

RUSSIAN ACADEMY OF SCIENCES

NATIONAL GEOPHYSICAL COMMITTEE

РОССИЙСКАЯ АКАДЕМИЯ НАУК

НАЦИОНАЛЬНЫЙ ГЕОФИЗИЧЕСКИЙ КОМИТЕТ



**NATIONAL VOLCANOLOGICAL REVIEW
OF RUSSIA**

for the

International Association of Volcanology
and Chemistry of the Earth's Interior

of the

International Union of Geodesy and Geophysics

2007–2010

**НАЦИОНАЛЬНЫЙ
ВУЛКАНОЛОГИЧЕСКИЙ ОБЗОР РОССИИ**

Международной ассоциации вулканологии

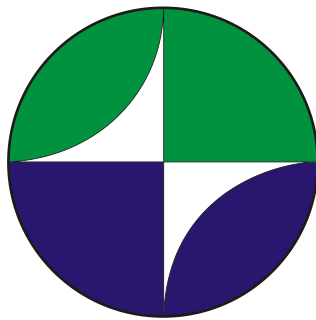
и химии недр Земли

Международного

геодезического и геофизического союза

2007–2010

Москва 2011 Moscow



**Presented to the XXV General Assembly
of the
International Union of Geodesy and Geophysics**

**К XXV Генеральной ассамблее
Международного геодезического и геофизического
союза**

RUSSIAN ACADEMY OF SCIENCES

National Geophysical Committee

**NATIONAL VOLCANOLOGICAL REVIEW
OF RUSSIA**

for the
International Association of Volcanology
and Chemistry of the Earth's Interior
of the
International Union of Geodesy and Geophysics
2007–2010

Presented to the XXV General Assembly
of the
IUGG

2011

Moscow

In the National Volcanological Review, major results are given of research conducted by Russian scientists in 2007–2010 on the topics of the International Association of Volcanology and Chemistry of the Earth's Interior of the International Union of Geodesy and Geophysics. Kamchatka Peninsula with its famous Klyuchevskaya Group of volcanoes is the most volcanically active area in Russia and one of the most active in the world. Majority of researches and scientific results on Volcanology and Geochemistry of the Earth's Interior during 2007–2010 were achieved in this region. Besides it, the scientific results on the magmatism of Far East of Russia and Northern Caucasus are also included in this review. Major achievements in the chemistry of the Earth, geothermy, geodynamics, and deep mantle structure are featured. The studies as for the single volcanoes as well the regional observations are outlined. The theoretical and applied efforts connected to the volcanological processes are considered. All the required references are given.

Editorial Board

T.G. Churikova (*Chief Editor*), B.N. Gordeychik (*Deputy Chief Editor*), S.A. Fedotov.

© 2011 Geophysical Center RAS

DOI: 10.2205/2011-IAVCEI-NRR2007-2010

ISBN: 978-5-904509-05-7

CONTENTS

INTRODUCTION.....	7
1 Volcanological and geochemical studies in Kamchatka area.....	7
1.1. Complex study of the Kluchevskaya Group of volcanoes and Central Kamchatka Depression.....	7
1.1.1. The Magmatic Feeding System of the Klyuchevskaya Group of Volcanoes Inferred From Data on Its Eruptions, Earthquakes, Deformation, and Deep Struc.....	8
1.1.2. Petrological and geochemical research on the volcanoes of Kluchevskaya Group and Central Kamchatka Depression.....	17
1.1.2.1. The petrological relationship between Kamen volcano and adjacent volcanoes of Klyuchevskaya group.....	17
1.1.2.2. Shisheysky complex.....	22
1.1.2.3. Research on mantle xenoliths in Central Kamchatka Depression.....	24
1.1.2.4. Tolbachik volcano.....	27
1.1.2.5. Southern part of the Central Kamchatka Depression.....	29
1.1.3. Volcanological research on the volcanoes of Kluchevskaya Group.....	29
1.1.3.1. Monitoring of active volcanoes.....	29
1.1.3.2. Bezimianny volcano.....	31
1.1.3.3. Shiveluch volcano.....	32
1.1.3.4. Klyuchevskoy volcano.....	36
1.1.3.5. Ushkovsky volcano.....	43
1.2. Regional study of the Kamchatka arc in 2007-2010.....	45
1.2.1. Geochemical variations across the Kamchatka arc.....	45
1.2.1.1. Previous results on major-, trace and high field strength elements.....	45
1.2.1.2. Volatile (S, Cl and F) and fluid mobile trace elements.....	47
1.2.2. Geochemistry of Primitive Lavas of the Central Kamchatka Depression: Magma Generation at the Edge of the Pacific Plate.....	49
1.2.3. South-North transect through the Sredinny Ridge of the Kamchatka.....	51
1.2.4. Pre-Holocene caldera-forming eruptions.....	54
1.2.5. New age data for Cainozoic magmatizm in Kamchatka.....	57
1.2.6. Cretaceous–Paleogene Magmatism of the Sredinnyi Range.....	57
1.2.7. Ocean–Continent Transition Zone: Kamchatka.....	58
1.2.8. Impuls nature of the areal volcanism on Kamchatka.....	60

1.2.9. Largest eruptions of Kamchatka in middle Pleistocene-Holocene: tephrakronological studies.....	61
1.2.10. Late Pleistocene-Holocene Volcanism on the Kamchatka.....	61
1.2.11. The Identification and Diagnostics of Active volcanoes.....	63
1.2.12. Marine geological-geophysical researches.....	65
1.3. Complex research of the active volcanoes of the Eastern Volcanic Front of Kamchatka and Kurile volcanic arc in 2007-2010.....	66
1.3.1. Chikurachki volcano (Kurile arc).....	66
1.3.2. Koriaksky volcano.....	67
1.3.3. Karymshina, a Giant Supervolcano Caldera.....	67
1.3.4. Karimsky volcanic center.....	69
1.3.5. Cape Nalycheva and the Shipunskii Peninsula.....	75
1.3.6. Kizimen volcano.....	77
1.3.7. Valley of Geysers.....	79
1.3.8. Ultra-depleted melts from Kamchatkan ophiolites.....	80
1.3.9. Method of water balance at Kurile arc.....	81
1.3.10. Gorely volcano.....	81
1.4. Kamchatka's minerals.....	82
1.4.1. Mutnovsky volcano and it's Geothermal Reservoirs.....	82
1.4.2. Asachinskoe epithermal Au-Ag deposit.....	87
1.4.3. Platibum-Group minerals.....	88
1.4.4. Fe-Mn crusts formation.....	89
1.4.5. Diomondiferous complexes of Kamchatka.....	89
1.4.6. Oil and Gas Potential.....	90
2. Volcanology, geodynamics and deep mantle structure of the Far East region of Russia in 2007-2010.....	91
2.1. Intraplate alkaline- basaltic volcanism of arctic shelf and continental margin of North- East Asia.....	91
2.2. Research of the modern volcanoes in Far East of Russia.....	91
3. Volcanology of Northern Caucasus.....	93
3.1. Cenozoic fluid-magmatic centers, geodynamics, seismotectonics and volcanism in Elbrus volcano area.....	93

3.1.1. Pulsating Vertical Evolution of the Elbrus Volcanic Region (as a Consequence of Migration of the Mantle Plume?).....	93
3.1.2. Relation between Structural and Material Circular Motions in a Volcanic Center.....	96
3.2. Mud volcanoes in North-Western Caucasus.....	98
3.3. Thermal resources of Northern Caucasus.....	102
4. Theoretical evidences in Volcanology.....	106
4.1. The temporal organization of global volcanic activity.....	106
4.2. Mechanism of lava fields generation.....	106
4.3. Interaction of NaNO ₃ -NaOH fluids with sandstone rocks.....	111
4.4. Simulation of earthquake ground motion.....	112
4.5. Processes in the feeders of basaltic volcanoes.....	113
4.6. Volcanology and climate.....	115
4.7. Rotational processes in geology.....	116
4.8. Volcanic plumes and wind.....	116

INTRODUCTION

T. G. Churikova, tchurikova@mail.ru. *National Geophysical Committee RAS. Institute of Volcanic Geology and Geochemistry, Piip Avenue 9, Petropavlovsk–Kamchatsky, Russia.*

This review submitted to the International Association of Volcanology and Chemistry of the

Earth's Interior (IAVCEI) of the International Union of Geodesy and Geophysics (IUGG) contains results obtained by Russian volcanologists and geochemists in 2007-2010. In the review prepared for the XXV General Assembly of IUGG (Australia, Melbourne, 28 June - 7 July 2011), the results are briefly outlined of basic research in volcanology, geochemistry, isotopic systematics, geodynamics, geothermy, as well as in some other directions.

The period from 2007 to 2010 was still difficult for Russian volcanologists and geochemists. Owing to economic reasons scientific career in Russia is still believed to be lacking in prestige. Thus recruiting younger scientists for fundamental research in volcanologists and geochemists actually failed. Economic difficulties were redoubled by difficulties arising from reorganizing the Russian Academy of Sciences, Russian science and the educational system of Russia initiated by the leaders of the country. The number of Russian scientists in governing bodies of IUGG, IAVCEI, IASPEI, and their commissions is decreasing. In spite of the difficulties, Russian scientists participated in practically all conferences of the International Association of Volcanology and Chemistry of the Earth's Interior (IAVCEI), in the General Assemblies, international projects and international centers.

Even in such difficult conditions high scientific potential, great experience in research and the traditions of Russian volcanologists and geochemists allowed obtaining a number of fundamentally important new results in the period under review. Many of them are presented in the following sections of this review.

One of the most pronounced publications of Russian volcanologists during reviewing period was Volum 172 of Geophysical Monograph Series "Volcanism and subduction: the Kamchatka region." (Eichelberger J., Gordeev E., Izbekov P., Kasahara M., Lees J. (eds.). – Washington, DC: American Geophysical Union, 2007), which combined the most important results on the Kamchatka volcanism. Some of these researches would be presented in this review. Each of the sections has a list of the most interesting scientific papers published in 2007–2010 including publications prepared in cooperation of Russian scientists and their colleagues from other countries.

For a number of reasons not all results obtained by Russian scientists on the problems of volcanologists and geochemists of the Earth's interior in 2007-2010 are included in the review. At the same time it is hoped that authors may present these results at symposia of IUGG XXV General Assembly.

1. Volcanological and geochemical studies in Kamchatka area

1.1. Complex study of the Kluchevskaya Group of volcanoes and Central Kamchatka Depression

The Kluchevskaya Group of Volcanoes (KGV, Fig. 1.1.1) has been the foremost object of volcanological research in Russia since the early 1930s. The beginnings of these researches were associated with the names of such outstanding scientists as academicians F.Yu. Levinson-Lessing, A.N. Zavaritskii, V.I. Vlodayets, corresponding member of the USSR Academy of Sciences B.I. Piip, S.I. Naboko, and others. Several volcanological expeditions worked in the KGV during the period from 1931 to 1935; the Kamchatka Volcanological Station of the USSR

Academy of Sciences was inaugurated in the village of Klyuchi near the northern foot of Klyuchevskoi Volcano on September 1, 1935. The Station has been conducting continuous valuable observations of the KGV volcanoes since that time. This research has expanded since the Laboratory of Volcanology of the USSR Academy of Sciences with its Kamchatka Volcanological Station were set up in 1945–1962 and afterward successfully continued in the 1960s after the Institute of Volcanology of the Siberian Branch (SB) of the USSR Academy of Sciences was set up in the city of Petropavlovsk-Kamchatskii. By the present time the study of the KGV volcanoes has been conducted for nearly 80 years. Fundamental scientific results have emerged from the comprehensive study of major eruptions. These include the paroxysmal summit eruption of 1944–1945 on Klyuchevskoi, the disastrous eruption and directed explosion of the andesitic volcano Bezimyannyi in 1955–1956, and the Great Tolbachik Fissure Eruption GTFE of 1975–1976, which is the greatest basaltic eruption to have occurred in Kamchatka during historical time.

The most intense Holocene activity in Kamchatka is found in KGV (Fig. 1.1.1) of the Central Kamchatka Depression with Kluchevskoy volcano (4750 m) being the most productive arc volcano in the world (63*10⁶ t magma/year). Additionally it was shown previously (Kersting and Arculus, 1995; Tsvetkov et al., 1989; Turner et al., 1998), that the amount of the sedimentary component is limited, offering the chance to investigate a relatively simple system. All these advantages make the Kluchevskaya Group one of the best volcanic laboratories not only for Russian scientist, but also one of the best volcanic places in the world. In this section we will consider the investigations done by Russian volcanologists, geochemists and geophysicists in the area of Kluchevskaya Group.



Fig. 1.1.1. Kluchevskaya Group of volcanoes (view from the South): from left to right are volcanoes: Ploskie Sopky, Kluchevskoy, Kamen, Bezimianny. (foto by B. Gordeychik and T. Churikova).

1.1.1. The Magmatic Feeding System of the Klyuchevskaya Group of Volcanoes Inferred From Data on Its Eruptions, Earthquakes, Deformation, and Deep Structure

S. A. Fedotov, karetn@list.ru. *Institute of Volcanology and Seismology, Far East Division, Russian Academy of Sciences, Petropavlovsk-Kamchatsky, 683006, Russia; Institute of Physics of Earth, Russian Academy of Sciences, Moscow, 123995, Russia*

N. A. Zharinov, nzhar@kscnet.ru. *Institute of Volcanology and Seismology, Far East Division, Russian Academy of Sciences, Petropavlovsk-Kamchatsky, 683006, Russia*

L. I. Gontovaya, glarissa@i.kiev.ua. *Institute of Volcanology and Seismology, Far East Division, Russian Academy of Sciences, Petropavlovsk-Kamchatsky, 683006, Russia*

The study of magmatic feeding systems of volcanoes (roots of volcanoes) is one of the main tasks facing volcanology. One major object of this research is the Klyuchevskoi group of volcanoes (KGV, Fig. 1.1.1.1), Kamchatka, which is the greatest found at island arcs and subduction zones. We summarize the comprehensive research that has been conducted there since 1931. Several conspicuous results derived since the 1960s are reported emerging from the study of magma sources, eruptions, earthquakes, deformation, and deep structure for the KGV. Our discussion of these subjects incorporates the data of physical volcanology relating to the mechanism of volcanic activity and data from petrology on magma generation. The following five parts can be distinguished in the KGV magmatic feeding system and the associated geophysical model: the source of energy and material at the top of the Pacific Benioff zone at a depth of about 160 km, the region of magma ascent in the asthenosphere, the region of magma storage in the crustmantle layer at depths of 40–25 km, magma chambers and channelways in the crust, and bases of volcanic edifices. We discuss and explain the properties of the relationships between these parts, the mechanisms of volcanic activity and of the KGV magmatic feeding system as existing today. There are methods available for calculating magma chambers and conduits, the amount of magma in the system and its other properties.

These studies were based on the data on eruptions, seismicity, ground deformation and other geophysical data, with appeal to the theory of the mechanism of volcanic activity. In all, five basic parts can be distinguished in the KGV plumbing system:

The upper part of the plunging Pacific plate, at a depth of approximately 160 km beneath the KGV. The source of material and energy. Seismological evidences suggest that it is at this depth the source of energy and volatiles necessary for magma generation is situated. The heat that is released from deformation in the Benioff zone can be sufficient to start partial melting. Figure 1.1.1.2 contain plots of the cumulative total weight of juvenile volcanic rocks discharged in 1930–2008 by the Klyuchevskoi, Bezmyannyi, and Ploskii Tolbachik volcanoes, together with the Tolbachik zone of monogenic cones and by the entire KGV. The total average magma discharge from these volcanoes of the KGV (155 million t/yr) was more than half the total magma discharge from all 70 active volcanoes of the Kuril–Kamchatka arc (250 million t/yr). Figure 1.1.1.1d indicates the years and magnitudes of the $M \geq 7.3$ earthquakes which occurred in Kamchatka during the period from 1930 to 2008. The basic data on these events are given in [Fedotov et al., 2010]. All the four major eruptions in the KGV were preceded by $M \geq 7.3$ earthquakes occurring in the Benioff zone of Kamchatka 2–4 years before the eruptions. The segment of the Benioff zone beneath the KGV where magma generation begins extends for about 100 km along the Kuril–Kamchatka arc. According to seismological data for the thickness of the subducted plate is about 50 km. According to geodetic data, the plate moves at a rate of 8–10 cm/yr. Using these data, we deduce that the part of the plate that is annually submerged under the KGV has a volume of approximately 0.5 km^3 and weighs $1.5 * 10^9$ tons. The average annual discharge from the greatest KGV volcano, Klyuchevskoi, is equal to $60 * 10^6$ t/yr, while the figure for the entire KGV was $155 * 10^6$ t/yr during the most active period from 1930 to 2008. The weight of all discharged KGV rocks thus amounts to 4–10% of the weight of the plunging plate. The percentage may be a few times greater for the top of the plate. The area of the Benioff zone beneath the KGV is 10000 times the crater area of the active KGV volcanoes. The ascent of magmas results in an enormous concentration of material and energy in the asthenosphere and lithosphere. This process can begin from the top of the Benioff zone.

The asthenosphere, the region of magma generation and ascent toward the intermediate magma chambers in the KGV, depths of 160–40 km. According to geophysical and geochemical data, partial melting of mantle material and the generation of deep seated magmas beneath the KGV are taking place in the lower asthenosphere. Melting is intensified as volatiles come in from the plunging plate and because of decompression as the material that is melting is ascending. The principal force that is responsible for magma ascent is due to

decreased density of molten rocks. The ascent of magmas in the asthenosphere can occur by gravitational convection in diapirs, asthenoliths, magmatic asthenosphere columns, and jets. The most rapid ascent can occur in extended magmatic asthenosphere columns.

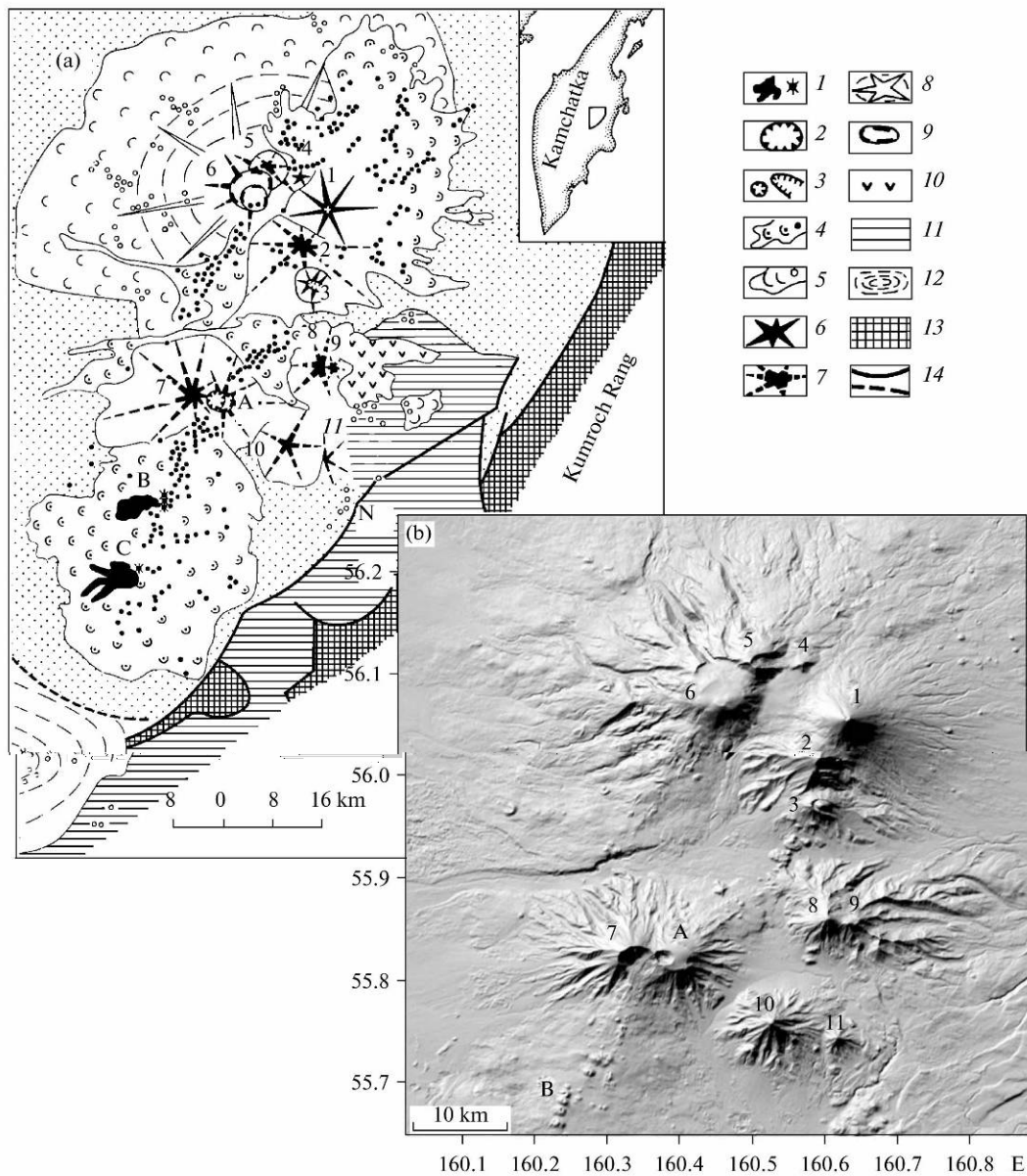


Fig. 1.1.1.1. A map of the Klyuchevskaya group of volcanoes (KGV). (a) locations of active and extinct volcanoes: (1) lava flows from the North (B) and South (C) vents of the GTFE, (2) fresh collapse caldera on the summit of Ploskii Tolbachik which was generated during the GTFE (A), (3) larger craters, (4) Holocene cinder cones and lava flows from these, (5) Late Pleistocene cinder cones and lava flows from these, (6) major Holocene stratovolcanoes, (7) major Late Pleistocene volcanoes, (8) shield volcano at the base of Ushkovskii and Krestovskii volcanoes, (9) Holocene collapse calderas on the summits of Ploskii Tolbachik and Ushkovskii volcanoes, (10) strongly damaged Gornyi Zub Volcano, (11) lava plateaus, (12) Nikolka, shield volcano, (13) pre-Quaternary rocks of folded basement, (14) faults, those having relief expression and buried ones. Numbers in Fig. 1.1.1.1a mark the following volcanoes: 1 Klyuchevskoi, 2 Kamen', 3 Bezmyanni, 4 Srednii, 5 Krestovskii, 6 Ushkovskii, 7 Ostryi Tolbachik, 8 Bol'shaya Zimina, 9 Malaya Zimina, 10 Bol'shaya Udina, 11 Malaya Udina. (b) map-view space image of the KGV, numbers mark the same volcanoes.

Seismic tomography shows that there is a region of low shear velocity in the KGV area extending upward from the Benioff zone toward the crust.

total plot's average line, (3) dates of major eruptions, (4) years and magnitudes of $M \geq 7.3$ Kamchatka earthquakes for the period 1930–2008.

According to our calculations, when the base of a magmatic asthenosphere column is at a depth of 150 km or when basaltic or andesitic magma is rising in it, and the difference in density between magma and host rock $\Delta\rho$ is about 0.5 g/cm³, we find that the excess pressure of deep-seated magmas at the crustal bottom equals 1000–2000 bars. Basaltic and andesitic magmas must quickly be squeezed from under the crust.

The excess pressure of deep-seated magmas at the crustal bottom is frequently in the range 500–1500 bars. The main mantle conduit of the KGV is at present beneath Klyuchevskoi Volcano, whose age is about 6000 years. It is along this conduit that more than 75% of all KGV mantle magma is supplied. Another Hawaiian-type active volcano, Ploskii Tolbachik, together with its Tolbachik zone of cinder cones is the second only to Klyuchevskoi in output in the KGV during Holocene time, erupting an average of $20 \cdot 10^6$ tons of basalt per year in the Holocene. However, at present we do not have solid geophysical data on its existence.

The crust–mantle layers and the lower crust, the intermediate magma chamber, depths of 40–25 km. According to geophysical data the average depth to the bottom of the crust–mantle layer beneath the KGV is equal to 40 km, the crystalline part of the crust is at depths of 25–7 km, while the sedimentary layers of the crust lie above 7–5 km. The character of the KGV magmatic activity experiences a change above that boundary. Under it, in the upper mantle, the initial melting and ascent of magmas occur. The processes above it include magma storage, the generation of the KGV intermediate magma chamber, conduits, crustal magma chambers beneath their respective volcanoes, and terminal conduits.

Figure 1.1.1.4 presents a diagram of the structure and a geophysical model for the upper parts of the KGV plumbing system above the mantle on a vertical cross section passing along the KGV axial line through the active Klyuchevskoi, Bezmyannyi, and Ploskii Tolbachik volcanoes. Figure 1.1.1.4 shows how the KGV magma chambers can be connected.

We indicate approximate volumes of the magma chambers, the excess magma pressure in these, as well as the content of SiO₂ and MgO (in %) in various places of the KGV plumbing system.

According to seismological and geodetic data, the Intermediate magma chamber of Klyuchevskoi Volcano or the magma storage region beneath it is situated at depths of 35–25 km (Fig. 1.1.1.3). This location is identified from swarms of small earthquakes with many long-period earthquakes among these, which are characteristic for volcanic roots. This intermediate chamber is the source of basalt for the summit and adventive eruptions on Klyuchevskoi. It is from there that intrusions of ultramafic and basic magmas can be emplaced; these magmas are moving beneath the KGV along layers of neutral buoyancy near the crustal bottom at depths of 20–30 km. The volume of that chamber was estimated from the amount of rocks discharged by Klyuchevskoi major eruptions and from the pressure decrease in the chamber after eruptions. This layer contains more than 80% of all KGV magmas and most intrusive activity may occur there.

Magma chambers and conduits, magma movement in the crust beneath the KGV. Depths of 25–5 km, 5–0 km, and volcanic edifices. The depth range from 25 to 5 km contains a continuous, vertical magma conduit along which magma is rising from the intermediate chamber to depths of 5 km or less into the sedimentary layers that underlie the volcano and into its edifice (Fig. 1.1.1.4). This region contains the upper magma storage area, the peripheral chamber, the source of basaltic magmas for the summit and adventive eruptions of Klyuchevskoi Volcano. The excess magma pressure can reach 500 bars and be diminished by 100 bars or more during major eruptions. Many radial dikes are generated to supply adventive eruptions with magma as far as 20 km from the volcano's summit.

The upper bound on the volume of the Klyuchevskoi peripheral chamber was obtained from the amount of lavas discharged by the largest adventive eruption of high alumina basalts on the volcano - Piip eruption of 1966, altitude of 2000 m.

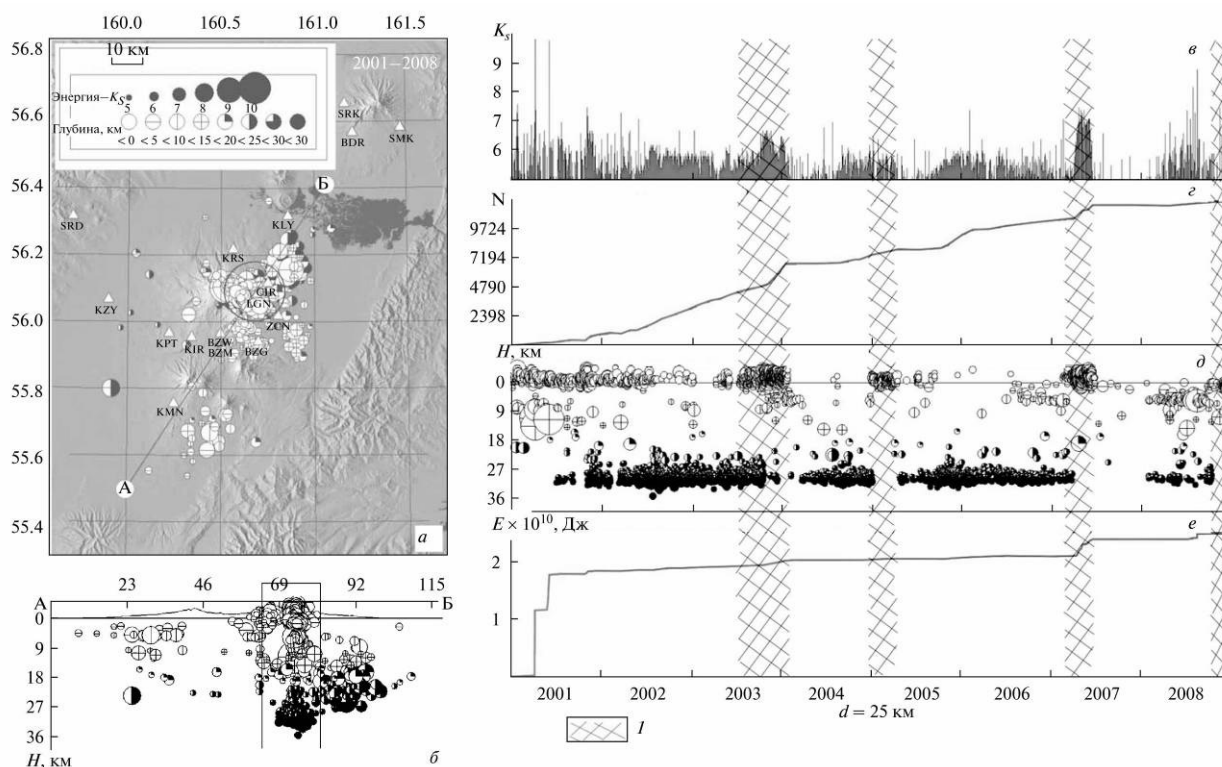


Fig. 1.1.1.3. Map showing the distribution of earthquakes over depth and time for the epicenter zone of Klyuchevskoi Volcano (the zone is 25 km across) for 2001–2008: (a) epicenter map and the identified epicenter zone, (b) cross section along AB, (b–f) variation over time in the epicenter zone for energy class, number of events, depth, and total energy of earthquakes; map (a) shows the locations of telemetry seismic stations (triangles), the circle marks the central epicenter zone around Klyuchevskoi Volcano (the zone is 25 km across); the notation shows energy class K_S and depth of focus. The vertical rectangle shows the cross section of the volcano’s central epicenter zone indicated in panel (a). The data are catalogs of the KB GS RAS. 1 cross_hatching shows periods of summit eruptions.

According to our calculations, the volume of the peripheral chamber is $B \leq 100 \text{ km}^3$ (Fig. 1.1.1.4). According to geodetic and seismological data, magma ascent from the intermediate to the peripheral chamber begins a few months before a summit eruption. Seismic probing of the KGV revealed that the crustal magma chamber of the andesitic Bezymyanni Volcano may be at depths of 5–10 to 20 km beneath the volcano (Fig. 1.1.1.4), which confirms by earthquakes occurring beneath the volcano down to depths of 15 km.

A catastrophic eruption of Bezymyanni occurred on March 30, 1956 discharging fresh pyroclastic andesite flows from the crater produced by the explosion, 1 km^3 in volume and with a density 2 g/cm^3 . The new crater was 600–700 m deep, and the pressure at the source was diminished by 150 bars. The magma chamber of Bezymyanni Volcano is centered 10–15 km higher than the Klyuchevskoi intermediate chamber, and the magma compressibility is greater in it. Assuming $\beta = 5 * 10^{-6} \text{ bar}^{-1}$ or $K = 2 * 10^5 \text{ bars}$, we obtain the result that the source that supplied magmas for the catastrophic eruption of Bezymyanni Volcano might be as large as 1050 km^3 in volume (Fig. 1.1.1.4).

A Hawaiian_type caldera 3 km in diameter is situated on top of the basaltic Ploskii Tolbachik Volcano. The top of the magma chamber beneath the caldera is at a depth of 2 km,

and the chamber is 4–5 km across. The chamber contains megaplagiophyre alumina basalts. A collapse crater 100–200 m deep had been in the volcano's summit caldera prior to the GTFE, with a lava lake appearing and disappearing on the bottom. At that time the plumbing system of the volcano was in a stationary state. The excess magma pressure in the plumbing system was previously estimated for the crustal density profile beneath the KGV. Assuming the magma of megaplagiophyre alumina basalts to have a density of 2.65 g/cm^3 , we obtain the result that the source of these magmas beneath Ploskii Tolbachik Volcano is deeper than 23 km, and the excess magma pressure is equal to 300 bars at the bottom of the sedimentary layer at a depth of about 7 km (Fig. 1.1.1.4).

Magnesian basalts are rocks of the most basic composition in the KGV. They were erupted again in 1975 at the North vent of the Great Tolbachik Fissure Eruption in the Tolbachik zone of cinder cones 18 km southwest from the summit caldera of Ploskii Tolbachik. According to geophysical data, the source of those basalts was at a depth of 16–22 km beneath the North vent, Fig. 1.1.1.4. The excess magma pressure near the ground surface was equal to 100–250 bars.

The preceding eruption of high-magnesian basalts took place in that zone of cinder cones during May 5–14, 1941 at a distance of 4 km from the summit caldera (Fig. 1.1.1.4).

Less than 2000 years ago high-magnesian basalts were erupted in that same zone 27 km from the summit caldera. The source of these eruptions was the segment of the conduit that allows passage for the KGV magnesian basalts; the segment is situated in the lower half of the crust under the southwestern end of the KGV axial line (Fig. 1.1.1.4).

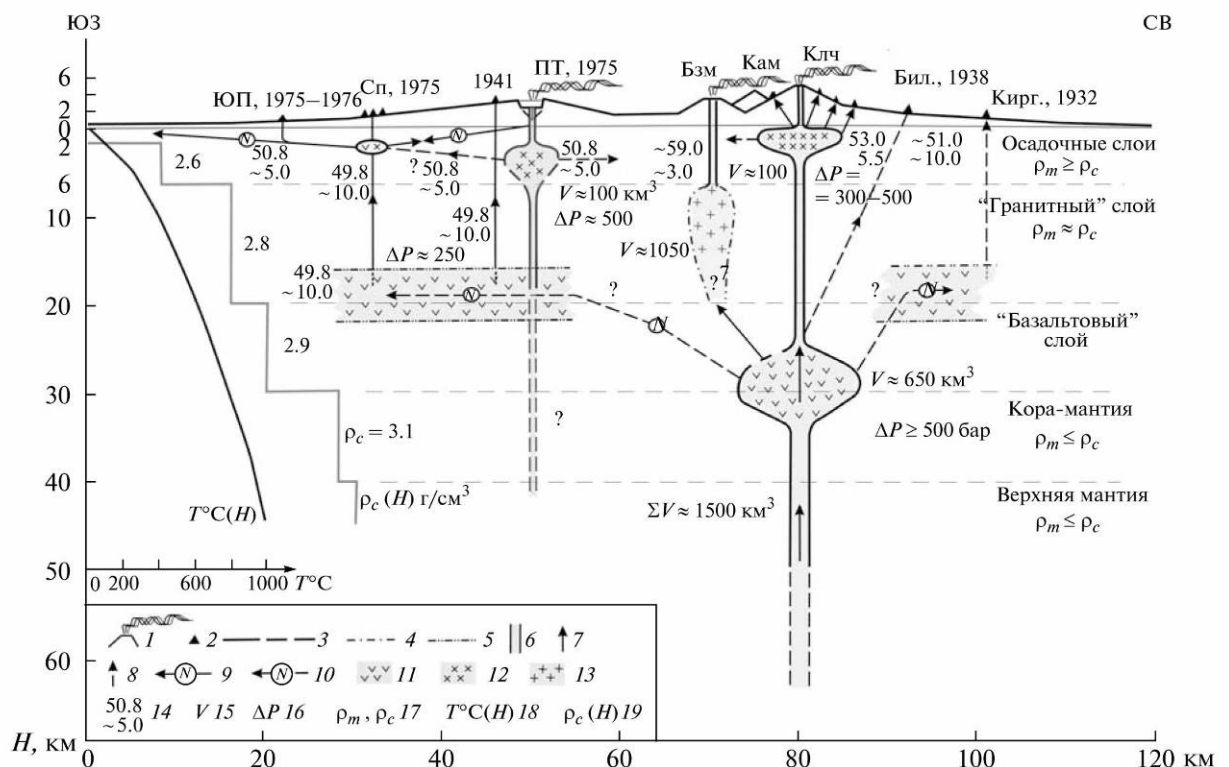


Fig. 1.1.1.4. The KGV plumbing system: present day structure, movement and storage of magmas. Geophysical model. Vertical cross section along the KGV axial line: (1) active volcanoes, (2) cones of 1930–2008 monogenic eruptions, (3) boundaries of basaltic magma chambers, (4) boundary of a possible source of andesite magmas for Bezymyannyi Volcano, (5) possible boundaries of storage and movement regions for magnesian basalts, (6) vertical conduits, (7) observed locations of magma ascent, (8) possible lines of magma ascent, (9) observed magma movements in layers of neutral buoyancy, (10) possible

magma movements in layers of neutral buoyancy, (11) magnesian basalts, (12) alumina basalts, (13) andesite, (14) concentration of SiO₂ and MgO in magmas, %, (15) volumes of magma chambers, km³, (16) excess magma pressure, in bars, (17) rock and magma densities, ρ_m and ρ_c , g/cm³, (18) variation in rock temperature with depth, T°C (H) km, (19) rock density variation with depth, $\rho_c(H)$, g/cm³. Locations of active volcanoes in the KGV, the 1932 areal Kirgurich eruption, the 1938 adventive Bilyukai eruption, the North and South vents of the 1975–1976 GTFE.

Using geophysical data the location of a chamber was determined at a depth of 2–4 km beneath the GTFE North vent; the chamber was formed at the beginning of that eruption. The chamber may have been responsible for mixing of magnesian and megaplagiophyre alumina basalts during the GTFE (Fig. 1.1.1.4).

Magmas are supplied to peripheral chambers and to the craters of active central-type volcanoes along extended vertical conduits, i.e., the channelways for magmas coming to the locations of hundreds of monogenic cones, with adventive eruptions and extrusions in the KGV being fissures that solidify after eruptions.

The volume of hundreds of radial dikes as long as 20 km beneath Klyuchevskoi Volcano may equal the volume of the entire edifice. The dikes of its adventive eruptions are shown diagrammatically in figure 1.1.1.4.

Quick emplacement, mixing, and flow of basalts was occurring for one and a half years during the GTFE at depths of a few kilometers for 50 km along the Tolbachik zone of cones (Fig. 1.1.1.4). This magma movement was similar to that of basalts in zones of neutral buoyancy along volcanic rifts in Iceland and other regions.

The magma pressure decrease during the GTFE, 100–250 bars, the mass of erupted basalts, $3.8 * 10^9$ tons, and the magma bulk modulus $K = 10^5$ bars were used to derive an approximate volume of that part of the plumbing system from which magmas were issuing during the GTFE; this figure might well be $(1.6–4.0) * 10^3$ km³.

The total volume of the magma chambers of the active Klyuchevskoi, Bezmyannyi, and Ploskii Tolbachik volcanoes shown in figure 1.1.1.4 is below $1.9 * 10^3$ km³. Based on these approximate estimates, we infer that comparable magma volumes in the KGV may reside in the magma chamber of the decaying Ushkovskii Volcano, in the large intrusions throughout the KGV, and in the magma channelways beneath the KGV axial line. Mantle magmas are probably for the most part emplaced and stored at the base of the crust.

The above estimates are consistent with determinations of the volume ratios between the pressure sources in the peripheral and intermediate chambers of Klyuchevskoi Volcano obtained from geodetic data. The latter yield the result that the scale of intrusive activity beneath Klyuchevskoi Volcano at depths of 25 km is six times that at a depth of about 3 km.

The interrelationships among magma chambers and sources over the entire KGV area could be seen during the greatest basaltic eruption (GTFE) in 1975–1976 and subsequent eruptions in 1977–1978.

The eruptions of the most basic rocks in the KGV, magnesian basalts, only occur in the Tolbachik zone of cones, for 30 km from the summit caldera of Ploskii Tolbachik, and in the areal zone of cones 10–20 km north-east from the Klyuchevskoi crater. These places lie at the ends of the KGV axial line passing through Klyuchevskoi, Bezmyannyi, and Ploskii Tolbachik volcanoes along the trend of the Kamchatka volcanic belt. The layer of neutral buoyancy for magnesian basalts, which can transport these in the basaltic crustal layer beneath the KGV, must extend along the KGV axial line (Fig. 1.1.1.4).

The basaltic magmas of Klyuchevskoi Volcano and the andesitic magmas of Bezmyannyi Volcano have a common deep-seated source; their channelways branch out at a depth of about 30 km. This is confirmed by the fact that when either of the adjacent Klyuchevskoi and Bezmyannyi volcanoes shows increased activity the other is quiescent.

A genetic relationship between the magmas of Klyuchevskoi, Bezmyanni, and Kamen' volcanoes is quite probable. The active Klyuchevskoi and Bezmyanni volcanoes formed in the Holocene at the edges of the extinct Upper Pleistocene Kamen' Volcano. These three volcanoes are arranged in a 10 km row along the KGV axial line (Fig. 1.1.1.1). Ushkovskii Volcano, which shows little present day activity, has a different mantle source.

These conclusions from petrologic research are corroborated by data on the distribution of earthquake hypocenters beneath the KGV and are consistent with the geophysical model (Fig. 1.1.1.4). The model sheds light on the positions, significance, and relationships among the magma chambers of the three volcanoes referred to above in the entire plumbing system of the KGV.

The high-magnesian and high-alumina magmas of Klyuchevskoi Volcano are generated during the ascent and differentiation of mantle magmas in the channelways and chambers of the KGV plumbing system situated beneath the volcano in the asthenosphere, in the transitional layer, and in the crust. According to seismological and geodetic data the time intervals during the period from 1978 to 2008 when magma was rising from the intermediate chamber of Klyuchevskoi Volcano toward its peripheral chamber lasted less than a third of this time. The longest periods of time were those which favored magma differentiation.

Magmas of magnesian alumina basalts and andesites are generated in the KGV plumbing system. Eruptions of alumina basalts are occurring throughout the KGV area, but andesites are discharged in its middle only (Fig. 1.1.1.4).

According to the properties of the geophysical model, the movements of alumina basalts throughout the KGV can take place in intrusions along the layer of neutral buoyancy for these basalts, which is situated in the crustal sedimentary layer. In this case the accumulation of andesites in the middle of the KGV may be due to the thicker volcanogenic-sedimentary layer there. Such a distribution of igneous rocks with differing compositions exists in many volcanic centers. Further examination of this geophysical model for the KGV plumbing system may form the subject of future publications.

We considered and accounted for many properties of the present day KGV plumbing system. It should be borne in mind that other volcanoes had been active in the KGV area during Upper Pleistocene time, and the KGV plumbing system had a substantially different structure at that time. It should be noted that we are in a position at present to calculate many properties of the model set forth here: the parameters and properties of dikes, sills, cylindrical conduits, spherical and lens-like magma chambers, and the mechanisms of different eruptions and of plumbing systems. The theory of volcanic activity is used to study various properties of the KGV, its volcanoes and eruptions. Geophysical data are helpful for the formulation and interpretation of results from petrologic, geochemical and other research.

S. A. Fedotov, N. A. Zharinov, and L. I. Gontovaya. The Magmatic System of the Klyuchevskaya Group of Volcanoes Inferred from Data on Its Eruptions, Earthquakes, Deformation, and Deep Structure. Journal of Volcanology and Seismology, 2010, Vol. 4, No. 1, pp. 1–33.

Gontovaya, L.I., Khrenov, A.P., Stepanova, M.Yu., and Senyukov, S.L., A Deep Model of the Lithosphere in the Area of the Klyuchevskaya Group of Volcanoes, Kamchatka, Vulkanol. Seismol., 2004, no. 3, pp. 3–11.

Gorel'chik, V.I., Garbuzova, V.T., and Storcheus, A.V., Deep-Seated Volcanic Processes beneath Klyuchevskoi Volcano from Seismological Data, Vulkanol. Seismol., 2004, no. 6, pp. 21–34.

Seliverstov, N.I., Geodinamika zony sochleneniya Kurilo-Kamchatskoi i Aleutskoi ostrovnykh dug (The Geodynamics of the Junction Zone between the Kuril-Kamchatka and Aleutian Island Arcs), Petropavlovsk-Kamchatskii, 2009.

Senyukov, S.L., Droznina, S.Ya., Nuzhdina, I.N., Garbuzova, V.T., and Kozhevnikova, T.Yu., Studies in the Activity of Klyuchevskoi Volcano by Remote Sensing Techniques between January 1, 2001 and July

- 31, 2005, *Volcanol.Seismol.*, 2009, no. 3, pp. 50–59 [*J. Volcanol. Seismol.*, vol. 3, no. 3, pp. 191–199].
- Fedotov, S.A., *Magmaticcheskie pitayushchie systemy I mekhanizm izverzhenii vulkanov (Magmatic Feeding Systems and the Mechanism of Volcanic Eruptions)*, Moscow: Nauka, 2006.
- Fedotov, S.A., *Fifty Years of Detailed Seismological Investigations: The Kuril–Kamchatka Arc*, *Volcanol. Seismol.*, 2008, no. 2, pp.153–160 [*J. Volcanol. Seismol.*, 2008, vol. 2, no. 2, pp. 135–141.]
- Fedotov, S.A. and Zharinov, N.A., *On the Eruptions, Deformation, and Seismicity of Klyuchevskoy Volcano, Kamchatka in 1986–2005 and the Mechanism of Its Activity*, *Vulkanol. Seismol.*, 2007, no. 2, pp. 3–31 [*J. Volcanol. Seismol.*, 2007, vol. 1, no. 2, pp. 71–97].
- Fedotov, S.A., Zharinov, N.A., and Gontovaya, L.I., *On the Activity, the Plumbing System, and Deep Structure of the Klyuchevskaya Group of Volcanoes, in Vulkanizm i Geodinamika (Volcanism and Geodynamics), Proc. IV All_Russia symp. on Volcanology and Paleovolcanology (September 22–27, 2009, Petropavlovsk-Kamchatskii)*, vol. 1, *Petropavlovsk_Kamchatskii: IViS DVO RAN*, 2009, pp. 24–27.
- Fedotov, S.A., Zharinov, N.A., Gontovaya, L.I., and Sobisevich, A.L., *Klyuchevskoi Volcano, Kamchatka: Activity, Plumbing System, Seismic Tomography, in Izmenenie okruzhayushchei sredy i klimata, prirodnye I svyazannye s nimi tekhnogennye katastrofy (Environmental and Climate Changes, Natural and Related Manmade Disasters)*, vol. 2, *Noveishii vulkanizm Severnoi Evrazii: zakonomernosti razvitiya, vulkanicheskaya opasnost', svyaz' s glubinnymi protsessami i izmeneniyamiprirodnoi sredy i klimata (Recent Volcanism in North Eurasia: Evolutionary Patterns, Volcanic Hazards, the Relationships to Deep Seated Processes and Environmental and Climate Change)*, Moscow: IGEM RAN, 2008, pp. 273–294.
- Khrenov, A.P., Fedotov, S.A., Zharinov, N.A., et al., *Klyuchevskoi Volcano, in Deistvuyushchie vulkany Kamchatki (Active Volcanoes of Kamchatka)*, vol. 1, Fedotov, S.A. and Masurenkov, Yu.P., Eds., Moscow: Nauka, 1991, pp. 106–155 (in Russian and English).
- Khubunaya, S.A., Gontovaya, L.I., Sobolev, A.V., and Nizkous, I.V., *Magma Chambers beneath the Klyuchevskaya Volcanic Group, Kamchatka*, *Volcanol. Seismol.*, 2007, no. 2, pp. 32–54 [*J. Volcanol. Seismol.*, vol. 1, no. 2, pp. 98–118].
- Churikova, T.G., Gordeichik, B.N., Ivanov, B.V., and Maksimov, A.P., *Petrogenetic Features in Rocks of Kamen' Volcano, Kamchatka, in Magmatizm I rudoobrazovanie (Magmatism and Ore Formation), Proc. conf. dedicated to the 125th birthday anniversary of Academician A.N. Zavaritskii, March 18–19, 2009, Moscow: IGEM RAN*, 2009, pp. 139–143.
- Lees, J.M., Symons, N., Chubarova, O., et al., *Tomographic Images of Klyuchevskoy Volcano P_Wave Velocity, in Volcanism and Subduction: The Kamchatka Region*, Eichelberger, J. et al., Eds., *Geophysical Monograph 172*, Washington: AGU, 2007, pp. 293–302.
- Nizkous, I., Kissling, E., Gontovaya, L., et al., *Correlation of Kamchatka Lithosphere Velocity Anomalies with Subduction Processes, in Volcanism and Subduction: The Kamchatka Region Geophysical Monograph Series 172*, pp. 97–106.

1.1.2. Petrological and geochemical research on the volcanoes of Kluchevskaya Group and Central Kamchatka Depression

1.1.2.1. The petrological relationship between Kamen volcano and adjacent volcanoes of Klyuchevskaya group

Churikova T., tchurikova@mail.ru. National Geophysical Committee RAS. Institute of Volcanic Geology and Geochemistry, Piip Avenue 9, Petropavlovsk–Kamchatsky, Russia.

Gordeychik B., gordei@mail.ru. Institute of Physics of Earth, Russian Academy of Sciences, Moscow, 123995, Russia.

Wörner G., gwoerner@gwdg.de. GZG Abteilung Geochemie, Universität Göttingen, Germany.

Ivanov B., ivanovbv@kscnet.ru. Institute of Volcanology and Seismology, Far East Division, Russian Academy of Sciences, Petropavlovsk7Kamchatskii, 683006, Russia.

The Klyuchevskaya Group (KG) of volcanoes has the highest magma production rate across the Kamchatka arc and in fact for any arc worldwide. However, modern geochemical studies of Kamen volcano, which is located between Klyuchevskoy, Bezymianny and Ploskie Sopky volcanoes (Fig. 1.1.1), were not carried out and its relation and petrogenesis in comparison to other KG volcanoes is unknown. Space-time proximity of KG volcanoes and the common zone of seismicity below them may suggest a common source and genetic relationship. However, the lavas of neighboring volcanoes are rather different: high-Mg and high-Al basalts occur at Klyuchevskoy volcano, Hbl-bearing andesites and dacites dominate at Bezymianny and medium-high-K subalkaline rocks at Ploskie Sopky volcano. Moreover, previously it was shown that distinct fluid signatures were observed in different KG volcanoes [Churikova et al., 2007]. In this review we present geological, petrographical, mineralogical and petrochemical data on the rocks of Kamen volcano in comparison with other KG volcanoes.

Three consecutive periods of volcano activity were recognized in geological history of Kamen volcano: stratovolcano formation, development of a dike complex and formation of numerous cinder and cinder-lava monogenetic cones. The stratovolcano stage is characterized by rather uniform magma evolution: the earliest lavas are essentially olivine-bearing; higher up in the geological section olivine-pyroxene-bearing rocks are developed with mafic minerals decreasing from base to top. The younger stages of the volcano are characterized by olivine-free and hornblende-bearing lavas. The rocks of the dike complex are olivine-bearing (up to 25% olivine) and hornblende-bearing basalts. Monogenetic cinder and cinder-lava cones are olivine-clinopyroxene basalts and basaltic andesites. Mantle xenoliths are represented by harzburgites and pyroxenites.

The rock series of volcano are divided into four groups: olivine-bearing (Ol-2Px and Ol-Cpx), olivine-free (2Px-Pl, Cpx-Pl and abundant Pl), Hb-bearing and subaphyric rocks. While olivine-bearing rocks are observed in all volcanic stages, olivine-free lavas are presented only in the stratovolcano edifice. Lavas of the monogenetic cones are presented by olivine-bearing and subaphyric rocks. Dikes are olivine-bearing and hornblende-bearing rocks. Olivines of the Kamen stratovolcano and dikes vary from Fo₆₀ to Fo₈₃. They have unimodal distribution with maximum at Fo₇₉. NiO, Cr₂O₃ and CaO in olivines vary significantly: 0,009%÷0,124%, 0,007%÷0,06% and 0,1%÷0,378%, respectively. NiO/Cr₂O₃ and NiO/CaO ratios are rather low: 3,5 and 0,38, respectively. Due to low Mg# and NiO, olivines of Kamen volcano do not fall into the mantle array of primary magmas after Ozawa [1984]. Clinopyroxenes are augites in composition with magnesian number similar to magnesian number of olivines. Plagioclases have a bimodal distribution with maximum modes at An₅₀ and An₈₆. Oxides are represented by high-Al spinel, magnetite and titaniferous magnetite. Mineral compositions of the rocks from monogenetic cones are systematically different from minerals of dikes and stratovolcano. Olivines in monogenetic cones varies from Fo₇₀ to Fo₉₂, Mg# of clinopyroxenes from 72 to 80 and plagioclases are represented by An₆₀₋₈₀.

All rocks of the volcano belong to medium-K calc-alkaline basalt-basaltic-andesitic series. The rocks of the stratovolcano are high-Al low-Mg (MgO=7%, SiO₂=50÷56%) and form the stable trends on all petrological diagrams with increasing K₂O, decreasing Al₂O₃, TiO₂, CaO, FeO and MgO from basalts to andesites. The melts of the dike complex are likely the least fractionated members of the same mantle source which is confirmed by the same mineral composition. Lavas of the monogenetic cones are high-Mg basalts (MgO>6%, SiO₂=50.5÷52.5%). They systematically differ from the stratovolcano samples by mineral composition and by higher MgO and CaO and low FeO, TiO₂, Al₂O₃ and P₂O₅ at similar SiO₂ content.

Kamen – Ploskie Sopky

Ploskie Sopky volcano rocks are systematically enriched in K₂O and P₂O₅ which probably result of higher fluid addition at Ploskie Sopky mantle source.

Mineral composition of Ploskie Sopky and Kamen volcanoes show similarities in scale of major elements. However, olivines from Ploskie Sopky volcano rocks are systematically enriched in CaO in comparison with all other basalts of Kluchevskaya Group.

Kamen-Kluchevskoy

Kluchevskoy volcano lavas are represented by three rock types in scale of MgO and Al₂O₃ content: high-Al basalts (HAB: MgO < 7 wt. % и Al₂O₃ ≥ 16 wt. %), magnesian basalts (MB: MgO = 7-10 wt. % и Al₂O₃ < 17 wt. %) and high-Mg basalts (HMB: MgO > 10 wt. % и Al₂O₃ < 17 wt. %).

KAMEN - PLOSKIE SOPKY

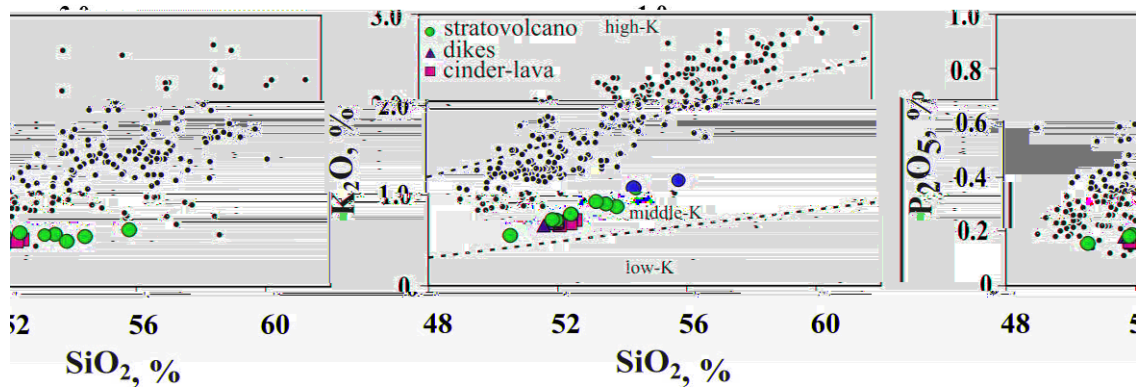


Fig. 1.1.2.1.1. SiO₂ versus K₂O and P₂O₅ in the rocks of Ploskie Sopky and Kamen volcanoes. Small black points – the rock composition of the Ploskie Sopky volcano after [Churikova, 1993]. Circles – stratovolcano rocks, triangles – dikes samples, squares – lavas and bombs of the monogenetic cones.

KAMEN - KLUCHEVSKOY

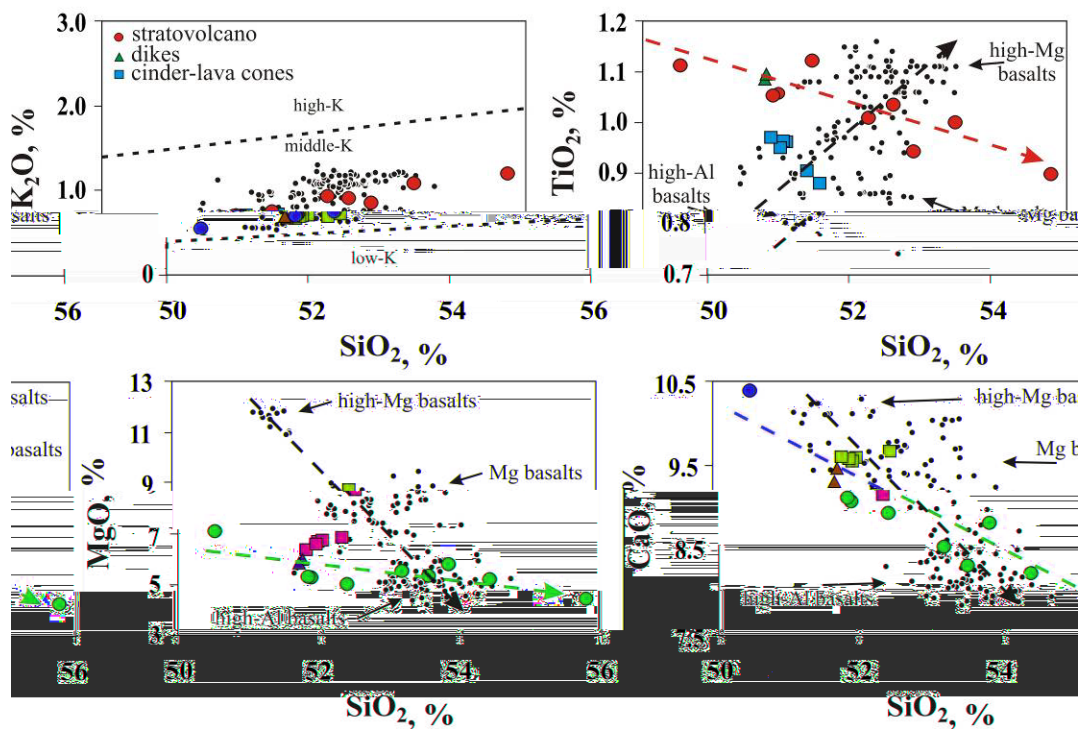


Fig. 1.1.2.1.2. Diagrams SiO₂ versus other major elements in rocks of Kamen and Kluchevskoy volcanoes. Small black points – the rock composition of the Kluchevskoy volcano using database from [Portnyagin et al., 2007]. Other symbols like on figure 1.1.2.1.1.

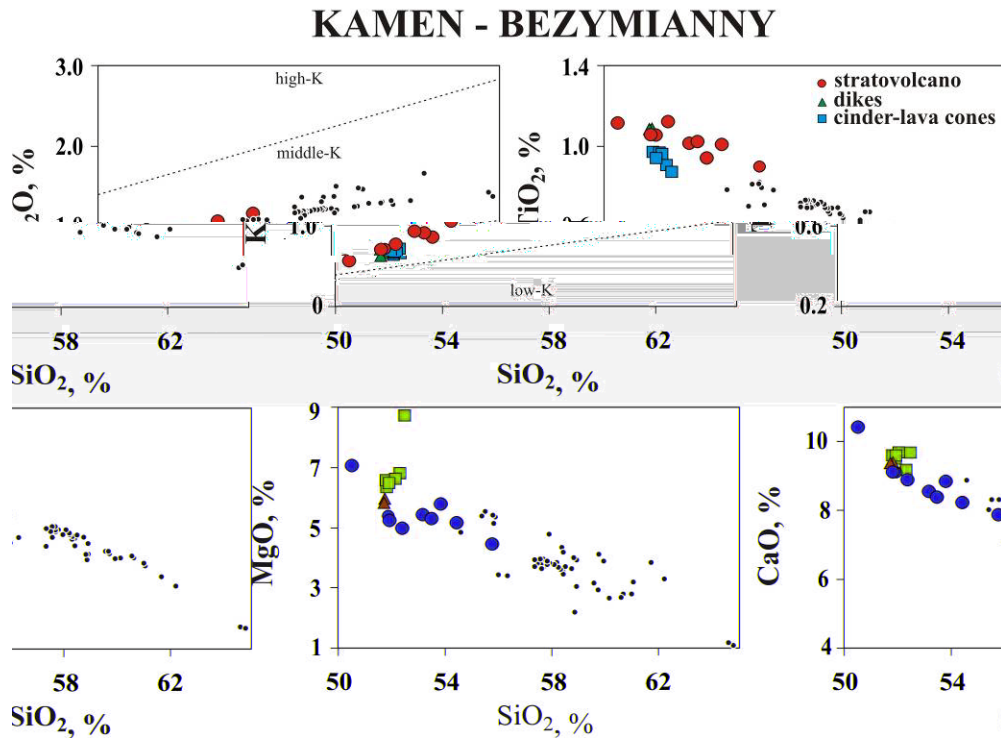


Fig. 1.1.2.1.3. Diagrams SiO₂ versus other major elements in rocks of Kamen and Bezymianny volcanoes. Small black points – the rock composition of the Bezymianny volcano using database from [Portnyagin et al., 2007]. Other symbols like on figure 1.1.2.1.1.

Kamen and Kluchevskoy volcanoes form multidirectional crystallization trends on most petrological diagrams, which overlap at SiO₂ = 53%-55% at of Kluchevskoy HAB field. Despite that Ol and Cpx from both rock groups are similar in major elements, they are systematically different in trace element composition: olivines and pyroxenes from HAB are enriched in Ni/CaO and Na₂O/TiO₂ ratios, correspondingly, in comparison with mafic minerals from Kamen lavas.

The fields of cinder-lava cones, which were erupted at Kamen volcano, and MB of Kluchevskoy are nearly identical. Their close relationship is confirmed by the same mineral composition.

Kamen- Bezymianny

Kamen and Bezymianny stratovolcanoes form the narrow single geochemical trends. Basalts and basaltic andesites of Kamen volcano comprise a mafic part of the trend while Bezymianny data points comprise a more silica-rich part – basaltic andesites – andesites – dacites of the overall trend.

Mineral composition of Ol and Cpx from Bezymianny volcano rocks show Fe enrichment in comparison with mafic minerals from Kamen lavas. On diagram Fo – CaO in Ol the olivines from both volcanoes form single geochemical trends, where Bezymianny data points comprise a more calcium-rich part of the overall trend.

We argue that Bezymianny volcano is keeps on the Kamen volcano evolution. These confirmed by arising of the Hb-bearing rocks at the last stages of Kamen stratovolcano activity and during dike complex formation.

P-T diagram, calculated from whole rock analyses (Fig. 1.1.2.1.4), show the relationship of the KGV volcanoes. The temperatures and pressures of the rocks crystallization were calculated using models of Albarede [1992] and Putirka [2008]. Diagram shows clearly that Ploskie Sopky rocks take separate place out of all studied volcanoes of KGV. They were crystallized at higher pressures. High-Al, moderate-Mg and high-Mg rocks of the Kluchevskoy volcano occupy three areas. high-Mg basalts were crystallized at the highest temperatures and pressures ($T = 1320-1350^{\circ}\text{C}$, $P = 10-12$ Kbar). Moderate-Mg and high-Al melts were crystallized at similar depth ($P = 6-8$ Kbar), but at different temperatures ($T = 1200-1270^{\circ}\text{C}$ and $T = 1100-1200^{\circ}\text{C}$, respectively). Points of the cinder cones of Kamen volcano are situated inside the field of moderate-Mg rocks, confirming their genetical similarities. The rocks of the Kamen and Bezymianny stratovolcanoes form one trend, which starts around the field of high-Al basalts of Kluchevskoy and follow to the area of lower temperatures and pressures (T decreases up to 1000°C , P decreases up to 1-2 Kbar (Fig. 1.1.2.1.4).

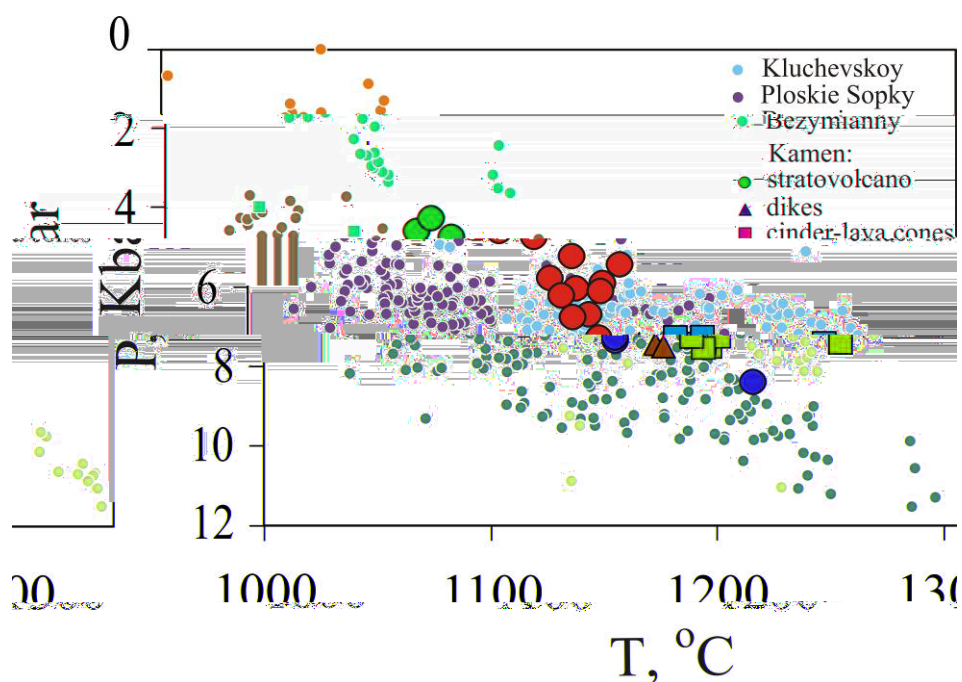


Fig. 1.1.2.1.4. P-T diagram for KGV rocks calculated from whole rock analyses. Temperatures and pressures were calculated using models of [Albarede, 1992] and [Putirka, 2008], correspondingly.

Thus, using petrological and mineralogical data we conclude that:

- (1) Kamen and Bezymianny volcanoes have a common mantle source;
- (2) monogenetic cones, which were erupted at Kamen volcano, belong to the group of high-Mg cones of Kluchevskoy;
- (3) the rocks of Ploskie Sopky and Kluchevskoy stratovolcanos are systematically different from stratovolcano Kamen in major elements and mineral composition and thus can not originate from the same mantle source by fractional crystallization.

Churikova T., Gordeychik B., Wörner G., Ivanov B., Maximov A. Mineralogy and petrology of Kamen volcano rocks, Kamchatka // Mitigating natural hazards in active arc environments. Linkages among tectonism, earthquakes, magma genesis and eruption in volcanic arcs, with a special focus on hazards posed by arc volcanism and great earthquakes: 6-th Biennial Workshop on Japan-Kamchatka-Alaska subduction processes (JKASP-2009). June 22-26, 2009. – Fairbanks, Alaska: Geophysical Institute, University of Alaska, 2009. – P. 117-118.

Churikova T., Gordeychik B., Wörner G., Ivanov B., Maximov A., Lebedev I., Griban A. *The petrological relationship between Kamen volcano and adjacent volcanoes of Klyuchevskaya group // Geophysical Research Abstracts: 7th EGU General Assembly. – 2010, vol. 12. – EGU2010-12866-2.*

Churikova T., 1993. *Geochemistry and modeling of magmatic process of the Kluchevskaya Group volcanoes". Ph.D. Thesis, Moscow State University, Geological Faculty: pp. 155.*

Portnyagin M., Bindeman I., Hoernle K., Hauff F. *Geochemistry of Primitive Lavas of the Central Kamchatka Depression: Magma Generation at the Edge of the Pacific Plate // Volcanism and subduction: the Kamchatka region. Geophysical Monograph Series. Vol. 172. / Eichelberger J., Gordeev E., Izbekov P., Kasahara M., Lees J. (eds.). – Washington, DC: American Geophysical Union, 2007. – P. 199-239.*

1.1.2.2. Shisheysky complex

In Collaboration with Department of Earth and Ocean Sciences, University of South Carolina, lavas of the northern Kamchatka area were studied. In this research primitive arc magmatism and mantle wedge processes are investigated through a petrologic and geochemical study of high-Mg# ($Mg/(Mg + Fe) > 0.65$) basalts, basaltic andesites and andesites from the Kurile-Kamchatka subduction system. Primitive andesitic samples are from the Shisheysky Complex, a field of Quaternary-age, monogenetic cones located in the Aleutian–Kamchatka junction, north of Shiveluch Volcano, the northernmost active composite volcano in Kamchatka. The Shisheysky lavas have Mg# of 0.66–0.73 at intermediate SiO_2 (54–58 wt%) with low CaO (< 8.8%), CaO/Al_2O_3 (< 0.54), and relatively high Na_2O (> 3.0 wt%) and K_2O (> 1.0 wt%). Olivine phenocryst core compositions of Fo_{90} appear to be in equilibrium with whole-rock ‘melts’, consistent with the sparsely phryic nature of the lavas. Compared to the Shisheysky andesites, primitive basalts from the region (Kuriles, Tolbachik, Kharchinsky) have higher CaO (> 9.9 wt%) and CaO/Al_2O_3 (> 0.60), and lower whole-rock Na_2O (< 2.7 wt%) and K_2O (< 1.1 wt%) at similar Mg# (0.66–0.70). Olivine phenocrysts in basalts have in general, higher CaO and Mn/Fe and lower Ni and Ni/Mg at Fo_{88} compared to the andesites.

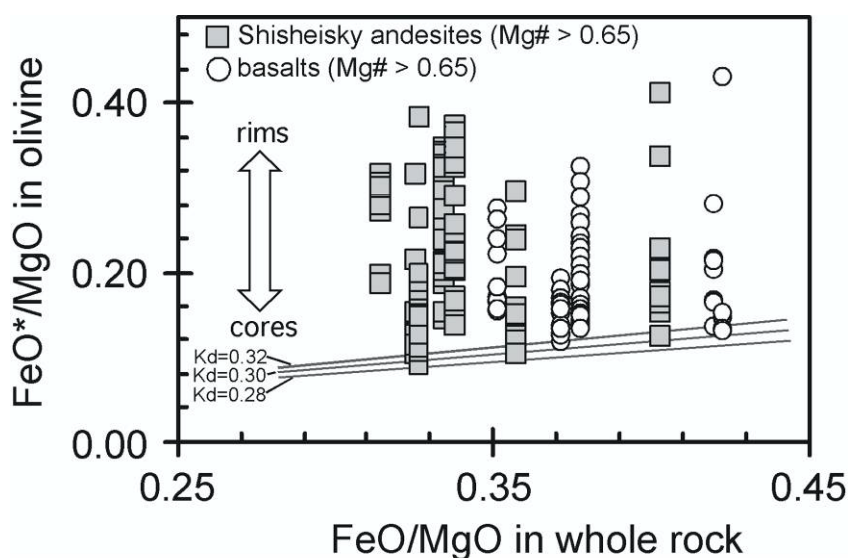


Fig. 1.1.2.2.1. Whole-rock and olivine FeO/MgO for primitive andesitic lavas of the Shisheysky Complex compared to primitive Kurile-Kamchatka basalts. Dashed lines are olivine and whole-rock compositions predicted to be at equilibrium based on Fe–Mg exchange coefficients (K_d 's) of 0.28 and 0.32 ($K_d = [FeO^*/MgO_{olivine}]/[FeO/MgO_{melt}]$) from Roeder and Emslie (1970)

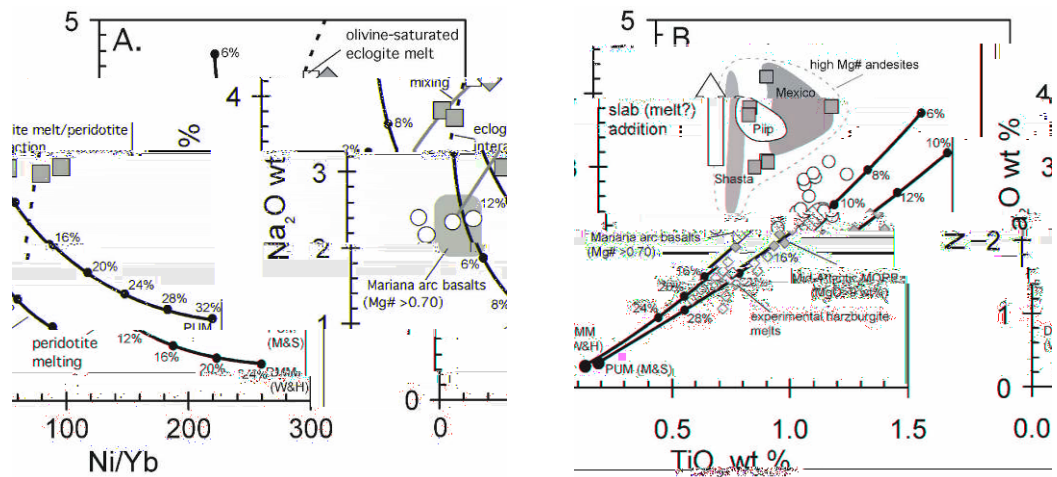


Fig. 1.1.2.2.2. Na_2O versus Ni/Yb and TiO_2 for Shisheisky Complex and Kurile-Kamchatka lavas compared to various models, natural samples and experimental compositions. Solid black lines with circles are peridotite batch melting models using the equations of Shaw (1970). Peridotite compositions are the primitive upper mantle (PUM— $\text{Na}_2\text{O} = 0.36$ wt%, $\text{TiO}_2 = 0.2$ wt%, $\text{NiO} = 0.25$ wt%, $\text{Yb} = 0.441$ ppm) from McDonough and Sun (1995) and the average depleted MORB mantle (DMM— $\text{Na}_2\text{O} = 0.28$ wt%, TiO_2 wt% = 0.13 wt%, $\text{NiO} = 0.24$ wt%, $\text{Yb} = 0.365$ ppm) from Workman and Hart (2005). Bulk distribution coefficients for Ti ($\text{DTi} = 0.04$) and Na ($\text{DNa} = 0.02$) are from Kelley et al. (2006). Bulk distribution coefficients for Ni ($\text{DNi} = 6.7$) and Yb ($\text{DYb} = 0.115$) are from Kelemen et al. (2003c). High Na at a given Ti for high-Mg# andesites from Piip (Yogodzinski et al. 1994), Shasta (Baker et al. 1994), Mexico (Blatter and Carmichael 1998), and the Shisheisky Complex (Table 1) clearly distinguish primitive andesitic compositions from experimentally produced melts of harzburgite (Falloon and Danyushevsky 2000), primitive Mariana arc basalts (Stern et al. 1990), and Atlantic MORB (Schilling et al. 1983). The solid gray line is a mixing model between olivine-saturated eclogite melt from Wang and Gaetani (2008) and a primitive basalt.

The absence of plagioclase phenocrysts from the primitive andesitic lavas contrasts the plagioclase-phyric basalts, indicating relatively high pre-eruptive water contents for the primitive andesitic magmas compared to basalts. Estimated temperature and water contents for primitive basaltic andesites and andesites are 984–1,143°C and 4–7 wt% H_2O . For primitive basalts they are 1,149–1,227°C and 2 wt% H_2O . Petrographic and mineral compositions suggest that the primitive andesitic lavas were liquids in equilibrium with mantle peridotite (Fig. 1.1.2.2.1) and were not produced by mixing between basalts and felsic crustal melts, contamination by xenocrystic olivine, or crystal fractionation of basalt. Key geochemical features of the Shisheisky primitive lavas (high Ni/MgO , Na_2O , Ni/Yb and $\text{Mg}\#$ at intermediate SiO_2) combined with the location of the volcanic field above the edge of the subducting Pacific Plate support a genetic model that involves melting of eclogite or pyroxenite at or near the surface of the subducting plate, followed by interaction of that melt with hotter peridotite in the over-lying mantle wedge. The strongly calc-alkaline igneous series at Shiveluch Volcano is interpreted to result from the emplacement and evolution of primitive andesitic magmas similar to those that are present in nearby monogenetic cones of the Shisheisky Complex (Fig. 1.1.2.2.2).

J.A. Bryant, G.M. Yogodzinski, T.G. Churikova, 2010. High Mg# Andesites of the Shisheisky Complex, Northern Kamchatka: Implications for Primitive Magmatism in Subduction Systems. Accepted to CMP.

1.1.2.3. Research on mantle xenoliths in Central Kamchatka Depression

Xenoliths from Shiveluch volcano (in cooperation with Department of Earth and Ocean Sciences, University of South Carolina, USA)

Ultramafic xenoliths of spinel dunite, harzburgite, lherzolite, amphibole/phlogopite-bearing pyroxenite, and clinopyroxenite occur in andesitic pyroclastic debris from the 1964 eruption of Shiveluch volcano, Kamchatka. Peridotites have coarse/protogranular, porphyroclastic, and granuloblastic textures (Fig. 1.1.2.3.1), abundant kink-banded olivine, and refractory mineral compositions with forsteritic olivine (Fo88–94) and Cr-rich spinel ($100 \cdot \text{Cr}/\text{Cr} + \text{Al} = 47\text{--}83$).

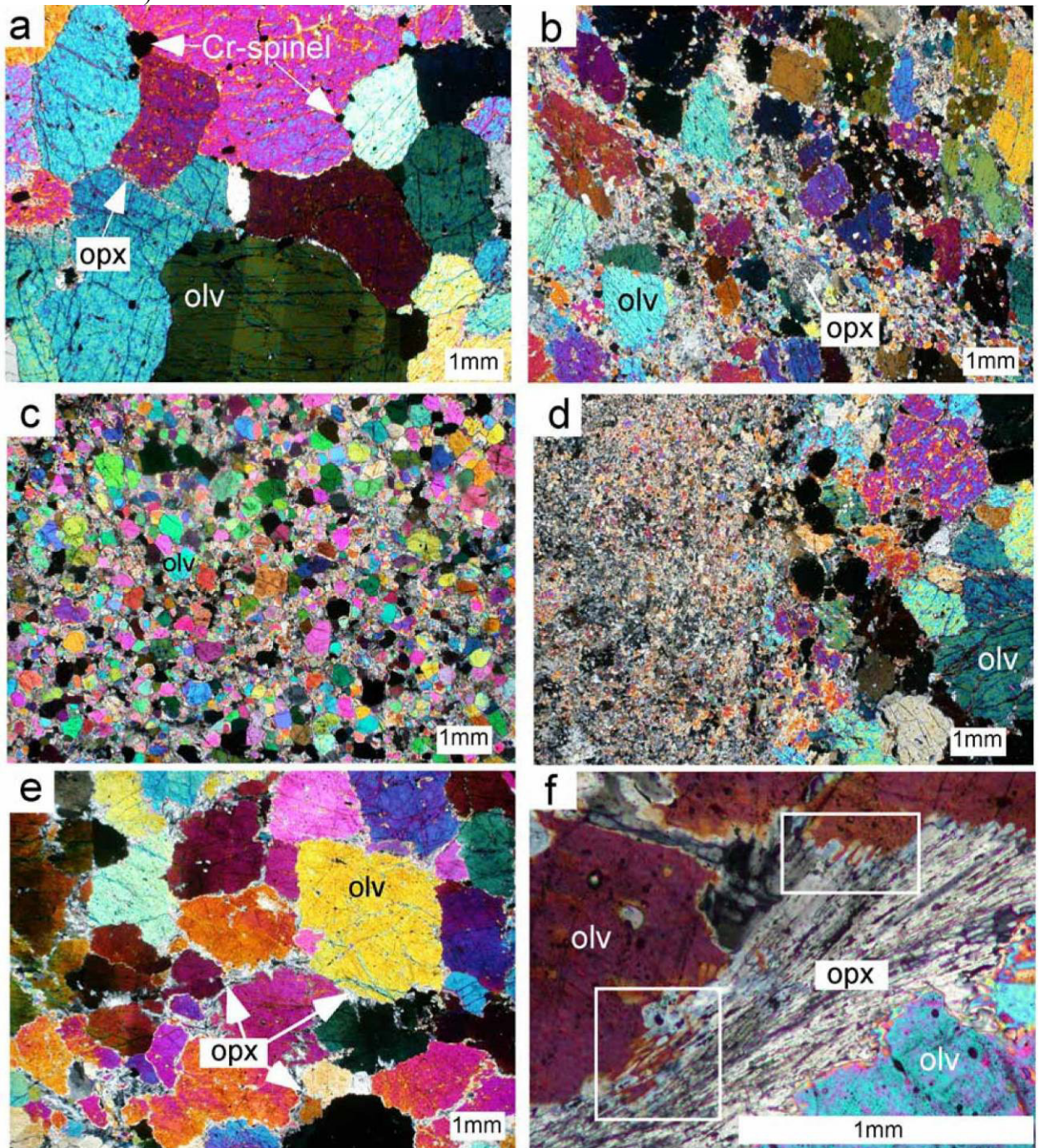


Fig. 1.1.2.3.1. Cross-polarized photomicrographs of Shiveluch xenoliths: (a) coarse dunite showing kink-banding in olivine, (b) porphyroclastic harzburgite, (c) granuloblastic harzburgite, (d) spinel lherzolite

showing a sharp contact between fine-grained and coarse-grained textures, (e) coarse harzburgite showing the growth of opx along olivine grain boundaries, and (f) fibrous opx adjacent to coarse olivine grains. Note the jagged and interpenetrating contact between fibrous opx and coarse olivine (white boxes), interpreted to indicate that opx was produced by replacement of olivine.

Orthopyroxene (opx) is also Mg-rich but occurs only as a fibrous mineral present along olivine grain boundaries, in monomineralic veins that crosscut coarse olivine, and in veins with amphibole and phlogopite that crosscut coarse-grained peridotites. Textural evidence and mineral compositions indicate that the peridotites and hydrous pyroxenites were replacement dunites that formed by melt-rock reactions involving the dissolution of pyroxene and precipitation of olivine. The fibrous opx and millimeter-scale veins of phlogopite, amphibole, and opx are interpreted as the autometasomatic products of hydrous magmas that were trapped in the uppermost mantle (<45 km). In this interpretation, opx was produced by reaction between late-stage, silica-rich, hydrous fluids/melts and olivine in the dunite protolith, and the millimeter-scale veins of phlogopite, amphibole, and opx are the volatile-enriched, deuteritic products that were liberated during the final stages of magma crystallization. The absence of textural equilibrium suggests that the late-stage replacement process which produced the fibrous opx occurred shortly prior to the eruption that carried the xenoliths to the surface. On the basis of two-pyroxene thermometry and Ca-in-olivine barometry, the xenoliths equilibrated between 800 and 1000°C and 1.03 and 2.21 GPa (Fig. 1.1.2.3.2). This implies that the xenoliths were carried from sub-Moho depths, a result consistent with geophysical estimates of crustal thickness. Olivine-opx-spinel equilibria indicate that the xenoliths are strongly oxidized with fO_2 from +1.4–2.6 log units above the fayalite-magnetite-quartz (DFMQ) buffer in peridotites, +1.7–2.3 DFMQ in hydrous pyroxenites, and +2.4–3.3 DFMQ in cumulate clinopyroxenites (Fig. 1.1.2.3.3). High fO_2 in the peridotites is attributed to the melt-rock reactions that formed the dunite protolith. These results therefore suggest that interaction between oxidized melts and peridotite wall rock at shallow mantle depths plays a significant role in creating and modifying the uppermost mantle and deepest crust in some subduction settings.

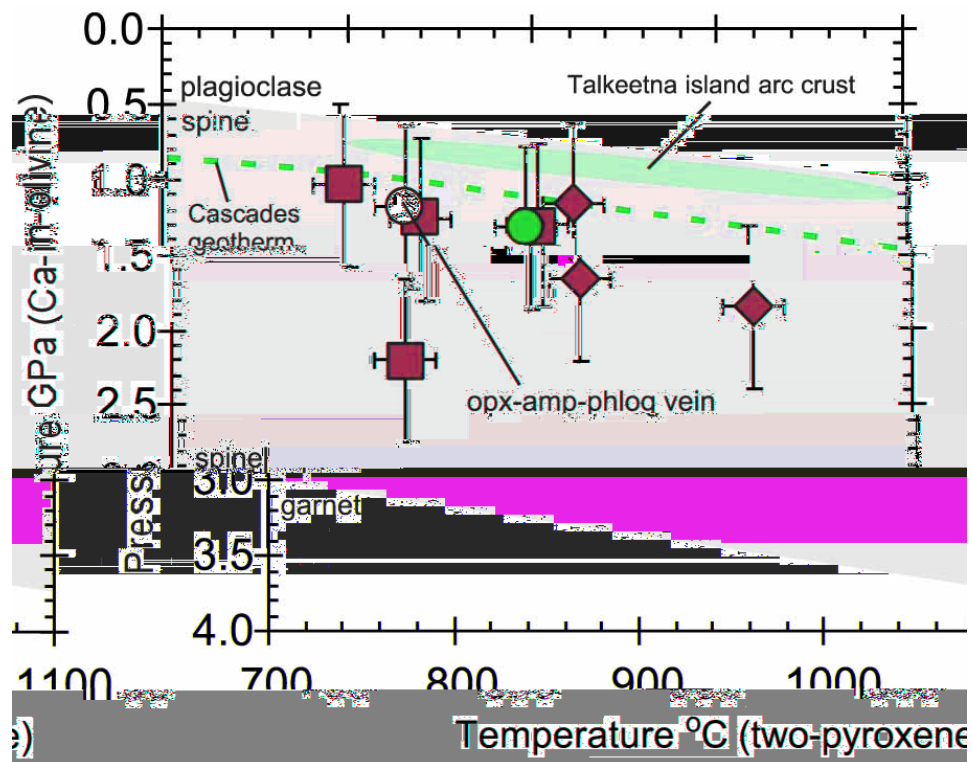


Fig. 1.1.2.3.2. Equilibration P-T estimates for Shiveluch xenoliths using two-pyroxene thermometry [Brey and Köhler, 1990] and Ca-in-olivine barometry [Köhler and Brey, 1990]. Analytical techniques and errors are described in the text. The Fe^{2+} component, which was estimated assuming pyroxene stoichiometry [Droop, 1987], was used in the two-pyroxene temperature calculations. The plagioclase-spinel-garnet stability field is from Herzberg [1978] and O'Neill [1981]. The spinel-garnet transition is calculated for spinel with $\text{Cr}\# = 0.72$, which is the average of the eight xenoliths. Cascades geotherm is from the thermal model of van Keken et al. [2002], based on a crustal density of 2.6 g/cm^3 . Talkeetna arc crust is based on P-T estimates for garnet gabbros and gabbro-norites from Kelemen et al. [2003] and DeBarri and Coleman [1989]. Square – harzburgites; diamonds – lherzolites; circles – hydrous pyroxenites; triangles – clinopyroxenites.

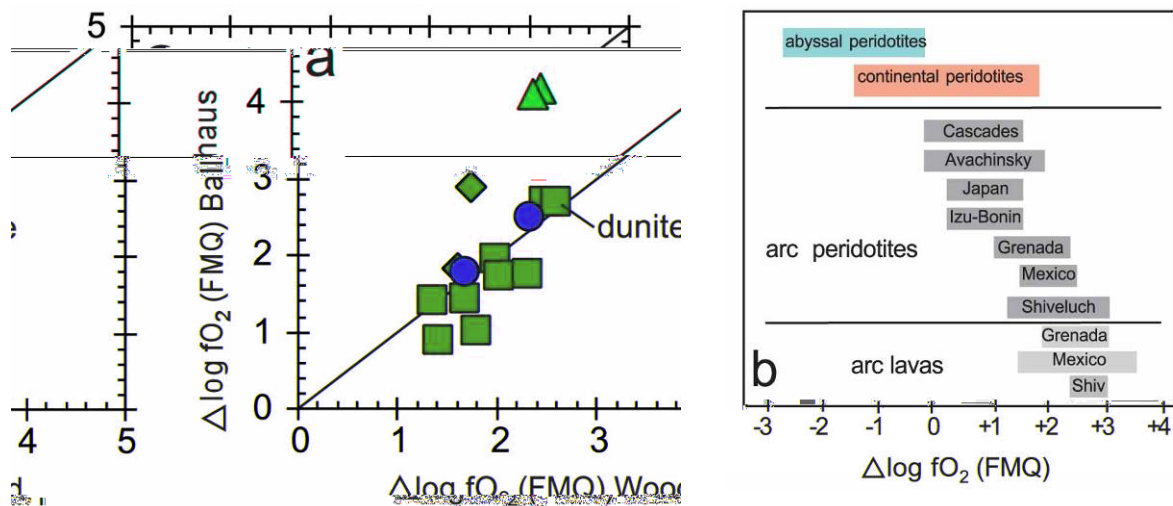


Fig. 1.1.2.3.3. Oxygen fugacity calculated for Shiveluch xenoliths compared to published data for peridotites and arc lavas. Estimates of $f\text{O}_2$ plotted in Figure 1.1.2.3.3a were made using the methods of Ballhaus et al. [1991] and Wood et al. [1990] and are plotted as log $f\text{O}_2$ units from the fayalite-magnetite-quartz buffer reaction. Symbols for Shiveluch xenoliths are as in Figure 1.1.2.3.2. Figure 1.1.2.3.3b shows the total range of $f\text{O}_2$ calculated from the Shiveluch xenoliths (bottom gray bar under “arc peridotites”) compared to published data from other peridotites and from arc lavas. Oxygen fugacities for other data sources are as follows: abyssal [Bryndzia and Wood, 1990], continental [Wood and Virgo, 1989], Cascades [Brandon and Draper, 1996], Avachinsky Volcano, Kamchatka [Arai et al., 2003], Japan [Wood and Virgo, 1989], Izu-Bonin-Mariana [Parkinson and Pearce, 1998], Grenada [Parkinson et al., 2003], Mexican hornblende-bearing peridotites and websterites [Blatter and Carmichael, 1998], Mexican hornblende andesites [Carmichael, 1991], and Shiveluch (Shiv) andesites [Humphreys et al., 2006].

Bryant J.A., Yogodzinski G.M., Churikova T.G. Melt-mantle interactions beneath the Kamchatka arc: Evidence from ultramafic xenoliths from Shiveluch volcano // *Geochemistry, Geophysics, Geosystems*. – 28 April 2007, vol. 8, no. 4. - P. 1-24. - Q04007. - doi: 10.1029/2006GC001443.

Xenoliths from Kharchinsky volcano (in cooperation with Department of Earth and Ocean Sciences, University of South Carolina, USA)

Abundant ultramafic xenoliths from Kharchinsky Volcano provide a rare opportunity to study the physical conditions and processes in the upper mantle and lower crust of the Kamchatka arc. Forty-five peridotite and pyroxenite xenoliths, which are representative of the 250 samples that were collected from an alkaline dike at the summit of the late Pleistocene volcano, have been studied petrographically and analyzed for their whole-rock major element and mineral compositions. Peridotite xenoliths are primarily harzburgites with protogranular textures and olivine and pyroxene compositions that are uniformly Mg-rich (Fo_{91-92} , CPX Mg-no. 0.94-0.96). Spinel compositions are Cr-rich, and several samples contain mm-scale and veins

of parasitic amphibole. Kink banding in olivine is common in the peridotites, consistent with deformation under mantle conditions. Silicate mineral compositions in the pyroxenites are more Fe-rich and more variable (FO76-o76-82, CPX Mg-no. 0.75-0.88) than in the peridotites. Oxide compositions are also relatively Fe-rich (magnetite, hercynitic spinel). Pyroxenites contain up to 50% hornblende, which occurs in mm-scale veins and as coarse poikilitic crystals. Texturally, the pyroxenites, which show mm-scale layering in some large samples, are generally more finely crystalline and less intensely deformed than the peridotites. Two-pyroxene thermometry (Brey & Köhler, 1990, *J. Petrology*) indicates that the peridotites, which we interpret as depleted upper mantle, equilibrated at temperatures that were 200-250°C hotter (1000-1050°C) than the pyroxenites (80-900°C), which we interpret as cumulates related to basalt fractionation near the crust-mantle boundary. The higher temperatures recorded peridotite xenoliths imply a somewhat greater depth of burial and equilibration compared to the pyroxenites. These results indicate higher temperatures at mocho depths beneath Kharchinsky Volcano, compared those inferred from studies of peridotite xenoliths at nearby Shiveluch Volcano (Bryant et al., 2007, G-Cubed). These differences may be related to different primitive melt genesis and evolution processes at these distinctively different volcanoes.

Mobley Reid, Dektor Christine, Yogodzinski Gene, Churikova Tatiana Mineralogy and Petrology of Ultramafic Xenoliths from Kharchinsky Volcano, Kamchatka // 2008 Joint Meeting of The Geological Society of America, Soil Science Society of America, American Society of Agronomy, Crop Science Society of America, Gulf Coast Association of Geological Societies with the Gulf Coast Section of SEPM. – http://gsa.confex.com/gsa/2008AM/finalprogram/abstract_150822.htm

1.1.2.4. Tolbachik volcano

New mineral at Tolbachik eruption 1875-1976

Krivovichev S.V., Filatov S.K., *Department of Crystallography, St. Petersburg State University, University Emb. 7/9, St. Petersburg 199034*

Vergasova L.P., Ananiev V.A., *Institute of Volcanology and Seismology FED RAS, Petropavlovsk-Kamchatski, Russia*

Britvin S.N., *Department of Mineral Deposits, St. Petersburg State University, University Emb. 7/9, St. Petersburg 199034*

Kahlenberg V., *Institut für Mineralogie und Petrographie, Leopold-Franzens-Universität Innsbruck, Innrain 52, A-6020 Innsbruck*

Pauflerite, β -VO(SO₄), is a new mineral species from the fumaroles of the Great Fissure Tolbachik eruption (GFTE), Kamchatka Peninsula, Russia. It was found in 1977 in the first cinder cone of the North breach of the GFTE. The mineral occurs as light green prismatic crystals up to 0.1 mm in length, associated with shcherbinaite (V₂O₅), an unknown Tl–Bi sulfate and finely crystalline Mg, Al, Fe and Na sulfates. Pauflerite is light green with a white streak and vitreous luster; the mineral is transparent and non-fluorescent. The Mohs hardness is 3–4. Pauflerite is brittle, and without visible cleavage. The density is 3.36(4) (measured) and 3.294 g/cm³ (calculated). The mineral is biaxial, optically positive, α 1.731(4), β 1.778(2), γ 1.845(4), with $2V_{\text{meas}} \approx 90^\circ$, and $2V_{\text{calc}}$ equal to 83° . The orientation was determined as $X = a$; further details are unclear. Pleochroism is clear in green tones: X light green, Y bluish green, Z light green-blue. A chemical analysis with an electron microprobe gave VO₂ 50.40, SO₃ 49.30, total 99.70 wt.%. The empirical formula, calculated on the basis of 5O, is V_{0.99}S_{1.01}O₅. The simplified formula is VO(SO₄). Pauflerite is orthorhombic, *Pnma*, a 7.3890(13), b 6.2740(11), c 7.0788(11) Å, V 328.16(10) Å³, $Z = 4$. The structure has been solved by direct methods and refined to R_1 of

0.034, calculated for the 457 unique observed reflections ($|F_o| > 4\sigma|F_o|$). The structure contains one symmetrically independent V^{4+} cation in distorted octahedral coordination to the O atoms (one vanadyl V^{4+} -O bond of 1.607 Å, four bonds of 1.992–1.996 Å, and one bond of 2.267 Å). One symmetrically independent S^{6+} cation is tetrahedrally coordinated by four O^{2-} anions with the mean $\langle S^{6+}$ -O \rangle bond length of 1.470 Å. The structure of pauflerite consists of a three-dimensional framework of distorted $V^{4+}O_6$ octahedra and SO_4 tetrahedra with a titanite-type topology. Pauflerite is a natural analog of β -VO(SO₄). The powder-diffraction pattern was not obtained because of the paucity of natural material. The calculated powder-diffraction pattern is in excellent agreement with that reported for the synthetic analogue (PDF 19–1400). The name chosen honors Peter Paufler, professor at the Technical University of Dresden in recognition of his important contributions to physical and structural crystallography and mineralogy.

Krivovichev S.V., Vergasova L.P., Britvin S.N., Filatov S.K., Kahlenberg V. and Ananiev V.A. Pauflerite, β -VO(SO₄), a new mineral species from the Tolbachik volcano, Kamchatka Peninsula, Russia // Canadian Mineralogist. Vol. 45. № 4. 2007. P. 921-927.

Morphometric and morphological development of Holocene cinder cones

Inbar M., *Department of Geography and Environmental Studies, University of Haifa, Israel*

Gilichinsky M., *Department of Forest Resource Management, SLU, Umea, Sweden*

Melekestsev I., Melnikov D., *Institute of Volcanology and Seismology, RAS, Petropavlovsk-Kamchatsky, Russia*

Zaretskaya N., *Geological Institute, RAS, Moscow, Russia*

The evolution of landscape over time is a central aspect of geological, paleogeographical and geomorphological studies. Volcanic features like cinder cones offer the opportunity to monitor the processes and development of the landscape. Cinder cones are perhaps the simplest and most common volcanic landforms in the world. Morphological and morphometric study of cinder cones has proven an efficient tool for determining their relative dates, and the erosional processes affecting them. The extensive Kamchatka volcanic province (Russian Far East), with its large Tolbachik cinder cone field, is an excellent case study for spatial and temporal classification and calibration of changes in morphometric values with time.

We show how the morphological and morphometric values of the monogenetic cinder cones, measured in the field and by digital elevation models, can be used to validate their age and erosional processes.

Field data were GPS measurements of cinder cones formed at the Tolbachik 1975–1976 eruption and of Holocene cinder cones; erosion processes on the cinder cones and lava flows were identified and evaluated. For every studied cinder cone morphometric parameters were assessed on the basis of remotely sensed data and digital elevation model. Morphometric measurements were taken of cone height and slope and average axis diameter and the height–width ratio was obtained.

The comparison of morphometric parameters calculated from ASTER DEM and topographic map clearly supports the concept of relative morphometric dating as the most recent cinder cones are always associated with the highest slopes and h/W ratio. The measured morphometric values of the recent Tolbachik cinder cones are valuable benchmark data for determining erosion rates, such as the measured values for the Paricutin cone in Mexico after the 1943 eruption. The variability of the morphometric values of the recent cinder cones is due to their lithological coarse composition. A comparison with the older cinder cones in the area shows that the climatic conditions of the Kamchatka peninsula and the slow development of

vegetation cover determine a high rate of erosion and rapid change in the morphometric values, as compared to published values for other volcanic fields.

Inbar M., Gilichinsky M., Melekestsev I., Melnikov D., Zaretskaya N. Morphometric and morphological development of Holocene cinder cones: a field and remote sensing study in the Tolbachik volcanic field, Kamchatka // Journal of Volcanology and Geothermal Research. 2010. doi: 10.1016/j.jvolgeores.2010.07.013;

Gilichinsky M., Melnikov D., Melekestsev I., Zaretskaya N., Inbar M. Morphometric measurements of cinder cones from digital elevation models of Tolbachik volcanic field, central Kamchatka // Can. J. Remote Sensing (in press).

1.1.2.5. Southern part of the Central Kamchatka Depression

Koloskov A.V., kolosav@kscnet.ru, **G.B. Flerov**, flerov@kscnet.ru, *Institute of Volcanology and Seismology FED RAS, Petropavlovsk-Kamchatski, Russia*

Kovalenko D.V., Dmitry@igem.ru, *Institute of Geology of Ore Deposits, Petrography Mineralogy and Geochemistry, Russian Academy of Science, Moscow, Russia*

A comparative study was done of the data on Late Cretaceous-Paleocene volcanism of four areas of Kamchatka: Prav. Tolbachik – Lev. Shchapina – Adrianovka rivers interfluvium (northern Tumrok Ridge), the area south of the Ipuin River - Mt Hrebtovaya (northern Valaginsky Ridge), the area of Mt Savulch (Kitilgina River upper reaches, northern Valaginsky Ridge), and: Kirganik – Lev. Kolpakova rivers interfluvium (Sredinnyy Ridge). New data on petrochemical, geochemical and isotopic composition of volcanic rocks from these areas are offered. The analysis of these materials together with the already published data on volcanics and also on plutonic rocks of close composition and age made it possible to establish the following: 1) the basaltoids under study are referred to the trachyandesite series with transition to the maymechite-picrite rock association, 2) in the rocks of the Valaginsky - Tumrok – Sredinnyy ridges alkali content increases with simultaneous increase in Rb concentration; the contents of highly charged and radioactive elements first drop and then grow. In the coordinates Ybn-Cen the presence of two trends is established: positive, which embraces the majority of volcanic and plutonic rocks; and negative, peculiar to the maymechite-picrite association. The former trend reflects rock evolution during crystallization differentiation; and the latter, a different degree of melting of initial substrate. Possible reconstructions of geodynamic conditions of volcanism manifestation are discussed.

Koloskov V.A., G.B. Flerov, D.V. Kovalenko. Late Cretaceous – Paleocene magmatic complexes of Central Kamchatka, magmatic sources, and geodynamic conditions of their formation. Tikhookeanskaya geologiya, 2009, V. 28, N 4, pp. 16–34

1.1.3. Volcanological research on the volcanoes of Kluchevskaya Group

1.1.3.1. Monitoring of active volcanoes

O. A. Girina, S. V. Ushakov, N. A. Malik, A. G. Manevich, D. V. Mel'nikov, A. A. Nuzhdaev, Yu. V. Demyanchuk, and L. V. Kotenko, *Institute of Volcanology and Seismology (IVS), FED, RAS, Petropavlovsk-Kamchatsky, Russia*

The comprehensive monitoring of active volcanoes in Kamchatka and North Kurils is carried out under the KVERT project in close cooperation with colleagues from the Institute of Volcanology and Seismology (IVS) of the Far East Division of the Russian Academy of

Sciences, the Kamchatka Branch of the Geophysical Survey (KBGS) of the RAS, and the Alaska Volcano Observatory (AVO), USA. The monitoring of volcanoes involves daily analysis of their seismic activity carried out by the KBGS, visual observations, both from field surveys close to volcanoes and by video cameras directed at the Klyuchevskoi, Shiveluch, and Bezmyannyi volcanoes (operated by the KBGS), and satellite information for recognition of thermal anomalies, ash ejection, ash and steam–gas plumes.

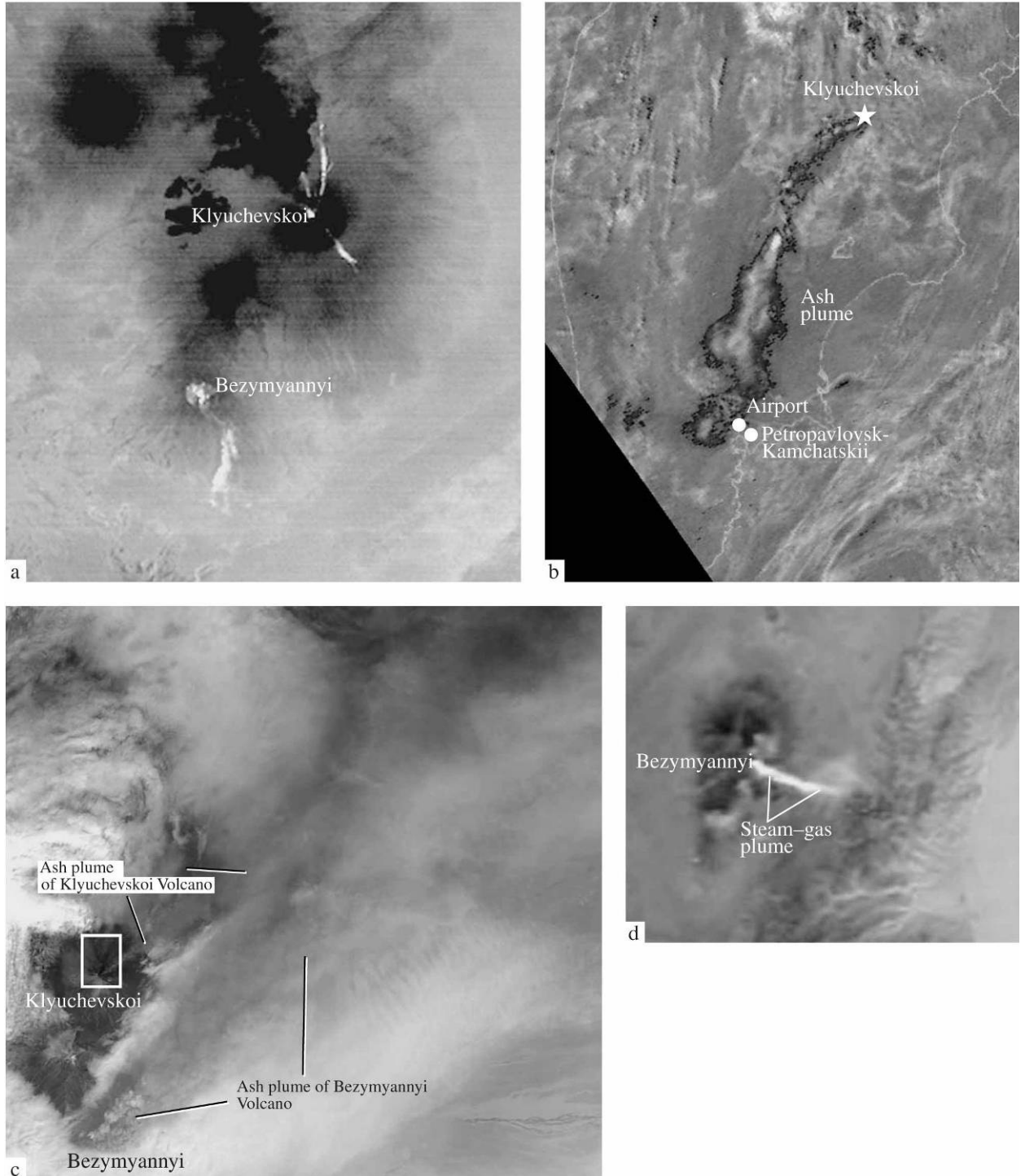


Fig. 1.1.3.1.1. Thermal anomalies in the area of Klyuchevskoi and Bezmyannyi volcanoes on an ASTER satellite image at 11:02 UTC on July 7, 2007 (a); ash plume from Klyuchevskoi Volcano in the areas of

Petropavlovsk-Kamchatskii and airport at 04:30 UTC on June 20, 2007 on an image NOAA-12, AVHRR (4m5), courtesy the AVO (USA) (b); the moment of simultaneous eruptions of Klyuchevskoi and Bezymyanni volcanoes on an ASTER VNIR satellite image at 00:38 UTC on May 12, 2007, courtesy M. Ramsey, USA (c); bright steam–gas plume from Bezymyanni Volcano at 23:59 UTC on November 9, 2007 on an image of TERRA MODIS, courtesy ROSGEOLFOND, MNR RF (d).

In 2007 six strong explosions of four Kamchatka volcanoes (Bezymyanni, Klyuchevskoi, Shiveluch, and Karymskii) and two of Chikurachki Volcano of North Kurils took place. In addition, an explosive event occurred on Mutnovskii Volcano, and higher fumaroles activity was observed on Avacha and Gorelyi volcanoes in Kamchatka as well as on Ebeko Volcano, Paramushir I., North Kurils.

The Northern Group of Volcanoes was the most active in 2007. Explosive–effusive eruption of Klyuchevskoi Volcano was unusual: three lava flows poured onto different volcano slopes at the same time; during strong explosions ash clouds rose up to 12 km ASL; ash plumes stretched for 5400 km and more in all directions from the volcano; eruption continued for about 5 months. Three explosive eruptions of the Merapi type took place at the Bezymyanni Volcano: two of them were related to juvenile matter supply, and one, with the collapse of the frontal parts of lava flows, originated during the eruptions of 1989–2001; eruptive columns rose to 10 km ASL, and ash plumes extended to the southeast and east of the volcano. At the Shiveluch Volcano continued explosive eruption, and almost uninterrupted squeezing of juvenile material were accompanied by rare powerful explosive events, when ash rose up to 12 km ASL, ash plumes stretched primarily to the southeast and east of the volcano. On Karymskii Volcano moderate explosive eruption was occurring with ash ejection up to 5 km ASL for almost the entire year; ash plumes propagated primarily to the southeast and east of the volcano. Satellite monitoring of Kamchatka and North Kuril volcanoes allowed KVERT staff to detect and observe an explosive event (probable a phreatic explosion) on Mutnovskii Volcano and two explosive eruptions of the Chikurachki Volcano (Paramushir Island). Owing to the close cooperation of KVERT project colleagues, the Elizovo Airport Meteorological Center, and the volcanic ash advisory centers in Tokyo, Anchorage, and Washington (Tokyo VAAC, Anchorage VAAC, and Washington VAAC), all necessary precautions were taken for flight safety near Kamchatka and no fatal accidents related to the explosive activity of these volcanoes took place.

Girina O. A., S. V. Ushakov, N. A. Malik, A. G. Manevich, D. V. Mel'nikov, A. A. Nuzhdaev, Yu. V. Demyanchuk, and L. V. Kotenko. The Active Volcanoes of Kamchatka and Paramushir Island, North Kurils in 2007. Journal of Volcanology and Seismology, 2009, Vol. 3, No. 1, pp. 1–17.

1.1.3.2. Bezimianny volcano

Olga Girina and Yurii V. Demyanchuk, yuridem@emsd.iks.ru, *Institute of Volcanology and Seismology (IVS), FED, RAS, Petropavlovsk-Kamchatsky, Russia*

Adam J. Carter, Michael S. Ramsey, *Department of Geology and Planetary Science, University of Pittsburgh, Pittsburgh, PA 15260, USA*

An explosive eruption occurred at Bezimianny Volcano (Kamchatka Peninsula, Russia) on 24 December 2006 at 09:17 (UTC). Seismicity increased three weeks prior to the large eruption, which produced a 12–15 km above sea level (ASL) ash column. We present field observations from 27 December 2006 and 2 March 2007, combined with satellite data collected from 8 October 2006 to 11 April 2007 by the Advanced Spaceborne Thermal Emission and Reflection Radiometer (ASTER), as part of the instrument's rapid-response program to volcanic eruptions. Pixel-integrated brightness temperatures were calculated from both ASTER

90 m/pixel thermal infrared (TIR) data as well as 30 m/pixel short-wave infrared (SWIR) data. Four days prior to the eruption, the maximum TIR temperature was 45 °C above the average background temperature (– 33 °C) at the dome, which we interpret was a precursory signal, and had dropped to 8 °C above background by 18 March 2007. On 20 December 2006, there was also a clear thermal signal in the SWIR data of 128 °C using ASTER Band 7 (2.26 µm). The maximum SWIR temperature was 181 °C on the lava dome on 4 January 2007, decreasing below the detection limit of the SWIR data by 11 April 2007. On 4 January 2007 a hot linear feature was observed at the dome in the SWIR data, which produced a maximum temperature of 700 °C for the hot fraction of the pixel using the dual band technique. This suggests that magmatic temperatures were present at the dome at this time, consistent with the emplacement of a new lava lobe following the eruption. The eruption also produced a large, 6.5 km long by up to 425 m wide pyroclastic flow (PF) deposit that was channelled into a valley to the south–southeast. The PF deposit cooled over the following three months but remained elevated above the average background temperature. A second field investigation in March 2007 revealed a still-warm PF deposit that contained fumaroles. It was also observed that the upper dome morphology had changed in the past year, with a new lava lobe having in-filled the crater that formed following the 9 May 2006 eruption. These data provide further information on effusive and explosive activity at Bezymianny using quantitative remote sensing data and reinforced by field observations to assist in pre-eruption detection as well as post-eruption monitoring.

Adam J. Carter, Olga A. Girina, Michael S. Ramsey, and Yurii V. Demyanchuk, ASTER and field observations of the 24 December 2006 eruption of Bezymianny Volcano, Russia // Remote Sensing of Environment. 112. 2008. pp. 2569–2577.

1.1.3.3. Shiveluch volcano

Shiveluch volcano – one of most active volcanoes of Kamchatka. Sheveluch is one of the biggest volcanic structures in Kamchatka. The volcano includes three main units: Stary Sheveluch, the old caldera and active apparatus Molodoy Sheveluch. Moderate potential hazards are caused by ash plumes, ash falls, pyroclastic flows, hot avalanches and lahars. The volcano constitutes a potential hazard to international and local airlines at Kamchatka because its eruptive clouds can rise to a height of 3-20 km ASL and extend for hundreds of kilometers from the volcano. Active monitoring on this volcano is organized the clock round by Institute of Volcanology and Seismology of Far East Division of Russian Academy of Sciences. These observations are includes seismic, visual, satellite monitoring and web video camera. A lot of researches are elaborated during 2006-2010 on this volcano in Russia. We present just small part of it.

Zharinov N. A., Yu. V. Demyanchuk, Institute of Volcanology and Seismology (IVS), FED, RAS, Petropavlovsk-Kamchatsky, Russia

Observations in 1980–2007 of an intracrater extrusive dome growing on Shiveluch Volcano are collected. Information is provided on the main phases in the generation of the lava dome. The rate of growth and discharge of erupted lava are shown to vary over time. The 1980–1981 discharge was very low during the initial phase in the generation of the lava dome, not above 0.1–0.2 million cubic meters per day. When the extrusion began to grow again, the highest discharge of ejecta was recorded in 1993, as much as 1.25 million cubic meters per day. The maximum rates of growth and discharge of ejecta are generally observed during the first few

months of extrusion generation following the resumption of the eruptive process. Powerful explosive eruptions that accompany the extrusive process provoke an acceleration of dome growth. The periods of explosive eruptions had discharges three orders of magnitude greater than those during the most productive extrusive periods. This nonuniformity in extrusion generation reflects nonuniformities in magma supply, and also indicates the existence of a shallow magma chamber at depths of 4–6 km.

Zharinov N. A. and Yu. V. Demyanchuk. *The Growth of an Extrusive Dome on Shiveluch Volcano, Kamchatka in 1980–2007: Geodetic Observations and Video Surveys. Journal of Volcanology and Seismology*, 2008, Vol. 2, No. 4, pp. 217–227.

Olga Girina, girina@kscnet.ru, **Ushakov S.V.**, ushakov@kscnet.ru and **Yurii V. Demyanchuk**, yuridem@emsd.iks.ru, *Institute of Volcanology and Seismology (IVS), FED, RAS, Petropavlovsk-Kamchatsky, Russia*

Using the field work observations on 2004 eruption of Young Shiveluch volcano, as well as satellite, seismic and visual data, the sequence of events before and during this paroxysmal eruption was shown. Geological effect and all volcanic products were described. The volume of pyroclastic material, which was deposited on the Earth surface during volcano eruption 9th of May 2004, including deposits of the pyroclastic flows, waves and tephra, was evaluated as 0.06 km³

Girina O.A., Ushakov S.V., Yurii V. Demyanchuk. *Paroxysmal eruption of the Young Shiveluch volcano, Kamchatka, May 9 2004 // Vestnik KRAUNC. Nauki o Zemle*, 2007, N 2, issue 10, pp. 65-73 (in Russian).

Ponomareva V., *Institute of Volcanology and Seismology FED RAS, Petropavlovsk-Kamchatski, Russia*

Philip Kyle, Melanie Hartman, *Department of Earth and Environmental Science, New Mexico Institute of Mining and Technology, Socorro, New Mexico, USA*

Maria Pevzner, Leopold Sulerzhitsky, *Geological Institute, Moscow, Russia*

The Holocene eruptive history of Shiveluch volcano (Fig. 1.1.3.3.1), Kamchatka Peninsula, has been reconstructed using geologic mapping, tephrochronology, radiocarbon dating, XRF and microprobe analyses. Eruptions of Shiveluch during the Holocene have occurred with irregular repose times alternating between periods of explosive activity and dome growth. The most intense volcanism, with frequent large and moderate eruptions occurred around 6500–6400 BC, 2250–2000 BC, and 50–650

AD, coincides with the all-Kamchatka peaks of volcanic activity. The current active period started around 900 BC; since then the large and moderate eruptions has been following each other in 50–400 yrs-long intervals. This persistent strong activity can be matched only by the early Holocene one.

Most Shiveluch eruptions during the Holocene produced medium-K, hornblende-bearing andesitic material characterized by high MgO (2.3–6.8 wt %), Cr (47–520 ppm), Ni (18–106 ppm) and Sr (471–615 ppm), and low Y (<18 ppm). Only two mafic tephra erupted about 6500 and 2000 BC, each within the period of most intense activity.

Many past eruptions from Shiveluch were larger and far more hazardous than the historical ones. The largest Holocene eruption occurred ~1050 AD and yielded >2.5 km³ of tephra. More than 10 debris avalanches took place only in the second half of the Holocene.

Extent of Shiveluch tephra falls exceeded 350 km; travel distance of pyroclastic density currents was >22 km, and that of the debris avalanches ≤20 km.

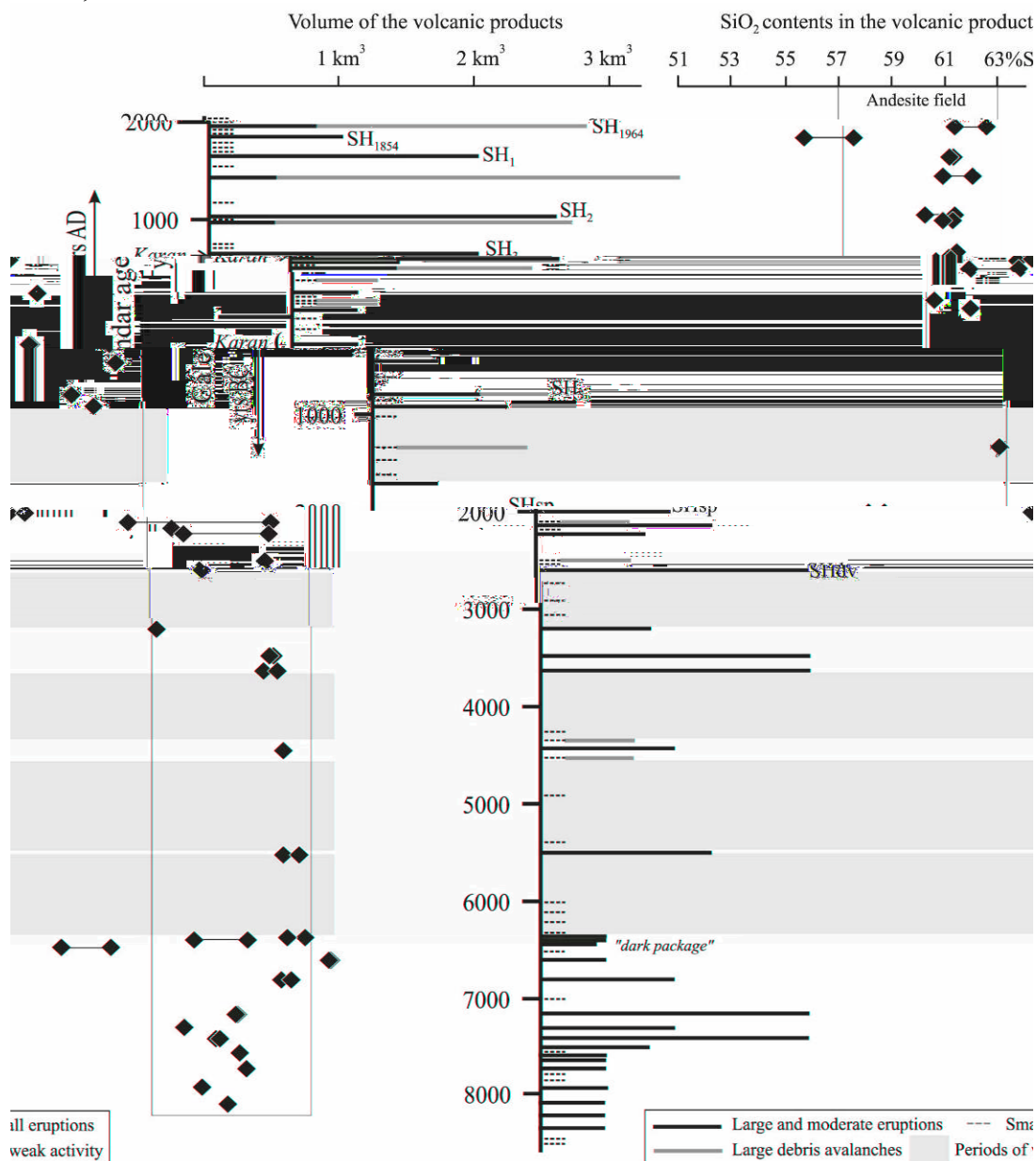


Fig. 1.1.3.3.1. Volumes of eruptive products and the Holocene eruptive history of Shiveluch volcano. Ages are in calendar years AD or BC. Codes of the eruptions are given in [Ponomareva et al., 2007]. Periods of Karan domes activity are shown to the left of the age axis. The SiO₂ contents of the erupted products show most eruptions were andesitic (the range in analyses for the same eruption are shown by tie lines). The figure is based on the data from “Table 3” and “Table 4” (available on the CD-ROM accompanying [Ponomareva et al., 2007]).

Vera Ponomareva, Philip Kyle, Maria Pevzner, Leopold Sulerzhitsky, Melanie Hartman. *Holocene Eruptive History of Shiveluch Volcano, Kamchatka Peninsula, Russia. Volcanism and subduction: the Kamchatka region* / Eichelberger John, Gordeev Evgenii, Kasahara Minoru, Izbekov Pavel, Lees Jonathan (editors). – *Geophysical Monograph Series, vol. 172*. – Washington, DC: American Geophysical Union, 2007. – P. 263-282.

Tatiana Churikova, tchurikova@mail.ru *Institute of Volcanology and Seismology FED RAS, Petropavlovsk-Kamchatski, Russia*
Gordeychik B., gordei@mail.ru *Institute of Physics of Earth, Russian Academy of Sciences, Moscow, 123995, Russia.*

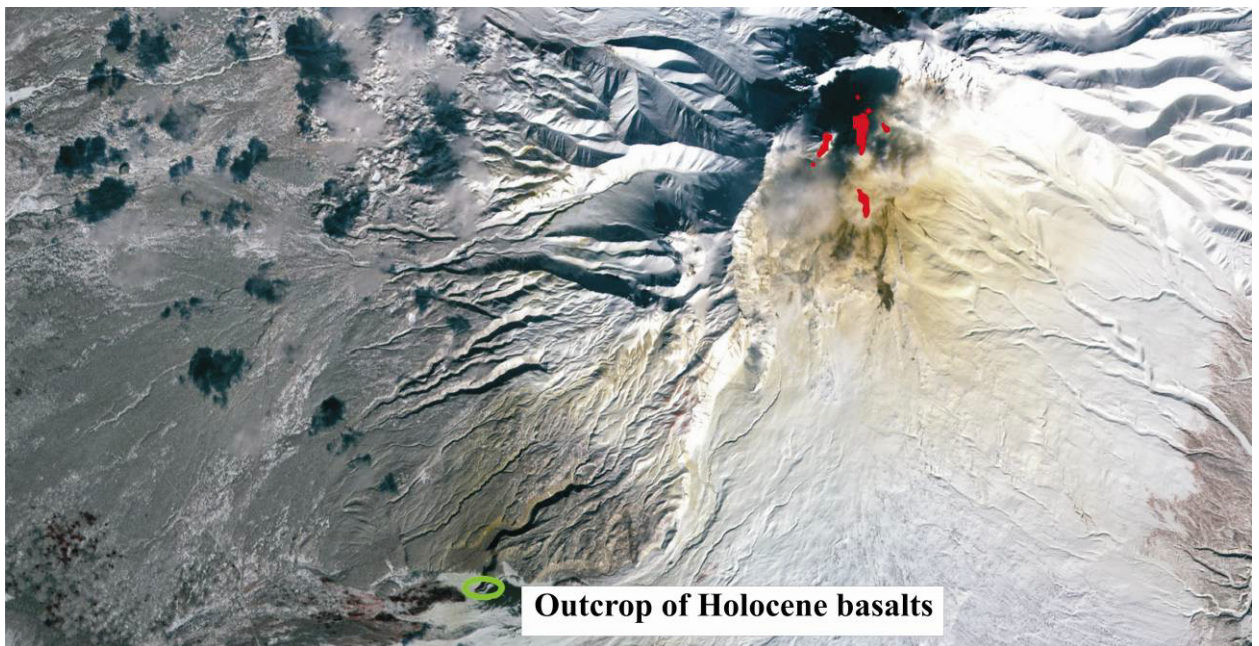


Fig. 1.1.3.3.2. The location of olivine basalts of age 7600 y.a. at Shiveluch volcano. Red – active Young Shiveluch dome.

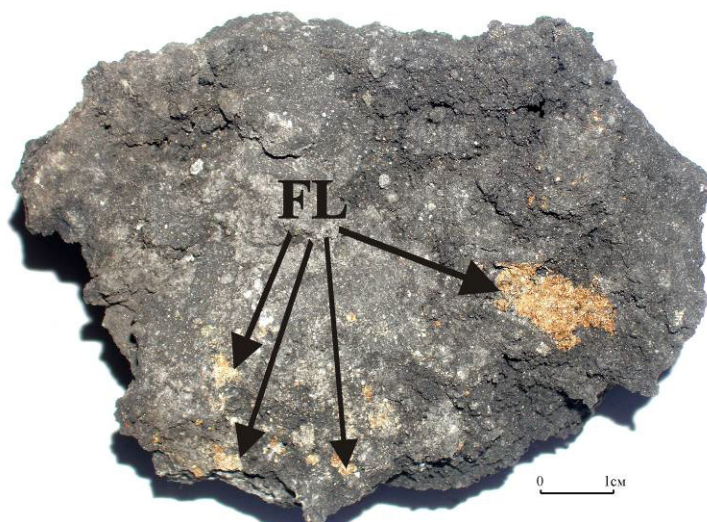


Fig. 1.1.3.3.3. Agregates of mica in olivine basalt from Shiveluch volcano.

Shiveluch volcano erupts in Holocene mainly high-Mg andesites [Yogodzinsky et al., 2001; Ponomareva et al., 2007]. It was known from previous studies only two basaltic eruptions during Holocene. Both of them were represented only by tephra layers in soil-pyroclastic sections of all sectors of the basement of Shiveluch volcano. Their age was determined as 3600 14C and 7600 14C [Ponomareva et al., 2007]. However, the natural outcrops of bath basalt eruptions were not known up to present time.

Due to strong pyroclastic eruption of Shiveluch volcano in 2005, Baydarnaya river changed its channel and opened the new narrow canyon in SW side of volcano (Fig. 1.1.3.3.2). In 2008 in new canyon the package of basalt-basaltic andesite pyroclastic with thickness about 50 meters was found. The size of basaltic bombs reach up to 2 m, which suggests the very close eruption centrum. The rocks are black weakly-foamed basalts with large (up to 1-1,5 sm) olivine grains. The distinctive feature of these rocks are fine-grained aggregates of mica in the pores (Fig. 1.1.3.3.3). Major- and trace elements as well as trace element ratios (Rb/Sr, Ba/Sr, Sr/Y) are similar with previously studied thephra of age 7600 y.a. The same age was confirmed by thephrakhronological studies in 2010.

Churikova T.G., Gordeychik B.N., Belousov A.B., Babnskiy A.D. Discovery of the centrum of the basaltic eruption at Shiveluch volcano // Gordeev E.I. (eds.) Materials to All-Russian conference to 75 anniversary of the Kamchatka volcanological station. Petropavlovsk-Kamchatsky, Institute of Volcanology and Seismology FED RAS, 2010 (in Russian).

Vera Ponomareva, Philip Kyle, Maria Pevzner, Leopold Sulerzhitsky, Melanie Hartman. Holocene Eruptive History of Shiveluch Volcano, Kamchatka Peninsula, Russia. Volcanism and subduction: the Kamchatka region / Eichelberger John, Gordeev Evgenii, Kasahara Minoru, Izbekov Pavel, Lees Jonathan (editors). – Geophysical Monograph Series, vol. 172. – Washington, DC: American Geophysical Union, 2007. – P. 263-282.

1.1.3.4. *Klyuchevskoy volcano*

Geochemistry and geophysics

Khubunaya S. A., L. I. Gontovaya, *Institute of Volcanology and Seismology, Far East Division, Russian Academy of Sciences, Petropavlovsk-Kamchatskii, 683006 Russia*

Sobolev A. V., *Institute of Geochemistry and Analytic Chemistry, Russian Academy of Sciences, Moscow, 111991 Russia*

Nizkous I. V., *Data Services Subsection, Data Consulting and Services Section, Schlumberger Logelco Inc., Moscow, 109147 Russia*

A 3D velocity model of the Earth's crust beneath the Klyuchevskoy volcanic group has been constructed using the seismic tomography method (Fig. 1.1.3.4.1). Anomalies of the velocity parameters related to the zones of magma supply to active volcanoes have been distinguished. Petrological data on the composition, temperature, and pressure of generation and crystallization of parental melts of Klyuchevskoy volcano magnesian basalts have been obtained. The parental melt corresponds to picrite (MgO = 13–14 wt %) with an ultimate saturation of SiO₂ (49–50 wt %), a high H₂O content (2.2–2.9%), and incompatible elements (Sr, Rb, Ba). This melt is formed at pressures of 15–20 kbar and temperatures of 1280–1320°C. Its further crystallization proceeds in intermediate magma chambers at two discrete pressure levels (i.e., greater than 6, and 1–2 kbar). The results of the petrological studies are in good agreement with the seismotomographic model.

The above assessments of the conditions of generation of high-magnesia melts from the Klyuchevskoy Volcano make it possible to generally represent the 3D model of formation of magnesian basalts based on the petrological and geophysical data.

The first level corresponds to the depth of melt separation from the melt residue (40–60 km) at a temperature of 1280–1320°C. Here, picritic melts can form and move along the system of fissures toward the site of fractionation in the intermediate magma chambers. This conclusion is in adequate agreement with the calculations of the asthenospheric depth and comparison of the theoretical and experimental velocity (V_p) models [Gontovaya and Gordienko, 2006; Nizkous, 2005]. This conclusion also does not contradict other previous studies. Many long-period

earthquakes are generated at depths of 20–40 km beneath Klyuchevskoy Volcano. Such events at the crust–mantle boundary are also registered at other volcanoes located worldwide. The origin of these events is related to the intrusion of a magma melt from a mantle diapir into the Earth’s crust [e.g. Gorel’ chik and Storcheus, 2001]. We should note that the existence of the magma source prior to the separation of this source from the mantle residue, at depths below those indicated above, suggests systematic repeated equilibrium between the melt and the mantle residue; therefore, the composition of this melt is unknown.

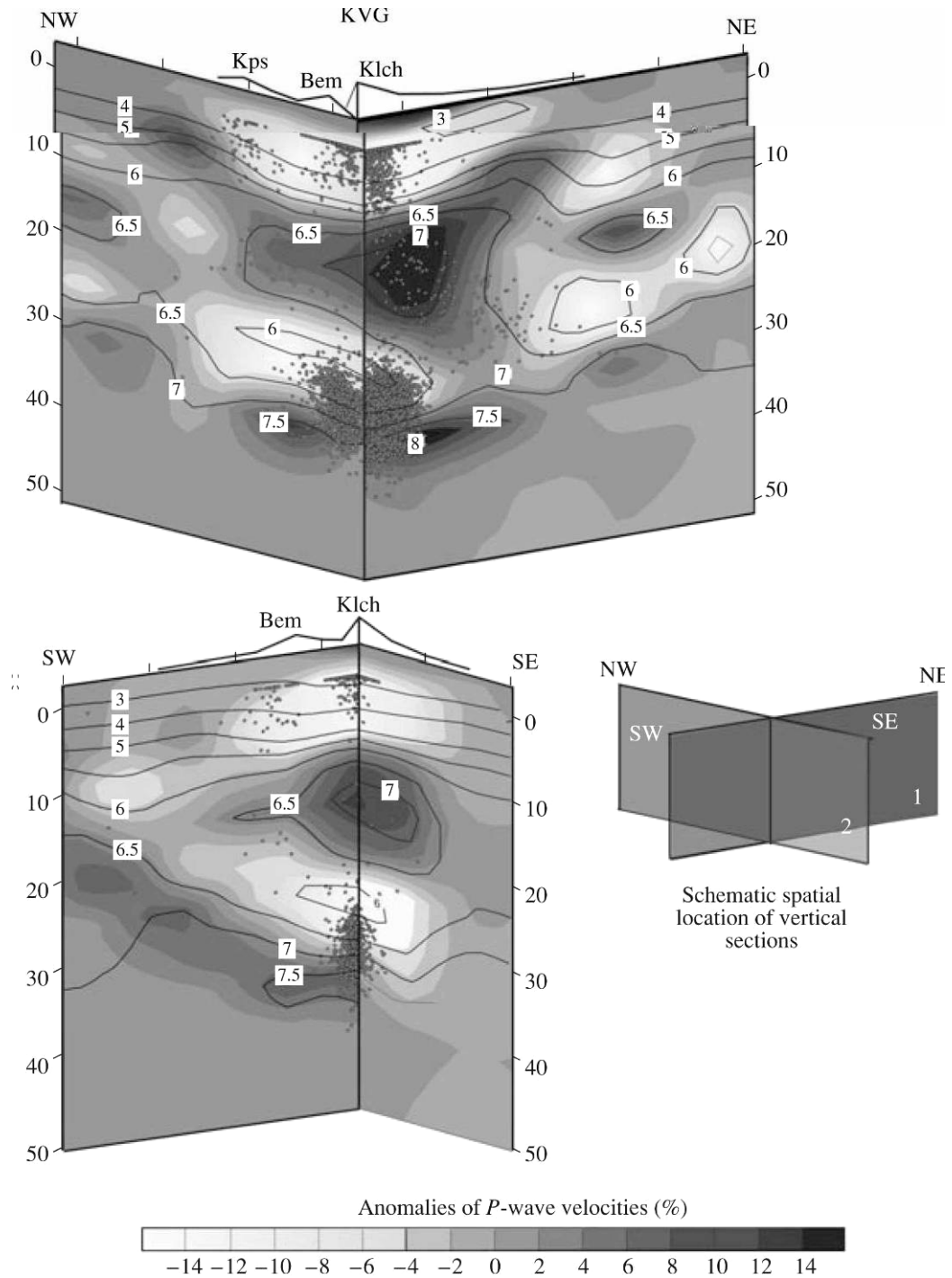


Fig. 1.1.3.4.1. A 3D image of the velocity model of the Earth’s crust beneath KVG. The sections present the contour lines of the absolute values of the V_p velocity (km/s, solid lines) and the projections of earthquake hypocenters onto these sections (circles).

The second level, through which magnesian basalts are formed and which is registered based on fluid microinclusions in olivines, corresponds to a minimal pressure of 5–6 kbar and a depth of more than 18–20 km at a maximal temperature of 1280°C (taking the 2.9% of water in the melt into account). Stable intermediate chambers, where picritic magmas crystallized and fractionated, are apparently generated here. Taking the errors of the method into account, this depth is in good agreement with the 25–30 km depths, where the method of seismic tomography makes it possible to reliably register low-velocity Vp and Vs anomalies and increased values of the Vp/Vs parameter, which are most likely related to a magma chamber. The results of other geophysical methods and theoretical calculations also indicate that a dynamically related system of magma chambers could exist in this layer.

A high-velocity discontinuity was reliably distinguished at a depth of 10–20 km beneath the Klyuchevskoy Volcano in the middle part of the Earth's crust (anomalies of the Vp and Vs velocities reach 10% in this region). This anomaly is most probably related to an ancient crystallized intermediate chamber, which supplied the Ushkovskii and Krestovskii volcanoes 40–50 ka ago. The presence of a high-velocity discontinuity is evidently an insurmountable obstacle for a direct magma duct from the mantle to the Klyuchevskoy crater. We should note that the methods of seismic tomography also made it possible to distinguish high-velocity zones, which are interpreted as large intrusions of crystallized ultrabasic–basic magmas, in the Earth's crust beneath other volcanoes located worldwide.

In addition to calc–alkaline magnesian basalts, calc–alkaline high-alumina basalts and andesites magnesian melts also erupt within the Klyuchevskoy volcanic group. According to modern petrological studies their occurrence is also related to a mantle supply and the further fractionation of magnesian melts [Al'meev, 2006; Mironov et al., 2001]. The genesis and conditions of generation of these igneous rocks are outside the limits of this publication. However, these eruptions stimulate researchers to study the spatial location of intermediate magma chambers, where magnesian and high-alumina magmas could fractionate, leading to the occurrence of andesite melts. These chambers could be located on both sides of the crystallized intrusion at depths of 10–20 km, where increased values of the Vp/Vs parameter were obtained from the data of seismic tomography.

The third level, where magnesian magmas can crystallize and fractionate, corresponds to low pressures, apparently, within several kilobars. This level can only be assessed indirectly based on the absence of a high-density fluid in the augite of magnesian basalts. Low crystallization pressures of augites are also confirmed by the ability of the augite-hosted melt inclusion to homogenize. Associations of high-pressure phenocrysts mix with low-pressure crystallization products in these shallow chambers. Boris Ivanovich Piip substantiated the existence of intermediate chambers at the same depth (5–7 km) beneath the northeastern flank of Klyuchevskoy Volcano based on xenoliths of Tertiary rocks from bocche. Velocity anomalies are confined to the same depth. The calculations in [Mironov et al., 2001] indicate that shallow-depth crystallization of clinopyroxenes in high-alumina magmas occurs beneath the northeastern flank of Klyuchevskoy Volcano. All these conclusions do not contradict the above seismotomographic model. For example, increased values of the Vp/Vs parameter are confined to the Earth's crust depths of 5–10 km. Anomalies of this parameters are most likely related to the presence of shallow-depth magma chambers. Differentiated magnesian and high-alumina magmas, which have provoked lateral eruptions of magnesian and high-alumina basalts on the northeastern flank of the Klyuchevskoy Volcano, could have come from this region during the entire Holocene.

- Khubunaya S. A., L. I. Gontovaya, A. V. Sobolev, I. V. Nizkous. *Magma Chambers beneath the Klyuchevskoy Volcanic Group (Kamchatka)*. *Journal of Volcanology and Seismology*, 2007, Vol. 1, No. 2, pp. 98–118.
- Gontovaya, D.I. and Gordienko, V.V., *Deep Processes and Geological Models of the Mantle within Eastern Kamchatka and the Kronotskii Bay*, in *Geologiya i poleznye iskopaemye Mirovogo okeana (Geology and Minerals of the World Ocean)*, Kiev: NANU, 2006, issue 2, pp. 107–121.
- Nizkous, I.V., *Tomographic Reconstruction of the Kamchatka Region with a High Spatial Resolution*, *Cand. Sc. (Geol.–Min.) Dissertation*, Moscow, 2005.
- Gorel' chik, V.I. and Storcheus, A.V., *Deep Long-Period Earthquakes beneath Klyuchevskoy Volcano, Kamchatka*, in *Geodinamika i vulkanizm Kurilo-Kamchatskoi ostrovoduzhnoi sistemy (Geodynamics and Volcanism of the Kurils–Kamchatka Island-Arc System)*, Petropavlovsk-Kamchatskii, 2001, pp. 173–189.
- Al' meev, R.R., *Geochemistry of Bezmyannyi Volcano Magmatism: Mantle Source Indications and Conditions of Initial Magma Fractionation*, *Cand. Sc. (Geol.–Min.) Dissertation*, Moscow: 2006.
- Mironov, N.L., Portnyagin, M.V., Plechov, P.Yu., and Khubunaya, S.A., *Final Stages of Evolution in Klyuchevskoy Volcano, Kamchatka: Evidence from Melt Inclusions in Minerals of High-Alumina Basalts*, *Petrologiya*, 2001, vol. 9, no. 1, pp. 51–69 [*Petrology (Engl. Transl.)*, 2001, vol. 9, no. 1, pp. 46–62].

Senyukov S. L., ssl@emsd.ru, S. Ya. Droznina, I. N. Nuzhdina, V. T. Garbuzova, and T. Yu. Kozhevnikova, *Kamchatka Branch, Geophysical Service of the Russian Academy of Sciences, Petropavlovsk-Kamchatskii, 683006 Russia*

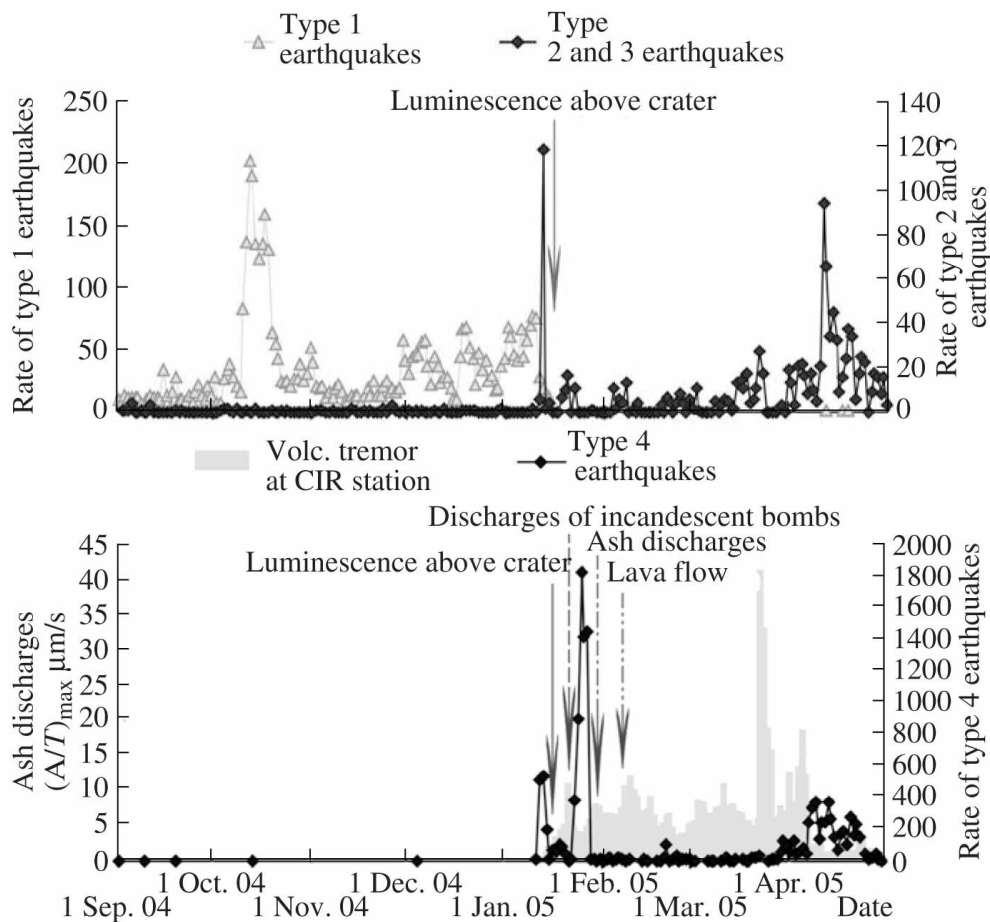


Fig. 1.1.3.4.2. Seismicity in the Klyuchevskoi area before, during, and after the 2005 eruption. The earthquake types are after Tokarev' s classification [Tokarev, 1981].

The Kamchatka Branch of the Geophysical Service (KB GS) of the Russian Academy of Sciences (RAS) has been observing the activity of Kamchatka volcanoes since 2000 in near real time using three methods: (1) seismicity monitoring (2) visual and video observations, and (3) satellite monitoring of thermal anomalies and ash discharges. The joint use of these data provides objective information on the state of the volcanoes from which to predict possible eruptions. During the period of time investigated, which culminated in the eruptions of March 10, 2003 to February 27, 2004 and January 12, 2005 to April 28, 2005, two active periods of Klyuchevskoi Volcano were identified. The results from our study of the first of these periods helped define an approximate scenario for the activity of the volcano before a summit eruption. The use of this experience in combination with an analysis of the literature enabled us to produce a successful short-term forecast of the January 2005 eruption.

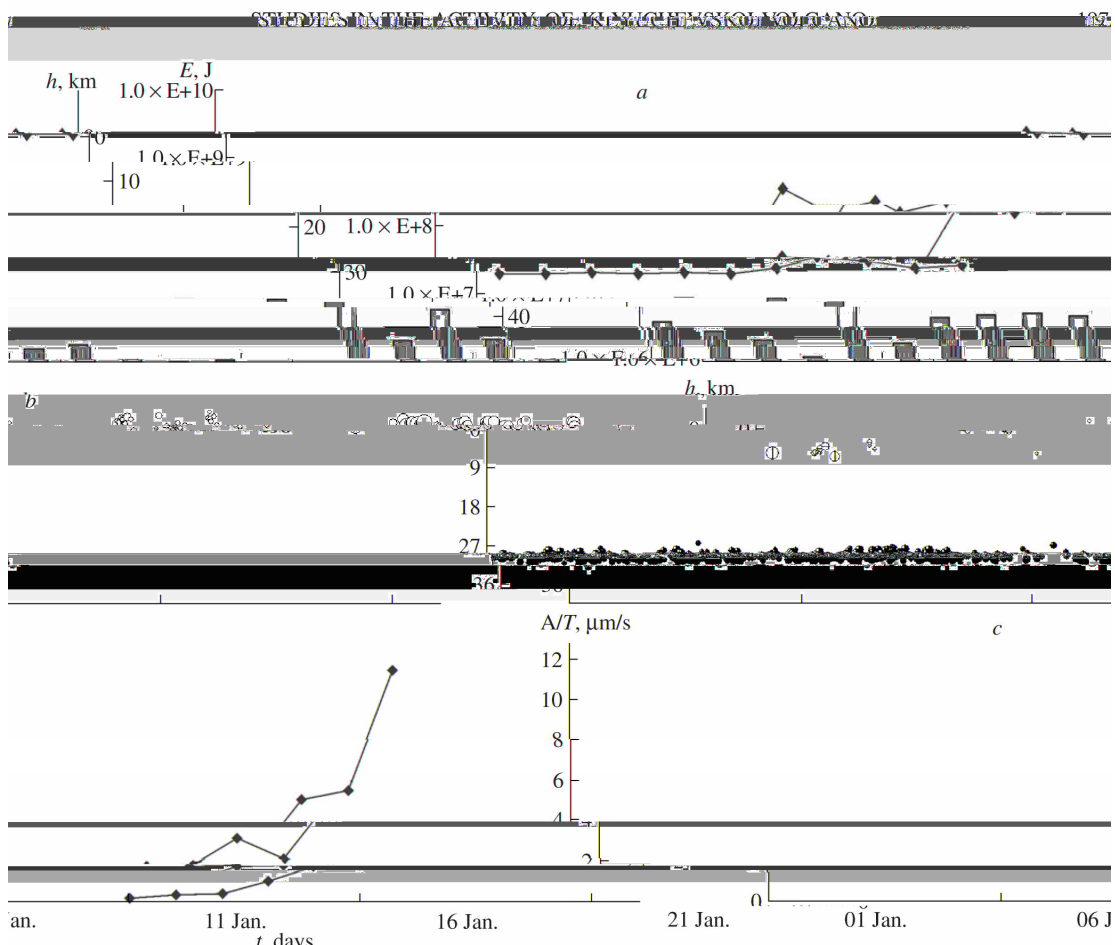


Fig. 1.1.3.4.3. Various seismicity parameters against time (from January 1 to 21, 2005) for Klyuchevskoi Volcano: (a) depth (km) and energy (J) of the center of released seismic energy, (b) depth of located hypocenters, km, (c) average amplitude of volcanic tremor at CIR, $\mu\text{m/s}$.

Two periods of activation that terminated in eruptions have been recorded on the volcano during the period of study:

(1) March 10, 2003 to February 27, 2004; the eruption started on March 21, 2003 with the first small discharges of ash rising as high as 200 m (the later discharges, which rose to 500 m, occurred on April 15, 2003, while the first thermal anomaly was recorded on May 15, 2003), the place of eruption was the central crater;

(2) January 12 to April 28, 2005; the eruption started on January 21 with the first ejection of incandescent bombs (ash discharges were first recorded on January 31, a lava flow was first observed visually on February 7, the flow propagated for a few kilometers), the place of eruption was the central crater.

During these periods the seismicity exceeded the “normal” (or “background”) level. A first definition of the “normal” seismicity was suggested from an analysis of accumulated data and those found in the literature. The practical use of the definition showed that it was suitable. For Klyuchevskoi Volcano the “normal” level is equal to no more than 50 earthquakes per day at a depth of about 30 km. The “normal” level for earthquakes in the depth range from the summit to 5 km is no more than 10 earthquakes with $K_S \geq 4.0$ or no more than 5 earthquakes with $K_S \geq 5.0$ or no more than 3 earthquakes with $K_S \geq 6.0$. For volcanic tremor the threshold of “normal” seismicity is given by the daily average of $1.0 \mu\text{m/s}$ at the CIR station.

In both cases the eruptions were preceded by swarms of deep-focus earthquakes (as many as 100 events per day at 30 km depth and the maximum class equal to 6.5). A swarm of deep-focus earthquakes before the first eruption was recorded February 13–15, 2003, that before the second eruption occurred during October 10–20, 2004.

In both cases the termination of visually observable volcanic activity was followed, first, by a gradual diminution in the rate of shallow earthquakes and afterward the instrumentally located hypocenters moved downward from sea level to a depth of about 30 km.

One can consider the seismicity that was recorded before, during, and after the early 2005 eruption in more detail as exhibiting the approximately typical scenario for the precursory period of a summit eruption on Klyuchevskoi (Fig. 1.1.3.4.2). Since mid-September 2004 earthquakes began to be recorded (at a daily rate of about 40 events) at a depth of about 30 km beneath the central crater. The rate was gradually increasing until 204 earthquakes were recorded during a single day (October 12), the highest number for this period. Subsequently, the rate decreased down to the background level. From November 29, 2004 to January 10, 2005 the daily rate of deeper earthquakes was gradually increasing to as many as 80 events. Figure 1.1.3.4.3 presents detailed data on the variation of several seismicity parameters for the period from January 1 to 21. Figure 1.1.3.4.3a shows the ascent of the center of released seismic energy from 30 km depth to 0 km and a concurrent decrease in energy release between January 12 and 18. The center of released seismic energy for a specified day was defined as an equivalent earthquake with the hypocentral coordinates equal to the mean 3D coordinates for the earthquakes located during the day. The energy of the equivalent event was found as the sum of energies of those earthquakes. The ascent of the center of released seismic energy can be explained by the occurrence of type 2 and 3 earthquakes (using P.I. Tokarev’s classification [Tokarev, 1981]) at depths of 0 to 7 km upon the background a decreasing seismicity rate at a depth of ~ 30 km. The central zone in the depth range 7 to 20 km remained aseismic; it was interpreted by Fedotov, Zharinov and Gorel’chik [Fedotov et al., 1988] as the trace of a heated, plastic zone around the central conduit. It appears that that zone is largely aseismic due to the high temperature and the plastic condition. From a depth of 7 km upward one notes a well-pronounced migration of hypocenters toward the summit at an ascent rate of the order of 1 km per day (Fig. 1.1.3.4.3b).

On January 12 the hypocenters reached the summit, the daily rate of type 2 and 3 earthquakes increased to reach 119; that of type 4 was as high as 500. The rate of deeper earthquakes became much lower. Since January 11 volcanic tremor began to be recorded with gradually increasing amplitude (Fig. 1.1.3.4.3c). It should be noted that earthquakes of class 4.5 or greater are clearly recorded upon the tremor background of amplitude below $1 \mu\text{m/s}$ at the CIR station. Consequently, the rapid diminution and subsequent disappearance of deeper earthquakes from January 9 to 13, 2005 can be regarded as a well-established fact. Earthquakes of

class 5 or greater above sea level were reliably located from January 14 to 21, but no deeper events of the same class occurred. During the period from January 22 to April 27, 2005 the identification of deep and shallow earthquakes was hampered by strong volcanic tremor.

Visual observations made by workers at the Klyuchi seismic station showed luminescence above the crater during the night hours, first appearing on January 16 (Fig. 1.1.3.4.2). Later the rate of volcanic type 4 earthquakes increased, the amplitude of volcanic tremor became greater, while the daily rate of type 2 and 3 earthquakes decreased down to 10–15, or else no such events were recorded at all. On January 21 the first discharges of incandescent bombs were recorded flying to heights of about 50–100 m above the crater, which can be viewed as the beginning of an explosive eruption. The first ash discharges were recorded by visual observation on January 31 following a dramatic increase in the rate of shallow volcanic events. On February 7, a lava flow was seen on the western flank of the volcano upon the background of a gradually increasing tremor amplitude.

After that, Klyuchevskoi erupted for two months, discharging a lava flow a few kilometers in length and hurling ash to as high as 4 km above the crater. On April 8 the tremor level dropped to 2.2 $\mu\text{m/s}$ at the CIR station and it became possible to identify type 2 and 3 earthquakes (about 100 events per day), as well as type 4 earthquakes. Discrete earthquakes occurring at 30 km depth began to be recorded on April 11. The seismicity was gradually decreasing during two weeks and at last reached the “background” level on April 29. A thermal anomaly around the Klyuchevskoi central crater was first detected on a satellite image (NOAA16) at 16:47 January 15. Subsequently the anomaly was recorded during the entire period of activity, unless the volcano was covered by clouds. The anomaly was the largest, about 50 pixels, on March 10–11. Visual and video observations made at that time showed discharges of incandescent material flying as high as 1000 m; ash was ejected to heights of 3200 m above the crater and a lava flow was observed on the volcano’s west flank.

The time, location, and size of a possible eruption on Klyuchevskoi were predicted during the 2005 activation based on the acquired experience of observing the 2003–2004 eruption and with an analysis of the literature. The forecast was reported to the Kamchatka Branch of the Russian Expert Council on Earthquake Prediction for Seismic Hazard and Risk Assessment by workers at the Laboratory of Seismic and Volcanic Activity Studies (SVAS, S.L. Senyukov, V.T. Garbuzova, S.Ya. Droznina, I.N. Nuzhdina, and T.Yu. Kozhevnikova) on January 17, 2005. The predicted parameters included:

The start of a possible eruption (probability 70%) was to be during the nearest month, from January 17 to February 17, 2005;

The size of eruption was predicted to be an explosive eruption from the central crater with ash discharged as high as 10 km above sea level with possible effusion of a lava flow several kilometers long;

The duration of eruption was predicted as a few days to a few months;

Ashfalls (a few millimeters) were expected at nearby population centers (Klyuchi, Kozyrevsk, Ust’ -Kamchatsk), depending on wind direction.

We wish to explain our forecast using widely accepted volcanological terms. The handbook of V.I. Vlodayets gives the following definition of an “eruption” [Vlodayets, 1984]:

“Eruption of a volcano is the process bringing to the surface incandescent or hot, solid, liquid and gaseous volcanic products. It may occur as a series of explosions or solely as effusion of lava, or as a gas explosion ejecting plastic and solid material” . We will employ the analogy with earthquake prediction where prediction concerns, not all possible earthquakes, but rather those posing a hazard, i.e., those having magnitudes of ≥ 6 . We also try to forecast, not eruption in the wide acceptance of that term, but only such hazardous and characteristic (for Klyuchevskoi Volcano in this case) volcanic phenomena, such as explosive eruption and

effusion of lava onto the volcano's flanks. We remember that [Vlodavets, 1984]: "Explosive eruption is (1) eruption proceeding by explosions, which is characterized by explosions and ejection of ash and coarser clastic products, or (2) eruption of a volcano resulting from an explosion of magmatic gases. It is accompanied by the ejection of large masses of older lava and host rock by the volcano's vent, followed by discharges of newer fresh unconsolidated products (ash, bombs, and blocks)." According to V.I. Vlodavets' definition, both the steam and gas activity of a volcano and crater luminescence are kinds of eruption in the wide sense, but we do not consider such phenomena hazardous and do not predict them. Such cases may more suitably be treated using the term "prediction of activation" instead of "prediction of eruption."

Senyukov S. L., S. Ya. Droznina, I. N. Nuzhdina, V. T. Garbuzova, and T. Yu. Kozhevnikova, Studies in the Activity of Klyuchevskoi Volcano by Remote Sensing Techniques between January 1, 2001 and July 31, 2005. Journal of Volcanology and Seismology, 2009, Vol. 3, No. 3, pp. 191–199.

Tokarev, P.I., Vulkanicheskie zemletryaseniya Kamchatki (Volcanic Earthquakes of Kamchatka), Moscow: Nauka, 1981.

Fedotov, S.A., Zharinov, N.A., and Gorel' chik, V.I., Deformation and Earthquakes on Klyuchevskoi Volcano, a Model of Its Activity, Vulkanol. Seismol., 1988, no. 2, pp. 3–42.

Vlodavets, V.I., Spravochnik po vulkanologii (Handbook of Volcanology), Moscow: Nauka, 1984.

Periodicity of eruptions

Ivanov V.V., *Institute of Volcanology and Seismology FED RAS, Petropavlovsk-Kamchatski, Russia*

The peculiarities of the 2008 activity of the giant basaltic Kluchevskoy volcano were studied using for the first time suggested formalized criteria. This criteria allows us to distinguish different activity phases: 1) the volcano is characterizes by long-drawn activity periods up to 1-2 years, which are separated by the periods of relative repose; 2) each activity includes three phases: preparation, eruption and relaxation; 3) to the 2008 inside the ongoing activity period it was happened three eruptions: in 2003, 2005 and 2007. Using data of seriated volcano activity during 70 years it was possible to make the successful medium-term prediction of the start time of the new top volcano eruption, which started September 30th 2008.

Ivanov V.V. Ongoing cycle of activity of the Kluchevskoy volcano 1995-2008 years: development using seismic, photo-, video- and visual data// Abstracts to the annual Conference to Volcanology day March 27-29 2008, Petropavlovsk-Kamchatskiy, Institute of Volcanology and Seismology FED RAS, pp. 100-109

1.1.3.5. Ushkovsky volcano

Murav'ev Ya. D., murjd@kscnet.ru, **A. A. Ovsyannikov**, *Institute of Volcanology and Seismology FED RAS, Petropavlovsk-Kamchatski, Russia*

Shiraiwa T., *Institute of Low Temperature Research, Sapporo, 060-0819 Japan*

Long-term investigations in the Ushkovsky Volcano caldera were completed in June 1998 using deep drilling of the crater glacier filling the Gorshkov summit cone. A 212-m ice core containing 354 bands of volcanic ash was obtained. The possibility of using an analysis of these data in paleovolcanic reconstructions of the northern volcano group is discussed.

Our studies of the ice core from the Ushkovsky volcano crater significantly improve our understanding of the chronology and power of the Kamchatka volcano eruptions (especially for the active volcanoes of the northern group). Data on glacial accumulation for the last 50 years, marking ash layers, and mathematical modeling of the crater glacier dynamics [Salamatin et al., 2001], allows us to estimate the age of the ice layers at the borehole bottom at 600 ± 50 years. It is known that no powerful or moderate eruptions of the Ushkovsky volcano summit craters occurred during the period.

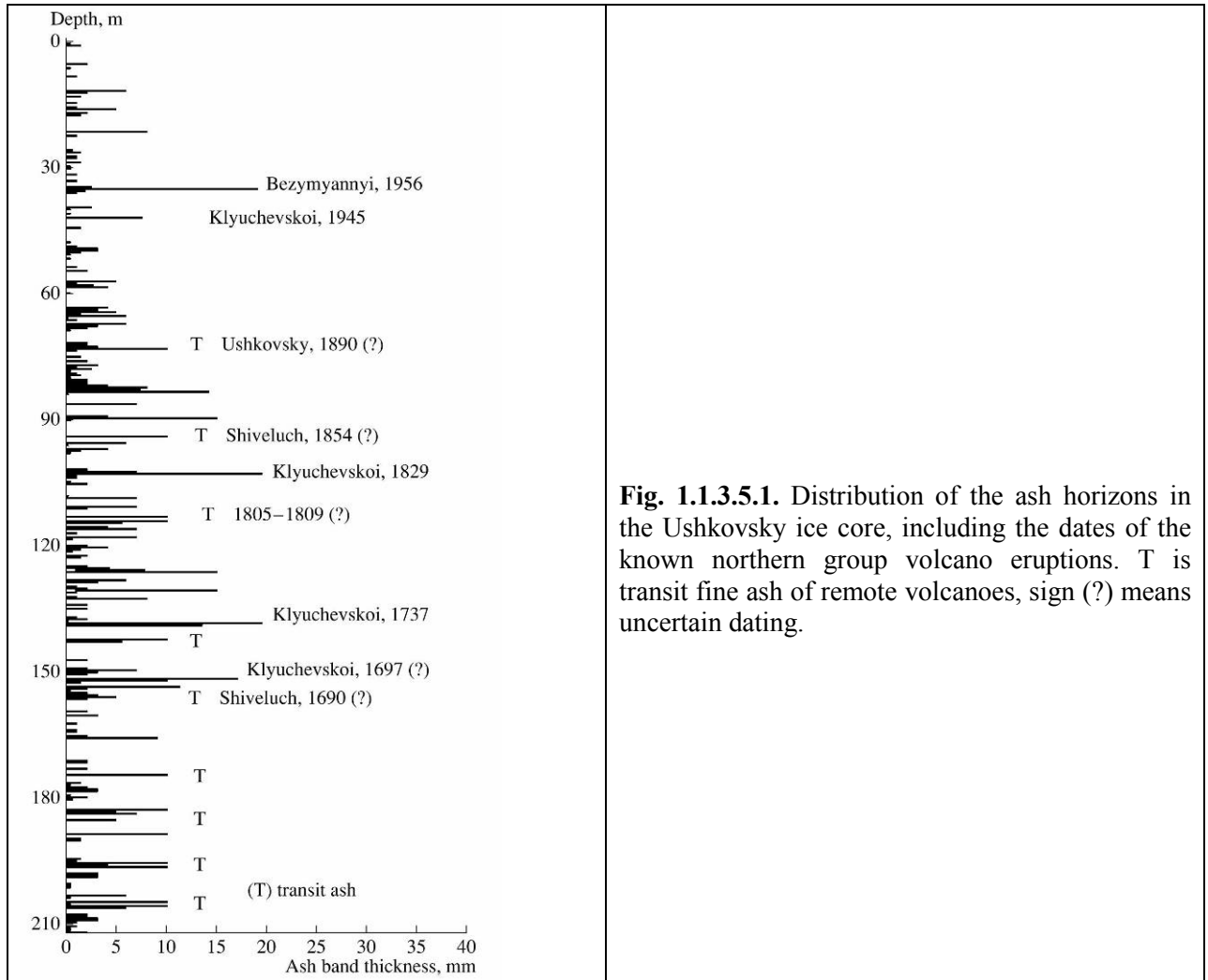


Fig. 1.1.3.5.1. Distribution of the ash horizons in the Ushkovsky ice core, including the dates of the known northern group volcano eruptions. T is transit fine ash of remote volcanoes, sign (?) means uncertain dating.

Ash from 180 volcanic eruptions (Fig. 1.1.3.5.1) is recognized in the core for the past centuries, including 49, 38, and 25–30 eruptions in the 20th, 19th, and 16–18th centuries, respectively. From this it follows that the activity of the northern group volcanoes was higher in the 20th century than in the past 500 years by a factor of 1.5. However, we should note that almost all powerful eruptions (mainly of the Klyuchevskoi volcano) occurred in the 18–19th centuries (ten of 13 events), while not more than one event occurred during each of the other centuries.

This analysis was performed only using observed ash horizons. It is clear that more precise geochemical and isotopic techniques will substantially increase the information value of the ice core. This is especially important for the Shiveluch volcano, which is the farthest volcano from the drilling site.

On the whole, we note that the Gorshkov crater glacier on the Ushkovsky volcano is not only a paleoclimatic archive for the northern Pacific sector of the Earth but can also be used to construct the 600-year chronology of volcanic activity in the region. Some Kamchatka volcano eruptions for this period will most likely be dated using acid and sulfate signals in ice cores from the Alaska Peninsula where volcanic activity is not so intense.

Murav'ev Ya. D., A. A. Ovsyannikov, T. Shiraiwa. Activity of the Northern Volcano Group According to Drilling Data in the Ushkovsky Crater Glacier, Kamchatka. Journal of Volcanology and Seismology, 2007, Vol. 1, No. 1, pp. 42–52.

Salamatin, A.N., Shiraiwa, T., Muravyev, Y.D., et al., Dynamics and Borehole Temperature Memory of Gorshkov Ice Cap on the Summit of Ushkovsky Volcano, Kamchatka Peninsula, Proc. Int. Symposium Atmosphere–Ocean–Cryosphere Interaction in the Sea of Okhotsk, Sapporo, 2001, pp. 120–121

1.2. Regional study of the Kamchatka arc in 2007-2010

The Kamchatka Peninsula, forming the northern part of the Kurile-Kamchatka volcanic arc, is located in the northwest Pacific Ocean and represent one of the most volcanically active regions on Earth. More than 200 Quaternary volcanoes, including 32 active ones, have been identified on Kamchatka. Interest for this area is caused by in particular large magma production rate, abundance of Recent to historical eruptions and rather mafic lava composition.

The Kamchatka Peninsula, forming the northern part of the Kurile-Kamchatka volcanic arc, is located at the NE convergent boundary of the Eurasian and Pacific plates, which is presently subducted at the rate of ~9 cm/a (Geist and Scholl, 1994). With it, the 65 Ma old Emperor Seamount chain is also subducted below Kamchatka. Active volcanism continues southwards to the Kurile Island arc. The termination of volcanic activity to the N at Shiveluch volcano is related to the Aleutian-Kamchatka triple-junction (Yogodzinski et al., 2001).

1.2.1. Geochemical variations across the Kamchatka arc

(in collaboration with GZG Abteilung Geochemie, Universität Göttingen)

Tatiana Churikova, tchurikova@mail.ru. Institute of Volcanology and Seismology FED RAS, Petropavlovsk-Kamchatski, Russia

Gerhard Wörner, gwoerner@gwdg.de. GZG Abteilung Geochemie, Universität Göttingen, Germany

Münker Carsten, muenker@nwz.uni-muenster.de. Zentrallabor für Geochronologie (ZLG), Institut für Mineralogie, Corrensstr. 24, Universität Münster, Münster D-48149, Germany

Mironov Nikita, nikita_mir@rambler.ru. Vernadsky Institute of Geochemistry and Analytical Chemistry, Kosygin Str, 19, 117975 Moscow, Russia

Kronz Andreas, akronz@gwdg.de. GZG Abteilung Geochemie, Universität Göttingen, Germany

1.2.1.1. Previous results on major-, trace and high field strength elements

Arc volcanism on Kamchatka comprises from E to W three zones parallel to the subduction trench (Fig. 1.2.1.1.1): (1) the Eastern Volcanic Front (EVF), 2) the Central Kamchatka Depression with the large Kluchevskaya Group (CKD) and three more northern volcanoes (NCKD) and (3) Sredinny Ridge (SR) of the back arc. The slab depth increases from 90-110 km below the EVF to 180-200 km below CKD and to 300-400 km below SR (Gorbatov, 1997). Mafic samples (> 5% MgO) of Upper Pleistocene and Holocene age were sampled along

the 220 km E-W traverse from stratovolcanoes and monogenetic cones in three volcanically active zones (Fig. 1.2.1.1.1).

Rocks are medium to high K-calkalkaline and have typical but variable arc-like trace element signatures. Systematic geochemical variations in major and trace elements from the volcanic front to the back arc exist (Fig. 1.2.1.1.2a) : K and most incompatible trace elements, i.e. HFSE, LILE, LREE, and certain element ratios (K/Na, La/Yb, Ce/Yb, Sr/Y, Nb/Yb) increase with slab depth from the arc front (EVF) to back arc (SR). HREE abundances are unfractionated and lower than in NMORB by a factor of 1.3 – 1.9, which suggests that the Kamchatka mantle wedge is variably depleted possibly due to earlier MORB- or intra-arc rifting and melting events (Churikova et al, 2001). HFSE and Hf isotope systematics (Münker et al, 2004) show that EVF and CKD magmas formed from a depleted mantle source (low Ta/Yb ratios). By contrast, lavas from the SR back arc have a significant contribution of a source relatively rich in HFSE (higher Ta/Yb, low Zr/Nb and Ba/Nb ratios). Based on the amount of an OIB component in the mantle source Churikova et al (2001) distinguished two groups of back arc rocks: (I) back arc basalts (IAB), which are only slightly (up to 5%) enriched by an OIB-type mantle component in their source and (II) within-plate types basalts (WPT) with a minor slab fluid signature, which are enriched by an OIB component in their source up to 35%. However, in the present melt inclusion study, only samples from the group (I) were analyzed (Fig. 1.2.1.1.2a-c).

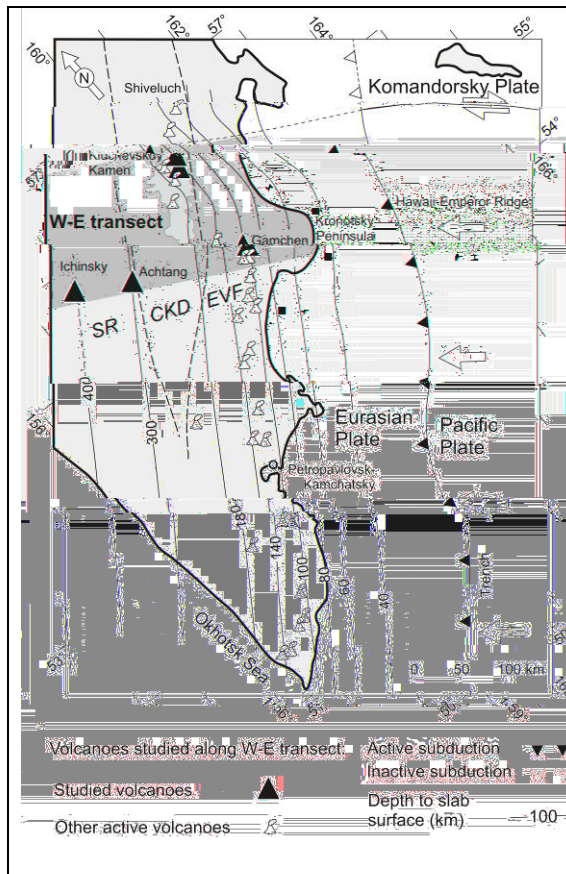


Figure 1.2.1.1.1. Plate tectonic setting of the Kamchatka arc and location of the transect in N-Kamchatka (shaded zone). The depth to Benioff zone is from (Gorbatov, 1997). Studied volcanoes are marked by shaded symbols. CKD borders are from Masurenkov (1991).

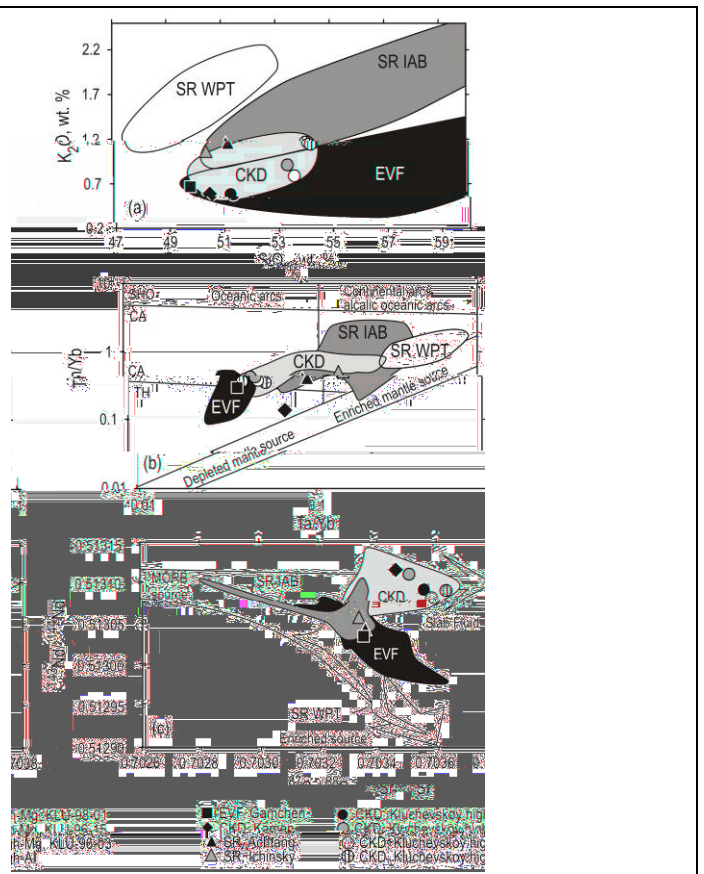


Figure 1.2.1.1.2. Representative compositional features of the lavas selected for the melt inclusion study. The fields of additional whole rock data from each zone are shown for comparison (data from Churikova et al., 2001). The most magnesian samples were chosen from each volcanic zone: (a) for a given SiO₂ potassium increases from the arc front to back arc; (b) demonstrates depleted and enriched mantle sources for Kamchatka arc

rocks; (c) CKD magmas are relatively enriched in $^{87}\text{Sr}/^{88}\text{Sr}$ at constant Nd isotopes; SR samples lie on the mantle array from MORB to OIB sources.
--

Forsteritic olivine in CKD rocks show enrichment compared to MORB in ^{18}O -isotopes (up to 7,5‰) while their hosts are only slightly enriched in $^{87}\text{Sr}/^{86}\text{Sr}$ (0.70366) at nearly constant Nd-isotopes. This observation was attributed to a relatively large fluid flux from the subducted Emperor Seamount chain in this area (Dorendorf et al, 2000a).

From these studies we know that several components were involved in magma generation below Kamchatka: a depleted MORB source, an OIB component (in SR rocks) and slab fluids that were variably enriched in ^{18}O and $^{87}\text{Sr}/^{86}\text{Sr}$ -isotopes (EVF, CKD). The data of Dorendorf et al (2000a, 2000b) and Churikova et al (2001) show that Pb isotopic variations do not correlate with any slab fluid parameters (e.g. $^{87}\text{Sr}/^{86}\text{Sr}$, fluid mobile elements). Therefore sediments did not contribute in any significant way to these magmas, and fluids are for clearly dominated by devolatilization of the subducted oceanic crust and the Emperor Seamount Chain.

In order to investigate the properties of HFSE in subduction regimes, we performed high precision measurements of Nb/Ta, Zr/Hf, and Lu/Hf ratios together with $^{176}\text{Hf}/^{177}\text{Hf}$ analyses on arc rocks from Kamchatka and the western Aleutians. The volcanic rocks of the Kamchatka region comprise compositional end members for both fluid and slab melt controlled mantle regimes, thus enabling systematic studies on the HFSE mobility at different conditions in the subarc mantle. Hf–Nd isotope and systematic Zr/Hf and Lu/Hf covariations illustrate that Zr–Hf and Lu are immobile in fluid-dominated regimes. Hf–Nd isotope compositions furthermore indicate the presence of “Indian” type depleted mantle beneath Kamchatka, as previously shown for the Mariana and Izu–Bonin arcs. In addition to a depleted mantle component, Hf–Nd isotope compositions enable identification of a more enriched mantle wedge component in the back-arc (Sredinny Ridge). The ratios of Nb/Ta and Zr/Hf are decoupled in rocks from fluid-dominated sources, indicating that Nb and Ta can be enriched in the mantle by subduction fluids to a small extent.

Churikova T., Dorendorf F., Wörner G. Sources and fluids in the mantle wedge below Kamchatka, evidence from across-arc geochemical variation // Journal of Petrology. - 2001, vol. 42, no. 8. - P. 1567-1593.

Münker C., Wörner G., Yogodzinski G., Churikova T. Behavior of high field strength elements in subduction zones: constraints from Kamchatka–Aleutian arc lavas. Earth and Planetary Science Letters 224 (2004) 275– 293.

1.2.1.2. Volatile (S, Cl and F) and fluid mobile trace elements

Research on the Northern Kamchatka transect was continued during 2007-2010 and was focused on volatile and fluid mobile elements in the rocks and melt inclusions previously studied samples. Because the volatile elements in whole rocks are strongly affected by degassing process before and during eruption (Hansteen and Gurenko, 1998; Metrich, 1999, Edmonds et al, 2001; de Moor et al, 2005; Wallace, 2005), melt inclusions trapped in pristine igneous minerals are potentially the best data source to study initial volatile contents in primary and parental melts (Danyushevsky et al, 2002). Melt inclusions provide also an opportunity to extend our data on melt compositions beyond the range covered by whole rocks towards more primitive compositions (Sobolev et al, 2000). The combination of electron microprobe and SIMS analyses on glass inclusions also provides a great advantage since variable trace element patterns can be directly related to variable fluid signatures and thus allow to constrain different fluids and their capacity to carry certain trace elements. To study the across-arc geochemical zonation in volatile

elements, their behavior during magma evolution and correlation with trace elements, we analyzed the major, trace and volatile elements (S, Cl, F) contents in melt inclusions from 19 mafic samples from 12 Holocene volcanoes of the E-W transect across the Kamchatka arc.

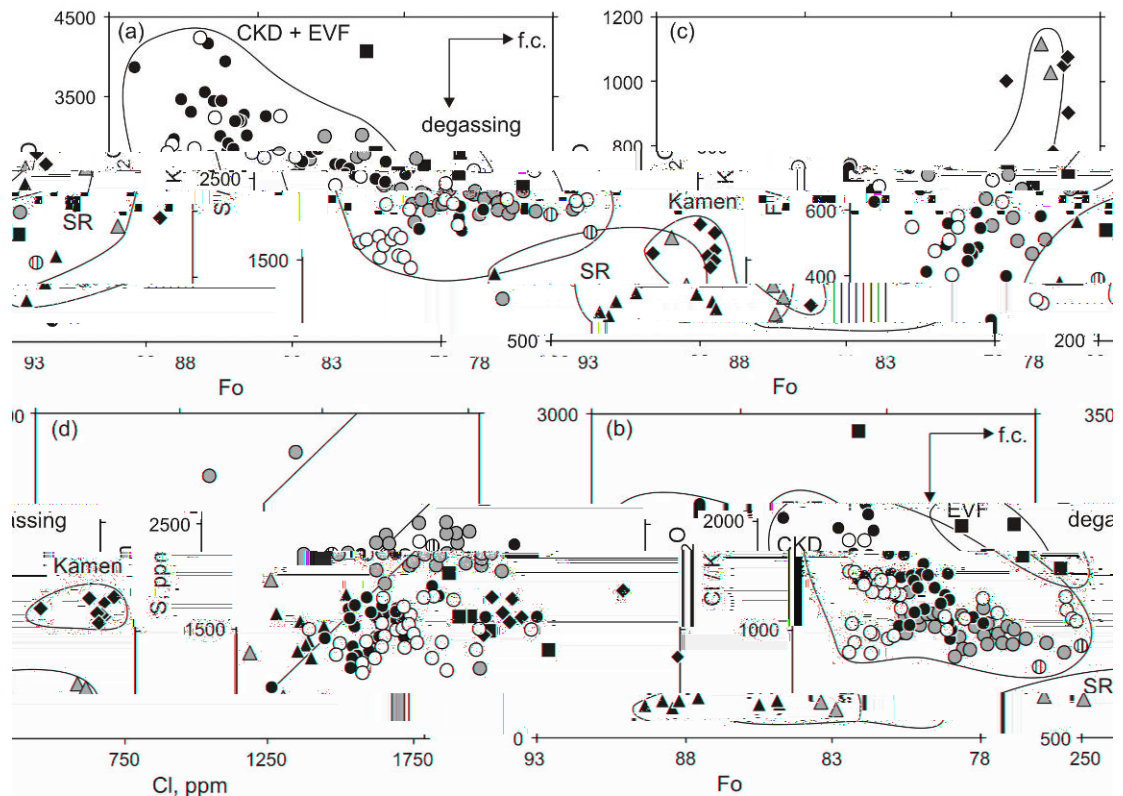


Fig. 1.2.1.2.1: Variation in V/K_2O (V = volatile element) with $Mg\#$ of host olivines. The S vs Cl diagram (d) shows that sulphur is more strongly degassed than chlorine. f.c. – fractional crystallization. Symbols as in Fig. 1.2.1.1.2.

Volatile element–trace element ratios correlated with fluid-mobile elements (B, Li) suggesting successive changes and three distinct fluid compositions with increasing slab depth. The Eastern Volcanic arc Front (EVF) was dominated by fluid highly enriched in B, Cl and chalcophile elements and also LILE (U, Th, Ba, Pb), F, S and LREE (La, Ce). This arc-front fluid contributed less to magmas from the central volcanic zone and was not involved in back arc magmatism. The Central Kamchatka Depression (CKD) was dominated by a second fluid enriched in S and U, showing the highest S/K_2O and U/Th ratios. Additionally this fluid was unusually enriched in ^{87}Sr and ^{18}O . In the back arc Sredinny Ridge (SR) a third fluid was observed, highly enriched in F, Li, and Be as well as LILE and LREE. We argue from the decoupling of B and Li that dehydration of different water-rich minerals at different depths explains the presence of different fluids across the Kamchatka arc. In the arc front, fluids were derived from amphibole and serpentine dehydration and probably were water-rich, low in silica and high in B, LILE, sulfur and chlorine. Large amounts of water produced high degrees of melting below the EVF and CKD. Fluids below the CKD were released at a depth between 100 and 200 km due to dehydration of lawsonite and phengite and probably were poorer in water and richer in silica. Fluids released at high pressure conditions below the back arc (SR) probably were much denser and dissolved significant amounts of silicate minerals, and potentially carried high amounts of LILE and HFSE.

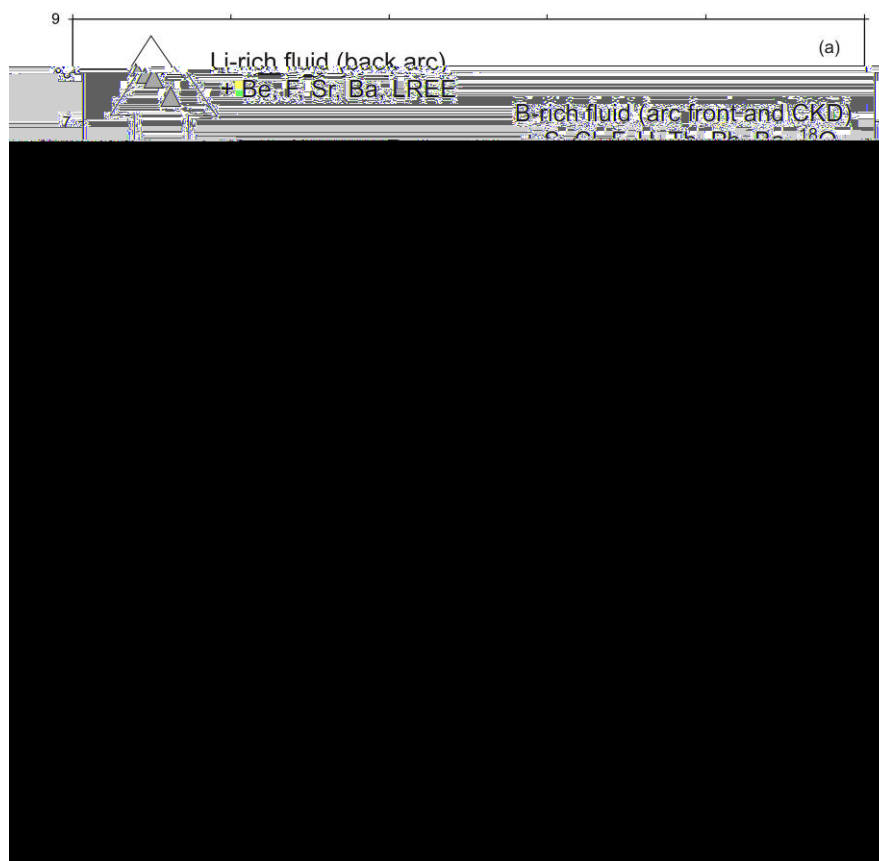


Fig. 1.2.1.2.2: B-Li-Be systematics across the Kamchatka arc. Our data provide clear evidence for decoupling of B and Li. This results in high B/La (a, b) and B/Nb values in arc front magmas and a strong increase in Li/Yb (a), Li/B (c) and Be/B ratios towards the back arc. Symbols as in Fig. 1.2.1.1.2.

Churikova, T., G. Wörner, N. Mironov, and A. Kronz, 2007. Volatile (S, Cl and F) and fluid mobile trace element compositions in melt inclusions: Implications for variable fluid sources across the Kamchatka arc, *Contributions to Mineralogy and Petrology*, vol. 154, number 2, August: 217–239. DOI 10.1007/s00410-007-0190-z.

Churikova T. Seeing through tectonic plates. – *Nature Geoscience*. – June 2008, vol. 1. – P. 350-351.

Wörner, G., Churikova, T., Leeman, W., Liebetrau, V., Tonarini, S., Heuser, A., 2001. Fluid-Mobile Trace Element and U-series Isotope Variations Across Kamchatka: Timing and effects of slab dehydration. *Margins Meeting, Schriftenreihe D. Geol. Ges.* 14: 236-237.

1.2.2. Geochemistry of Primitive Lavas of the Central Kamchatka Depression: Magma Generation at the Edge of the Pacific Plate

(in cooperation with GEOMAR)

Maxim Portnyagin, mportnyagin@ifm-geomar.de. Leibniz Institute for Marine Sciences, IfM-GEOMAR, Kiel, Germany; Vernadsky Institute of Geochemistry and Analytical Chemistry, Moscow, Russia.

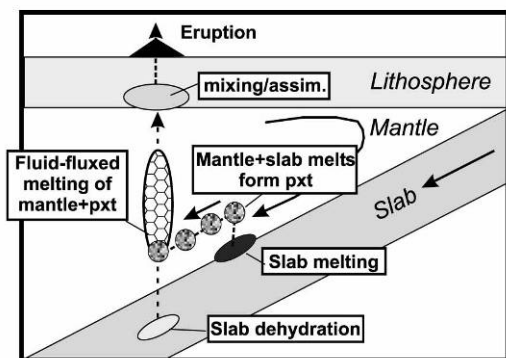
Ilya Bindeman, bindeman@uoregon.edu. Department of Geological Sciences, University of Oregon, Eugene, Oregon, USA.

Kaj Hoernle. Leibniz Institute for Marine Sciences, IfM-GEOMAR, Kiel, Germany; SFB574, University of Kiel, Kiel, Germany

Folkmar Hauff. Leibniz Institute for Marine Sciences, IfM-GEOMAR, Kiel, Germany.

New and published major and trace element and isotope (O, Sr, Nd) compositions of the Late Quaternary rocks from the Central Kamchatka Depression (CKD) are used to demonstrate systematic changes in magma genesis along the northern segment of the Kamchatka Arc, above and north of the subducting Pacific slab edge. We envision a number of possible petrologic scenarios for magma generation beneath the CKD and formulate quantitative mass-balance models which lead to three major conclusions departing significantly from previous interpretations of the CKD rocks. First, this study demonstrates that eclogite melts contribute to the composition of virtually all CKD lavas and could be the major agent transferring material from the subducted slab to the mantle wedge, including fluid-mobile elements (e.g., K, Ba).

Mixing or pyroxenite model (Model 1)



Reaction or fluxed melting model (Models 2A and 2B)

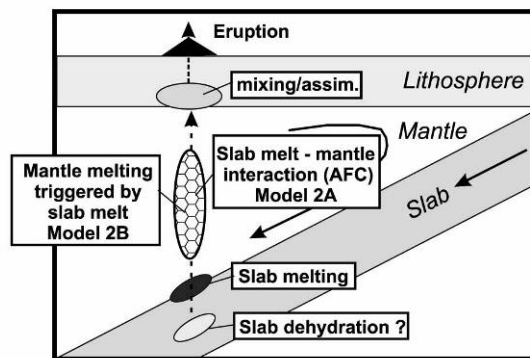


Fig. 1.2.2.1. Schematic illustration of possible scenarios for magma generation beneath the CKD. Model 1 assumes reaction of eclogite melts with mantle peridotite producing secondary high-Mg# pyroxenites in the mantle wedge, which are melted on later stage together with surrounding peridotite material. Model 2 suggests continuous reactive interaction between eclogitic melts and mantle wedge peridotite. Hydrous eclogitic melt triggers mantle melting (model 2A) or, in alternative view, assimilates mantle material as the slab melt rises, heats and decompresses in the mantle wedge (model 2B). All models assume that some shallow assimilation may follow mantle melting and occurs in the overriding plate. Combination of different mechanisms of magma origin can certainly take place beneath the CKD.

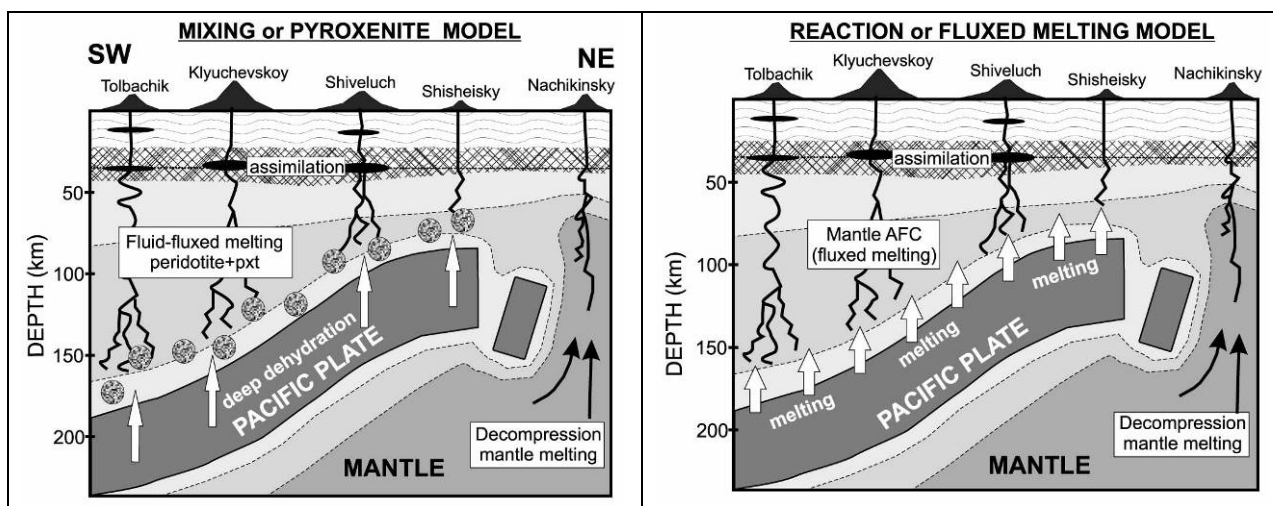


Fig. 1.2.2.2. Geodynamic models of primary magma origin along the CKD. Schematic distribution of temperatures in the mantle is shown by gradations of grey; darker grey tone corresponds to hotter temperature. Characteristic feature of the mantle wedge is inverted thermal gradient above the subducting

Pacific Plate. Normal gradient is proposed to characterize mantle column beneath Nachikinsky volcano to the north of the slab edge. The temperature field is qualitatively similar to numerically predicted by *Manea et al.* [2007]. (A) Mixing model suggests that major and trace element zoning along the CKD originates due to mixing of basaltic and dacitic melts, which originate from fluid-fluxed melting of hybrid mantle consisting of pyroxenite “blobs” in peridotite matrix. The pyroxenite is proposed to form through reaction between mantle wedge and eclogitic melts at shallow mantle depths. Absolute amount of pyroxenite involved in melting could be similar beneath all volcanoes but their relative amount compared to mantle increases toward the slab edge. (B) Reaction model implies that slab melting occurs beneath all volcanoes and could be particularly abundant at the slab edge. Eclogite melts leave the slab and interact with the mantle wedge on their rise according to the AFC or flux mantle melting scenario. The average extent of this interaction and increase of liquid mass as expressed in the average compositions of erupted primitive magmas correlate with the length of mantle column, distance from the slab-edge and the thermal state of the mantle wedge. Extent of this interaction is larger beneath the southern Klyuchevskoy Group volcanoes and smaller beneath the northern Shiveluch Group. Short mantle columns can favor incomplete mixing between magmas originating in different parts of the mantle wedge and can explain larger variability of primitive magmas toward the slab edge. Magmas to the north of the slab edge are thought to originate due to short-lived upwelling and decompression melting of fertile mantle. The upwelling could be caused by detachment of slab fragments as discussed in the text. All magmas in the CKD could also interact with the shallow lithosphere. The assimilation of lithospheric material could be particularly large beneath the largest and highly active Kamchatkan volcanoes, where lithosphere could be hotter and melted more easily.

Second, thermal state of the mantle wedge beneath the CKD has primary control on the major composition of primitive magmas, favoring production of low temperature andesitic and dacitic mantle melts toward the slab edge. Third, hydrous slab-fluids might not be required to generate CKD magmatism. Instead, strong enrichment in LILE, high $\delta^{18}\text{O}$ and $^{87}\text{Sr}/^{86}\text{Sr}$, in some CKD magmas could originate from assimilation of hydrothermally-altered mafic lithosphere. Several concurring factors could facilitate partial melting of the subducting slab beneath the all CKD volcanoes and favor variable modification of the eclogite melts during interaction with the mantle wedge (Figs. 1.2.2.1 and 1.2.2.2). Large input from slab melting makes CKD magmatism unique in Kamchatka and may contribute to the CKD volcanoes being the most productive arc volcanoes on Earth.

Portnyagin, M. V., K. Hoernle, and G. P. Avdeiko (2003), Evidence for decompressional melting of garnet peridotite at the Kamchatka-Aleutian junction, Geochim. Cosmochim. Acta, 67 (18), Suppl. 1, Goldschmidt Conference Abstracts, A381.

Portnyagin, M., K. Hoernle, G. Avdeiko, F. Hauff, R. Werner, I. Bindeman, V. Uspensky, and D. Garbe-Schönberg (2005a), Transition from arc to oceanic magmatism at the Kamchatka-Aleutian junction, Geology, 33 (1), 25–28.

Portnyagin, M. V., K. Hoernle, P. Y. Plechov, N. L. Mironov, and S. A. Khubunaya (2007), Constraints on mantle melting and composition and nature of slab components in volcanic arcs from volatiles (H_2O , S, Cl, F) and trace elements in melt inclusions from the Kamchatka Arc, Earth Planet. Sci. Lett., 255 (1-2): 53–59.

Sara Auer, Ilya Bindeman, Paul Wallace, Vera Ponomareva, Maxim Portnyagin (2009). The origin of hydrous, high-d18O voluminous volcanism: diverse oxygen isotope values and high magmatic water contents within the volcanic record of Klyuchevskoy volcano, Kamchatka, Russia. Contrib Mineral Petrol (2009) 157:209–230 DOI 10.1007/s00410-008-0330-0

1.2.3. South-North transect through the Sredinny Ridge of the Kamchatka

Anna O Volynets, a.volynets@gmail.com, **Tatiana Churikova**, tchurikova@mail.ru *Institute of Volcanology and Seismology FED RAS, Petropavlovsk-Kamchatski, Russia*

Gerhard Wörner, gwoerner@gwdg.de. *GZG Abteilung Geochemie, Universität Göttingen, Germany*

Gordeychik B., gordei@mail.ru. *Institute of Physics of Earth, Russian Academy of Sciences, Moscow, 123995, Russia.*

Paul Layer, pwlayer@alaska.edu. *University of Alaska Fairbanks, Department of Geology and Geophysics, Fairbanks, USA.*

The results of this research are based on two transects which were carried out through Kamchatka peninsula during the last decade: (1) a SE-NW cross-arc transect and (2) a SW-NE Sredinny Range (SR) along-arc transect. These data together with the first Ar-Ar dating offer an opportunity to study the geochemical feature distribution of the volcanic rocks in space and time. The cross-arc transect (Fig. 1.2.3.1, Churikova et al., 2001, 2007), extending from the Gamchen Volcano in the Eastern Volcanic Front (EVF) through the Central Kamchatka Depression (CKD) to Ichinsky Volcano in the SR, is based only on Quaternary rocks; it showed a continuous geochemical zonation from the arc front to the back arc of the present subduction zone, including strong and gradual increases in LILE, LREE, and HFSE in whole rocks. The transect along the SR back arc from the Achtang lava field to Tekletunup Volcano (Fig. 1.2.3.1) comprises two age groups, each uniform in geochemical features. Late Miocene-Pliocene rocks (3.05-6.19 Ma) represent voluminous plateau lavas of depleted basalts with low HFSE and HREE. Fluid-mobile elements are enriched; enrichment patterns are in fact similar to typical arc front lavas. The younger group of Quaternary rocks (<1 Ma) is represented by monogenetic cones and stratovolcanoes that combine the typical LILE/HFSE-enrichment of a subduction setting with enrichment in all incompatible elements.

Geological and geophysical studies (Legler, 1977; Avdeiko et al., 2007) suggest that in Eocene-Miocene time the present back arc represented the active volcanic front of the Proto-Kamchatka subduction zone. Later, the Kamchatka arc system was modified by a step-by-step accretion of the Kronotsky terranes from south to north. The time of that accretion and the outward southeast 200 km shift of the subduction zone to the presently active EVF is estimated to have occurred from 40 to 2 Ma (Alexeiev et al., 2006; Lander & Shapiro, 2007).

Our data can help to better constrain the timing of this event. We argue that the systematic change in SR rock geochemistry with time is the result of this arc shift, and has been facilitated by a massive slab roll-back event. In this scenario, the SR plateau lavas represent the volcanic front until as recently as 3 Ma; the area west of the Miocene Sredinny arc front constituted the back arc region at that time. Volcanic rocks of that region (Mt. Khukhch: 3.78 Ma, Fig. 1.2.3.1) are indeed characterized by the absence of an arc signature; some even exhibit true within-plate trace element patterns (Perepelov et al. 2006). The younger Quaternary rocks at SR are the present back arc lavas of the recent subduction zone. Both the systematic across-arc geochemical zonation from the contemporary arc front to the back arc and the uniform geochemistry of young volcanic rocks along the SR show that the volcanism of the whole region is explained by only one mechanism – subduction of the Pacific Plate below Kamchatka. A trend is documented from fluid-dominated melting in the EVF, through the upwelling of a strongly fluid-fluxed mantle below the CKD (Dorendorf et al. 2000), to melting of a fluid-enriched mantle aided by strong upwelling and decompression in the SR back arc region.

SR magmatism has continued to be active up to the Holocene, even though seismic data today do not signal a downgoing plate below this region. Geophysical studies have shown that the depth of Kamchatka seismicity decreases from south to north. Kirby et al. (1996) showed that the absence of seismicity does not mean the absence of a plate, because at temperatures higher than 600-700°C seismicity is lost. Davaille & Lees (2004) argued that the seismicity of the subducted Pacific slab is gradually decreasing to the north as result of its heating.

Yogodzinski et al. (2001) argued that the edge of the Pacific Plate is traced below Shiveluch Volcano while Portnyagin et al. (2005) show that the slab edge may be traced somewhat further north at the Shisheisky complex (Fig. 1.2.3.1). We argue that the northern edge of the Pacific Plate is represented by a wide (150 km) boundary as a set of transform faults that can be projected on Kamchatka's surface from the morphology of the downgoing oceanic plate (Fig. 1.2.3.1). At the depth where fluid release is possible, this edge is marked by the termination of Holocene volcanoes on the surface. The absence of young volcanism to the north of the on-land projection of the Alpha fault, then, marks the plate boundary at depth (Fig. 1.2.3.1). The movements of the melts across the vector of subduction and small scale convection motions could be strong at the slab edge (Davaille and Lees, 2004) and thus magmatism will show a diffuse image of the slab edge. However, this slab edge is weak at best at the volcanic front, probably due to the fact that the slab edge has not been sufficiently heated at this position (Davaille & Lees, 2004).

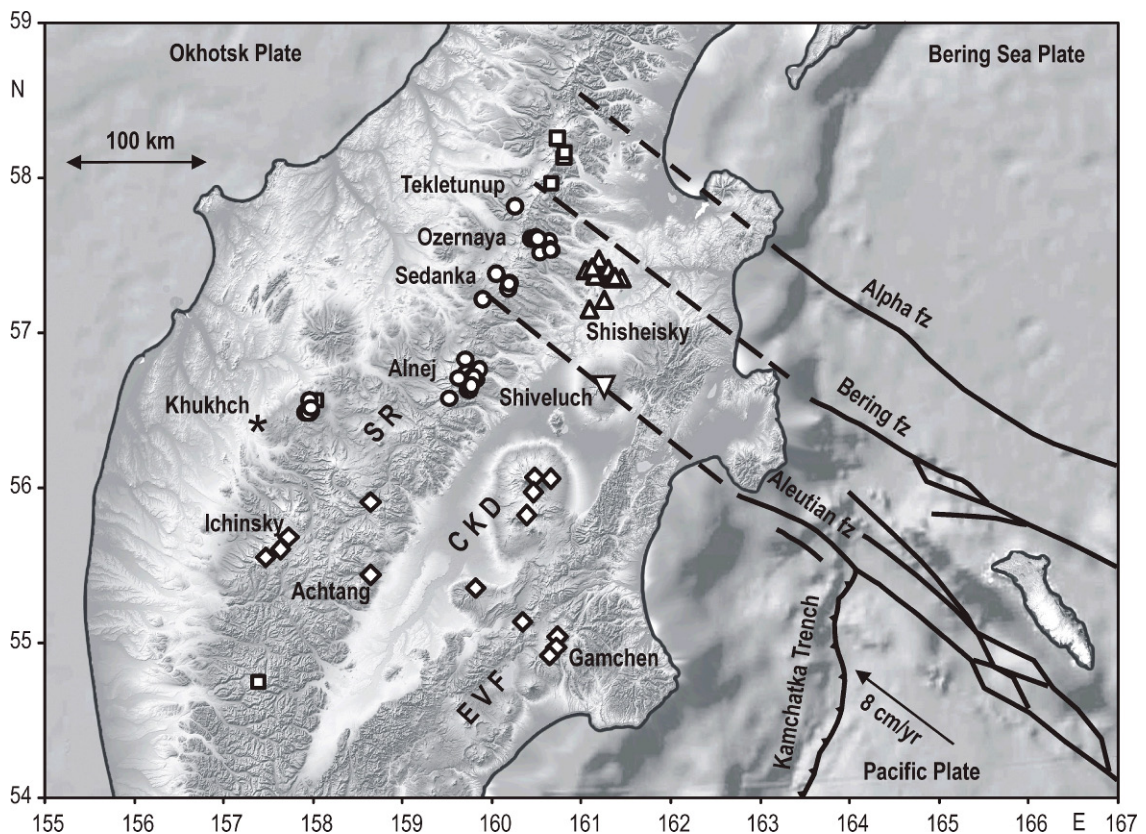


Fig. 1.2.3.1. Tectonic sketch map of the region, where three plates are joined based on Seliverstov (1998). Relative motion of the Pacific and Bering Sea plates produces the system of transform fault zones Aleutian, Bering, and Alpha. Dashed lines show the extension of these transform zones under the Okhotsk Plate. Data sources for Quaternary volcanism: upturned triangle – Shiveluch (Yogodzinski et al, 2001), triangles – Shisheisky complex (Portnyagin et al., 2005), squares – data from Pevzner & Volynets (2006), rhombs – cross-arc transect from Churikova et al. (2001), circles – SR long-arc transect from Volynets et al. (this meeting), star – from Perepelov et al. (2006).

Anna O Volynets, Tatiana Churikova, Gerhard Wörner, Boris Gordeychik, Paul Layer. Mafic Late Miocene–Quaternary volcanic rocks in the Kamchatka back arc region: implications for subduction geometry and slab history at the Pacific-Aleutian junction // Contributions to Mineralogy and Petrology. – 2010, vol. 159. – P. 659–687. – DOI 10.1007/s00410-009-0447-9.

Boris Gordeychik, Tatiana Churikova, Gerhard Wörner, Anna Volynets, Paul Layer Geodynamical conditions at the north of the Kamchatka subduction zone: geochemical evidence // Mitigating

natural hazards in active arc environments. Linkages among tectonism, earthquakes, magma genesis and eruption in volcanic arcs, with a special focus on hazards posed by arc volcanism and great earthquakes. 6-th Biennial Workshop on Japan-Kamchatka-Alaska subduction processes (JKASP-2009). June 22-26, 2009. – Fairbanks, Alaska: Geophysical institute, University of Alaska, 2009. – P. 76-77.

A.O. Volynets, T.G. Churikova, G. Wörner Geochemical modeling of the composition and amount of slab fluid for Kamchatka Sredinny Range volcanic rocks // Mitigating natural hazards in active arc environments. Linkages among tectonism, earthquakes, magma genesis and eruption in volcanic arcs, with a special focus on hazards posed by arc volcanism and great earthquakes. 6-th Biennial Workshop on Japan-Kamchatka-Alaska subduction processes (JKASP-2009). June 22-26, 2009. – Fairbanks, Alaska: Geophysical Institute, University of Alaska, 2009. – P. 89-90.

Volynets A., Churikova T., Wörner G. Mantle sources and fluids in the Northern Kamchatka back-arc // Geochimica et Cosmochimica Acta. Abstracts of the 19th Annual V.M. Goldschmidt Conference, Davos, Switzerland. – 2009, Vol. 73, Issue 13. – P. A1393.

Boris Gordeychik, Tatiana Churikova, Anna Volynets, Gerhard Wörner, and Paul Layer. The northern edge of Pacific plate position near Kamchatka-Aleutian junction // Geophysical Research Abstracts: 7th EGU General Assembly. – 2010, vol. 12. – EGU2010-12504.

1.2.4. Pre-Holocene caldera-forming eruptions

Leonov V.L., vl@kscnet.ru, **V.V. Ponomareva**, **L.I. Bazanova**, *Institute of Volcanology and Seismology FED RAS, Petropavlovsk-Kamchatski, Russia*

Bindeman I.N., bindeman@uoregon.edu, **K.E. Watts**, **N.K. Shipley**, *Geological Sciences, 1272 University of Oregon, Eugene, OR 97403, USA*

Izbekov P.E., *Geophysical Institute, University of Alaska, Fairbanks, AK, USA*

Perepelov A.B., *Vinogradov Institute of Geochemistry, Irkutsk, Russia*

Jicha B.R., **B.S. Singer**, *Geology and Geophysics, University of Wisconsin, Madison, WI, USA*

Schmitt A.K., *Earth and Space Sciences, UCLA, Los Angeles, CA, USA*

Portnyagin M.V., *Leibnitz Institute for Marine Sciences, IfM-GEOMAR, Kiel, Germany*

Chen C.H., *Institute of Earth Sciences, Academia Sinica, P.O. Box 1-55 Nankang, Taipei 11529, Taiwan*

The Kamchatka Peninsula in far eastern Russia represents the most volcanically active arc in the world in terms of magma production and the number of explosive eruptions. We investigate large-scale silicic volcanism in the past several million years and present new geochronologic results from major ignimbrite sheets exposed in Kamchatka (Fig. 1.2.4.1). These ignimbrites are found in the vicinity of morphologically-preserved rims of partially eroded source calderas with diameters from ~2 to ~30 km and with estimated volumes of eruptions ranging from 10 to several hundred cubic kilometers of magma. We also identify and date two of the largest ignimbrites: Golygin Ignimbrite in southern Kamchatka (0.45 Ma), and Karymshina River Ignimbrites (1.78 Ma) in southcentral Kamchatka. We present whole-rock geochemical analyses that can be used to correlate ignimbrites laterally. These large-volume ignimbrites sample a significant proportion of remelted Kamchatkan crust as constrained by the oxygen isotopes. Oxygen isotope analyses of minerals and matrix span a 3‰ range with a significant proportion of moderately low- $\delta^{18}\text{O}$ values. This suggests that the source for these ignimbrites involved a hydrothermally-altered shallow crust, while participation of the Cretaceous siliceous basement is also evidenced by moderately elevated $\delta^{18}\text{O}$ and Sr isotopes and xenocryst contamination in two volcanoes.

The majority of dates obtained for caldera-forming eruptions coincide with glacial stages in accordance with the sediment record in the NW Pacific, suggesting an increase in explosive volcanic activity since the onset of the last glaciation 2.6 Ma. Rapid changes in ice volume

during glacial times and the resulting fluctuation of glacial loading/unloading could have caused volatile saturation in shallow magma chambers and, in combination with availability of low- $\delta^{18}\text{O}$ glacial meltwaters, increased the proportion of explosive vs effusive eruptions. The presented results provide new constraints on Pliocene–Pleistocene volcanic activity in Kamchatka, and thus constrain an important component of the Pacific Ring of Fire.

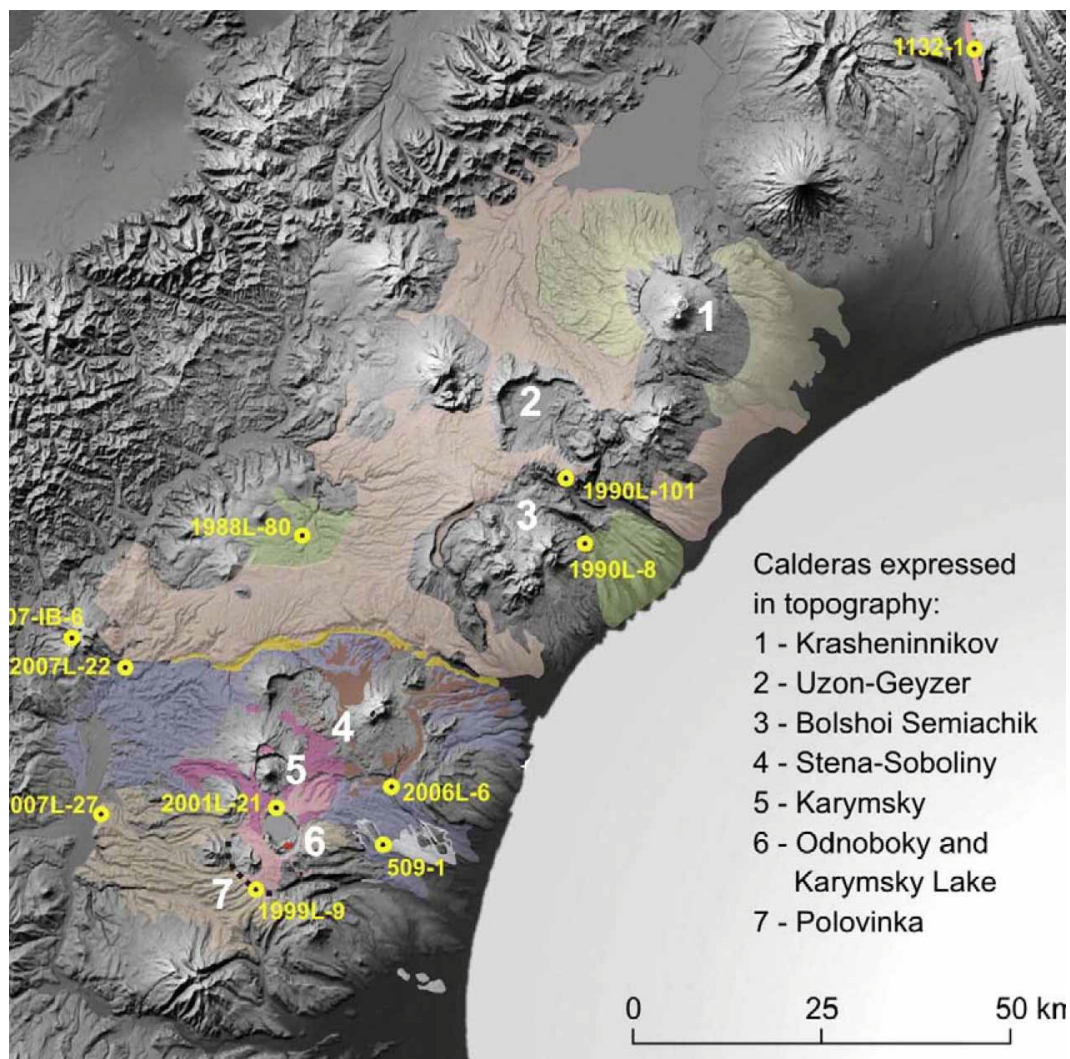


Fig. 1.2.4.1. Calderas and associated ignimbrites of the central part of Eastern Kamchatka. Location of this area is shown in [Bindeman et al., 2010]. Ignimbrite sheets associated with the individual caldera complexes are shown with different colors; their outlines are based on the maps of Masurenkov (1980), Florensky and Trifonov (1985), Leonov and Grib (2004). Location of the dated samples is shown with yellow circles. Some ignimbrite sheets are covered by younger sediments and are exposed only in river banks. See Table 1 for ages and text for details. Uzon, Polovinka and Stena–Soboliny ignimbrites are multi-stage sheets and may represent a suite of repetitive eruptions from these eruptive centers. Distribution of the individual ignimbrite sheets somewhat differs when mapped by different researchers and requires further refining.

What causes explosive eruptions and low- $\delta^{18}\text{O}$ values during the glacial times?

The observation presented here that the majority of eruptions happened during a maximal (“75% glacial”) period is counterintuitive and deserves discussion. There were many attempts to describe periodicity of volcanic eruptions, both basaltic and silicic, explosive and effusive, to external factors varying from sea-level change, tides, to glaciations (Kennett and Thunell, 1977;

Rampino et al., 1979; Wallman et al, 1988; Glazner et al., 1999; Gusev et al., 2003; Jellinek et al., 2004; Jicha et al., 2009). It appears that glaciations have documented influences on volcanism in Iceland, Sierra Nevada, and NE Pacific, with increased mantle melting productivity and formation of the crustal magma chambers. However the connection between deglaciation and increased volcanism is not straightforward: melting glaciers (glacial unload) do not automatically cause volcanic eruptions because lithostatic and hydrostatic pressure differential remains the same. Thus, association of the thickest ice with calderas makes them most susceptible to pressure fluctuation during interstadial and deglaciation episodes: caldera walls may experience cone failure during deglaciation (Waythomas and Wallace, 2002; Huggel et al., 2007).

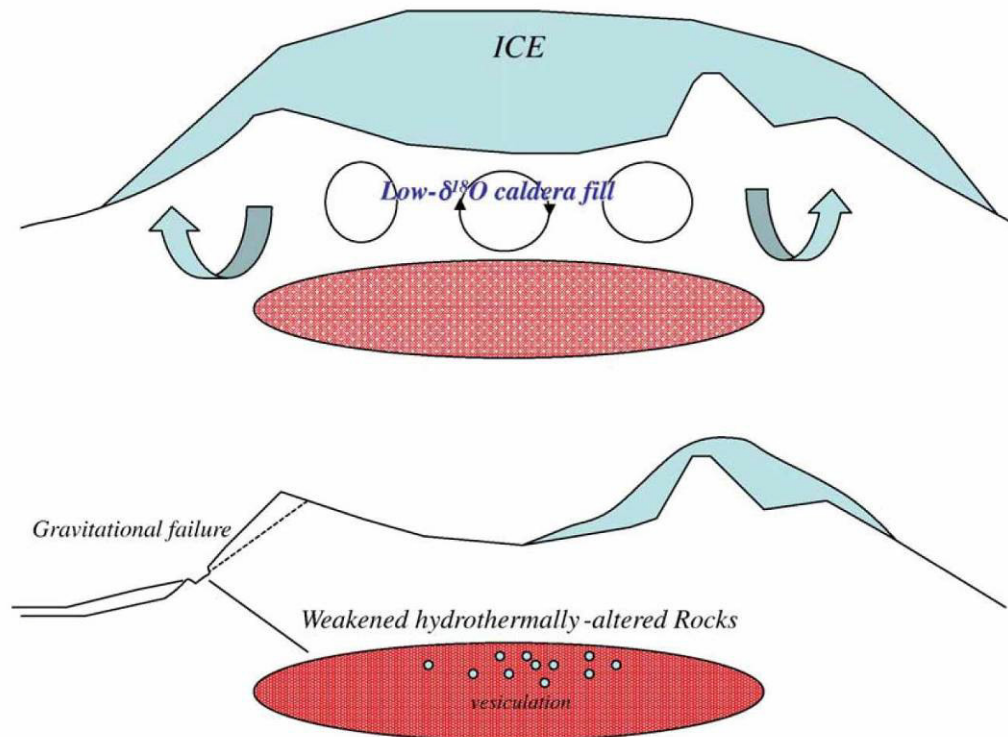


Fig. 1.2.4.2. A cartoon showing glacial–interglacial transition affecting shallow magma chambers and initiating caldera-forming eruptions.

Jellinek et al. (2004) attributed the rate of change — first derivative of $\delta^{18}\text{O}$ -time foraminifera SPECMAP data — as a leading cause of triggering volcanic eruptions. Peaks of basaltic and silicic eruptions in eastern Sierra Nevada (Glazner et al., 1999) demonstrated delay after deglaciation at 3 ka (basaltic) and 11 ka (silicic) eruptions. These delays were explained by the elastic response of the mantle and the crust (Slater et al., 1998; Jellinek et al., 2004).

Our observation that the majority of studied Kamchatkan eruptions happen during glacial times supports this view. Glacial times represent the more dynamic conditions for change, with multiple fluctuation of the amount of ice, while ice-free or ice poor interglacial periods do not cause oscillating pressure over magma chambers (Fig. 1.2.4.2). The other factors that may promote greater explosivity during glacial periods involve specific hydrogeologic conditions for hydrothermal circulation around caldera-covered volcanic centers (Fig. 1.2.4.2). Confined hydrothermal circulation under ice may cause greater weakening of the intracaldera roof rock, formation of structurally-weak and permeable tuyas and hyaloclastites like in Iceland, that are more prone to subsequent collapse in interstadial. This hydrothermal weakening may contribute

to catastrophic volcanic edifice failures caused by glacial erosion and deglaciation (e.g. Waythomas and Wallace, 2002). An additional consideration for explosive eruptions happening during glacial periods may be related to increased accumulation of gas phase in their parental magma chamber (Fig. 1.2.4.2), both due to magma chamber saturation with volatiles, and by water inherited from assimilation of the surrounding meteoric–hydrothermal system.

An independent memory of glaciations in erupted volcanic products is delivered by their low- $\delta^{18}\text{O}$ values, making Kamchatka one of the provinces around the world with abundant low- $\delta^{18}\text{O}$ magmas. The appearance of low- $\delta^{18}\text{O}$ signature in magma is related to remelting of hydrothermally-altered rocks altered by low- $\delta^{18}\text{O}$ snow water, and seasonally-averaged $\delta^{18}\text{O}$ values of meteoric waters tend to be lower during the glacial, than interglacial times, which (other conditions being the same) should fingerprint the upper crust with lower $\delta^{18}\text{O}$ values.

It is hard to distinguish which of these factors played the dominant role but the abundant low- $\delta^{18}\text{O}$ values in volcanic products from Kamchatka (this work and Bindeman et al., 2004) suggest that the assimilation of hydrothermally-altered rocks from adjacent meteoric–hydrothermal systems played an equally-important role, in addition to the physical changes associated with glacial–interglacial pressure oscillations. While availability of water is likely to be similar in glacial vs. interglacial time in wet Kamchatkan climate, it is the lower- $\delta^{18}\text{O}$ value of glacial precipitation that has greater isotopic leverage to fingerprint the crust, aiding identification of the shallow petrogenetic processes.

Bindeman I.N., V.L. Leonov, P.E. Izbekov, V.V. Ponomareva, K.E. Watts, N.K. Shipley, A.B. Perepelov, L.I. Bazanova, B.R. Jicha, B.S. Singer, A.K. Schmitt, M.V. Portnyagin, C.H. Chen. Large-volume silicic volcanism in Kamchatka: Ar–Ar and U–Pb ages, isotopic, and geochemical characteristics of major pre-Holocene caldera-forming eruptions. Journal of Volcanology and Geothermal Research 189 (2010) 57–80.

1.2.5. New age data for Cainozoic magmatism in Kamchatka

Koloskov A.V., kolosav@kscnet.ru, *Institute of Volcanology and Seismology FED RAS, Petropavlovsk-Kamchatski, Russia*

Kovalenko D.V., Dmitry@igem.ru, *Institute of Geology of Ore Deposits, Petrography Mineralogy and Geochemistry, Russian Academy of Science, Moscow, Russia*

The authors analyzed rock samples from intrusive massifs in Kamchatka by K-Ar method. The results of this analysis revealed 17 new age data. The geological and isotope-geochronological analyses showed that a boundary between the late Cretaceous (Paleocene) – Paleogene is an important critical stage in development of magmatism in Kamchatka and adjacent territory. In early Paleozoic time the magmatism was basic and ultrabasic. It enclosed the whole territory of the peninsular in the late Cretaceous – Paleogene time. Since Eocene the magmatism has significantly changed in intensity and composition of volcanic products containing mostly andesites and andesite-dacites. Large granitoid massifs set up their formation at this time. The age of the boundary falls within the age span about 44-36 Ma.

Koloskov A.V., Kovalenko D.V., NEW AGE DATA FOR CAINOZOIC MAGMATISM IN KAMCHATKA. Vestnic KRAUNC. Nauki o Zemle, 2009, N 1, issue 13, pp. 231-236 (in Russian)

1.2.6. Cretaceous–Paleogene Magmatism of the Sredinnyi Range

Flerov G. B., flerov@kscnet.ru, *Institute of Volcanology and Seismology FED RAS, Petropavlovsk-Kamchatski, Russia*

Seliverstov V. A., *The Earth Sciences Museum, Moscow State University, Moscow, 119899 Russia*

Based on published and new data, a new petrological model of the preorogenic Late Cretaceous–Paleogene intrusive rock association is suggested. The principle of plume geodynamics is the essential one: homodromous intrusion of dunite–clinopyroxenite–gabbro magmas into upper layers of the lithosphere results from melting of a nonuniform substratum of the upper mantle caused by an ascending fluid and containing a phosphorus–potassium component. Different rock series are of comagmatic character: basalt–trachybasalt–latite and gabbro–monzogabbro–syenite, evolving in the process of crystallization differentiation of the basalt magma influenced by transmigmatic fluid. We suggest a petrogenesis of high-potassic basalt series.

Flerov G. B., V. A. Seliverstov. The Cretaceous–Paleogene Magmatism of the Sredinnyi Range of Kamchatka: Magma Sources. Journal of Volcanology and Seismology, 2008, Vol. 2, No. 2, pp. 71–82.

1.2.7. Ocean–Continent Transition Zone: Kamchatka

Gontovaya L. I., glarissa@i.kiev.ua, *Institute of Volcanology and Seismology, Far East Division, Russian Academy of Sciences, Petropavlovsk-Kamchatskiy, 683006, Russia*

Popruzhenko S. V., *AO LukinCholot, Petropavlovsk_Kamchatskii, 683016 Russia*

Nizkous I. V., *Data Services Subsection, Data Consulting and Services Section, Schlumberger Logelco Inc., Moscow, 109147 Russia*

The results from modeling were considered the crustal and upper mantle velocity structure in Kamchatka by seismic tomography and compare these with gravity data and present-day tectonics. We found a well-pronounced (in the physical fields) vertical and lateral variation for the upper mantle and found that it is controlled by fault tectonics. Not only are individual lithosphere blocks moving along faults, but also parts of the Benioff zone. The East Kamchatka volcanic belt (EKVB) is confined to the asthenospheric layer (the asthenosphere lens) at a depth of 70–80 km; this lens is 10–20 km thick and seismic velocity in it is lower by 2–4%. The top of the asthenosphere lens has the shape of a dome uplift beneath the Klyuchevskoi group of volcanoes and its thickness is appreciably greater; overall, the upper mantle in this region is appreciably stratified. A low-velocity heterogeneity (asthenolith) at least 100 km thick has been identified beneath the Central Kamchatka depression; we have determined its extent in the upper mantle and how it is related to the EKVB heterogeneities. Gravity data suggest the development of a rift structure under the Sredinnyi Range volcanic belt. The Benioff zone was found to exhibit velocity inhomogeneity; the anomalous zones that have been identified within it are related to asthenosphere inhomogeneities in the continental and oceanic blocks of the mantle.

The main results of this research are next:

(1) Results of geophysical studies, in particular, by the method of seismic tomography, show that the lithosphere and asthenosphere beneath Kamchatka down to depth 200 km, as studied thus far, involve considerable vertical and lateral velocity inhomogeneities; a layered block structure is clearly expressed in the velocity field. The greatest contrast and persistency in the lithosphere are shown by the interface between the lower and upper crust, the crust–mantle

interface, the asthenosphere top, and the dipping high velocity focal layer that separates the oceanic and the continental block in the upper mantle.

(2) Asthenospheric inhomogeneities have been identified in the upper mantle and their depths and positions were determined (Fig. 1.2.7.1). The East Kamchatka volcanic belt is confined to the asthenosphere lens at a depth of 70–80 km, its thickness is approximately 10–20 km there, with the velocity in the lens being lower by 2–4%. The asthenosphere lens is thicker in the area of the Klyuchevskoi group of volcanoes, the depth to its top is appreciably smaller beneath the volcanoes, forming the shape of an mantle dome uplift. Shear velocity anomalies helped the tracking of deep, and probably “thermal,” roots beneath the Klyuchevskoi volcanoes down to the depth where these intersect the focal layer and even deeper. For the first time we have identified a low velocity inhomogeneity (asthenolith) in the upper mantle beneath the Central Kamchatka depression, whose thickness is at least 100 km and have determined its dimensions and boundaries (the eastern, southern, and northern ones). The mantle “roots” of the asthenolith are probably confined to depths greater than those thus far studied and intersect with the focal layer at a depth of about 200 km. This inhomogeneity is probably due to a deeper mantle source, which is indirectly related to the present-day volcanism of the northern part of the East Kamchatka volcanic belt; gravity data suggest an extension of this feature under the Sredinnyi Range volcanic belt.

(3) We have found considerable lateral velocity variation in the focal layer and interrelationships of the layer characteristics (layer geometry, velocity structure, and seismicity features) with velocity features in the continental and oceanic upper mantle blocks. The pattern of velocity anomalies suggests horizontal eastward displacements of lithosphere blocks along weakened layers in the crust and upper mantle, with the displacements also involving the Benioff zone.

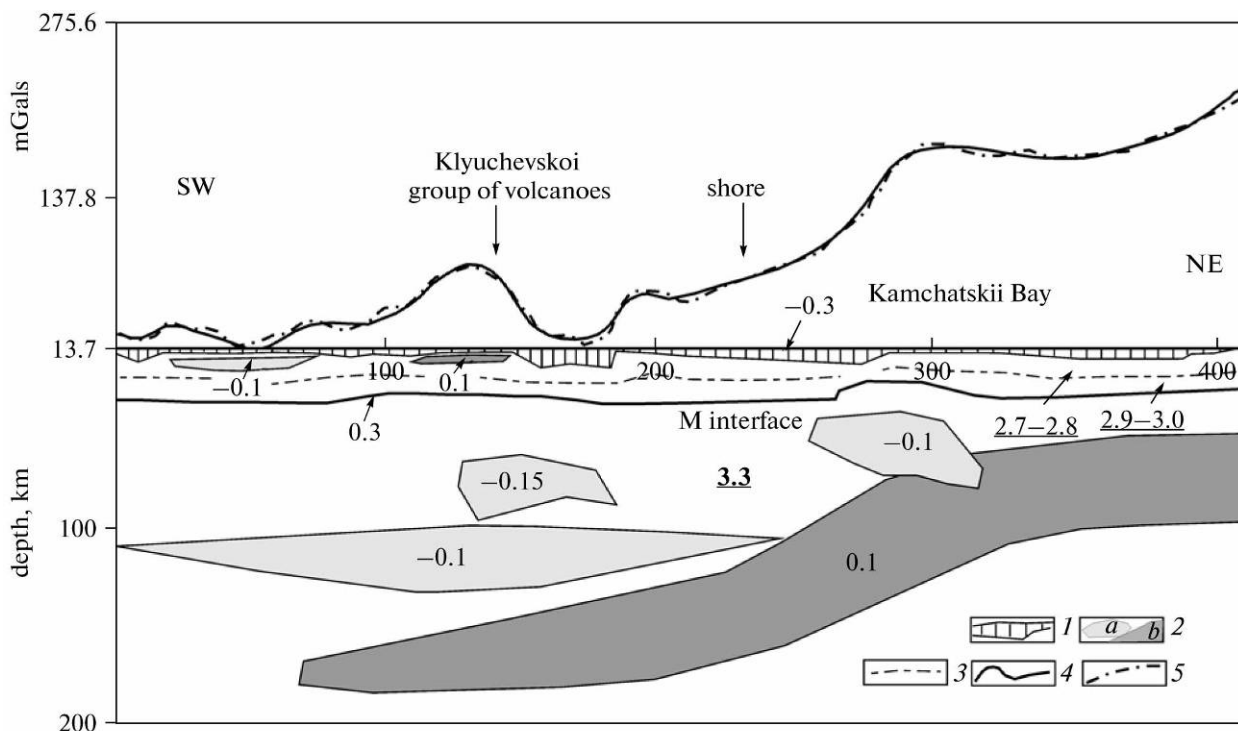


Fig. 1.2.7.1. Results of gravity modeling of the upper mantle along a profile corresponding to EW profile throughout of KGV: (1) sedimentary volcanogenic layer, (2) density anomalies, lows (a) and highs (b), anomaly values are in mGals, (3) interface between upper and lower crust, (4) observed gravity curve, (5)

theoretical anomaly due to the model. Numerals (underlined> give mean densities in crust and mantle (in g/cm³).

(4) The prevailing feature at several depth levels in the upper mantle is the control of the upper-mantle structure by fault tectonics. The velocity structure shows fault zones that are oriented along and across the Benioff zone. Of the latter, the one that is particularly well seen in the velocity field pattern is the fault zone in the area of Petropavlovsk-Kamchatskii. The zone has deep (at least 150 km deep) mantle roots and is expressed in the structure (horizontal displacement) of the focal layer. The neotectonic magmatic activity in the area between the Kamchatskii Bay and the Klyuchevskoi group of volcanoes is probably related to the transverse fault zone, which has been identified from the long intensive low velocity anomaly in that area in the depth range of 60–120 km. This zone was previously identified from anomalous resistivity measured on land.

(5) This combined analysis of the velocity structure, the transformed gravity field, and other data suggests the presence of a low-velocity mantle inhomogeneity in the western (not probed by seismic tomography) area of the Sredinnyi Range volcanic zone. Since anomalous velocity fields provide indirect evidence for the geodynamic setting, these new data on the deep velocity structure of the upper mantle beneath Kamchatka can be used for geodynamic analyses.

Gontovaya L. I., S. V. Popruzhenko, and I. V. Nizkous. Upper Mantle Structure in the Ocean–Continent Transition Zone: Kamchatka Journal of Volcanology and Seismology, 2010, Vol. 4, No. 4, pp. 232–247.

Gontovaya, L.I., Gordienko, V.V., Popruzhenko, S.V., et al., A Deep Model of Kamchatka Upper Mantle, Vestnik KRAUNTS, Nauki o Zemle, 2007, no. 1, part 9, pp. 78–92 (in Russian).

Nizkous, I., Kissling, E., Gontovaya, L., et al., Correlation of Kamchatka Lithosphere Velocity Anomalies with Subduction Processes, in Volcanism and Subduction: The Kamchatka Region Geophysical Monograph Series 172, pp. 97–106.

1.2.8. Impuls nature of the areal volcanism on Kamchatka

Dirksen O.V., *Institute of Volcanology and Seismology FED RAS, Petropavlovsk-Kamchatski, Russia*

It was established, that the activity of the areal volcanism on Kamchatka has impuls nature. The strongest impuls was occur about 50000-25000 14C y.a. That time all shield volcanoes as well as most of smaller eruptive centres were formed. It is possible to distinguish two impulses of activity during the Holocene time: 10000-7500 14C y.a. and 3500 14C y.a. up to present time. These impulses were synchronized with the active stages of the stratovolcanoes and caldera-forming eruptions in Kamchatka. Each impuls has the maximum of activity, which usually started 1000-700 years after it's beginning. The regions of most intensive areal volcanism are confined to zones of intersection of the regional tectonical structures of the NW and NE directions.

Dirksen O.V. Latequaternary areal volcanism of the Kamchatka (structural position, geology-geomorphology effect, space-time patterns of the occurrence) // Ph.D. thesis, Sankt-petersbourg State University, 2009. 172 p.

1.2.9. Largest eruptions of Kamchatka in middle Pleistocene-Holocene: tephrochronological studies

Ponomareva V., vera.ponomareva1@gmail.com, **Melekestsev I.V.**, **L.I. Bazanova**, **Leonov V.L.**, *Institute of Volcanology and Seismology FED RAS, Petropavlovsk-Kamchatski, Russia*
Sulerzhitsky L.D., *Geological Institute, Moscow, Russia*
Ilya Bindeman, bindeman@uoregon.edu, *Department of Geological Sciences, University of Oregon, Eugene, Oregon, USA.*

The largest explosive eruptions of Kamchatka during last 0,5 M.y. were considered. These eruptions cardiac changed the natural environment around the significant part of Kamchatka peninsula and may influence the climate change. The strongest Holocene eruption on Kamchatka happened about 8400 y.a. During this eruption 140-170 km³ of pyroclastics was erupted and large caldera with 7 rv diameter was formed. According to the volume of erupted material, this eruption is one of ten largest Holocene eruptions of the world-wide. Most of analogical eruptions of the world took place in the Pacific fire ring and in Indonesian island arcs. The analysis of the catalogs shows that the global picks of the explosive volcanism were during next periods of time: about 8600-7200 y.a., 4200-3000 y.a. and 2000-1400 y.a. The dating results on the surface pumices and ignimbrites as well as studies on ashes from the deep-sea wells in adjacent to Kamchatka area of water show that in Late Pleistocene the periods of often volcanological catastrophes with large calderas formation happened 0.03-0.04 M.y.a. and in Middle Pleistocene – between 0.3 and 0.5 M.y.a. These data allow inserting the significant contribution to world-wide chronicle of the explosive eruptions (about 14% eruptions, recognized to the present time, with erupted volume of material ≥ 0.1 km³. Using investigations of the tephra horizons of the largest Kamchatka eruptions it was created the unique system of the geochronological reference points (isochrones), which allow to date and to correlate the stages of the formation of the relief shapes and deposits in Holocene.

Ponomareva V., Melekestsev I.V., Bazanova L.I., Bindeman I., Leonov V.L., Sulerzhitsky L.D. Volcanological catastrophes on Kamchatka in middle Pleistocene-Holocene. In: Extremal natural phenomenons and catastrophes. Gliko A.O. (eds.). Moscow, Institute of Physics of the Earth RAS. 2010, pp. 219-238 (in Russian).

1.2.10. Late Pleistocene-Holocene Volcanism on the Kamchatka

Ponomareva V., vera.ponomareva1@gmail.com, **Melekestsev I.V.**, **Braitseva O.A.**,
Churikova T.G., tchurikova@mail.ru, *Institute of Volcanology and Seismology FED RAS,*
Petropavlovsk-Kamchatski, Russia
Pevzner M.M., suler@ginras.ru, **Sulerzhitsky L.D.**, *Geological Institute, Moscow, Russia*

Overview paper

Late Pleistocene-Holocene volcanism in Kamchatka results from the subduction of the Pacific Plate under the peninsula and forms three volcanic belts arranged in an echelon manner from southeast to northwest (Fig. 1.2.10.1). The cross-arc extent of recent volcanism exceeds 250 km and is one of the widest worldwide. All the belts are dominated by mafic rocks. Eruptives with SiO₂>57% constitute ~25% of the most productive Central Kamchatka Depression belt and ~30% of the Eastern volcanic front, but <10% of the least productive Sredinny Range belt.

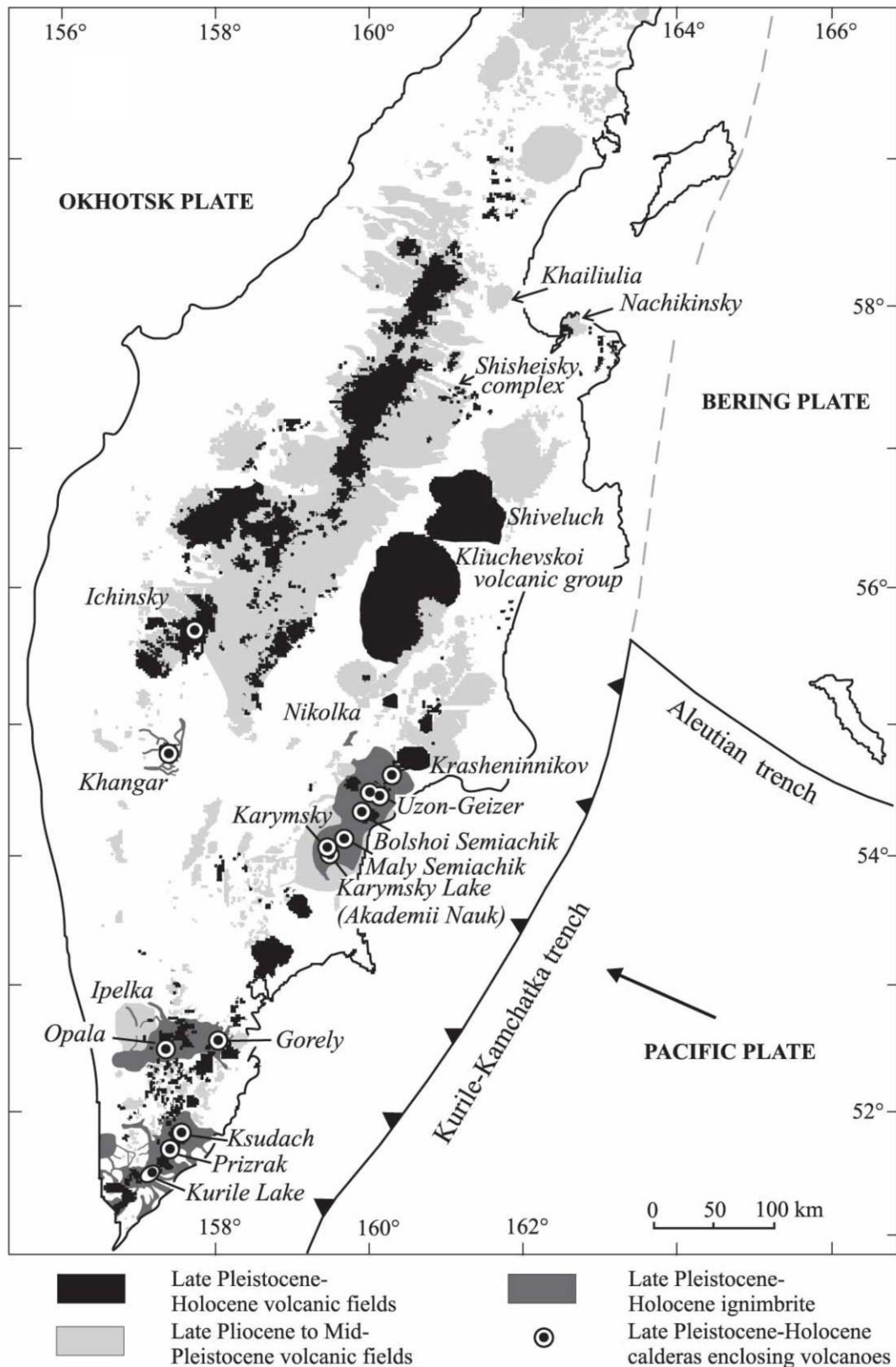


Fig. 1.2.10.1. Sketch map of late Pliocene-Holocene Kamchatka volcanic fields based on the 1:100 000 and 1:300 000 unpublished geological maps by Ivan Melekestsev, and *Map of Mineral Resources of Kamchatka region* (1:500 000) [1999]. Volcanic fields include debris avalanche and lahar deposits at the volcanoes foot. Gray dashed line shows a presumed boundary of the Bering plate [Lander et al., 1994]. Late Pleistocene-Holocene calderas and selected volcanoes are labeled.

All the Kamchatka volcanic rocks exhibit typical arc-type signatures and are represented by basalt-rhyolite series differing in alkalis. Typical Kamchatka arc basalts display a strong increase in LILE, LREE and HFSE from the front to the back-arc. La/Yb and Nb/Zr increase from the arc front to the back arc while B/Li and As, Sb, B, Cl and S concentrations decrease. The initial mantle source below Kamchatka ranges from N-MORB-like in the volcanic front and Central Kamchatka Depression to more enriched in the back arc. Rocks from the Central Kamchatka Depression range in $^{87}\text{Sr}/^{86}\text{Sr}$ ratios from 0.70334 to 0.70366, but have almost constant Nd isotopic ratios ($^{143}\text{Nd}/^{144}\text{Nd}$ 0.51307–0.51312). This correlates with the highest U/Th ratios in these rocks and suggest the highest fluid-flux in the source region.

Holocene large eruptions and eruptive histories of individual Holocene volcanoes have been studied with the help of tephrochronology and ^{14}C dating that permits analysis of time-space patterns of volcanic activity, evolution of the erupted products, and volcanic hazards.

Ponomareva V.V., Churikova T.G., Melekestsev I.V., Braitseva O.A., Pevzner M.M., Sulerzhitsky L.D. (2007) Late Pleistocene-Holocene Volcanism on the Kamchatka Peninsula, Northwest Pacific region // Volcanism and Subduction: The Kamchatka region. Ed. J. Eichelberger, E. Gordeev, P. Izbekov, J. Lees. Printed in the United States of America. Geophysical Monograph Series, Volume 173. 2007. P. 169-202.

1.2.11. The Identification and Diagnostics of Active volcanoes

Melekestsev I. V., *Institute of Volcanology and Seismology FED RAS, Petropavlovsk-Kamchatski, Russia*

It was considered the identification and diagnostics of active and potentially active volcanic features (regional zones of cinder cones, fields sheet volcanism, fields of concentrated multivalent extrusive volcanism, calderas, and underwater eruption centers in the sea) in the Kuril–Kamchatka island arc and in the Commander Islands link of the Aleutian island arc, as well as the condition of this region as of late 2007. We have identified and examined three periods in the research of active and potentially active volcanic features in the region: the early (1697–1934), the new (1935–1962), and the most recent, still in progress (1963 until today). We provide a new definition of the term “active volcano,” which is scientifically well-grounded, for the first time here. We present modified (compared with those available until now) catalogs of active and potentially active volcanic forms in Kamchatka and the Kuril Islands (Tabs. 1.2.11.1 and 1.2.11.2). For typical multieruption volcanoes now in phase I (the active) and II (the passive) of their evolution, we provide long-term forecasts of the character and parameters of future eruptions and the associated volcanic hazard.

(1) The long-term prediction of eruptions and volcanic hazard critically depends on reconstructions of the dynamics of activity and productivity of a volcano of interest for a long interval of its existence, at least a few thousand years. Based on these data, a long-term forecast of activity can be developed specifying the type and parameters of eruptions that can take place exactly during the current phase of the volcano’s existence.

(2) The dynamics of activity for a volcano is reconstructed based on special tephrochronologic geological–volcanological studies using ^{14}C dating techniques. Patterns are identified in the cyclic behavior of the volcano specifying its periods of activity and repose. Knowledge of how long such periods have lasted during the past cycles and of the volcano’s

productivity during the different phases of its evolution enables the approximate timing and parameters of future eruptions to be determined.

Type of volcanic feature	Identification criteria			Type of volcanic feature	Identification criteria	
	1	2	3		1	3
Multieruption volcanoes				Multieruption volcanoes		
1. Shiveluch (Molodoi Shiveluch)	+	+	+	1. Alaid	+	+
2. Klyuchevskoi	+	+	+	2. Shirinki?	-	-
3. Bezmyanni (Novyi Volcano)	+	+	+	3. Ekarma	+	+
4. Ploskii Tolbachik	+	+	+	4. Chirinkotan	+	+
5. Ushkovskii, Ploskaya Dal'nyaya Volcano	-	-	+	5. Raikoke	+	+
6. Kizimen	+	+	+	6. Broutona?	-	-
7. Vysokii	-	+	+	7. Ebeko	+	+
8. Komarova	-	+	+	8. Chikurachki	+	+
9. Gamchen	-	+	+	9. Tatarinova	+?	+
10. Kronotskii	+?	-?	-	10. Karpinskogo	+?	+
11. Krashennikova	-	+	+	11. Rasshua	+	+
12. Kikhpinych (Savich Cone)	-	+	+	12. Ketoï	+	+
13. Taunshits	-	+	-	13. Prevo Peak	+	+?
14. Mali Semyachik	+	+	+	14. Chernogo	+	+
15. Karymskii	+	+	+	15. Snou	+	+
16. Zhupanovskii	+	+	+	16. Brat Chirpoev	+	+
17. Koryakskii	+	+	+	17. Medvezhii-Kudryavii	+	+
18. Avacha (Molodoi Cone)	+	+	+	18. Chirip	-	+
19. Opala	+	+	-?	19. Bogdana Khmel'nitskogo	+	+
20. Gorelyi	+	+	+	20. Atsonupuri	+	+
21. Mutnovskii	+	+	+	21. Tyatya	+	+
22. Khodutka	-	+	-	22. Berutarube	+	+
23. Ksudach (Shtyubel' Cone)	+	+	-?	23. Severgina	+	+
24. Zheltovskii	+	+	+	24. Goryashchaya Sopka	+	+
25. Il'inskii	+	+	-?	25. Mendeleeva	+	+
26. Dikii Greben'	-	+	-	26. Sinarka	+	+
27. Kosheleva	+	+?	+	27. Ushishir	+	+
28. Kambal'nyi	+	+	-	28. Ivan Groznyi	+	+
29. Khangar	-	+	-	29. Golovnina	+	+
30. Ichinskii	-	+?	+	30. Fuss Peak	+	+?
Other volcanic features				31. Nemo Peak	+	+
A. Regional zones of cinder cones				32. Krenitsyna Peak	+	+
31. Tolbachik	+	+	+	33. Sarycheva Peak	+	+
32. Ploskie Sopki	-	-?	-	34. Berga	+	+
B. Fields of basaltic sheet volcanism				35. Trezubets	+	+
33. Tolmachev Dol	-	+	-	36. Kolokol?	+?	+?
34. Basin of Srednyaya and Levaya Avacha rivers	-	+	-	37. Baranskogo	+?	+
35. Northern Sredinnyi Range (at least 2-3 fields)	-	+	-	38. Teben'kova	-	+?
C. Fields of concentrated multivert extrusive volcanism				39. Stokap?	-	+?
36. Bol'shoi Semyachik	-	+?	-?	Other volcanic features		
D. Calderas				A. Calderas		
37. Lake Karymskii	+	+?	-?	40. Tao-Rusyr	+	+
38. Gorelyi	-	+	-?	41. Zavaritskogo	+	+
39. Opala	-	+	-	B. Underwater marine centers		
40. Ksudach V	+	+	-?	42. 1924	?	+?
41. Lake Kuril'skoe-Il'inskii	-	+	-?	43. 1967	+	?+

Table 1.2.11.1. Active and potentially active volcanic features of Kamchatka after [Melekestsev, 2006; Noveishii..., 2005] (1) documented historical eruptions; (2) eruptions during the last 3500 years dated by geological methods; (3) fumarole activity during the last few centuries; + present, - absent, ? checking and updating needed; parentheses enclose the active volcanic edifice

Table 1.2.11.2. Active and potentially active volcanic features on the Kuril Islands after [Vlodavets et al., 1957; Gorshkov, 1967] with this author's additions 1 documented historical eruptions, 3 fumarole activity during the last few centuries; + present, - absent; ? checking and updating needed.

(3) Groups of volcanoes have been identified which are in phase I (high and moderate activity and a growing volcanic edifice) and in phase II (low volcanic activity and the edifice beginning to disintegrate). Many of the active volcanoes in Kamchatka are in phase I. Klyuchevskoi, Bezymyannyi, Karymskii, Malyi Semyachik, and Ksudach volcanoes are in the first period of activity of the current cycle. Klyuchevskoi and Karymskii will show the current eruptive behavior for the nearest few hundred years. Bezymyannyi Volcano will produce eruptions for 100–200 years that have been typical of it after 1956, and which have built up Novyi dome and Novyi Bezymyannyi Volcano. Malyi Semyachik and Ksudach can produce violent eruptions in the near future. Krasheninnikova, Kikhpinych, and Kizimen volcanoes are in the period of relative repose of the current cycle. For Krasheninnikova the period will last a few hundred years, while for Kikhpinych the forecast is not as accurate: perhaps a few thousand years, or else an eruption can occur in the near future. A catastrophic eruption is expected for Kizimen Volcano during the nearest 50–100 years. Also for Ksudach, a large eruption can be expected in the nearest future.

(4) Predicting the future activity for volcanoes in phase II is difficult. In some cases, e.g., for Mutnovskii, the forecast can be sufficiently accurate. In other cases, where the volcano's eruptions have been infrequent and irregular, the forecast becomes indeterminate or else positively impossible.

(5) Reconstruction of the eruptive history for the active volcanoes of Kamchatka has revealed that their activity frequently contains long repose periods of 1000–3000 years; after such periods the volcano may resume its activity and remain active. The longest intermission we have found is 3500 years. It is therefore proposed to classify only those volcanoes as active that have had at least one eruption for the last 3000–3500 years reliably identified and dated. Tephrochronologic studies with radiocarbon dating have confirmed that Krasheninnikova and Kikhpinych were correctly classified as active, even though no evidence was available for historical eruptions on these volcanoes. We suggest setting up a subgroup of those active volcanoes, among the active ones, for which there are documented historical eruptions or the presence of fumarole activity, and a subgroup of potentially active volcanoes for which no such evidence is available, but their eruptions have been identified by geological methods and dated for the last 3500 years. The second group of active volcanoes should include Taunshits, Khodutka, Dikii Greben', and Khangar volcanoes, which are considered extinct and are absent from the catalogs.

Melekestsev I. V. The Identification and Diagnostics of Active and Potentially Active Volcanic Features in the Kuril–Kamchatka Island Arc and the Commander Islands Link of the Aleutian Arc. Journal of Volcanology and Seismology, 2009, Vol. 3, No. 4, pp. 221–245.

Melekestsev, I.V., Active and Potentially Active Volcanoes in the Kuril–Kamchatka Island Arc in the Beginning of the 21st Century: Periods of Research, Defining the Notion “Active Volcano,” Future Eruptions and Volcanic Hazard, Vestnik KRAUNTS, Ser. Nauki o Zemle, 2006, issue 7, no. 1, pp. 15–35.

Melekestsev I., Zaretskaya N., Gelichinsky M., Melnikov D., Inbar M. A morphometric and morphological study of cinder cones and their erosion in arid and humid conditions // International Geological Congress 2008, 6-14 August 2008, Oslo. Abstract 1338153).

1.2.12. Marine geological-geophysical researches

Seliverstov N.I., *Institute of Volcanology and Seismology FED RAS, Petropavlovsk-Kamchatski, Russia*

The review on the marine geological-geophysical researches, conducted in Kamchatka-Komandor region was presented. The relief of the sea floor, sediments structures and anomalous magnetic field of the area around the Kamchatka were analyzed in details. It was considered their main peculiarities of the geological construction and recent tectonics. The complex analysis was conducted on the results of morphologic structures studies and data of geothermal, gravimetrical, seismic and GPS observations. Based on this analysis, new ideas were elaborated about the geodynamics of the junction zone of the Kurile-Kamchatka and Aleutian island arcs in conception of lithospheric plates. Using the spatial analysis of the seismofocal zone it was confirmed the existence of the double seismofocal layer below Kamchatka. The ideas about deep aquation in the near Kamchatka water area of the Pacific plate taking into account the regional peculiarities of its structure were considered. It were discussed the possible geodynamical consequence of this event. As the scientific hypothesis it was considered the paleogeodynamical scheme of Neozoic history of the region development. It were represented the main positions of the hydro- convection hypothesis of the island arc magmatism. It was shown the close connection of the strongest volcanological events and the regressive stages of the glacioeustatic cycles in Pleistocene along the western border of the Pacific ocean. It were considered the possible mechanisms of the global hydrosphere processes influence on the volcano activity.

Seliverstov N.I., The geodynamics of the junction zone of the Kurile-Kamchatka and Aleutian island arcs. Petropavlovsk-Kamchatsky: KamGU of Vitus Bering, 2009, 191 p. (in Russian)

1.3. Complex research of the active volcanoes of the Eastern Volcanic Front of Kamchatka and Kurile volcanic arc in 2007-2010

1.3.1. Chikurachki volcano (Kurile arc)

O.A.Girina, girina@kscnet.ru, *Institute of Volcanology and Seismology FED RAS, Petropavlovsk-Kamchatski, Russia*

N.A. Malik, L.V. Kotenko, *Vitus Bering Kamchatkan State University, Petropavlovsk-Kamchatsky, Russia*

Chikurachki volcano resumed its eruptive activity in 2002 after strong explosive-effusive eruption in 1986. Over the period of 2002-2007: in 2002, 2003, 2005 and twice in 2007, the volcano produced five moderate explosive eruptions. The longest volcano eruption was observed in 2002 and the strongest in 2003. During this period ash column rose up to 6 km ASL (2003), ash plumes extended for 700 km from the volcano. Since 2002 Kamchatkan Volcanic Eruption Response Team staff in the Institute of Volcanology and Seismology FEB RAS has been realizing continuous satellite and episodic visual monitoring of the volcano and recording possibly any changes in its activity.

Girina O.A., N.A. Malik, L.V. Kotenko. 2002-2007 ACTIVITY OF CHIKURACHKI VOLCAN (PARAMUSHIR ISLAND, NORTHERN KURILES) BASED ON KVERT DATA. Vestnic KRAUNC. Nauki o Zemle, 2008, N 1, issue 11, pp. 67-73 (in Russian)

1.3.2. Koriaksky volcano

Girina O.A., girina@kscnet.ru, **Manevich A.G.**, **Melnikov D.V.**, **Nuzhdaev A.A.**, **Ushakov S.V.**, **Konovalova O.A.**, *Institute of Volcanology and Seismology FED RAS, Petropavlovsk-Kamchatski, Russia*

The activity of the Koriaksky volcano in 2008-2009 was studied. It was shown that during three periods in steam-and-gas clouds the ash existed, which means that volcano was dangerous for aviation: 23th-28th of December 2008 г., from 4th of March to 18th of Aprile and 13th-27th of August 2009. The highest altitude of ash-bearing steam-and-gas clouds was 5.5 km above the sea level, the maximal distance of clouds out of volcano was up to 680 km. In general the activity of the Koriaksky volcano in 2008-2009 was very similar to it's eruption in 1956-1957.

Girina O.A., Manevich A.G., Melnikov D.V., Nuzhdaev A.A., Ushakov S.V., Konovalova O.A. The activity of the Koriaksky volcano in 2008-2009 from October 2008 to October 2009 according to KVERT data. In press.

1.3.3. Karymshina, a Giant Supervolcano Caldera

Leonov V. L. & A. N. Rogozin, lvl@kscnet.ru, *Institute of Volcanology and Seismology FED RAS, Petropavlovsk-Kamchatski, Russia*

The new caldera (Figs. 1.3.3.1, 1.3.3.2) discovered in 2006, formed in southern Kamchatka during Eopleistocene time (1.2 to 1.5 Ma). The caldera boundaries have been reconstructed and its dimensions determined (approximately 15-25 km). An uplifted block has been identified in the northwestern part of the caldera, the block is considered to be the result of emplacement of viscous rhyolite magmas at a later time (approximately 0.5-0.8 Ma), that is, as a resurgent uplift. We have reconstructed the boundaries of a large lacustrine basin that formed in the caldera after the appearance of the resurgent uplift. Calculations are provided yielding the volume of the pyroclastics ejected during caldera generation. It is shown that the caldera-forming eruption was a major one in Kamchatka in regard to its volume of ejected material, and ranks as a major eruption worldwide. We examined the structural controls of present-day hydrothermal systems and mineral occurrences situated in the area of study to demonstrate their relations to the caldera and the resurgent uplift.

A new large caldera has been identified in the area of the Karymshina volcanic complex previously recognized in southern Kamchatka, and its dimensions have been determined (15 * 25 km). The caldera is not identical with the volcanotectonic depressions identified previously in the area of study, viz., the Karymshina and Bannaya–Karymshina depressions, so it has been given a new name, the Karymshina caldera.

A tectonic uplift has been reconstructed in the northwestern part of this caldera, the uplift being regarded as a resurgent dome. The uplift has been found to be 4 by 12 km in size and to be elongate northwest. The uplift amplitude was estimated as 200 m. The uplifted block is bounded by straight northeast and northwest trending faults. We also reconstructed the boundary of a lake that had existed in the caldera south of the resurgent uplift.

It was found that the Karymshina rocks (mostly acid tuffs and ignimbrites) that fill the caldera are everywhere adjacent to the lavas that compose the volcanoes of mounts Goryachaya, Yagodnaya, Levaya Karymchina, etc., which extend in a band trending northwest along the

western boundary of the caldera. It has thus been unambiguously established that the above volcanoes are older and must be considered as evidence of a major volcanic phase that preceded the caldera generation.

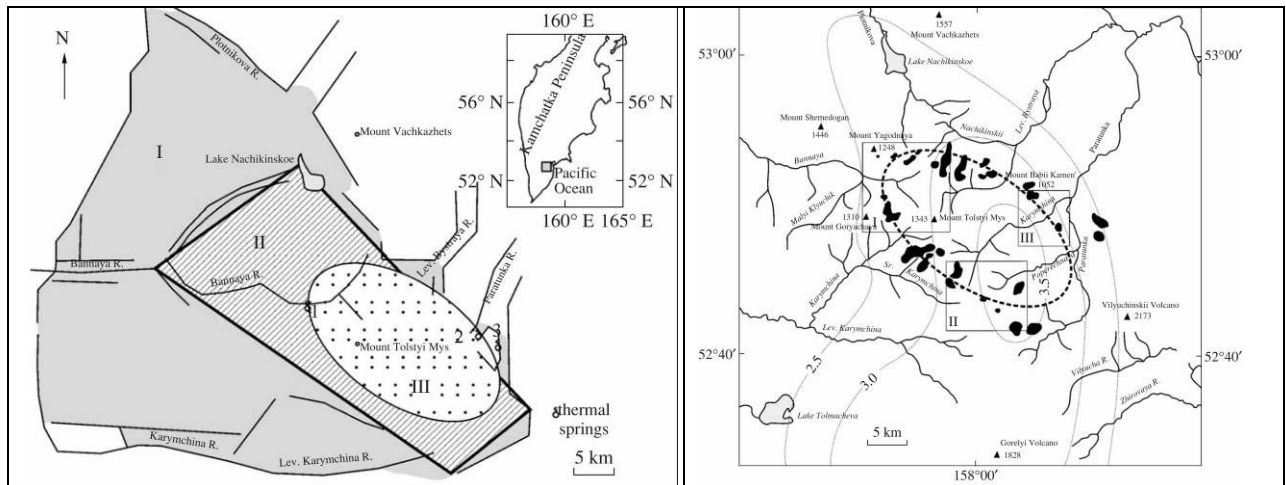


Fig. 1.3.3.1. Position of the Karymshina caldera and comparison with the volcanotectonic depressions that have previously been identified in the area: (I) Karymshina volcanotectonic depression, (II) Bannaya–Karymshina volcanotectonic depression, (III) Karymshina caldera (identified in this study for the first time). (1, 2, 3) Groups of thermal springs: (1) Bol’she-Bannaya, (2) Karymshina, (3) Verkhne-Paratunka. The inset in the top right corner shows the location of the area of study in Kamchatka.

Fig. 1.3.3.2. Reconstructed boundaries of Karymshina caldera (solid dashed line). Rectangles mark areas that have been studied in detail: (I) upper reaches of Bannaya R., (II) Karymshina–Karymshina pass, (III) Babii Kamen’. Black spots mark rhyolite extrusions that were emplaced during the postcaldera phase. Light dotted lines are isolines of depth to top of Cretaceous basement, in km.

New data were obtained on the setting of the rhyolite domes widely abundant in the area of study. It was shown that they are mostly confined to the boundaries of the caldera and to the boundary of the resurgent dome situated in it. Most of the domes were emplaced much later following caldera generation, they have ages of 0.5–0.8 Ma [19, 20], and they should be regarded as a consequence of postcaldera volcanism. We also identified a postcaldera basaltic volcanic phase whose manifestations are strictly confined to the boundary of the resurgent dome. An approximate volume of material erupted during the generation of the caldera has been calculated, viz., about 825 km³, which makes a weight of 2 * 10¹⁵ kg. This eruption should therefore be regarded as the largest so far known to have occurred in Kamchatka and be classed among the great eruptions worldwide.

The structural setting of the present-day hydrothermal systems in the area of study has been revised. It is shown that all larger hydrothermal systems (the Bol’she-Bannaya, Karymshina, and Verkhne-Paratunka ones) are confined to the boundaries of the Karymshina caldera. A new approach has also been advocated for determining the controls of the mineral occurrences and ore deposits known in the area. It is shown that the identification of the Karymshina caldera makes it possible to regard these ore deposits as a consequence of the existing large magma chamber above which the caldera was generated.

Leonov V. L. & A. N. Rogozin. Karymshina, a Giant Supervolcano Caldera in Kamchatka: Boundaries, Structure, Volume of Pyroclastics. *Journal of Volcanology and Seismology*, 2007, Vol. 1, No. 5, pp. 296–309.

1.3.4. Karimsky volcanic center

Tectonics

Leonov V. L., lvl@kscnet.ru, Institute of Volcanology and Seismology FED RAS, Petropavlovsk-Kamchatski, Russia

Unusual (for this location) events occurred near Karymskii Volcano, Kamchatka in early January of 1996: a magnitude 6.9 earthquake, the simultaneous eruptions of two volcanoes, and the generation of extensive ground breakage. This paper is concerned with the breaks, specifically, their positions, structure, and the character of the displacements. The breaks were studied with the help of trenches that were dug across them to expose their internal structure. Crosswise profiles were constructed on some of the breaks to analyze the variation of their geometry along the strike. This work revealed the specific features of the displacement episodes and whether these episodes were multiple ones, established their sequence, and suggested a mechanism of their generation and the overall mechanism responsible for the deformation observed.

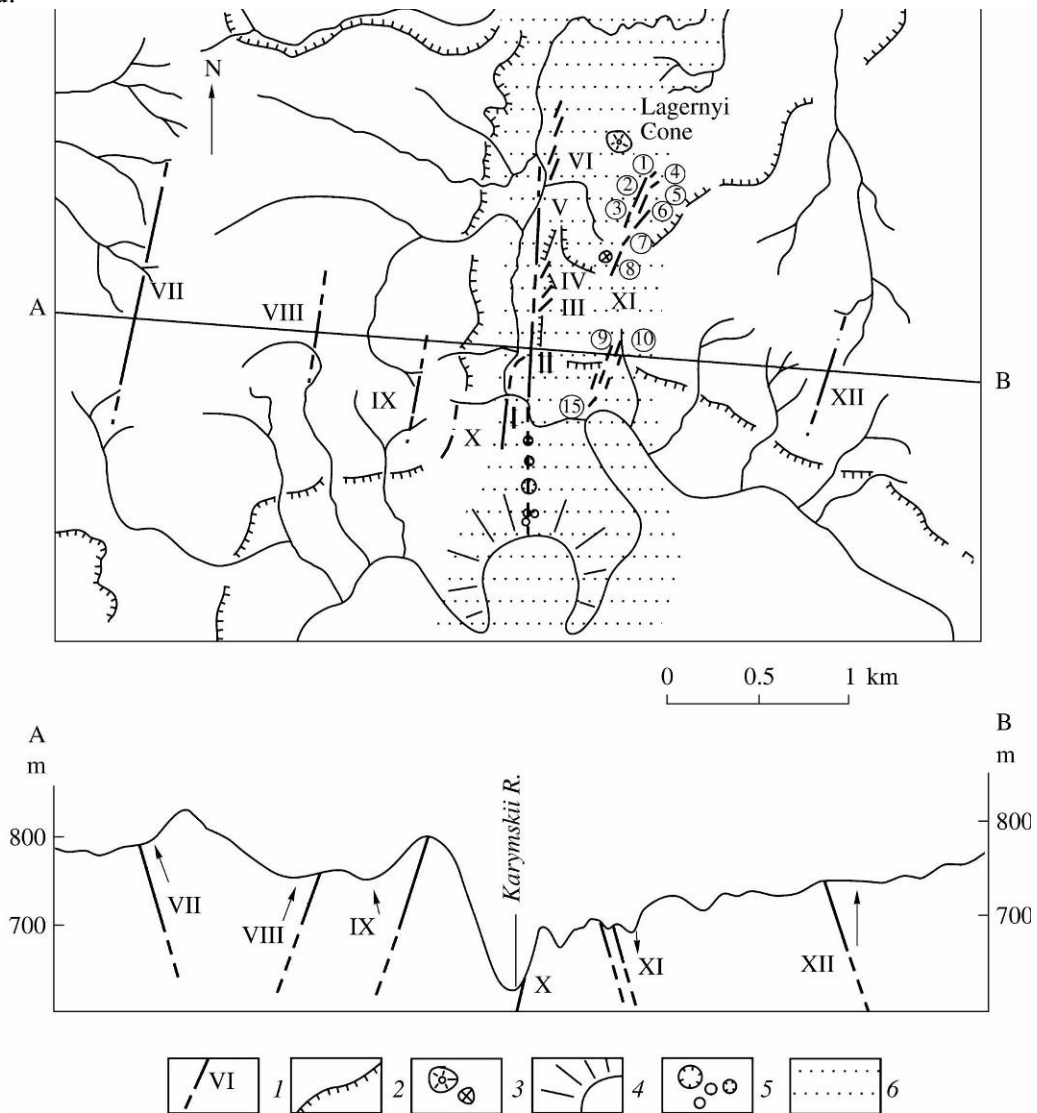


Fig. 1.3.4.1. The area of the largest surface breaks generated in early January 1996: (1) fault and its identification number [see also Leonov, 2009], (2) erosion scarps that bound the calderas (from above and from below) and the Karymskii River valley (at the center), (3) cinder cones and necks, (4) the main center of the eruption occurring in Lake Karymskii January 2–3, 1996, (5) minor explosive and collapse pits forming near the main center of lake Karymskii eruption, (6) north–south zone of extension and subsidence.

Most breaks that appeared near Karymskii Volcano in early January 1996 are reverse faults, the relevant movements frequently combining reverse and extensional displacements. Of lesser importance are the faults with normal displacements, all of these being confined to a narrow north–south zone in the center of the area that has experienced the deformation.

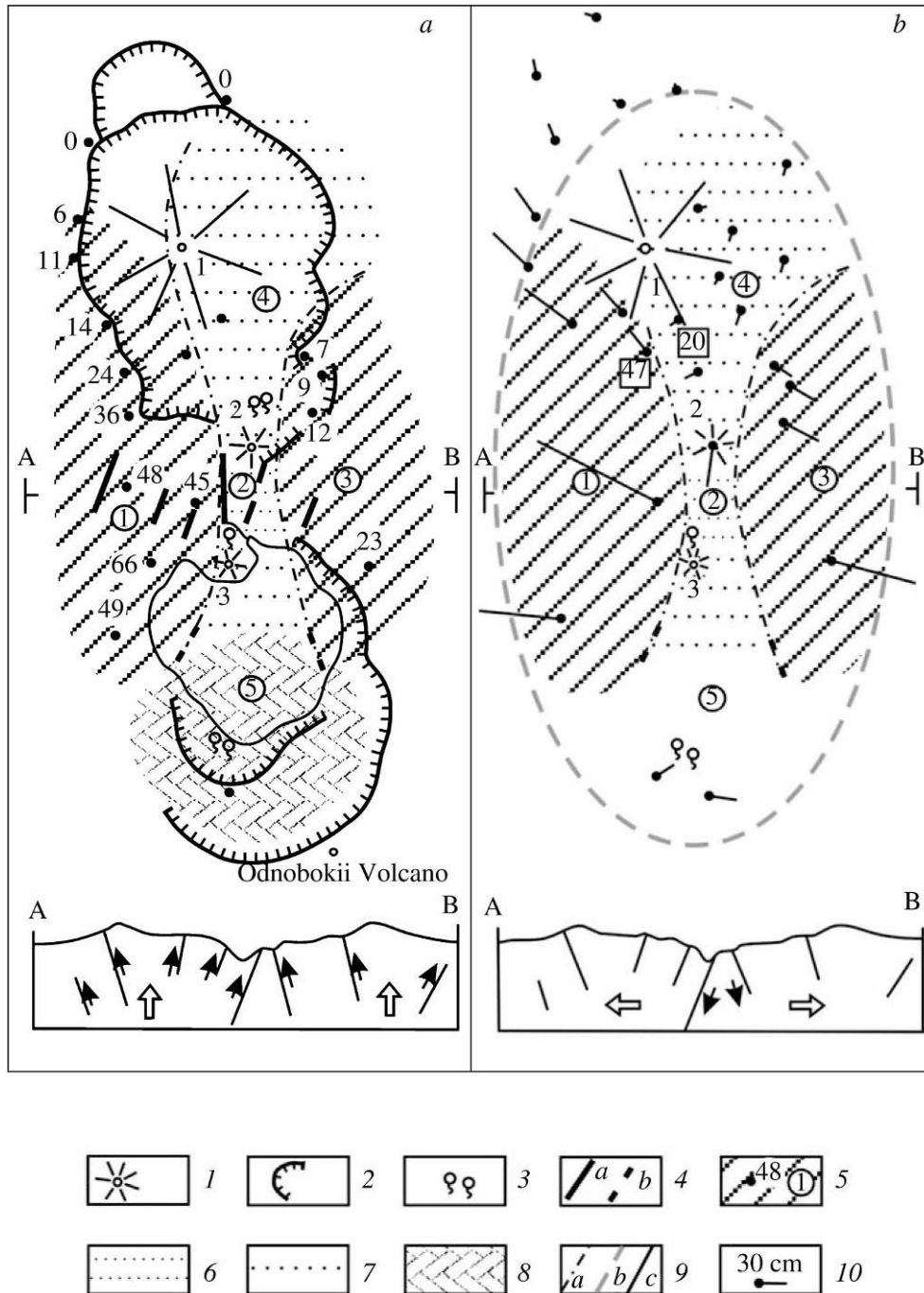


Fig. 1.3.4.2. Block movements near Karymskii Volcano in early January 1996 (*a* uplifts and subsidences during the first phase of deformation; *b* horizontal displacements occurring during the second phase of deformation). (1) Holocene volcanoes: (1) Karymskii, (2) Lagernyi, (3) main center of the 1996 eruption in Lake Karymskii); (2) calderas, (3) thermal springs, (4) faults : *a* certain, *b* inferred, (5–8) areas where block movements have been identified: (5) uplifts and northward tilts, a numeral in a circle denotes the identification number of a block, numerals in squares on the right of the figure are identification numbers of observation sites referred to in the text), (6) subsidences with amplitudes of up to 1.5–2.0 m and westward tilts, (7) subsidences with amplitudes of below 15 cm, (8) block of Akademii Nauk Volcano (a series of arcuate cracks formed along its boundaries, data on vertical movements are not available), (9) lines that bound: (*a*) uplifted and subsided areas, (*b*) area where block movements have been identified (in outline), (*c*) faults in cross-sections (arrows indicate the sense of movement on the faults), (10) direction and amplitude of horizontal movements. Large arrows in the cross-sections indicate the hypothetical block displacements during the first (*a*) and second (*b*) phases of deformation.

The breaks mostly have north–northeast orientations (about 20° NNE). Faults with other directions (north–south, northeast, and northwest) are less frequent and occur only in the zones of older faults that have been called to life by the deformation.

The movements are blocky, the blocks (mostly 1 to 4–5 km across) were not new formations; all of these were formed during the preceding phases in the evolution of the area. The block movements were not uniform: some of these were uplifting, some subsiding, and still others moved horizontally.

It has been found that the faulting occurred in two phases in the area of study. The first phase was to produce reverse faults upon the background of a general uplift in the area. The second phase involved a subsidence of some territory in the middle of the study area and some horizontal displacements; the resulting faults were reverse and extensional.

A likely mechanism has been suggested to explain the deformation. The fractures and block movements in the upper 3–4-km crustal layer are supposed to have occurred as a result of the top of a shallow magma chamber (which had a large area and a flat, sill-like shape) being broken through. The breakthrough, which was occasioned by increased pressure inside the chamber, was accompanied by eruptions and large earth- quakes (with magnitudes as large as 6.9). After the breakthrough in the chamber top the axes of principal stresses were reoriented and conditions arose to favor magma emplacement in horizontal directions. The orientation of the new faults is supposed to be controlled by the regional stress field that exists in the upper crust of Kamchatka.

Leonov V. L. The Faults That Appeared near Karymskii Volcano, Kamchatka on January 1–2, 1996: The Geometry and Mechanism of Generation. Journal of Volcanology and Seismology, 2009, Vol. 3, No. 3, pp. 150–167.

Geodesy

Magus'kin M. A., S. A. Fedotov, karetn@list.ru, V. I. Andreev, Institute of Volcanology and Seismology, Far East Division, Russian Academy of Sciences, Petropavlovsk-Kamchatsky, 683006

Levin V. E., V. F. Bakhtiarov, Kamchatka Branch, Geophysical Service, Russian Academy of Sciences, Petropavlovsk-Kamchatskii, 683006 Russia

A network of interconnected stations was established in the entire area of the Karymskii Volcanic Center and near the active Karymskii Volcano, Kamchatka in 1971–1988 for the purpose of studying ground deformation. Multiple observations by this network yielded quantitative characteristics of the ground deformation related to the following phenomena: the

eruption of Karymskii Volcano during the periods 1976–1982 and January 1, 1996, to 2005 (still continuing, written in February 2008); the discharge of basalt on January 2, 1996, in the bottom of Lake Karymskii situated in the caldera of Akademii Nauk Volcano (this volcano had previously been thought to be extinct) and the subsequent phreatomagmatic eruption lasting approximately 24 hours; and the large (M6.9) earthquake of January 1, 1996, occurring at 21 h 57 min local time in the Karymskii Volcanic Center at a depth of ~10 km. This paper discusses the relationships of ground deformation to volcanic activity and to the abovementioned unique natural occurrences, and their mechanism as deduced from geodetic data.

(1) The ground deformations in the Karymskii Volcanic Center were due to increasing pressure in the associated magma chamber during the period from 1972 to 1995 (the center of the chamber is at a depth of about 18 km) and to three almost simultaneous events: the shallow magnitude 6.9 earthquake, the start of the next (after a 13-year repose period) eruption on the andesite–dacite Karymskii Volcano, the outbreak of basalts, and the short-lived eruption in the caldera of Akademii Nauk Volcano generating surface breakage (cracks).

(2) The 1988 geodetic measurements revealed deformations (as large as $8 \times 10^{-6} \text{ yr}^{-1}$) that were extending the ground surface mostly east–west in the area between the calderas of Karymskii and Akademii Nauk volcanoes and farther south. The deformations continued in 1992–1995 and were precursors to the 1996 eruption in the area.

(3) The successive period of activity on Karymskii Volcano lasting from 1996 until now (February 2008) was preceded by a mostly northeast ground extension around the volcano's cone at a rate of $3.5 \times 10^{-6} \text{ yr}^{-1}$. The extension may have begun in 1991. The base of the volcano's cone was subsiding at a rate of 5 mm per year in 1991–1993, but arises by 5 mm in 1995 compared with 1992. The rise was a precursor to the eruption of Karymskii Volcano.

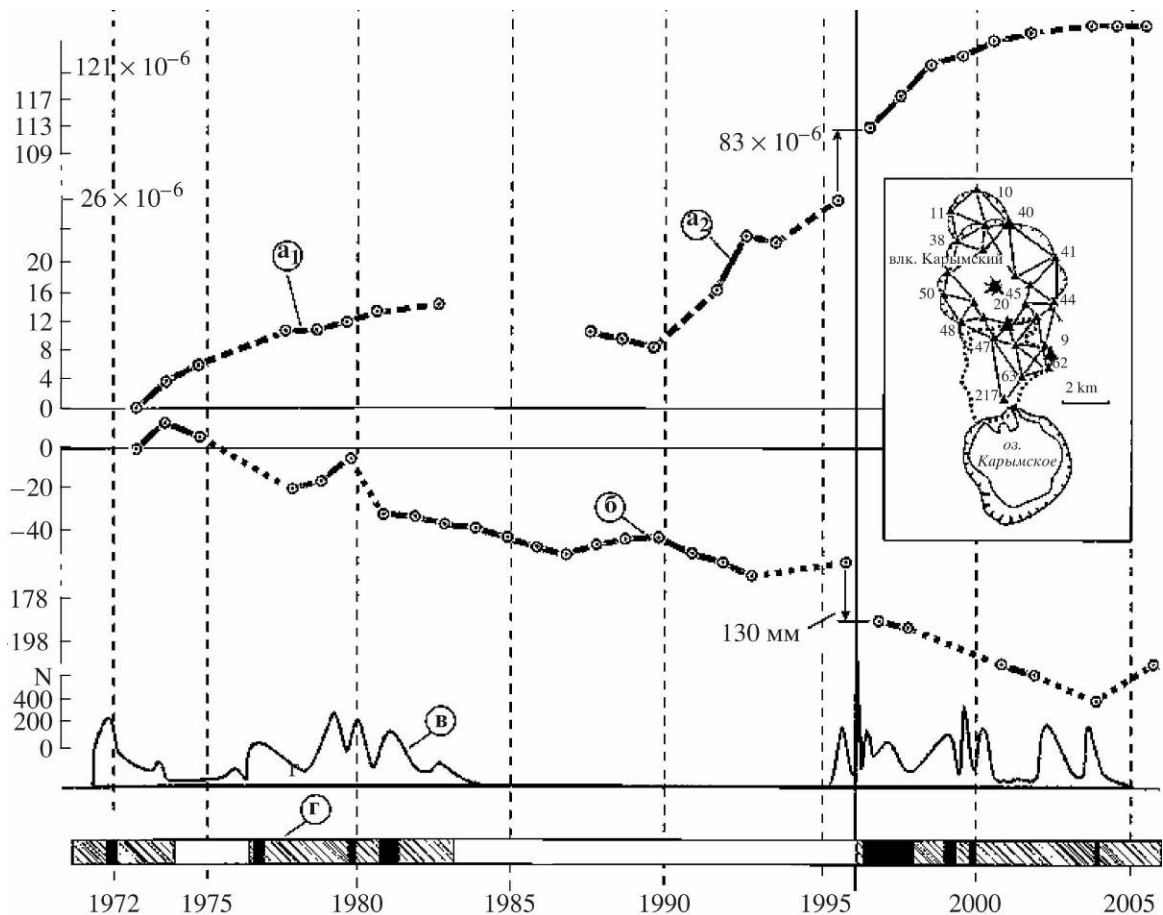


Fig. 1.3.4.3. Ground movements and the volcano's activity compared for 1972–2005: (a₁) mean value of changes in the lengths of lines (in 10⁻⁶) of the triangulation network around the volcano's cone delimited by the stations 48–50–38–11–10–40–41–44–9–47, (a₂) same for the area delimited by the stations 20–45–44–9–62–63–217–47, (b) vertical displacements of benchmark 20 relative to station 40 for the period 1972 to 1996, and relative to benchmark 9 for the period 1996 to 2005, (c) daily number of explosion earthquakes; (d) volcano's activity: (I) repose phase, (II) phase of explosive eruption, (III) phase of effusive–explosive eruption. The inset shows the triangulation network and the leveling line.

(4) The 1996–2003 eruption of Karymskii Volcano was occurring in an extensional and subsiding environment existing around the volcano's cone and caldera. An extension was occurring at a rate of $4.1 \cdot 10^{-6} \text{ yr}^{-1}$ during the period April 1996 to October 1998 in a 3*5 km area situated southeast of the volcano's cone and containing hot springs in a cuplike valley 1–2 km from the source of the Karymskii River. The extension was decreasing from 1999 to 2003, the average rate was $+1.8 \cdot 10^{-6}$. No significant (above the uncertainty) horizontal movements were found to occur between October 2003 and October 2005. At the same time, leveling revealed a beginning of uplift affecting the southeastern base of the volcano's cone. The benchmark arise +15 mm during these two years (Fig. 1.3.4.3).

(5) The epicenter of the magnitude 6.9 January 1, 1996, earthquake in the Karymskii Volcanic Center was situated near the region of compression for the upper crustal layers found from geodetic data.

(6) The greatest ground deformations observed by geodetic methods in the Karymskii Volcanic Center during the period 1972–2005 were horizontal extensions as large as 3 m occurring at the location where basalts were forced to the surface and discharged on January 2, 1996, between Karymskii and Akademii Nauk volcanoes. The distance between the vent of Karymskii Volcano and that of the phreatomagmatic eruption in Lake Karymskii, which erupted simultaneously on January 2, 1996, is equal to 6.5 km. The main fissure extending from the vent of the underwater eruption toward Karymskii Volcano is about 2.5 km long. This fissure of basalt penetration formed above the pressure center situated in the crustal magma chamber at a depth of 18 km.

(7) We conclude by noting that the deformation processes occurring in the Karymskii Volcanic Center can be comprehensively studied by continuous geodetic measurements conducted over the entire area. To a first approximation these processes can be found by discrete geodetic measurements. Continuous measurements are practically impossible without automatic equipment. Measurements in the entire area require considerable financial expenditures. Knowledge of the deformation and its further evolution over the entire area of the Karymskii Volcanic Center is important and necessary for understanding the processes responsible for magma emplacement in the upper crust, the depth, dimensions, and mechanism of magma chambers, and the mechanism of and hazards posed by volcanic eruptions.

Systematic measurements of the height of the summit crater rim on the active Karymskii Volcano showed that the variation of that parameter has been greater during its last eruption, lasting, with short intermissions, from January 1, 1996 until now (October 2007) compared with the earlier eruptions. The periodic increases in the height of Karymskii Volcano were due to explosion discharges of unconsolidated pyroclastic material, with most of this falling on the volcano's cone. The increased seismicity of Karymskii Volcano intensified the slope movement processes, resulting in a comparatively flat area forming periodically on the crater rim; during separate, not very long, periods the height of the volcanic cone was increasing in discrete steps and at a greater rate. The periodic decrease in the height of Karymskii Volcano is due to compaction of pyroclastic material and, to a much greater extent, after violent explosions which expand the crater by removing its nearsummit circumference. The other contributing

factor consists in sagging of the magma column due to partial emptying of the peripheral magma chamber, which makes the internal crater slope steeper, hence causes cone collapse and the cone lower. These occurrences are generally similar to the processes of crater and caldera generation described by previous investigators for other volcanoes of the world.

Magus'kin M. A., S. A. Fedotov, V. E. Levin, V. F. Bakhtiarov. Deformations Related to a Large (M=6.9) Earthquake, the Magma Discharge, and Eruptions in the Karymskii Volcanic Center in 1996–2005. Journal of Volcanology and Seismology, 2008, Vol. 2, No. 5, pp. 322–339.

Geochemistry

Grib E. N., *Institute of Volcanology and Seismology FED RAS, Petropavlovsk-Kamchatski, Russia*

Perepelov A. B., *Vinogradov Institute of Geochemistry, Siberian Branch, Russian Academy of Sciences, Irkutsk, 664033 Russia*

The olivine basalts of the Karymskii Volcanic Center (KVC) can be traced during the history of the area from the Lower Pleistocene until recently (the 1996 events); they are typical low- and moderate-potassium tholeiite basalts of the geochemical island-arc type. We have investigated the compositions of phenocryst minerals represented by plagioclase, olivine, clinopyroxene, as well as solid-phase inclusions of spinel in olivine, and more rarely in anorthite. The evolutionary trends of the rock-forming minerals provide evidence of the comagmaticity of these basalts, and thus of a long-lived intermediate magma chamber in the interior of the structure. The activity of this chamber is related to periodic transport of high temperature basalt melts to the surface. The geochemistry of the basalts is controlled by their origin at the same depleted magma source close to N-MORB, by successive crystallization of the primary melt, and by restricted mixing with magma components that are crystallizing at different depths. It is hypothesized that the solid-phase inclusions of high alumina spinel (hercynite?) found in olivine (and anorthite) of the basalts in the KVC north sector are of relict origin.

Grib E. N., A. B. Perepelov. Olivine Basalts at the Karymskii Volcanic Center: Mineralogy, Petrogenesis, and Magma Sources. Journal of Volcanology and Seismology, 2008, Vol. 2, No. 4, pp. 228–247.

Ecology

Karpov G. A., E. G. Lupikina, A. G. Nikolaeva, *Institute of Volcanology and Seismology FED RAS, Petropavlovsk-Kamchatski, Russia*

Bychkov A. Yu., S. A. Lapitskii, I. Yu. Nikolaeva, *Faculty of Geology, Lomonosov State University, Moscow, 119899 Russia*

The results of biohydrogeochemical monitoring are used to study time-dependent variations in the hydrogeochemical characteristics of the Lake Karymskii water mass, the state and characteristics of underwater discharge zones in the Tokarev crater (formed in 1996), hydrogeochemical characteristics of thermal springs around the lake, and the biota succession in the lake for the period 1996–2006 (2007). We detected a stratification in the chemical composition of water over depth and the presence of persistent zones of increased concentrations of dissolved oxygen. We found an alkalization of lake water and a decrease in its total salinity. The new thermal springs and underwater discharges of thermal water and gases were found to be continuing. The first data were obtained on the concentration of microelements in the thermal springs of the Karymskii basin. The biodiversity of algae in Lake Karymskii was largely

increased by the species diversity of benthic *Bacillariophyta*. The plankton phytocomponent of the precatastrophic period was found to have been regenerated in the lake as of April 2007.

Karpov G. A., E. G. Lupikina, A. G. Nikolaeva, Bychkov A. Yu., S. A. Lapitskii, I. Yu. Nikolaeva. The Time-Dependent Variation of Hydrogeochemical Characteristics, Thermal Regime, and Biocenoses in the Fresh and Thermal Waters of the Lake Karymskii Basin Following the Catastrophic Underwater Eruption of 1996 in the Akademii Nauk Caldera, Kamchatka. Journal of Volcanology and Seismology, 2008, Vol. 2, No. 5, pp. 303–321.

1.3.5. Cape Nalycheva and the Shipunskii Peninsula

Tsukanov N. V., *Shirshov Institute of Oceanology, Russian Academy of Sciences, Moscow, 119899 Russia*

Skolotnev S. G., *Geological Institute, Russian Academy of Sciences, Moscow, 109017 Russia*

Savel'ev D. P., *Institute of Volcanology and Seismology FED RAS, Petropavlovsk-Kamchatski, Russia*

The Vakhil' Uplift structure (Fig. 1.3.5.1) has different structural–material complexes combined tectonically. The formations of the Nalycheva sequence on Cape Nalycheva, the Kozlovskii and the Kubovskii suites in the Shipunskii Peninsula developed during Maastrichtian?–Eocene time within an active volcanic zone exhibiting a volcanism of the island arc type. This temporal phase is in good correlation with the active phase of volcanism in the Kronotskii and Kamchatskii Mys peninsulas. In the present-day structure of Kamchatka (inset in Fig. 1.3.5.1), the eastern peninsulas are separated from the eastern range composed of island-arc complexes of the Ozernovskii–Valaginskii segment of the Achaivayam–Valaginskii arc by the Vetlovskii complex-structured accretionary complex of backarc origin, which marks an Oligocene–Early Miocene collision suture in the presentday structure [Alexeiev et al., 2006].

The data we have obtained show that Cape Nalycheva is dominated by volcanic rocks of the moderately potassium calc-alkaline series. Comparison of the Cape Nalycheva magmatic rocks with those of the Shipunskii Peninsula shows certain differences. The Kozlovskii suite in the Shipunskii Peninsula mostly contains effusive rocks of the tholeiite island arc series, while the Kubovskii suite also contains representatives of the calc-alkaline series. In the character of their column and rock composition the formations of the Nalycheva sequence are similar to rocks of the Kubovskii suite found in the southern and eastern parts of the Shipunskii Peninsula. The structural setting of Cape Nalycheva (Fig. 1.3.5.1), which along with the Shipunskii Peninsula is a relative autochthon overthrust by the Vetlovskii allochthon, allows us to consider the volcanogenic complexes of these structures as a fragment of the southern segment of the Kronotskii paleoarc.

Earlier it was found that there are differences between the composition of Late Cretaceous volcanic rocks of the Kronotskii paleoarc found in the northern (Kamchatskii Mys and Kronotskii) segments and that the compositions of the Eocene island arc effusive within these segments are identical. The Upper Cretaceous island arc complexes in the Kamchatskii Mys peninsula are represented by island arc tholeiites. In the Kronotskii Peninsula, fragments of the arc are represented by plagiortholeiites of the Kamenistskii suite of Coniacian–Campanian–Maastrichtian age. The Eocene volcanic rocks found on Kamchatskii Mys and in the Kronotskii Peninsula are analogues and are represented by high alumina plagiortholeiites.

The magmatic rocks in the Shipunskii Peninsula and on Cape Nalycheva, which were generated simultaneously with the volcanic rocks found in the northern segment of the

Kronotskii arc, differ from these considerably. Rocks of the calc-alkaline series are widely abundant there, especially on Cape Nalycheva, and no plagiocliteites have been detected.

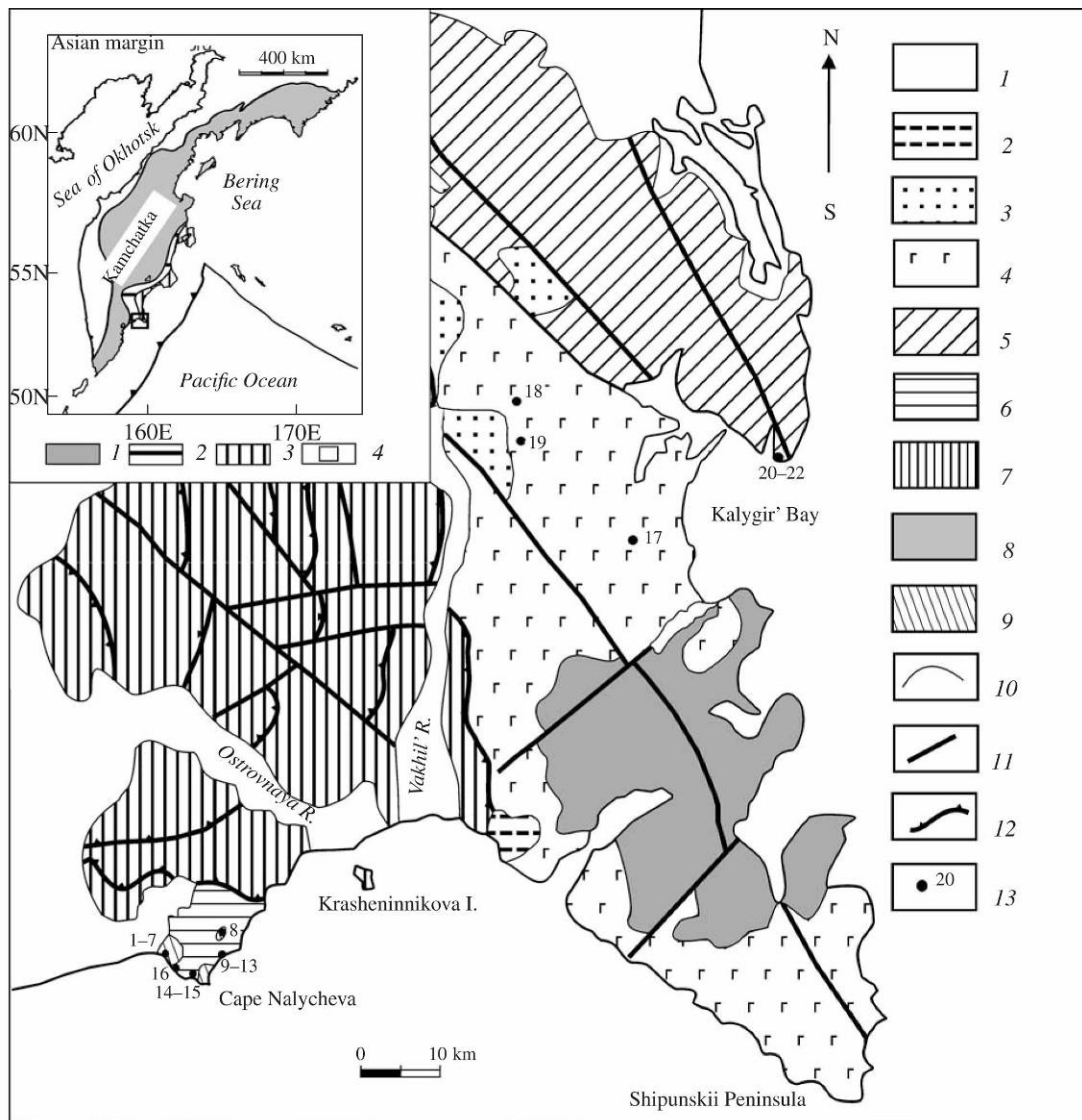


Fig. 1.3.5.1. A geological map of the Vakhil' Uplift after [6, 13] with these authors' modifications: (1) unstratified recent and Pliocene–Quaternary deposits, (2) Kornilovskii series (Miocene), (3) Tyushevskii series (Oligocene–Miocene), (4) Kubovskii suite (Eocene), (5) Kozlovskii suite (Eocene), (6) Nalycheva sequence (Maastrichtian?–Paleocene), (7) Vetlovskii complex, (8) Shipunskii gabbro–granodiorite intrusive complex (Oligocene), (9) subvolcanic andesite bodies in the Nalycheva sequence, (10) geological boundaries, (11) undifferentiated tectonic faults, (12) overthrusts, (13) sampling localities (numerals denote sample numbers corresponding to Table 1 in [Tsukanov et al., 2009]). The inset: (1–3) tectono-stratigraphic terrains: (1) Achaivayam–Valaginskii, (2) Vetlovskii, (3) of the eastern peninsulas, (4) area of study.

A change in the character of volcanism during the evolution of volcanic arcs and in different segments of the arcs is identified for many of these and is related to a change in the geodynamic regime in the subduction zone, and to the thickness and composition of the crust where the island arc originated [e.g. Avdeiko et al., 2003]. The Kronotskii paleoarc is ensimatic and was developing in an oceanic crust. This conclusion is corroborated by the tholeiitic character of island arc volcanism typical of the northern segments of the arc: the Kamchatskii

Mys and the Kronotskii, where the volcanism is specific to that locality. These specific features can be explained by the differences in geodynamic setting for different segments of the arc. In particular, the hypothesis was made that subduction for the Kula–Pacific spreading ridge occurred and the influence of the Hawaiian plume was hypothesized in the area of the Kamchatskii Mys segment [Skolotnev et al., 2009]. However, if the hypothesis that the island arc formations on Cape Nalycheva and in the southeastern part of the Shipunskii Peninsula are a common formational complex is correct, it follows that the differences between the southern and the northern segments of the Kronotskii paleoarc are greater. The calc-alkaline type of volcanism, mostly characteristic for the southern segment of the paleoarc, is evolving under different geodynamic conditions compared with the ensimatic arcs. Calc-alkaline volcanism is an indicator of maturity for this arc and of its originating in a thicker crust. More studies are required to elucidate the causes of calc-alkaline volcanism found in the southern Kronotskii paleoarc. One possible explanation may be the hypothesis that the Shipunskii segment of the Kronotskii paleoarc was superimposed on an older island arc system.

Alexeiev, D.V., Gaedicke, C., Tsukanov, N.V., and Freitag, R., Collision of the Kronotskiy Arc at the NE Eurasia Margin and Structural Evolution of the Kamchatka-Aleutian Junction, Intern. J. Earth Sci. (Geol. Rundsch.), 2006, vol. 95, no. 6, pp. 977–993.

Avdeiko, G.P., Savel'ev, D.P., Popruzhenko, S.V., and Palueva, A.A., The Principle of Uniformitarianism: Criteria for Paleotectonic Reconstructions for the Kuril–Kamchatka Region, Vestnik KRAUNTs, Ser. Nauki o Zemle, 2003, no. 1, pp. 32–59.

Tsukanov N. V., S. G. Skolotnev, D. P. Savel'ev New Evidence for the Composition and Structure of Volcanic Complexes on Cape Nalycheva and the Shipunskii Peninsula, Kamchatka. Journal of Volcanology and Seismology, 2009, Vol. 3, No. 1, pp. 18–26.

Skolotnev, S.G., Tsukanov, N.V., Savel'ev, D.P., and Fedorchuk, A.V., On the Compositional Heterogeneity of Island Arc Features in the Kronotskii and Kamchatskii Mys Segments of the Kronotskii Paleoarc, Kamchatka, Dokl. RAN, 2008, vol. 418, no. 2, pp. 232–236.

1.3.6. Kizimen volcano

Churikova T., tchurikova@mail.ru, **Ivanov B.**, ivanovbv@kscnet.ru, *Institute of Volcanic Geology and Geochemistry, Piip Avenue 9, Petropavlovsk–Kamchatsky, Russia.*

Wörner G., gwoerner@gwdg.de, *GZG Abteilung Geochemie, Universität Göttingen, Germany.*

Eichelberger J., jeichelberger@usgs.gov, *University of Alaska Fairbanks, Department of Geology and Geophysics Reichardt Building, Alaska, U.S.A. Currently at: U.S. Department of the Interior, U.S. Geological Survey, Office of Communication, 119 National Center, Reston, Va., 20192, U.S.A.*

Browne B., bbrowne@fullerton.edu, *Department of Geological Science, California State University, Fullerton, CA, USA*

Izbekov P., pavel@gi.alaska.edu, *Geophysical Institute, University of Alaska, Fairbanks, AK, USA*

Major and trace elements in whole rocks as well as major (Al, Si, Na, Ca, K), minor (Fe) and trace (Sr, Ba, Mg) elements in plagioclase phenocrysts were investigated in lavas from Kizimen volcano, Kamchatka. Quaternary Kizimen volcano was active during Holocene times and is intriguing in several aspects: (1) its lavas often contain unusually high proportions of incorporated basalt and basaltic andesite magma as enclaves; (2) banded texture is common in lavas; (3) large phenocrysts of plagioclase and hornblende associate with olivine and orthopyroxene in the same sample; (4) mafic enclaves and evolved dacites show a REE cross-over patterns; (5) MORB-like Sr-Nd isotope values exclude crustal contamination. Mafic

enclaves and host dacitic lavas are both hybrid and represented by mixtures of mafic and silicic end-members in different proportions. These end-members are likely derivatives of the same basaltic parent assuming a significant amount of amphibole fractionation. To understand magma chamber processes of the Kizimen volcano and the origin of its magmas, we used major and trace element zoning patterns in plagioclase phenocrysts from mafic enclaves and evolved hosts. According to our data, mafic and silicic magmas maintain some identity as physically distinct domains, while sometimes exchanging only heat but at other times heat, melt, and crystals between them. Processes in the magma chamber that occurred before eruption are: (1) crystal growth and fractionation, (2) recharge and magma mixing, and (3) resumed crystallization in high-temperature dacite heated by mafic magma.

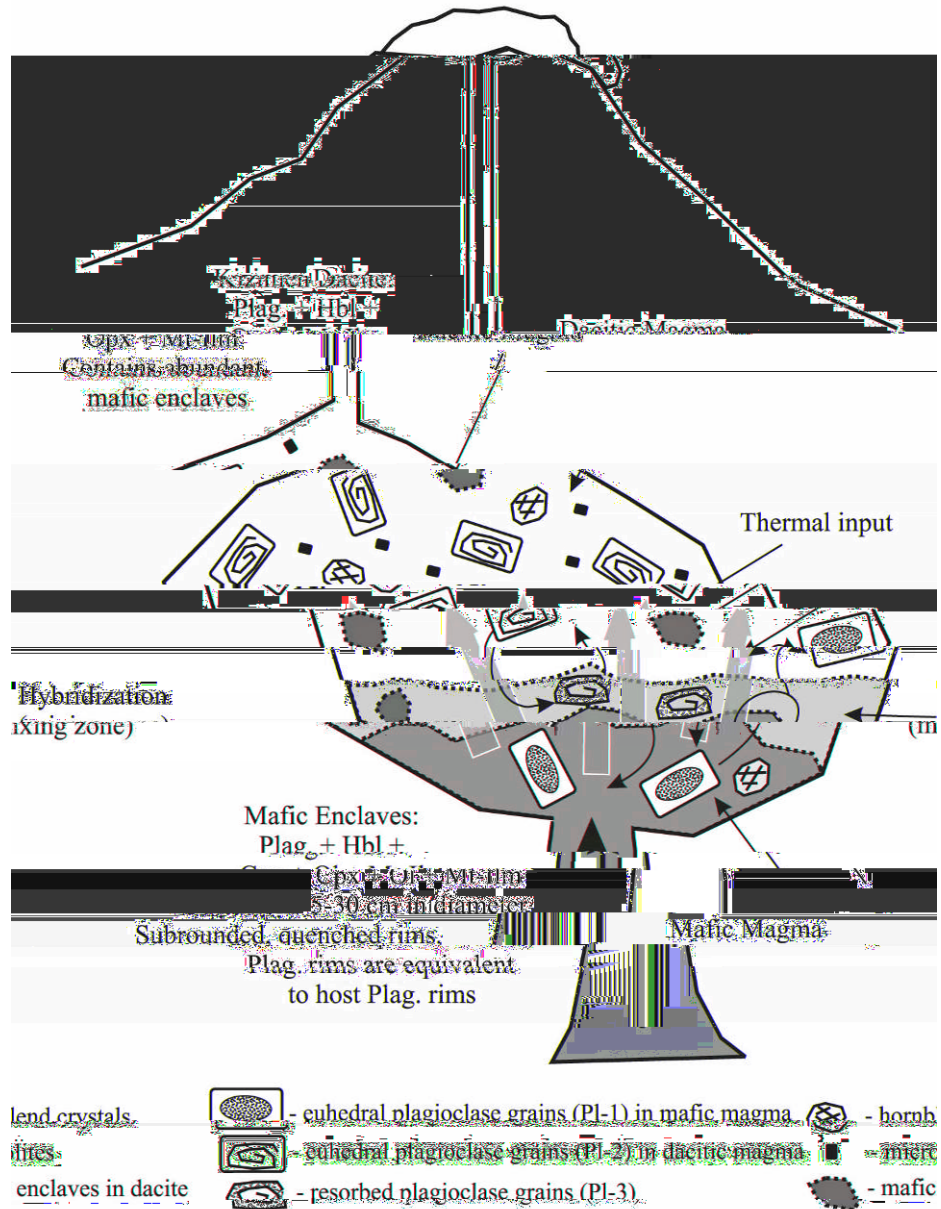


Fig. 1.3.6.1. Schematic cartoon illustrating different processes in magma chamber of the Kizimen volcano. Due to a recharge of the basaltic magma inside dacitic magma chamber interactions between two melts are complex. Melts and their crystals could be changed by direct physical and chemical mixing within the mixing zone forming hybrid magma and streaky lavas or by thermal conduction only. Mafic plagioclase grains from basalt would be not significantly influenced by these processes while acid

plagioclases would dissolve at higher temperature conditions and overgrow by new rims from surrounding hybrid and/or overheated melts. The movement of the plagioclase crystals are shown by arrows.

Based on textural evidence from plagioclase growth zones and major, minor and trace element contents, we conclude that:

1) All rocks of Kizimen volcano, including mafic enclaves, are hybrids and represent mixture of mafic and acid endmembers in different proportions. These end-members are likely to be derived melts from the same parental melt by crystal fractionation including amphibole.

2) The unusual negative correlation of Mg with An in high-An plagioclase can be explained by fractional crystallization of the high-Al basalt with Pl-only fractionation or by nonlinear behavior of KdMg in Pl-melt system.

3) Incomplete mixing maintains the physical identity of distinct, though somewhat hybridized, end-members. While (incomplete) chemical mixing is abundant, we also observe evidence for the transport of heat (or increased water content) only in the variation of An content in plagioclase at constant trace element concentrations.

4) The trend within mafic enclaves toward more mafic compositions with time at Kizimen indicates that generation (by fractional crystallization) of the evolved dacite is not keeping pace with mafic recharge and outputs are likely directly triggered by inputs.

All mentioned processes are schematically shown at the Fig. 1.3.6.1.

Using petrological experiments, an investigation of the pre-eruptive conditions (T, P and fO_2) of dacite magma erupted during the KZI cycle (12,000–8,400 years ago) of Kizimen Volcano was achieved. This cycle is the earliest, most voluminous, and most explosive eruption cycle in the Kizimen record. Titanomagnetite-ilmenite geothermometry calculations require that the dacite existed at a temperature of $823 \pm 20^\circ\text{C}$ immediately prior to eruption. Hydrothermal, water-saturated experiments on KZI dacite pumice reveal that at those temperatures the dacite was stable between 125-150 MPa. This estimate corresponds to a structural discontinuity between Miocene volcanoclastic rocks and Pliocene-Pleistocene volcanic rocks at a depth of 5-6 km beneath the Kizimen edifice, which may have facilitated the accumulation of dacitic magma below Kizimen during the KZI cycle.

Churikova T., Wörner G., Eichelberger J. Ivanov B. Minor- and trace element zoning in plagioclase from Kizimen volcano, Kamchatka: Insights on the magma chamber processes // Eichelberger John, Gordeev Evgenii, Izbekov Pavel, Kasahara Minoru, Lees Jonathan (eds.) / Volcanism and subduction: the Kamchatka region. Geophysical Monograph Series. Vol. 172. – Washington, DC: American Geophysical Union, 2007. – P. 303-324.

Browne B., Izbekov P., Eichelberger J., Churikova T. Pre-eruptive storage conditions of the Holocene dacite erupted from Kizimen Volcano, Kamchatka // International Geology Review. – 2010, vol. 52, no. 1. – P. 95-110. – DOI: 10.1080/00206810903332413

Churikova T., Ivanov B., Eichelberger J., Wörner G., Browne B., Izbekov P. Zonation on major- and trace elements in plagioclases of the Kizimen volcano (Kamchatka) as applied to the magma chamber processes // Volcanology and Seismology, in press.

1.3.7. Valley of Geysers

Gordeev, E.I.; Pinegina, T. K.; Droznin, V. A.; Dvigalo, V. N.; Melekestsev, I. V., Kiryukhin A.V., Muraviev J.D., murjd@kscnet.ru, Institute of Volcanology and Seismology FED RAS, Petropavlovsk-Kamchatski, Russia

The famous Valley of Geysers along with active volcanoes appears to be a beautiful visiting card of Kamchatka. It is well known in Russia and other countries as the most popular tourist place. Annually it is visited by thousands of Russian and foreign tourists. The Valley of

Geysers is the most potentially hazardous area in Kamchatka because of intense development of landslides, avalanches and frequent mudflows occurring within its boundaries. June 03, 2007 landslide, followed by a mudflow, resulted in a north - west faced horse-shoe amphitheater consisting of two adjacent cirques. The height of north-eastern sub-vertical wall is 150 m with a length 800 m; the length of a flatly inclined bottom 400 & 150; 600 m. Initially estimated volume of collapse and avalanche made up 8-15 millions cubic meters. Avalanching and formation of a dam at the Geysernaya River caused completion of some geysers and open thermal water discharge at sites blocked off by the avalanche and a dammed lake. However beyond the boundaries of the avalanche and the lake, the geysers are still operating. It is likely that some geysers could be brought back if water level in the lake decreases. Possibly new geysers could appear. Based on results of routine survey we estimated specific areas that nowadays pose a hazard as well as a possibility of new avalanches and landslides that may occur in the future. Estimation and forecast of new avalanches and landslides require continuous observations to be performed in the Valley of Geysers to monitor deformation and seismic processes.

Since 1990 cycling characteristics of five geysers (Maly, Bolshoy, Shel, Velican, Troynoy) were contentiously monitoring using automatic telemetric system (V A Droznin, <http://www.ch0103.emsd.iks.ru/>). The most powerful geyser Velikan erupted steam clouds at 300 m height. 1:20 UTC June 3-rd, 2007 lower basin of the Geysers Valley was in a few minutes buried under 10 mln m³ of mud, debris, and blocks of rocks. Some indications were found, that landslide triggered by steam eruption in the upstream area of Vodopadny creek. As a result of this three famous geysers (Pervenets, Sakharny, Troynoy) located at lower elevations were sealed under 10-30 m thick caprock as well as Vodopadny hot creek, a rock dumb trap Geysernaya river and lifted water into 20 m deep lake, which flooded three famous geysers (Conus, Bolshoy and Maly) terminating their cycling activity. Nevertheless Bolshoy and Maly activity continues in a form of discharge of water circulated in the former geysers channels and a clear plume at a lake surface above exits observed. Shortly after landslide continuous monitoring of the cycling characteristics of the upper basin geysers, including Velikan and lake level, accomplished by temperature loggers & 150; restarted. There are some indications time periods of the geysers cycling decrease.

Gordeev, E.I.; Pinegina, T. K.; Droznin, V. A.; Dvigalo, V. N.; Melekestsev, I. V. June 03, 2007 Natural Disaster in the Valley of Geysers in Kamchatka. Eos Trans. AGU, 88(52). 2007. Fall Meet. Suppl., Abstract T51A-0297

Droznin V.A., Kiryukhin A.V., Muraviev J.D. Geysers Characteristics Before and After Landslide June 3-rd 2007 (Geysers Valley, Kamchatka) // Eos Trans. AGU, 88(52). 2007. Fall Meet. Suppl., Abstract G41A-0146).

1.3.8. Ultra-depleted melts from Kamchatkan ophiolites

Portnyagin M., mportnyagin@ifm-geomar.de , *V.I.Vernadsky Institute of Geochemistry and Analytical Chemistry, Kosigin str. 19, 119991 Moscow, Russia; Leibniz Institute of Marine Sciences, IFM-GEOMAR, Wischhofstrasse 1-3, 24148 Kiel, Germany*

Hoernle K., *Leibniz Institute of Marine Sciences, IFM-GEOMAR, Wischhofstrasse 1-3, 24148 Kiel, Germany*

Savelyev D., *Institute of Volcanology and Seismology, Piip Boulevard 9, Petropavlovsk-Kamchatsky, 683006, Russia*

New data on the major and trace element composition of melt inclusions in spinel phenocrysts (Mg#=0.7–0.8, Cr/(Cr+Al)=0.32–0.52, TiO₂=0.06–0.60 wt.%) from Cretaceous MORB-like basalt (La/Yb=0.94, Th/Nb=0.055, Th/La=0.041) in the Kamchatsky Mys ophiolites

(Eastern Kamchatka) are reported. The melt inclusions preserved primitive melts (Mg# up to 0.72), which are remarkably depleted in incompatible trace elements compared to common MORBs. Numerous ultra-depleted inclusions from the studied sample have extraordinarily low Na₂O (0.20–0.67 wt.%), TiO₂ (0.16–0.5 wt.%), K (1.5–25 ppm), La (0.015–0.040 ppm), Zr (0.9–2 ppm), B (0.01–0.03 ppm), Ti/Zr=300–1074, La/Yb=0.008–0.075 and represent the most depleted melts known until now. The ultra-depleted melts from the Kamchatkan ophiolites are only comparable to a single melt inclusion from MORB of 9°N Mid-Atlantic Ridge [Sobolev and Shimizu, *Nature* 363 (1993) 151–154] yet have higher FeO, CaO, heavy rare-earth element (Dy, Er, Yb) contents and lower Na₂O and SiO₂. These melts, possibly the last melt fractions produced in an upwelling mantle column, could represent the highest degrees (up to ~20%) of near-fractional melting of mantle with $T_p \geq 1400$ °C, which started melting at ~75 km depth and continued to shallow depths of ~20 km. The presence of melts ranging in composition from ultra-depleted to compositions similar to Mauna Loa Volcano, Hawaii, high potential mantle temperature and association with rocks akin the Cretaceous Hawaiian tholeiites suggest that the trace element depleted melts preserved in spinel phenocrysts could have originated from extensive melting of a depleted component intrinsic to the Hawaiian plume or ambient upper mantle entrained and heated up at the plume margins.

Portnyagin M., Hoernle K., Savelyev D. Ultra-depleted melts from Kamchatkan ophiolites: Evidence for the interaction of the Hawaiian plume with an oceanic spreading center in the Cretaceous? // Earth and Planetary Science Letters. 2009. Volume 287. Issue 1-2. P. 194-204

1.3.9. Method of water balance at Kurile arc

Kalacheva, E.G., *Institute of Volcanology and Seismology, Piip Boulevard 9, Petropavlovsk-Kamchatsky, 683006, Russia*

Using the method of long-term water balance for the North part of Paramushir, we determined that about 400 mm of atmospheric precipitation replenish them every year. It makes up 13 % of the whole quantity. The calculations were made for the every water balance section of researching region. In the result sizable seats of relief of the underground waters were revealed in the basins of big rivers of the east slope and some river basins of the west slope of Vernadskii range. On these sections the surplus of moisture is from 9 % to 26 % from average long-term precipitation's value. The obtained data will be co-coordinated with geologyhydrogeological conditions of the region.

Kalacheva, E.G., Application of the Method of water balance for the study of the feeding conditions of underground waters of the North part of Paramushir Island. Vestnic KRAUNC. Nauki o Zemle, 2008, N 2, issue 12, pp. 87-94 (in Russian).

1.3.10. Gorely volcano

Gavrilenko M., max.gavrilenko@gmail.com, **Ozerov A.,** ozеров@ozеров.ru, *Institute of Volcanology and Seismology, Piip Boulevard 9, Petropavlovsk-Kamchatsky, 683006, Russia*

Gorely volcano, in southern Kamchatka, is a large, long-lived shield-type volcano that is currently in an eruptive phase. Prior eruptions occurred in 1980 and 1984. It is comprised of three structural units: Pra-Gorely volcano; thick ignimbrite complex, associated with a caldera forming eruption; modern edifice named 'Young Gorely'. An integrated mineralogical-

geochemical have been conducted on all structural units of the Gorely volcanic edifice to determine their genetic conditions.

After geochemical analysis two evolution series were found. First, Pra-Gorely volcano is represented by a suite of compositions ranging from basalt to rhyolite, with in this series, high-Mg basalts were discovered. Second, Young Gorely edifice is composed of only basalt, andesite and dacite. The reconstruction of chemical evolution trends shows that both volcanic series of Gorely volcano share the same genetic history with similar evolutionary stages. We suggest fractionation of an upper mantle peridotite as a common means to produce both volcanic series as a result of which the evolution of all rocks was generated. The magmatic series of Pra-Gorely and Young Gorely volcanoes were formed under different geodynamic conditions. Between these two series was a powerful stage of caldera formation, during which 100 km³ of ignimbrites were emplaced. The 12-km diameter caldera collapse was the catalyst for large-scale reorganization of the volcanic feeding system. Nevertheless following caldera collapse, Young Gorely was formed by activity inside the caldera and shows very similar evolutionary trends to that of Pra-Gorely. It can be confidently stated that crustal components are practically absent in the evolution of the series, and the compositional range is attributed directly to the evolution of the magmatic melts of Gorely volcano. Microprobe analyses conducted on olivine and pyroxene phenocrysts of Gorely volcano lavas, show that there were at least two stages of crystallization during the evolution of magmatic melt. In addition, accessory minerals enclosed as mineral inclusions in olivine and pyroxene phenocrysts were studied in order to reconstruct the magmatic melts evolution. The chemical composition of spinel crystals, which were found within the host-minerals, shows definite trends of mineral phase's evolution and confirm the two-stage nature of the magmatic melt evolution, which was detected by microprobe analysis of the phenocrysts of the Gorely volcano lavas. Cr-spinels (Cr₂O₃ is about 25 wt.%) were found in high-Mg olivines (Mg# 87-77). Fe-Ti spinels (TiO₂ is about 15 wt.%) were found in low-Mg pyroxenes (Mg# 72-69). The two-stage character of initial magmatic melt evolution is also confirmed by computer simulation results. The first stage is characterized by comparatively high pressures (6-8 kbar), which corresponds to formation at depth and low rates of oxygen fugacity (1% Fe³⁺ in total Fe). In contrast, the magmatic evolution of the second stage occurred in near-surface conditions (1-1.5 kbar) with high rates of oxygen fugacity (Ni-NiO buffer). The existing of this stage of crystallization testifies to shallow magmatic chamber presence which is responsible for generation of caldera and thick ignimbrite complex.

Gavrilenko M.G., Ozerov A.Yu. Geochemical similarities between the pre-caldera and modern evolutionary series of eruptive products from Gorely volcano, Kamchatka // 2010 AGU Fall Meeting, Abstract V21B-2333.

1.4. Kamchatka's minerals

1.4.1. Mutnovsky volcano and it's Geothermal Reservoirs

Kiryukhin A.V., avk@kcsnet.ru, **Сырцовов B.M.**, **Droznin V.**, **Dvigalo V.**, **Dubrovskaya I.**, **Manukhin Y.F.**, **Rychkova T.V.**, *Institute of Volcanology and Seismology FED RAS, Petropavlovsk-Kamchatski, Russia*

Asaulova N.P., **Obora N.V.**, **Vorozheikina L.A.**, *Kamchatskburgeotemia Enterprise, Krashennnikova-1, Thermalny, Kamchatka 684035, Russia*

Finsterle S., *Lawrence Berkeley National Laboratory, MS 90-1116, One Cyclotron Road, Berkeley, CA 94720, USA*

Ramsey M., **Carter A.**, **Rose S.**, *University of Pittsburgh, USA*

John Eichelberger, jeichelberger@usgs.gov, *University of Alaska Fairbanks, Department of Geology and Geophysics Reichardt Building, Alaska, U.S.A. Currently at: U.S. Department*

of the Interior, U.S. Geological Survey, Office of Communication, 119 National Center, Reston, Va., 20192, U.S.A.

Adam Simon, Department of Geoscience, University of Nevada – Las Vegas, 4505 South Maryland Parkway, Las Vegas, Nev., 89154-4010, USA

Geothermal Modeling

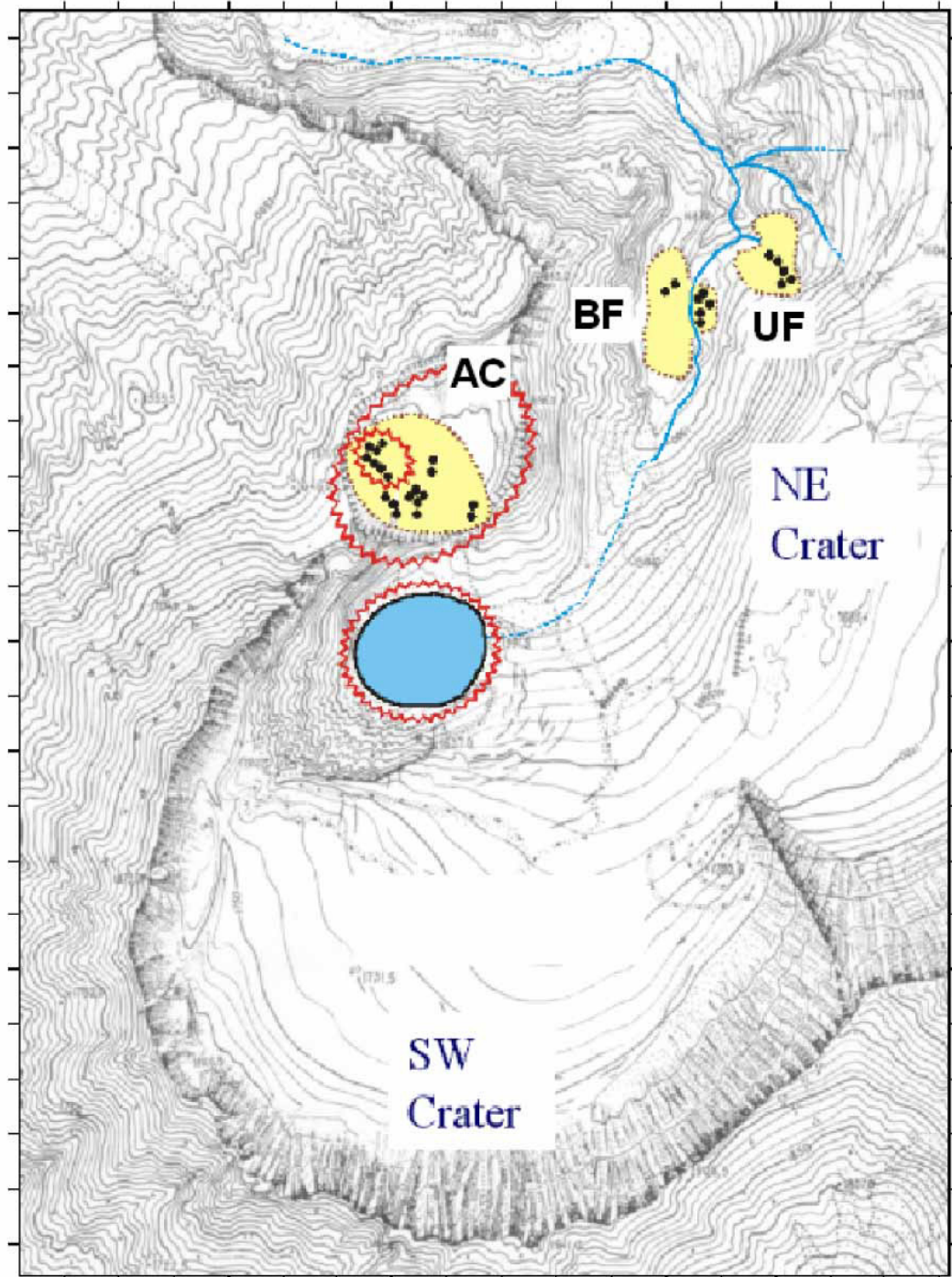


Fig. 1.4.1.1. Mutnovsky volcano thermal fields (Zelensky, 2006): UF – Upper Field, BF – Bottom Field, AC – Active Crater. Blue lake – site of the phreatic explosion 2000. Grid scale – 100 m.

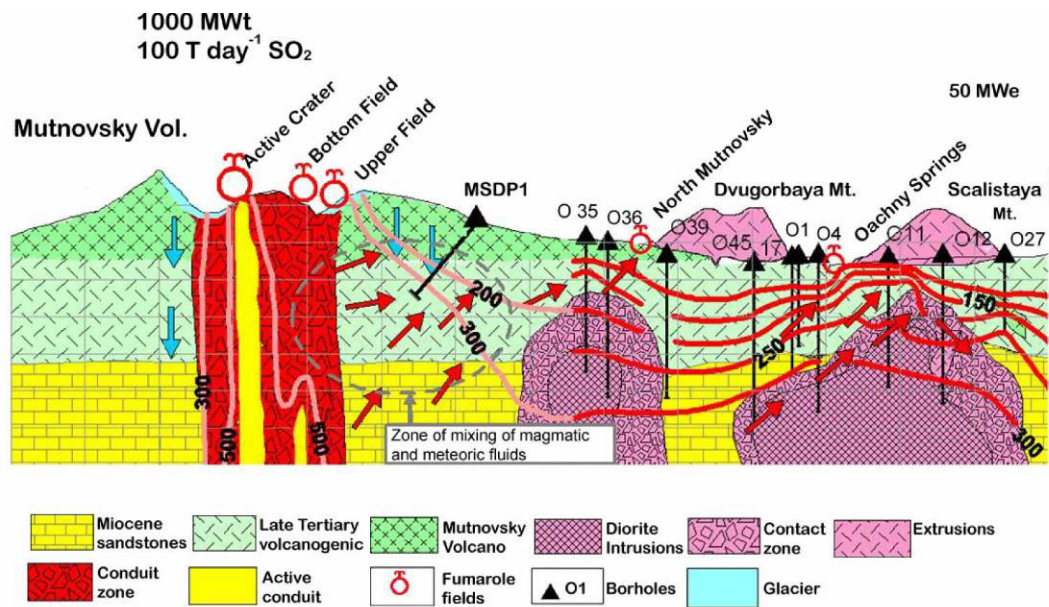


Fig. 1.4.1.2. Sub-meridional Cross-section and conceptual geothermal/hydrogeological model of the Mutnovsky volcano (Mutnovsky geothermal field system). MSDP1: potential borehole for the Mutnovsky Scientific Drilling Program. Upflow rates estimated based on numerical models are 50–60 kg s⁻¹ with enthalpies of 1270–1390 kJ kg⁻¹.

The TOUGH2 forward and iTOUGH2 inverse modeling codes were used to calibrate a model of the Pauzhetsky geothermal field (Figs. 1.4.1.1., 1.4.1.2) based on natural-state and 1960–2006 exploitation data. We identified and estimated key model parameters, i.e. geothermal reservoir fracture porosity, initial natural upflow, base-layer porosity and the permeabilities of the hydraulic windows in the upper layer of the model.

The computed heat and mass balances helped to identify the sources for the geothermal reserves in the field. The largest contribution comes from fluids stored in the reservoir, followed by meteoric water recharge, base-layer upflow, and injection waters.

Model predictions for the period 2007–2032 show the possibility of maintaining steam production at an average rate on the order of 30 kg/s (total flow rate about 290 kg/s), provided that five additional make-up wells are put into operation, and that the steam transmission lines from Wells 122 and 131 are improved to allow a reduction in wellhead pressures. This rate of steam production would be sufficient to support an average electricity generation of 7MWe at the Pauzhetsky power plant.

The calibrated model can be used for estimating overall reservoir behavior under future production scenarios. Nevertheless, to make reliable predictions of enthalpy and pressure declines, and to better match individual well data, the model should be improved by refining the model structure, increasing grid resolution, and capturing more accurately the cooling phenomena occurring in the geothermal system. We plan to develop such a model in the future since it likely will have improved predictive capabilities for scenarios that deviate more strongly from the current reservoir conditions.

We performed iTOUGH2 inverse modeling using a two-dimensional, radial model (cylindrical symmetry around a monitoring well) applied to Jan. 25, 2007 - Feb. 20, 2008 observational data of the water level monitoring well YZ-5 (Kamchatka). Before the inversion, the systematic component related to hydrogeological basin recharge/discharge conditions were removed, and water level was converted into well fluid pressures. The atmospheric pressure change was specified as time-dependent Dirichlet boundary conditions at the well head and earth surface. Reservoir permeabilities (on the order of 10⁻³ mD) were identified as the most sensitive

parameters, while porosity and compressibility are less sensitive. Moreover, the barometric pressure change mostly propagates into an aquifer directly through the well head, with pressure propagation limited to about one meter around the well.

Based on helicopter IR-survey (Figs. 1.4.1.3., 1.4.1.4) performed in 2007 the thermal anomalies of the Active Crater (AC), Bottom Field (BF) and upper field (UF), and a new thermal anomaly WF, located 300 m west to Bottom Field (BF) were characterized by the total area 37200 m² with temperatures above 30 °C, 4500 m² with temperatures above 40 °C, and 210 m² with temperatures above 60 °C. Total IR emission in the Mutnovsky volcano craters from surfaces above 30 °C is estimated as 5.2 MWt.

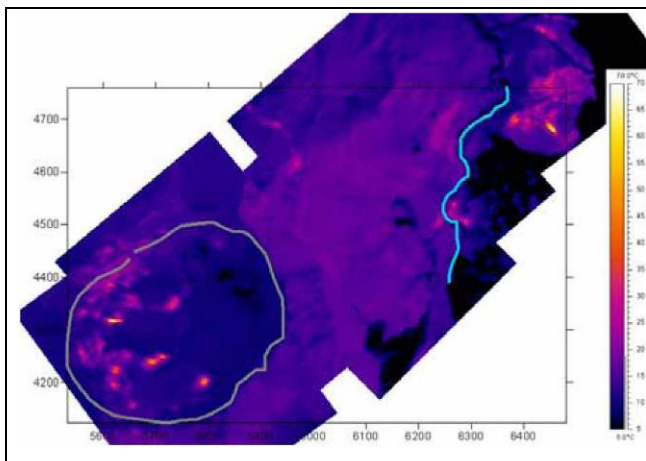


Fig. 1.4.1.3. IR-image of the Mutnovsky Volcano crater's. Active Crater rim shown as a gray circle, Volcannaya river is a blue line.

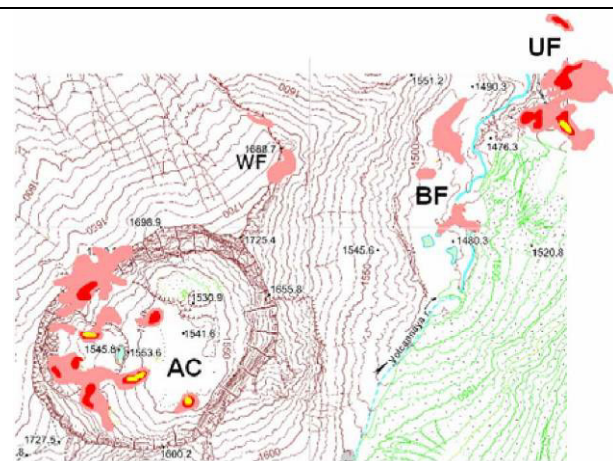


Fig. 1.4.1.4. IR-temperature distribution (August 2007) of the Mutnovsky Volcano craters. AC-Active Crater, BF – Bottom Field, UF- Upper Field, WF – West Field, thermal anomaly 300 m west from Bottom Field. IR-temperature areas: pink – above 30 °C, red – above 40 °C, yellow – above 60 °C.

If B. Polyak et al (1985) assumption, that the fraction of IR emission is the same in the heat output balances of the BF, UF and AC used, then the total heat discharge of Mutnovsky volcano craters estimated as ≈825 MWt.

Nevertheless, that value may reflect our underestimation of the AC because of difficulties to get IR images from subvertical crater's walls. This study is on-going.

Drilling program

The MSDP proposes a comprehensive geophysical and geochemical research program with stages wherein drilling will play an increasingly important role. Immediate priorities are magneto-telluric, seismic, geodetic, and gravity surveys to define the extent and behavior of the magma-hydrothermal system. The geothermal development company is currently drilling new 2000 m wells. This firm and the scientific drilling consortium formed at the workshop have agreed to collaborate in order to maximize scientific gain from drilled wells.

Based on results from this first phase, MSDP will drill a more proximal portion of the system that is hotter and more enriched in magmatic components than subsurface fluids previously sampled. Physical properties measurements on core will be used to refine initial

geophysical models, particularly rheological properties relevant to inversion of measured surface displacements. Tracer and hydraulic tests will be used to assess overall connectivity of the system, from crater to production zone. Natural events, the numerous strong regional earthquakes and occasional eruptions, will also provide pressure perturbation tests. Finally, if feasibility can be demonstrated, we hope that the project will attempt to penetrate Mutnovsky's active conduit. The goal of reaching magma in a decadal time frame is one endorsed by the International Continental Scientific Drilling Program White Paper (Harms et al., 2007).

Kiryukhin A.V., Asaulova N.P., and Finsterle S. *Inverse modeling and forecasting for the exploitation of the Pauzhetsky geothermal field, Kamchatka, Russia* // *Geothermics*, 2008. V. 37. P. 540-562.

Kiryukhin A.V. *MUTNOVSKY SCIENTIFIC DRILLING PROJECT (MSDP): MAGMA-HYDROTHERMAL CONNECTION STUDY* // 3-rd Taiwan-Russia Bilateral Symposium on Water and Environmental Technology, Tainan, Taiwan, Nov.1-2, 2007, p. 127-145.

Kiryukhin A.V., N.P. Asaulova, T.V. Rychkova, N.V. Obora, Y.F. Manukhin, L.A. Vorozheikina *MODELING AND FORECAST OF THE EXPLOITATION THE PAUZHETSKY GEOTHERMAL FIELD, KAMCHATKA, RUSSIA PROCEEDINGS, Thirty-Second Workshop on Geothermal Reservoir Engineering Stanford University, Stanford, California, January 22-24, 2007 SGP-TR-183*, 8 p.

Eichelberger J., A. Kiryukhin, and A. Simon. *The Magma-Hydrothermal System at Mutnovsky Volcano, Kamchatka Peninsula, Russia* // *Scientific Drilling* . 2009. № 7. 54-59

Kiryukhin A.V., Kopylova G.N. *ITOUGH2 analysis of the ground water level response to the barometric pressure change (WELL YZ-5, Kamchatka)* // *Stanford University* . 2009. 6

Kiryukhin A.V. *Conceptual Modeling of A Deep Seated NAPL Deposit in Volcanogenic Rocks* // *Lawrence Berkeley National Laboratory* . 2009. 7

Kiryukhin A., Ramsey M., Droznin V., Carter A., Rose S., Dvigalo V., Dubrovskaya I. *Heat Discharge of the Mutnovsky Volcano* // *Thirty-Third Workshop on Geothermal Reservoir Engineering Stanford University, Stanford, California, 2008*

Harms U., Koeberl, C., and Zoback M.D. 2007. *Continental Scientific Drilling: A decade of progress and challenges for the future*. Berlin, Springer, 366 pp.

Geochemistry

Rychagov S. N., R. G. Davletbaev, and O. V. Kovina, Institute of Volcanology and Seismology FED RAS, Petropavlovsk-Kamchatski, Russia

Nuzhdaev, A.A. I.I. Stepanov, Aleksandrov Experimental and Methodical Expedition, Ministry of Natural Resources of the Russian Federation, Krasnyi per. 6, Aleksandrov, Vladimir oblast 601650

The studies reported in this paper were carried out in the Pauzhetka and Nizhne-Koshelevskii geothermal fields situated in the southern Kamchatka Peninsula within the Pauzhetka-Kambalny-Koshelevskii geothermal area. Layer-by-layer sampling of clays was carried out by stripping, pitting, and hand-operated drilling of core holes in the Verkhne-Pauzhetka thermal field and the Nizhne-Koshelevskii thermal anomaly, which were studied previously using several geological, geophysical, and hydrogeothermal techniques. Hydrothermal clays were found to compose a nearly continuous sheet on the surface of the thermal field and of the thermal anomaly. The sheet has an average thickness of 1.3 to 1.5 m. The chemical and mineralogic composition of the clays have been characterized. The concentrations of Au, Hg, Pb, and Ag (a total of 41 elements) were determined in clay layers selected every 15–20 cm in vertical sections. The elements show inhomogeneous distributions, both along the strike and in vertical sections of the hydrothermal clay sheet, which can be accounted for by the physicochemical, hydrogeochemical, and temperature conditions prevailing during the generation of these clays in specific areas of the thermal fields. It was found that the

hydrothermal clay sheet lying on the ground surface of the geothermal fields has a significance of its own as an independent geological body, not only is it an aquifer and a heat-isolating horizon; it also serves as a dynamically active geochemical barrier in the structure of the present-day hydrothermal system. Pyrite is a concentrator of ore elements in hydrothermal clays, in addition to sulfates of Ca, Fe, Mg, Ba, and Al, and (possibly) aluminosilicates.

Mercury distribution was determined in all types of solid materials from the supergene zone of geothermal deposits in southern Kamchatka: rocks, hydrothermally altered rocks (metasomatic rocks), soils, soil-pyroclastic cover, bottom sediments of perennial and intermittent streams, hydrothermal clays, artificial siliceous precipitates, and iron sulfides formed owing to thermal water discharge from a well. The mercury content varies from background values for the Kurile-Kamchatka region in fresh rocks to high and extremely high values in hydrothermal clays and monomineralic pyrite samples. The sources, migration conditions, and concentration mechanisms of mercury were evaluated. Mercury is supplied to the surface of geothermal deposits and thermal fields by a deep hydrothermal flow and is concentrated on thermodynamic barriers in hydrothermal clays, siliceous sinters (silica gel), and soils showing high salinity owing to the deposition in them of silica, sulfates, and other compounds from a vapor-water mixture. Newly formed clay minerals, iron sulfides (pyrite), silica gel, and biological materials (peat) can probably efficiently sorb mercury under geothermal conditions at atmospheric pressure and temperatures from 20°C to 120°C.

Rychagov S. N., R. G. Davletbaev, and O. V. Kovina. Hydrothermal Clays and Pyrite in Geothermal Fields: Their Significance for the Geochemistry of Present-Day Endogenous Processes in Southern Kamchatka. Journal of Volcanology and Seismology, 2009, Vol. 3, No. 2, pp. 105–120.

Rychagov S. N., A.A. Nuzhdaev, I.I. Stepanov. Behavior of Mercury in the Supergene Zone of Geothermal Deposits, Southern Kamchatka. Geochemistry International, 2009, Vol. 47, No. 5, pp. 504–512..

1.4.2. Asachinskoe epithermal Au-Ag deposit

Takahashi R., Matsueda H., Ono Sh, Japan

Okrugin V., Institute of Volcanology and Seismology FED RAS, Petropavlovsk-Kamchatski, Russia

The Asachinskoe epithermal Au-Ag deposit is a representative low-sulfidation type of deposit in Kamchatka, Russia. In the Asachinskoe deposit there are approximately 40 mineralized veins mainly hosted by dacite–andesite stock intrusions of Miocene–Pliocene age. The veins are emplaced in tensional cracks with a north orientation. Wall-rock alteration at the bonanza level (170–200 m a.s.l.) consists of the mineral assemblage of quartz, pyrite, albite, illite and trace amounts of smectite. Mineralized veins are well banded with quartz, adularia and minor illite. Mineralization stages in the main zone are divided into stages I–IV. Stage I is relatively barren quartz–adularia association formed at 4.7 ± 0.2 Ma (K-Ar age). Stage II consists of abundant illite, Cu-bearing cryptomelane and other manganese oxides and hydroxides, electrum, argentite, quartz, adularia and minor rhodochrosite and calcite. Stage III, the main stage of gold mineralization ($4.5–4.4 \pm 0.1–3.1 \pm 0.1$ Ma, K-Ar age), consists of a large amount of electrum, naumannite and Se-bearing polybasite with quartz–adularia association. Stage IV is characterized by hydrothermal breccia, where electrum, tetrahedrite and secondary covellite occur with quartz, adularia and illite. The concentration of Au+Ag in ores has a positive correlation with the content of $K_2O + Al_2O_3$, which is controlled by the presence of adularia and minor illite, and both Hg and Au also have positive correlations with the light rare-earth elements. Fluid inclusion studies indicate a salinity of 1.0–2.6 wt% NaCl equivalent for the whole deposit, and ore-forming temperatures are estimated as approximately 160–190°C in stage

III of the present 218 m a.s.l. and 170–180°C in stage IV of 200 m a.s.l. The depth of ore formation is estimated to be 90–400 m from the paleo-water table for stage IV of 200 m a.s.l., if a hydrostatic condition is assumed. An increase of salinity ($>C_{NaCl} \approx 0.2$ wt%) and decrease of temperature ($>T \approx 30^\circ\text{C}$) within a 115 -m vertical interval for the ascending hydrothermal solution is calculated, which is interpreted as due to steam loss during fluid boiling. Ranges of selenium and sulfur fugacities are estimated to be $\log f_{Se_2} = -17$ to -14.5 and $\log f_{S_2} = -15$ to -12 for the ore-forming solution that was responsible for Au-Ag-Se precipitation in stage III of 200 m a.s.l. Separation of Se from S-Se complex in the solution and its partition into selenides could be due to a relatively oxidizing condition. The precipitation of Au-Ag-Se was caused by boiling in stage III, and the precipitation of Au-Ag-Cu was caused by sudden decompression and boiling in stage IV.

Takahashi R., Matsueda H., Okrugin V., Ono Sh. Epithermal Gold-Silver Mineralization of the Asachinskoe Deposit in South Kamchatka, Russia // Resource Geology. V.57. № 4. 2007. P. 354-373

1.4.3. Platibum-Group minerals

Tolstykh N., *Institute of Geology and Mineralogy, Siberian Branch, Russian Academy of Sciences, Koptyga Avenue 3, Novosibirsk, 630090, Russia*

Sidorov E., *Institute of Volcanology and Seismology, Siberian Branch, Russian Academy of Sciences, Bl. Pijpa, 9, Petropavlovsk–Kamchatskiy, 683006, Russia*

Kozlov A., *Institute of Problems of the Complex Development of Natural Resources, 111020, Kryukovsky tupik, 4, Moscow, Russia*

For the first time the systematization of the of the hardore occurrence of the minerals of platinum group (MPG) for the Koryak-Kamchatka region was realized. All MPG are connected to different formations of the basic-giperbasic bodies. The mineral forms of the elements of platinum group (EPG) are distinguished and studied (Fig. 1.4.3.1.). Oreformation types of the platinum hardore are determined. The factors, controlling their locations are shown. The typomorphic peculiarities of the silicate and ore minerals, which are associated with MPG, were discovered. For the first time it was found that minerals, associated with MPG, have significant amounts of Cl, Co, Ni, Zn, Cu, EPG. The role of the fluids is evidenced during mobilization, redistribution and concentration of EPG in oreforming processes for the studied formations.

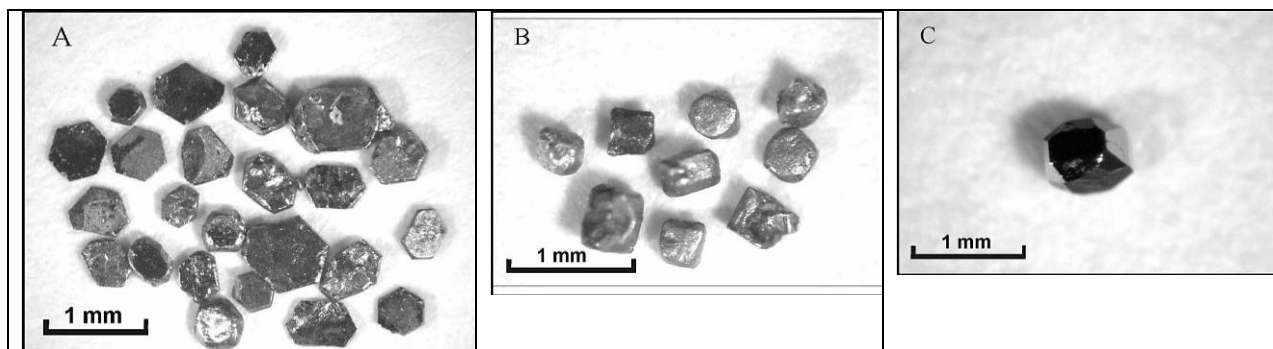


Fig. 1.4.3.1. The morphology of Os–Ir–Ru alloy grains (A), Pt–Fe alloy grains (B), and laurite (C).

Mineral assemblages from the Olkhovaya–1 River placers, in Kamchatka, Far-Eastern Russia, provide genetic information on their evolution. The minerals are dominated by Os–Ir–Ru alloys (80%), consisting of all possible mineral species, and Pt–Fe alloys consisting of native

platinum, Fe-rich platinum and isoferroplatinum. The following features of the mineral assemblage are characteristic of mineralization associated with an ophiolitic complex: (1) in the Os–Ru–Ir diagram, the compositions of the hexagonal alloy form a ruthenium trend; (2) there are two typical equilibrium magmatic parageneses of alloys: early osmium–iridium, and later isoferroplatinum–ruthenium, which both are associated with laurite and the solid solution laurite–irarsite (Ru, Ir)(S, As)₂. The cooperite, sperrylite and Pd minerals formed at the postmagmatic stage. Tetraferroplatinum–tulameenite, replacing the Pt–Fe alloys, as well as the multicomponent compounds of Ru, Os, Ir, Rh, Pt with Fe replacing the Os–Ir–Ru alloys and PGE sulfides, result from serpentinization of PGM-bearing rocks. The PGM assemblage in the Ol'khovaya–1 River placers is related to the Karaginsky ophiolite complex of the Kamchatskiy Mys Peninsula.

Tolstykh N., Sidorov E., Kozlov A. PLATINUM-GROUP MINERALS FROM THE OLKHOVAYA–1 PLACERS RELATED TO THE KARAGINSKY OPHIOLITE COMPLEX, KAMCHATSKIY MYS PENINSULA, RUSSIA. The Canadian Mineralogist Vol. 47, pp. 1057-1074 (2009).

1.4.4. Fe-Mn crusts formation

Anikeeva L.I., andreev@vniio.ru, **V.E. Kazakova**, *VNII Océangeologia, 190121 St. Petersburg, Russia*

Gavrilenko G.M., **V.A. Rashidov**, *Institute of Volcanology and Seismology, Siberian Branch, Russian Academy of Sciences, Bl. Pijpa, 9, Petropavlovsk–Kamchatskiy, 683006, Russia*

Chemical composition of hydrothermal hydrogenous ferromanganese crusts occurring in different sections of the West Pacific transition zone is variable because hydrothermal solutions contribute differently to crust formation. The hydrothermal origin of the Fe-Mn crusts from the back-arc basins of the WPTZ is evidenced by the contrasting variations of Mn and Fe content, low concentrations of non-ferrous and earth elements (domination of the middle/heavy rare earths elements, positive Eu anomaly, increased Sm/Nd rate), high content of Li and Ba. The formation of aureoles of oxide Fe-Mn crusts is associated with modern hydrothermal activity accompanying sulfide ore outcrops at the sea bottom. All geochemical varieties of the crusts of the ocean's rift systems have been discovered: essentially Mn- and Fe-Mn crusts and ferriferous and nontronite ones containing silicon. As for the hydrothermal crusts, their distance from the hydrotherm discharge areas is controlled by Mn/Fe. High contents of Fe are indicative for high-temperature hydrothermal process and associated shows of deep-sea polymetallic sulfides. The studied Fe-Mn crusts of unstable chemical and mineral composition are of hydrothermal-sedimentary nature at different degrees of involvement of the hydrogenous factor, which is most vividly demonstrated by the samples from the Kuril branch. These formations are the product of hydrothermal activity at the sea bottom and may be regarded as indicators for under bottom sulfide formation in the Kuril branch, similar to the major ore shows in the southern segments of WPTZ, i.e., the Sunrise (the Izu-Bonin arc) and the Jade (the Okinawa trough).

Anikeeva L.I., V.E. Kazakova, G.M. Gavrilenko, V.A. Rashidov. FERROMANGANESE CRUST FORMATIONS OF THE WEST PACIFIC TRANSITION ZONE. Vestnic KRAUNC. Nauki o Zemle, 2008, N 1, issue 11, pp. 10-31 (in Russian).

1.4.5. Diomondiferous complexes of Kamchatka

Seliverstov V.A., vaseliverstov@gmail.com, *Earth sciences Museum, Lomonosov Moscow State University. Moscow, 119899*

Geological peculiarities of the alkaline-ultramafic volcanic complex in Eastern Kamchatka (meimechites, lamproitoides, Na-alkaline basalts) are described. The ultramafic rocks contain a number of thermobarophyllitic minerals: olivine (F_{0.92-0.93,51}), Cr-diopsides, garnets (lilac, red, rose and orange pyropes), Cr-spinels and Ti-Cr-spinels, picroilmenite, ilmenite, Cr-ulvospinel, magnesioferrite, Ti-magnesioferrite, phlogopite and Ba-phlogopite, Ba-orthoclase, moissanite (polytype 6H), corundum, ruby and Cr-ruby (Cr₂O₃ up to 45 mass %), zircon, «exotic» glasses. The «exotic» glasses composition agrees the composition of orthopyroxene, clinopyroxene and andradite. The above minerals belong to certain parageneses, including diomondiferous ones: garnet clinopyroxenites, lhertsolites and wherlites, ilmenite and spinel peridotites, eclogites, alpine-type ultramafites etc. The combination of the following processes determines the meimechites and lamproitoides genesis: 1 – Selective melting of primitive mantle and reactions between melt and pyrolite accompanied by coherent elements loss caused by mantle metasomatism. 2 – Impact fragmentation and subtraction of the fragmented mantle ultramafic rocks and the dispersed melt into the upper lithosphere. 3 – Eruption of tuffs on the bottom of Cretaceous sea, their decompressed melting in the intermediate chambers and differentiation of the newly formed ultramafic magmas in the feeding systems of paleovolcanoes. The formation of the alkaline ultramafic complex on the deep differentiated crust concluded with the eruption of lamproitoides tuffs and effusion of nepheline basalt lavas.

Seliverstov V.A., THERMOBAROPHYLLIC MINERAL PARAGENESISES OF DIOMONDIFEROUS ALKALINE ULTRAMAFIC VOLCANIC COMPLEX IN EASTERN KAMCHATKA. Vestnic KRAUNC. Nauki o Zemle, 2009, N 1, issue 13, pp. 10-30 (in Russian).

1.4.6. Oil and Gas Potential

Pozdeev A. I. and I. N. Nazhalova, *Federal State Organization “Territorial Foundation for Information on Natural Resources and Environmental Protection, Ministry of Natural Resources of Russia for Kamchatka Oblast and the Koryak Autonomous District,” Petropavlovsk-Kamchatskii, 683016 Russia*

This paper considers the geology, hydrodynamics, and oil and gas occurrences in the Kosheleva vapor-dominated field related to the activity of the Kosheleva Volcano. The hydrodynamic peculiarities of this field allow the upper boundary of the vapor zone to be outlined. One notes an intimate connection between vapor-dominated hydrothermal occurrences and the occurrences of oil and gas containing heavy hydrocarbons, including even C₇H₁₂, as well as methane.

Pozdeev A. I. and I. N. Nazhalova. The Geology, Hydrodynamics, and the Oil and Gas Potential of the Kosheleva Steam-Water Field in Kamchatka. Journal of Volcanology and Seismology, 2008, Vol. 2, No. 3, pp. 170–183.

2. Volcanology, geodynamics and deep mantle structure of the Far East region of Russia in 2007-2010

2.1. Intraplate alkaline- basaltic volcanism of arctic shelf and continental margin of North-East Asia

Vladimir Sakhno, v_sakhno@mail.ru. *FAR east geological institute, Vladivostok, Russia.*
Alexey Surnin. *Institute geology of Diamond and precious, Yakutsk, Russia.*

In the Arctic zone of the continental margin of North-East Asia and on the shelf of the Arctic Ocean, the basaltoidal volcanism manifested itself widely in the Late Cenozoic time. These were isolated volcanoes, covers in the Anyui and Aluchin river basins (Aluchin-Anyui group of volcanoes), and valley lava sheets (Enmelenskaya group of volcanoes, East Chukotka, and Viliginsky volcanoes in the Viligi River basin, southern part of East Chukotka). On the shelf, the volcanic eruptions are known in the Late Pleistocene and Holocene on the De-Longa-Benetta Islands [Masurenkov, Flerov, 1989; Silantsev et al., 1991; Bogdanovsky et al., 1992; and others]. Basaltoids and xenoliths of ultrabasic rocks of these volcanoes were studied with determination of the rare-earth element spectra and Nd, Sr, and Pb, isotopes. Microprobe analyses were carried out for the mineral composition in lavas and xenoliths of lherzolites and xenogenic fragments of the crust substratum. The results obtained allow the following conclusions: The alkaline basaltoids belong to the intraplate volcanic associations whose petrological-geochemical and isotopic parameters are characteristic of the continental type of the lithosphere mantle. Comparison of them with the alkaline basalts and enclosed in them ultrabasic xenoliths of volcanoes of the continental margin (volcanoes of Anyui and Aluchin group) reveals many similar features. The petrogeochemical and isotopic data obtained for the volcanoes of Zhokhov and Bennett Islands suggest them to be the continental ones having the intraplate characteristics. The xenogenic material found in the basalts represents the basement of the continental slope.

2.2. Research of the modern volcanoes in Far East of Russia

Vladimir Sakhno, v_sakhno@mail.ru. *FAR east geological institute, Vladivostok, Russia.*

During 2007-2010 the investigations were conducted on the modern volcanoes in Far East of Russia, which were erupted as in historical time, as well in past. In papers during period 2007-2010 were considered the questions of the structure, chemistry of the rocks, geochronology, periodicity of eruptions, deep sources, and for the modern volcanoes (Chanbajshan, Udalanchi Group of volcanoes, Keluo and so on) - forecasting estimates of the possible future eruptions were made. The forecasting guidelines, discovered for the modern volcano Chanbajshan (Pectusan), based on the detail chronological data about eruptions and using petrological and geochemical studies of the rocks the time of eruption was predicted in very near future. At present this volcano is in active stage.

In following list of papers next questions were considered: relationship of the geodynamics, deep mantle structure (using tomography) and volcanism, fluids evolution, the nature of the explosive eruptions and the influence of the large pyroclastic volumes (more than 2

million km³) and gages on the climate in Cenomanian and Turonian time during the formation of the marginal-continental belts of the East Asia and so on.

- Vladimir Sakhno et al. *Recent volcanism: regularities of its evolution and attendant catastrophes. In: Natural and connected with them man-caused catastrophes. (edit by N.P. Laverov). Volume I. Change of the environment and climate. Moscow, IGEM RAS 2007, P. 35-90. (in Russian).*
- Vladimir Sakhno. *Recent and modern volcanism of the South of the Far East (latepleistocene-holocene stage). Book 1. Vladivostok, Galnauka. 129 pp. (in Russian).*
- Vladimir Sakhno et al. *Volcanism of intra-plate regions of the Central and Eastern Asia. In: Natural and connected with them man-caused catastrophes. (edit by N.P. Laverov). Volume I. Change of the environment and climate. Moscow, IGEM RAS 2007, P. 81-148. (in Russian).*
- V. G. Sakhno. *Chronology of Eruptions, Composition, and Magmatic Evolution of the Paektusan Volcano: Evidence from K–Ar, 87Sr/86Sr, and $\delta^{18}O$ Isotope Data. Doklady Earth Sciences, Vol. 412, No. 1, 2007. P. 22-28.*
- V. G. Sakhno. *Isotopic–Geochemical Characteristics and Deep-Seated Sources of the Alkali Rocks of the Pektusan Volcano. Doklady Earth Sciences, Vol. 417A, No. 9, 2007. P. 1386-1392.*
- V. G. Sakhno and V. V. Akinin. *First U–Pb Dating of Volcanics from the East Sikhote-Alin Belt. Doklady Earth Sciences, Vol. 418, No. 1, 2008. Part 1. Geology. P. 32-36.*
- V. A. Lebedev, G. T. Vashakidze, and V. G. Sakhno. *Potential Volcanic Danger in the Keli Highland (Greater Caucasus): Evidence from Isotopic–Geochronological Study of the Youngest Lavas. Doklady Earth Sciences, Vol. 418, No. 1, 2008. Part 2. Geochemistry, Geophysics, Oceanology, Geography. P. 169-173.*
- S. O. Maksimov and V. G. Sakhno. *Geochronology of Basalt Volcanism on the Shufan Plateau (Primorye). Doklady Earth Sciences, Vol. 422, No. 7, 2008. Part 1. Geology. P. 1044-1049.*
- V. A. Lebedev, V. G. Sakhno, and A. I. Yakushev. *Late Cenozoic Volcanic Activity in Western Georgia: Evidence from New Isotope Geochronological Data. Doklady Earth Sciences, Vol. 427, No. 5, 2009. Part 2. Geochemistry, Geophysics, Oceanology, Geography. P. 819-825.*
- V. A. Lebedev, V. G. Sakhno, and A. I. Yakushev. *Long-Lived Center of Youngest Volcanism in the Borzhomi Region of Georgia: Isotopic–Geochronological Evidence. Doklady Earth Sciences, Vol. 427A, No. 6, 2009. Part 2. Geochemistry, Geophysics, Oceanology, Geography. P. 1020-1024.*
- V. G. Sakhno and I. V. Utkin. *Ashes of Chanbaishan Volcano in Sediments of the Sea of Japan: Identification from Data on Micro- and Rare Earth Elements and Datings of Their Eruptions. Doklady Earth Sciences, Vol. 429, No. 8, 2009. Part 1. Geology. P. 1249-1255.*
- V. G. Sakhno, A. N. Derkachev, I. V. Melekestsev, N. G. Razzhigaeva, and N. V. Zarubina. *Volcanic Ash in Sediments of the Sea of Okhotsk: Identification Based on Minor and Rare Earth Elements. Doklady Earth Sciences, Vol. 434, Part 1, 2010. Part 1. Geology. P. 1156-1153.*
- Sakhno V.G., Surnin A.A. *The intraplate alkaline-basaltic volcanism of arctic shelf and continental margin of North-East Asia // 33 Intern. Geological Congr., 6-14 August 2008. Oslo, Norway. EID-05 Mantle petrology.*
- Sakhno V.G., Polin V.F., Alenicheva A.A. *Large-volume pyroclastic eruptions in Late Mesozoic, Cenozoic and recent times: relationship to catastrophes events // Proc. Lip Asia conference. Novosibirsk, Russia. 2009. P. 279-282.*

3. Volcanology of Northern Caucasus

3.1. Cenozoic fluid-magmatic centers, geodynamics, seismotectonics and volcanism in Elbrus volcano area

The new geophysical observatory for fundamental scientific studies of geophysical processes in the Elbrus volcanic area (Northern Caucasus) has been organized recently as a result of merging of five geophysical laboratories positioned round the Elbrus volcano and equipped with modern geophysical instruments including broadband triaxial seismometers, quartz tiltmeters, magnetic variometers, geo-acoustic sensors, hi-precision distributed thermal sensors, gravimeters, and network-enabled data acquisition systems with precise GPS-timing and integrated monitoring of auxiliary parameters (variations on ambient humidity, atmospheric pressure etc). Two laboratories are located in the horizontal 4.3 km deep tunnel drilled under the mount Andyrchi, about 20 km from the Elbrus volcano.

3.1.1. Pulsating Vertical Evolution of the Elbrus Volcanic Region (as a Consequence of Migration of the Mantle Plume?)

Alexei L. Sobissevitch, alex@ifz.ru, Leonid E. Sobissevitch, Yuri P. Masurenkov, Yuri V. Nechaev, Irina N. Pouzich, and Ninel I. Laverova, Ivan N. Filippov

Russian Academy of Sciences, Schmidt Institute of Physics of the Earth, Moscow, Russian Federation

Konstantin Kh. Kanonidi, Pushkov Institute of Terrestrial Magnetism, Ionosphere and Radiowave Propagation, Troitsk, Russia

The central segment of Alpine mobile folded system of the Greater Caucasus is characterized by complex crossing of the active faults of different structural directions. On the crossings of disjunctive knots of Caucasian WNW and Trans-Caucasian NS faults the two Cenozoic fluid-magmatic centers are located featuring dormant yet not extinct volcanoes of Elbrus and Kazbek. Mentioned centers are known as the Elbrus volcano-plutonic center, the Kazbek volcano-plutonic center, they are outlined according to the results of geological, geomorphological and geophysical studies.

Geodynamic position of the Elbrus volcano within the Transcaucasia uplift is considered with respect to evolution of volcanic processes and possible resumption of volcanic activity in this region. In order to carry out the multidisciplinary study of geological and geophysical processes in the vicinity of the volcanic dome it is essential to obtain reliable information about basic parameters of local magmatic structures.

Results of complimentary geological and geophysical studies carried out in the Elbrus volcanic area are presented and compared to the results of theoretical approaches as well as with numerical simulations and processing of remote sensing data. In particular, the satellite imagery processing carried out according to original technology based on determination of surface lineaments and consequent transition to analysis of the field of tectonic disintegration of the lithosphere may allow one to obtain independent knowledge about deep subsurface structures for the given territory. As a result, the 3D model of tectonic disintegration field under the Elbrus volcano has been constructed. The two anomalous domains have been outlined and they were associated with local deep magmatic source and peripheral magmatic chamber of the Elbrus volcano. Comparative analysis of experimental geophysical data obtained by means of microgravity studies over the same territory, magneto-telluric profiling and determination of

subsurface thermal anomalies reflected in the temperature regime of carbonaceous mineral waters has shown appropriate correlation in terms of shape, size and position of magmatic structures in the Elbrus volcanic area.

Analysis of multi-parameter streams of experimental data allows one to study the structure of geophysical wave fields induced by earthquakes and regional catastrophic events (including snow avalanches).

On the basis of continuous observations carried out since 2007 there have been determined anomalous wave forms in ULF geomagnetic variations preceding strong seismic events with magnitude 7 or more. Mentioned wave forms may be natively related to processes of evolution of dilatational structures in a domain of forthcoming seismic event. Specific patterns in anomalous ULF wave forms are distinguished for undersea earthquakes and for earthquakes responsible for triggering tsunami events. Thus, it is possible to consider development of a future technology to suggest the possible area and the time frame of such class of catastrophic events with additional reference to forecast information (including acoustic, hydro-acoustic and geo-acoustic) being concurrently analyzed.

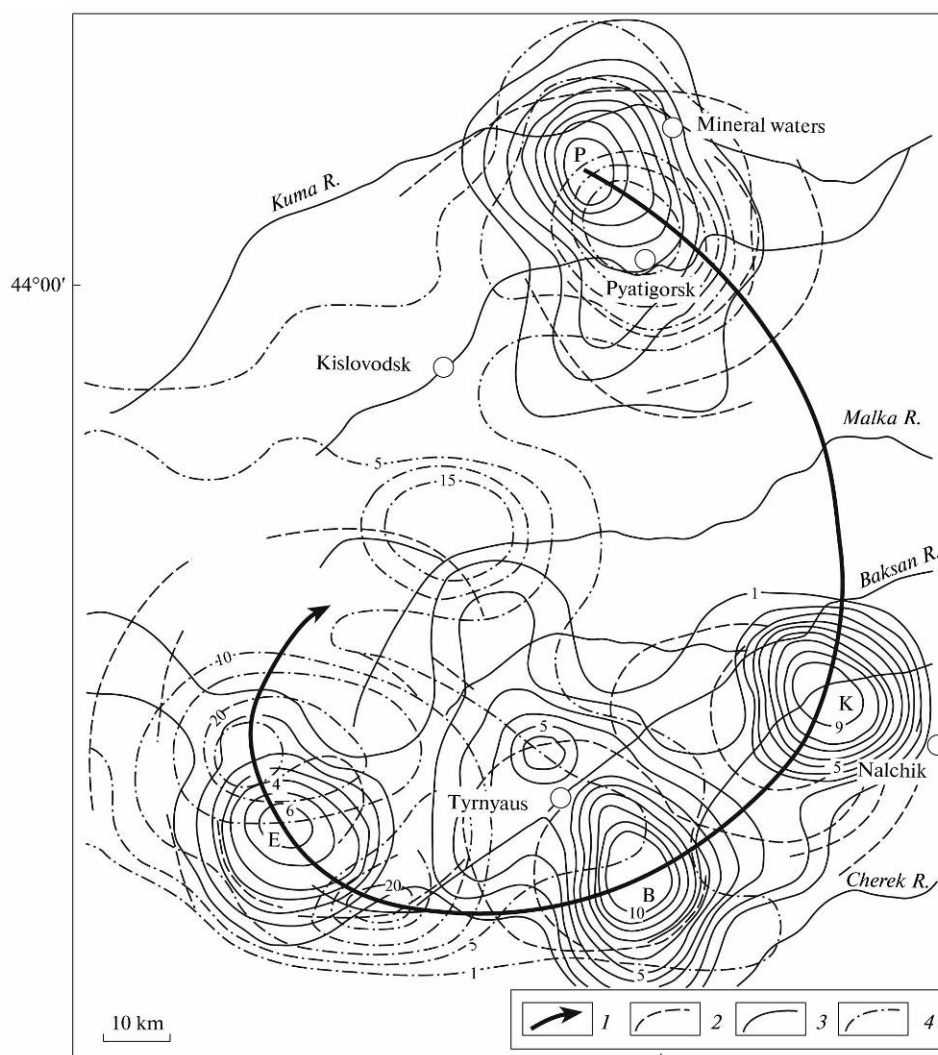


Fig. 3.1.1.1. The density of volcanic sources and mineral water springs distribution in the Elbrus volcanic region. (1) Trajectory of sequential appearance of VCs: Pyatigorsk (P), Kabardinsk (K), Balkar (B), and Elbrus (E); (2) Ring fractures; (3) Contour lines of volcanic sources and intrusions by distribution density (units per square unit) with a step of one unit; (4) Contour lines of the density distribution of mineral water springs with a step of five units.

The Elbrus volcanic region is a location of broad manifestation of Neogene–Quaternary volcanism. Despite the relatively shallow depth of erosion corresponding to this time interval, traces of subvolcanic and near-surface intrusion formations of this time outcrop to the day-time surface here. Together with volcanic sources, they form an extremely inhomogeneous distribution density at the present surface of the Earth (Fig. 3.1.1.1). The latter was determined using the method of a running square over the volcanic region. The step of the square was a half-square, within which the number of breaking out sources was counted (based on the results of field research). The obtained number corresponded to the center of the square. Thus, the entire region was covered with a network of numbers, and contour lines of their density distribution were plotted. The regions of their increased density are presented as VCs: Pyatigorsk, Kabardinsk, Balkar, and Elbrus.

Such a presentation of VCs instead of the usual geological maps has several advantages [1–4]. First, they clearly bound the regions of the Earth’s surface, which had become the main sources of deep material. Second, individual regions of increased density of elevating sources and breaking out of the deep material distinguish localized zones of magma generation, being their projections to the Earth’s surface. The zones of magma formation distinguished on this basis usually have characteristic features of ring (centricline) distribution of energetic and petrological properties within these concentrations. Third, concentrations of volcanic sources and subvolcanic intrusions reveal a clear correlation with ring fractures, which are mandatory elements of dome depression telescopic structures, within which breakout sources are mainly concentrated. Fourth, hydrothermal systems are confined near the concentrations of breakout sources, which can be pronounced at the Earth’s surface as sources of mineral and thermal mineral waters. Fifth, mapping of these factors as contour lines of the density of breakout sources and other structural and material characteristics gives the possibility for quantitative correlation of all these properties and for distinguishing of the structural material composition of the autonomous fluid magmatic system that drains the mantle.

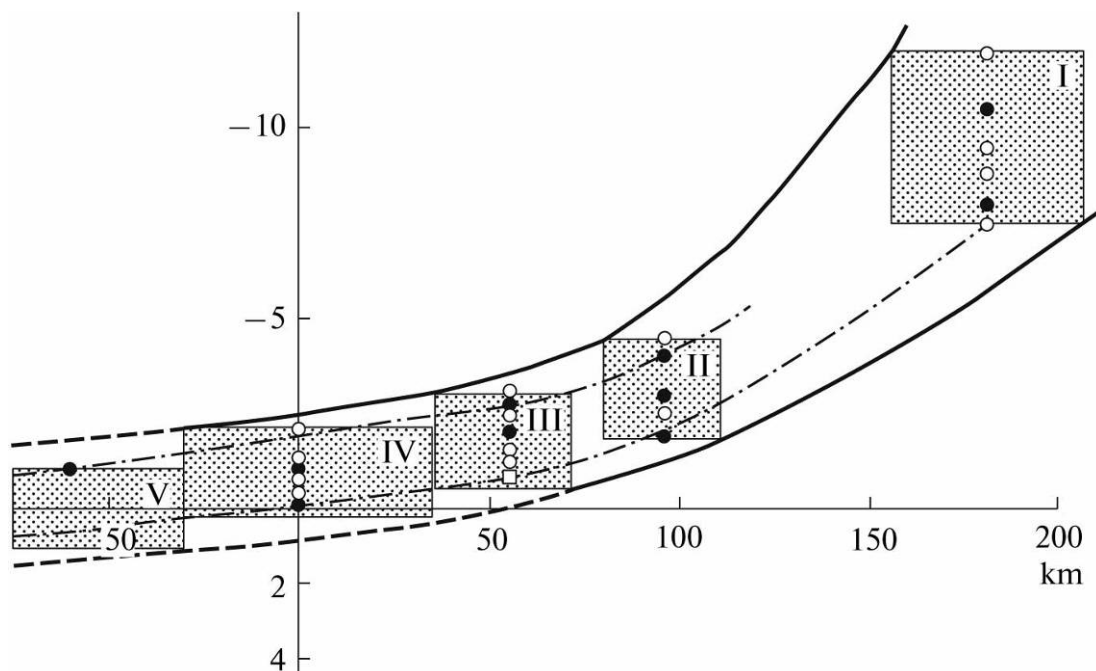


Fig. 3.1.1.2. Formation time of VCs versus their distance from Elbrus along the vortical trajectory. Volcanic centers: (I) Pyatigorsk, (II) Kabardinsk, (III), Balkar, and (IV) Elbrus, (V) place and time of possible appearance of the next VC. Open circles denote the dates of the absolute age of volcanic and

intrusive rocks. Black circles denote the dates that are considered most reliable. Rectangles denote the approximate age of volcanism based on geological data. Solid lines outline the spatiotemporal location of VCs based on maximum and minimum values of the age of volcanic rocks. Dashed dotted lines denote the location based on the most reliable data; dashed lines denote extrapolation. Past is above the abscissa axis; future is below the axis. East and north are to the right of the ordinate axis, west and north are to the left.

A combination of the scatter of these data with the distance of the nearest and most distant boundaries of each VC from Elbrus determines the size and location of rectangles corresponding to these centers.

Pyatigorsk VC: distance from Elbrus is 155–205 km (middle distance 180 km); magmatism was manifested in the interval 12–7.5 Ma.

Kabardinsk VC: distance from Elbrus is 80–110 km (middle distance 95 km); magmatism was manifested in the interval 4.4–1.8 Ma.

Balkar VC: distance from Elbrus is 35–72 km (middle distance 55 km); magmatism was manifested in the interval 3 to 0.7–0.1 Ma.

Elbrus VC: distance from Elbrus is –30 to +35 km (middle distance 0 km); magmatism was manifested in the interval 2–0 Ma.

Very interesting and important conclusions follow from this research:

First, they are related to the perspectives of further evolution of volcanic and postvolcanic phenomena in the entire Elbrus volcanic region. These perspectives can be expected owing to the location of the curves drawn through the minimum values of the most reliable dates and other dates of vulcanite age. The first crosses the abscissa (zero value of the ordinate at the point where the past changes to the future) near Elbrus, while the second crosses the abscissa 50–60 km to the east of Elbrus (Fig. 3.1.1.2). This means that volcanism will continue in the future, and its continuation and revival are possible not only in the immediate vicinity of the modern Elbrus cone but also in the Balkar VC. If this tendency will last and the minimum values of all obtained dates have geological sense, we can expect manifestation of volcanic processes in the Elbrus VC for one million years more. In the Balkar VC, the volcanic threat will last most likely not longer than 400 ky.

Second, approaching the VC in time and space engages our attention. This approach was very clearly pronounced during the formation of the Balkar and Elbrus VCs, which were reasonably joined by E.E. Milanovskii and N.V. Koronovskii into the Elbrus–Kyugenskii volcanic region. It is not clear what this approach indicates, but undoubtedly it evidences the dawning of a new epoch in the formation of VCs and maybe a transition to a principally new stage signifying the appearance of a mega center. Such huge structural material fluid magmatic systems are known from the literature. If this merging actually indicates the onset of a new large VC, we can expect absolutely new regularities in the further history of volcanic tectonic events and their manifestation in the spatiotemporal continuum.

Third, we have to note one more peculiarity of pulsating vortical evolution of volcanism in the Elbrus region. We are speaking about the possible place of the next manifestation of volcanic plutonic processes. According to the presented data, they can be expected in the region of the Elbrus and Balkar VCs as prolonged but, however, final events. During the possible transition to the next stage of the vortical evolution, activation of magmatism and tectonics will most likely occur to the north_northeast of Elbrus with the center in the region of the Narzan Valley (Khasaut River)–Western Kinzhal Mountain (Fig. 3.1.1.1). This region is characterized by episodic events of Early Pleistocene volcanism (andesites and Tyzyl andesite basalts) and concentration of numerous springs of carbonate mineral waters. It is likely that both of them are forerunners of expected large_scale volcanic tectonic events during the possible appearance of a new VC. Its spatiotemporal location is shown in Figure 3.1.1.2 by means of extrapolation of pulsating vortical process of volcanic evolution in the anticipated direction. Its possible

characteristics are as follows: distance from the Elbrus along the vortical trajectory is –30 to –80 km (middle at –60 km), interval of manifestation is –0.9 to > +1.5 My.

Masurenkov Yu. P., Sobisevich A. L. Pulsating Vortical Evolution of the Elbrus Volcanic Region (as a Consequence of Migration of the Mantle Plume?) // Doklady Earth Sciences, 2010, Vol. 432, Part 1, pp. 608–612. DOI: 10.1134/S1028334X10050132

Sobissevitch A.L., Masurenkov Y.P., Nechaev Y.V., Pouzich I.N., and Laverova N.I. Cenozoic fluid-magmatic centers, geodynamics, seismotectonics and volcanism in Northern Caucasus // European Geosciences Union General Assembly 2010, Vienna, Austria, May 2 – 7, 2010.

Sobissevitch L.E., Sobissevitch A.L., Kanonidi K.Kh., and Filippov I.N. The new geophysical observatory in Northern Caucasus (Elbrus volcanic area) and results of studies of ULF magnetic variations preceding strong geodynamic events // European Geosciences Union General Assembly 2010, Vienna, Austria, May 2 – 7, 2010.

3.1.2. Relation between Structural and Material Circular Motions in a Volcanic Center

Yuri P. Masurenkov, Alexei L. Sobissevitch, alex@ifz.ru, Ninel I. Laverova, Russian Academy of Sciences, Schmidt Institute of Physics of the Earth, Moscow, Russian Federation

For the first time, comparison of the petrogeochemical features of magmatic types from Pyatigorsk volcanic center with Mohorovichich area structure has been performed, and on the basis of the analysis, correlation signs of their correspondence to a uniform system are established.

We constructed the mantle area on the basis of the author's quoted work about three geophysical profiles made in terms of interpretation of records of exchange waves from earthquakes and waves from industrial explosions, made by scientists from the Neftegeofizika Scientific Development and Production Center, and a variant that represents a smoothed picture of the mantle area (sliding quadrature method on an area 400×400 km² at 10 km intervals). Despite the essential differences in details, the specified variants are uniform in one point: the mantle area at the basis of the volcanic center represents a dome with vertex fan pressure.

In Fig. 3.1.2.1. the distribution of porphyritic phenocrysts of the second generation as the most typical is shown. In the very middle of the volcanic center, the quantity of crystals of the second generation in magma is quite large—27%. Toward the periphery, at first it gradually decreases to 13% in all directions, and then gradually increases to values close to those in the middle: 24–30%. Owing to this fact, a concentric zone field with maximums both in the middle and at the edges with a circular zone of minimum between them is created. The zone of minimum configuration is an ellipse extended in the north–south direction. Its axes have the following parameters, 27 and 13 km. The type distribution in phenocryst laccoliths of the first, most likely deeper and certainly earlier, generation shows an obvious similarity to the distribution of phenocrysts of other generations: in the middle of the center 25%, in the elliptic minimum zone 15%, on periphery 24–29%.

It is possible to surmise that the greater the quantity of dissolved water that was in the melt, the greater the amount of it that would remain in residual form. This could serve as a certain orientator, specifying what quantity of water there was in transformation of melting rock. Actually, the pattern of residuary water distribution shows a similarity to the distribution of phenocrysts but with the opposite sign: it is fixed concentrically to the zone structure of the system and of particular importance is the presence of a minimum in the center (10% and less) and on the periphery (3–24%) of the structure and the maximum (30–79%) between them in circular form that surrounds the center. The size of elliptic axis of this positive anomaly is $33 \times$

18 km. Thus, a comparison of the distribution of residual water and primary crystallization and secondary crystallization of inversely proportional dependence types is planned.

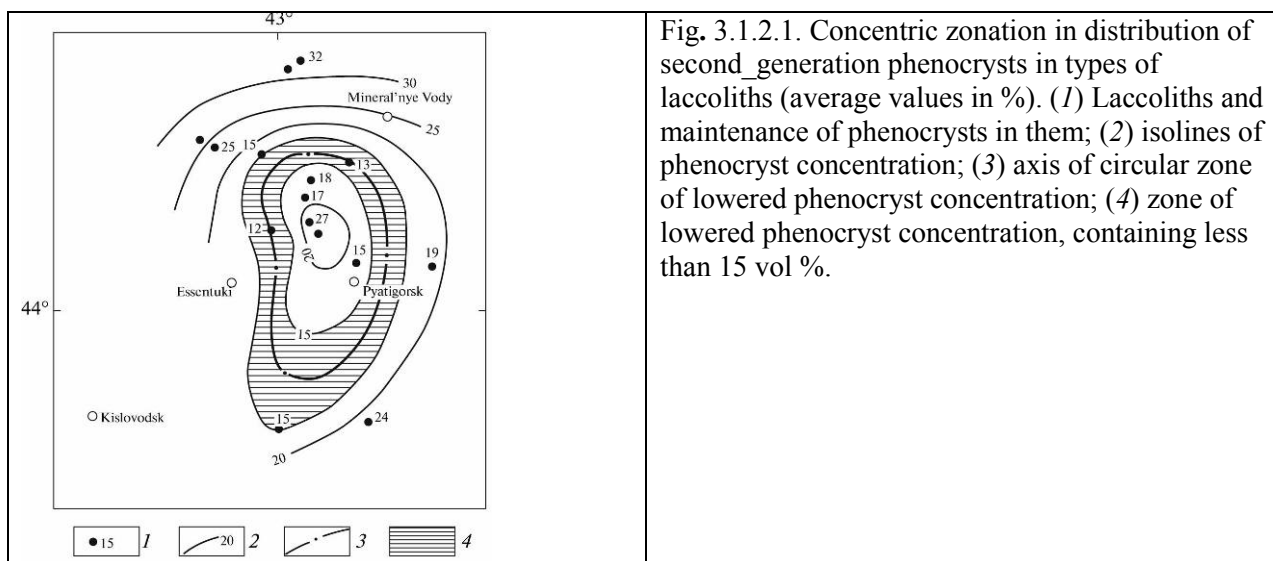


Fig. 3.1.2.1. Concentric zonation in distribution of second-generation phenocrysts in types of laccoliths (average values in %). (1) Laccoliths and maintenance of phenocrysts in them; (2) isolines of phenocryst concentration; (3) axis of circular zone of lowered phenocryst concentration; (4) zone of lowered phenocryst concentration, containing less than 15 vol %.

The distribution of fluorine content in types of laccoliths is like the distribution of the water content: minimum in the structure center, a circle of maximum around it, and concentration decrease toward the periphery. This is understandable as H₂O and HF are dissolved in silicate melting. However, their behavior, which coincides in the main, is characterized with rather considerable independence, forming in the timetable ellipses that are quite independent and strongly differing in size, form, and orientation. CO₂ as an antipode of water, and fluoric acid in the solubility in silicate melting behaves accordingly: the maximum in the center and the minimum on the periphery.

The cited data specify the high probability of the following geological objects and factors belonging to a uniform interconnected system: ring faults with a difficult pattern of intermittent concentric reclamations and deflections on the Earth's surface; subvolcanos in the circular structure with concentrically zoned distribution of petrogeochemical signs; the dome structure on the area of the geophysical stratum at a depth of 7–16 km; the circular dome fan pressure structure on the Mohorovichich area at a depth of 40–46 km.

All these elements of unified system, as a whole coinciding in plan, differ in sizes and are characterized by some displacement relative to each other. Subvolcanic intrusions, projected on a horizontal plain of the daylight surface chemical and temperature structure of the zone of magma formation and crystallization, possibly also contain information about the vertical heterogeneity of this zone. The differences in the concentration of water and carbonic gas in intrusion types of sites of different structures reach such high values that it is necessary to admit the difference in pressure for these sites, which is correlated to a difference of depths of 12 km. Such an overfall at a distance of only 5–6 km can be presented as the apical prominence of the magma chamber roof, which forms a resemblance to a large ring dike on its arch. Its relative enrichment with water, fluorine, sulfur, alkalis (mainly sodium), and earth silicon reduced the crystallization temperature. Therefore, the quantity of crystal phase is significantly lower at the same or even at lower temperature than in the chamber center. Certainly, this is one of the possible variants for explaining the phenomenon described above. It is possible to imagine another model but not in the form of a single magma chamber, as the area that is under a premelting condition and, therefore, in a position for disjunctive dislocation. Then the circular faults, which go through the entire crust and mantle thickness and are conductors of mantle gas and fluid streams, provide for the occurrence of local magma chambers, the properties of which submit to the concentric zonal

structure of the general intratelluric substance and energy stream. Detailed information about the geological aspects of the crust in the interval between the mantle and the daylight surface within a volcanic center are necessary to solve this problem.

Masurenkov Yu. P., A. L. Sobisevich, and N. I. Laverova. Relation between Structural and Material Circular Motions in a Volcanic Center. Doklady Earth Sciences, 2009, Vol. 429, No. 8, pp. 1359–1363.

3.2. Mud volcanoes in North-Western Caucasus

Alexei L. Sobissevitch, alex@ifz.ru, **Andrey V. Gorbatikov**, **Alexander N. Ovsuychenko**, **Leonid E. Sobissevitch**, **Irina N. Pouzich**, *Russian Academy of Sciences, Schmidt Institute of Physics of the Earth, Moscow, Russian Federation*
Boris A. Morev, *Voronezh State University, Voronezh, Russia*

Intense mud-volcanic activity is observed in the territory of Russia, first of all, on the Taman Peninsula, which is an integral part of the modern evolution of fluid-magmatic systems in the Northern Caucasus.

Complementary geological and geophysical studies of mud volcanic phenomena in North-Western Caucasus (Taman mud volcanic province) were established. Geophysical field works have been carried out in 2005 – 2009 on the two different mud volcanoes: the Gora Karabetova and the Shugo mud volcano.

Usage of methods of vibroseismic sounding, traditional magneto-telluric sounding and relatively new method of low-frequency microseismic sounding allows obtaining several independent vertical cross-sections for the two different mud volcanoes down to the depth of 25 km. For the two different mud volcanoes their deep subsurface structure has been revealed and discussed with respect to regional tectonic settings, geology and geomorphology.

The Gora Karabetova mud volcano is one of the most active mud volcanoes in the Taman peninsula with primarily explosive behaviour while the Shugo mud volcano's activity pattern is different, explosive events are rare and both types of phenomena may be explained by the configuration of their feeding systems, tectonic position and deep pathways of migration of fluids.

Gora Karabetova

During the last few years, Mt. Karabetov, which is one of the most active mud volcanoes in the Taman region, has been the object of multidisciplinary geological–geophysical and geochemical investigations [3, 4]. This volcano is characterized by explosive type of eruptions with periodic manifestation of the whole power of this seemingly harmless natural phenomenon. During the field works a detailed geological-geomorphological mapping of Mt. Karabetov mud volcano was carried out and supplemented by remote sounding data. As a result, it became possible to trace the tectonic deformations of young forms of topography and various manifestations of exogenous geological processes in the study region. Simultaneously, profile geophysical measurements were carried out using the microseismic sounding method.

From our data, we can suppose that the formation of the Mt. Karabetov mud volcano and the eponymous anticline is related to the conditions of subhorizontal extension along the fracture in the fold axis. In this case, the extension is oriented in the sublatitudinal direction, while contraction is in the submeridional direction. Such orientation of the strain axes agrees with the reconstruction of the Quaternary stress field based on the data of geological–structural investigations and analysis of focal mechanisms of earthquakes. This anticline is characterized by a NNE orientation, which is atypical for normal NE-oriented diapirs of the ridge, and the deep

location (1 km) of the Maikopian diapir core. We can suppose that this orientation caused maximal concentration of extension stresses and the most favorable conditions for fluid pressure discharge. Therefore, the diapir core piercing was not exposed.

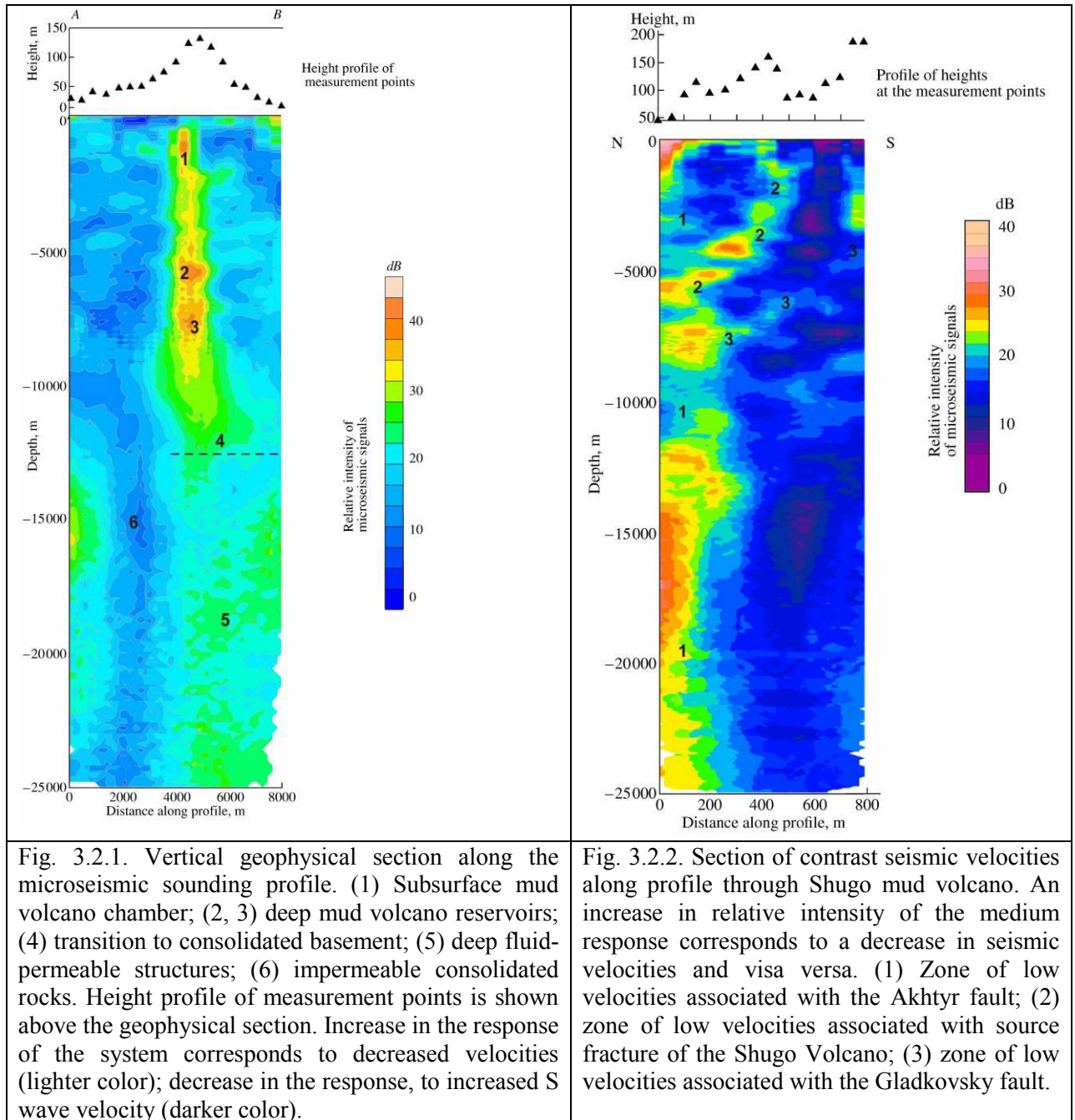


Fig. 3.2.1. Vertical geophysical section along the microseismic sounding profile. (1) Subsurface mud volcano chamber; (2, 3) deep mud volcano reservoirs; (4) transition to consolidated basement; (5) deep fluid-permeable structures; (6) impermeable consolidated rocks. Height profile of measurement points is shown above the geophysical section. Increase in the response of the system corresponds to decreased velocities (lighter color); decrease in the response, to increased S wave velocity (darker color).

Fig. 3.2.2. Section of contrast seismic velocities along profile through Shugo mud volcano. An increase in relative intensity of the medium response corresponds to a decrease in seismic velocities and visa versa. (1) Zone of low velocities associated with the Akhtyr fault; (2) zone of low velocities associated with source fracture of the Shugo Volcano; (3) zone of low velocities associated with the Gladkovsky fault.

A relatively narrow vertical low-velocity zone associated with the fluid-saturated conduit was distinguished from the results of microseismic sounding beneath the Karabetov Volcano. Based on the experimental data, the recharge zone for conduit is located at a depth of 4.5–9 km (Fig. 3.2.2). In the deeper zone, the contrasts of seismic velocities of S waves are not so clear. However, the anomaly associated with the recharge zone can possibly continue to a depth greater than 15 km. Hence, the core of Karabetov diapir anticline composed of Maikopian clays and the mud volcano can be interpreted as products of deep processes governed by the dynamic features of dilatancy structures. In this case, the formation of the anticline structure is not related to the

regional compression, but mainly to the response of the sediments overlying the Maikop Group to the injection of friable mobile masses along the fractures.

The deep structure of the Taman Peninsula was studied before, but the materials of drilling and seismic prospecting based on the reflected wave method allow us to determine only approximate depths of the location of rocks of different ages. It was found that the depth interval 4.5–9 km corresponds conditionally to the Cretaceous terrigenous-carbonate zone. The petroleum potential of Lower Cretaceous clayey sediments has been recognized in many deposits of the Ciscaucasus including the Taman Peninsula (e.g., the Fontalov deposit). The deeper zone is likely composed of Jurassic terrigenous rocks and the Permian–Triassic transitional terrigenous–carbonate complex. The industrial petroleum potential of the Lower Triassic carbonate rocks has been confirmed in the Eastern Ciscaucasus, while gas seeps from the Lower Triassic limestones have been found in the western depression of the Maikop Uplift. Hence, we do not also exclude their participation in the generation of fluids in this depth interval. The crystalline basement in the Taman Peninsula is presumably located at a depth of 13–15 km. This interval is marked by decrease in the contrasts of seismic velocities of S waves distinguished from the microseismic sounding data.

We also found the correlation between the regional geodynamics and the fluid activity and traced the fluid migration pathways down to the depths of 15–25 km.

Shugo Mud Volcano

The activity of Shugo Volcano located within the Akhtyr flexure-fracture zone is characterized by continual alternation of active and calm periods over a long period of time with systematic ejection of gases and volcano mud with an insignificant content of coarse clastic material.

The Shugo mud volcano is located within the Akhtyr flexure-fracture zone. Unlike the majority of mud volcanoes in the region, it is confined not to the axis of the anticlinal diapir fold, but to a synclinal depression in native Cretaceous–Pliocene deposits. The Upper Pliocene sediments at the foot of the mud-volcanic cone do not participate in processes of fold formation. The Shugo mud volcano associates with the NW-oriented fracture manifested in the topography. The fracture influences the endogenic processes. The southeastern limb of the fracture is elevated. The dextral component is manifested in the displacement of the circular ridge bounding the volcano caldera. The velocity of horizontal displacements measured by geomorphological methods for the last 10 000 yr (Holocene) is 3.7–5 mm/yr, while the velocity of the vertical displacements is 0.7–1 mm/yr [Ovsyuchenko, 2005].

Multidisciplinary geological–geophysical investigations including works on deep sounding of the zone were conducted in the Shugo Volcano region. The investigation included the microseismic sounding method [Gorbatikov et al., 2008; Gorbatikov, 2006] based on inversion of the amplitude–frequency spatial distribution of the microseismic field. The method is based on the following assumption: the vertical component of the microseismic field in the low-frequency range is determined by the dominating contribution of the fundamental modes of Rayleigh surface waves. The vertical section along contrast seismic velocities is shown in Fig. 3.2.2. The section based on the microseismic sounding method shows the location and form of geological heterogeneities of the medium on the basis of the contrasts of seismic velocities. The horizontal resolution of the method is estimated as 4% of the length of the sounding wave (correspondingly, 8% of the depth of the heterogeneity location). The vertical resolution is estimated as 15% of the depth of the location [Gorbatikov et al., 2008]. The regions with low seismic velocities correspond to more fractured and fluid-saturated structures.

Our attention is attracted by the near-surface fluid reservoir, which is confined to a synclinal fold and structurally similar to the later fold. This feature is likely responsible for fluid inflow to the Shugo Volcano according to the mechanism of an artesian spring. Fluid sources are clearly seen in the depth range 3500–4000 m.

A revision of the concept of the structure roots of the Shugo Volcano was carried out with the account for data on the structure and age of effusive rocks. The eruption products include abundant Lower Cretaceous siderite concretions along with Upper Cretaceous fucoid marls and limestones. The products also include fragments of igneous rocks, mainly quartz porphyries and Jurassic coral limestones. One can also see Lower Cretaceous conglomerates composed of pebbles of eroded Upper Jurassic igneous rocks. In general, ejecta of the Shugo mud volcano are mainly composed of Cretaceous rocks and a smaller amount of Paleocene, Upper Miocene (Sarmatian), and Pliocene (Pontian and Kimmerian) rocks, whereas Maikopian rocks are absent

- Sobisevich L.E., Sobisevich A.L. Study of deep underground structure of mud volcanoes in North-Western Caucasus by means of geological and geophysical methods // Геофизический журнал, № 4. Т. 32, 2010. С. 158.*
- Sobisevich A.L., Gorbatikov A.V., Ovsuychenko A.N., Sobisevich L.E., Pouzich I.N., Morev B.A. Results of study of deep underground structure of mud volcanoes in North-Western Caucasus by means of geological and geophysical methods // International Conference "Cities on Volcanoes 6. Tenerife, Canary Islands, Spain. May 31 – June 4, 2010.*
- Sobisevich A.L., Gorbatikov A.V., Ovsuychenko A.N., Sobisevich L.E., Pouzich I.N., and Morev B.A. Study of deep underground structure of mud volcanoes in North-Western Caucasus by means of geological and geophysical methods // European Geosciences Union General Assembly 2010, Vienna, Austria, May 2 – 7, 2010.*
- Sobisevich A. L., A. V. Gorbatikov, and A. N. Ovsuychenko. Deep Structure of the Mt. Karabetov Mud Volcano // Doklady Earth Sciences, 2008, Vol. 422, No. 7, pp. 1181–1185.*
- Gorbatikov, A. V., A. L. Sobisevich, and A. N. Ovsuychenko. Development of the Model of the Deep Structure of Akhtyr Flexure-Fracture Zone and Shugo Mud Volcano. Doklady Earth Sciences, 2008, Vol. 421A, No. 6, pp. 969–973.*
- Ovsuychenko A. N., in Modern Methods of Geological-Geophysical Monitoring of Natural Processes in the Caucasus Territory (IFZ RAN, Moscow, 2005), pp. 235–248 [in Russian].*
- Gorbatikov A. V., M. Yu. Stepanova, and G. E. Korablev, Izv. Phys. Solid Earth 44 , 50 (2008) [Izv. Akad. Nauk, Fiz. Zemli, No. 1, 75 (2008)].*
- Gorbatikov A. V., in Modern Methods of Processing and Interpretation of Seismological Data Proc. International Seismological School (Obninsk, 2006), pp. 66–71 [in Russian].*

3.3. Thermal resources of Northern Caucasus

Alexei L. Sobisevitch, alex@ifz.ru, **Yuri P. Masurenkov**, **D. V. Likhodeev**, *Russian Academy of Sciences, Schmidt Institute of Physics of the Earth, Moscow, Russian Federation*
A. V. Shevchenko, *Kabardino-Balkarian State University, Nal'chik*

Thermal Anomalies

Amongst the thermal anomalies of Northern Caucasus, the region of Elbrus volcanic center holds first place because the Elbrus is an active volcano in a resting state. It has been determined that the peripheral and parent magmatic chambers of the volcano are located at depths of 0–7 and 20–30 km below sea level, respectively, and the geothermal gradient beneath the volcano is 100°C/km. At present, in relation to the newly obtained data on thermal anomalies in the region of Elbrus volcanic center [Modern..., 2005; Sobisevich & Likhodeev, 2007], it is important to clarify the effect of the character of volcanic magmatic chambers on the temperature of carbonaceous mineral waters. The migration of deep fluids to the surface through faultblock structures leads to the formation of thermal anomalies of various scales, which are revealed in changes in the carbonaceous mineral waters (CMW) thermal regime.

The temperatures of CMW in the Elbrus region and adjacent territories (more than 500 springs in all) measured in natural conditions varied insufficiently (7–12°C); the temperature is seldom below 3–5°C or above 15°C. The notable thing is the distinct difference in temperatures of carbonaceous mineral waters of the northern and southern slopes of the Main Caucasian ridge; the temperature is higher in the south.

Analysis of the data on debits of more than 200 springs has shown that springs of the northern slope of the Main Caucasian ridge, having a debit of 500 l/day and more, reveal a positive correlation between debit and temperature (Fig. 3.3.1). Therefore, the higher temperatures of carbonaceous mineral waters of the Elbrus Region reflect, in general, the effect of endogenous factors. For the low-debit springs (less than 500 l/day), whose number is relatively low, the increase in temperature is likely related to the surface heating of water, because it directly depends on the decrease in their debits, revealing the surface conditions during summer sampling of water.

A clear dependence between temperature and debit values in the southern slope of the Main Caucasian is not observed, the area of data scattering is such that it implies the possibility of such a dependence, in particular, along the upper margin of the scattering area, where the most heated water springs are located. Carriers of relict deep temperatures might be among them. Meanwhile, the lower border of the scattering area testifies to the inverse phenomenon, namely to the prevalent influence of surface heating on water temperature. Somehow, the effect of the climate factor on the temperature of CMW springs should not be denied, because it is revealed to a greater or lesser degree anyway. In this connection, it is useful to eliminate this factor for a more exact determination of the role played by the deep temperature component.

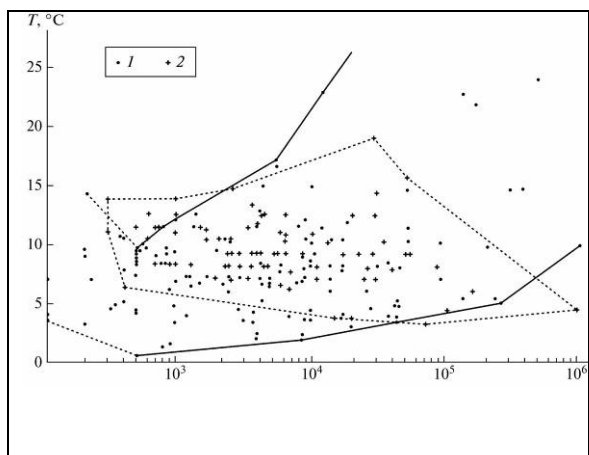


Fig. 3.3.1. Dependence between temperature and debit of CMW springs in the Elbrus Region: (1) springs of the northern slope of the Main Caucasian ridge, (2) springs of the southern slope of the Main Caucasian ridge.

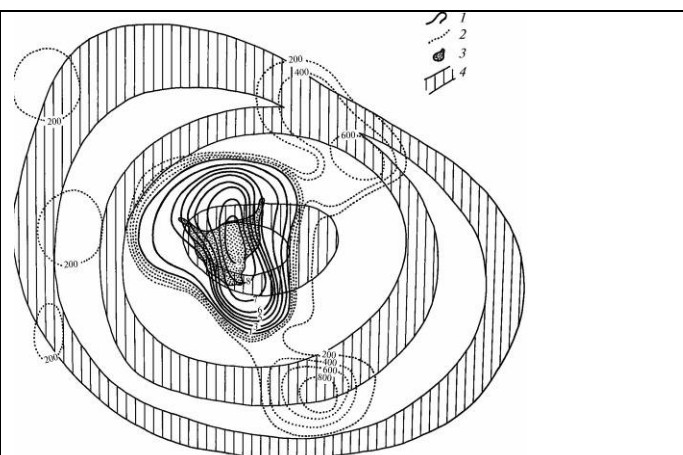


Fig. 3.3.2. Heat outflux of CMW in the Elbrus volcanic area: (1) isolines of trend of heat outflux made by springs in millions kcal/day, from 400 km², (2) the same in billions kcal/day, from 400 km², (3) the Elbrus volcano, (4) zones of ring deformations in dome-formation.

We calculated the outflux of deep heat by high_debit CMW springs of the Elbrus Region, whose number is more than 100. It was 21 277 000 kcal/day, or 1030 kW. The pattern of spatial distribution of this deep energy flux is of special interest. Even when all the hidden and unrecorded heat losses are taken into consideration, the total leaving is much less than the energy of the average volcano productivity during its active period and is about 40–400 MW. The calculations and their graphical pattern are interesting as a thermal projection of the peripheral magmatic chamber to the day surface (Fig. 3.3.2). The zone of manifold increased heat outflux forms an anomaly that coincides with the Elbrus volcanic edifice. By the trend of 3 million

kcal/day, from which a sharp increase is started, the diameter of the zone in the sublatitudinal direction is 10 km and that in the submeridional direction is 30 km. In this connection, particular attention should be paid to the fact of coincidence in the sizes of the anomaly and supposed magmatic chamber zone beneath the volcano, which was revealed using various geophysical methods; the magmatic chamber zone has a diameter of 10 km in the sublatitudinal direction [Modern..., 2005] and of 20 km and more in the submeridional direction.

The analysis of the modern heat outflux through carbonaceous springs in the Elbrus Region reflects the active state of the magmatic chamber. The thermal effect of the magmatic chamber on the environment exceeds the background values of heat flux many times, and includes both conductive and convective heat transfer, where the important role is played by carbonaceous mineral waters.

Masurenkov Yu. P., A. L. Sobisevich, D. V. Likhodeev, and A. V. Shevchenko, Thermal Anomalies of the Northern Caucasus. Doklady Earth Sciences, 2009, Vol. 429, No. 8, pp. 1318–1321.

Modern and Holocene Volcanism in Russia, Ed. by N. P. Laverov (Nauka, Moscow, 2005) [in Russian]. Sobisevich L. E. and D. V. Likhodeev, Ekol. Vestn. Nauch. Tsentrov ChES, No. 3, 47–54 (2007).

Pyatogorsk Volcanic Center

The temperature of waters from natural sources and from wells reflects their varied depth state in the interval from the Earth's surface down to 1600 m (the deepest of the known wells). It is a priori obvious that, in the ideal case, the dependence between depth and temperature in the considered intervals is a straight line corresponding to the geothermal gradient. Theoretically, it is slightly greater than 25°C per km for the so-called “projection of Caucasus Mineral Waters”. In fact, this gradient varies in 80 objects of Pyatigorsk from 50°C to 500°C per km.

The highest values of the geothermal gradient, almost coincide with laccoliths of Beshtau, Mashuk, and Zheleznaya Mounts (Fig. 3.3.3). The area of the hydrocarbonate maximum is located 7–10 km westwards from Beshtau Mount. In the same place, at the central portion of Blagodarnenskoe springs of mineral waters (well no. 46), the greatest helium content is revealed in the composition of spontaneous gases. The area of boron content is located 5–12 km southwestwards from Beshtau Mount. Southeastwards from it, near Mashuk Mount base (cryptolaccolith), mineral waters with high radon and radium content are without all peradventure related to postmagmatic processes. In the same place, in Pyatigorsk, and to the north of here, in Zheleznovodsk springs of mineral waters, the highest hydrogen contents in the CMW are found in composition of the accompanying gas. There is the supposition concerning the water genesis for these springs that they “are formed under conditions of a common source of liparite magmas”. These data are not only proved by the presented materials, but are also supplemented by new arguments for the hypothesis of a mantle source for other components of mineral waters. They also allow us to distinguish the place at the mantle surface that is the main drainage structure of mantle fluid and, apparently, the mantle magmatic flux. Its situation is determined by the location of portions with maximal hydrocarbonate, boron, helium, hydrogen, and radon concentrations in mineral waters and accompanying gases. It is outlined with a dashed line in Fig. 3.3.3. A highly raised segment of the dome-annular structure is located to the north and northeast of it, and the depression of the lowered segment is located to the southwest. Fluid flowing out from the drainage structure enters the basaltic layer of the crust and fills a certain volume with a shift to the southwest, to the trough side, because propagation in the northeasterly direction is bordered by a raised segment of the dome. The uplift of fluid in the granitic layer is accompanied with formation of a peripheral magmatic source, whose projection, apparently, corresponds to the position of the drainage mantle structure, but overcomes it by area.

We suggest that there may be portions containing magmatic melt inside this drainage system, somewhere close to its center, at the level of basaltic and granitic layers, or maybe

higher as well. The presence of high-temperature mineral waters above the supposed magmatic source, just near the Earth's surface, is evidence for this assumption; these waters also evidence the presence of a significant geothermal gradient, which is able to provide rock melting within the crust limits. Such a long (~8 Ma) existence of a supposed magmatic source in the center of the dome_ annular structure can be caused by constant migration of mantle fluids through it and by convection of the magmatic melt, which support its active state and implement thermal and material transfer to the Earth's surface.

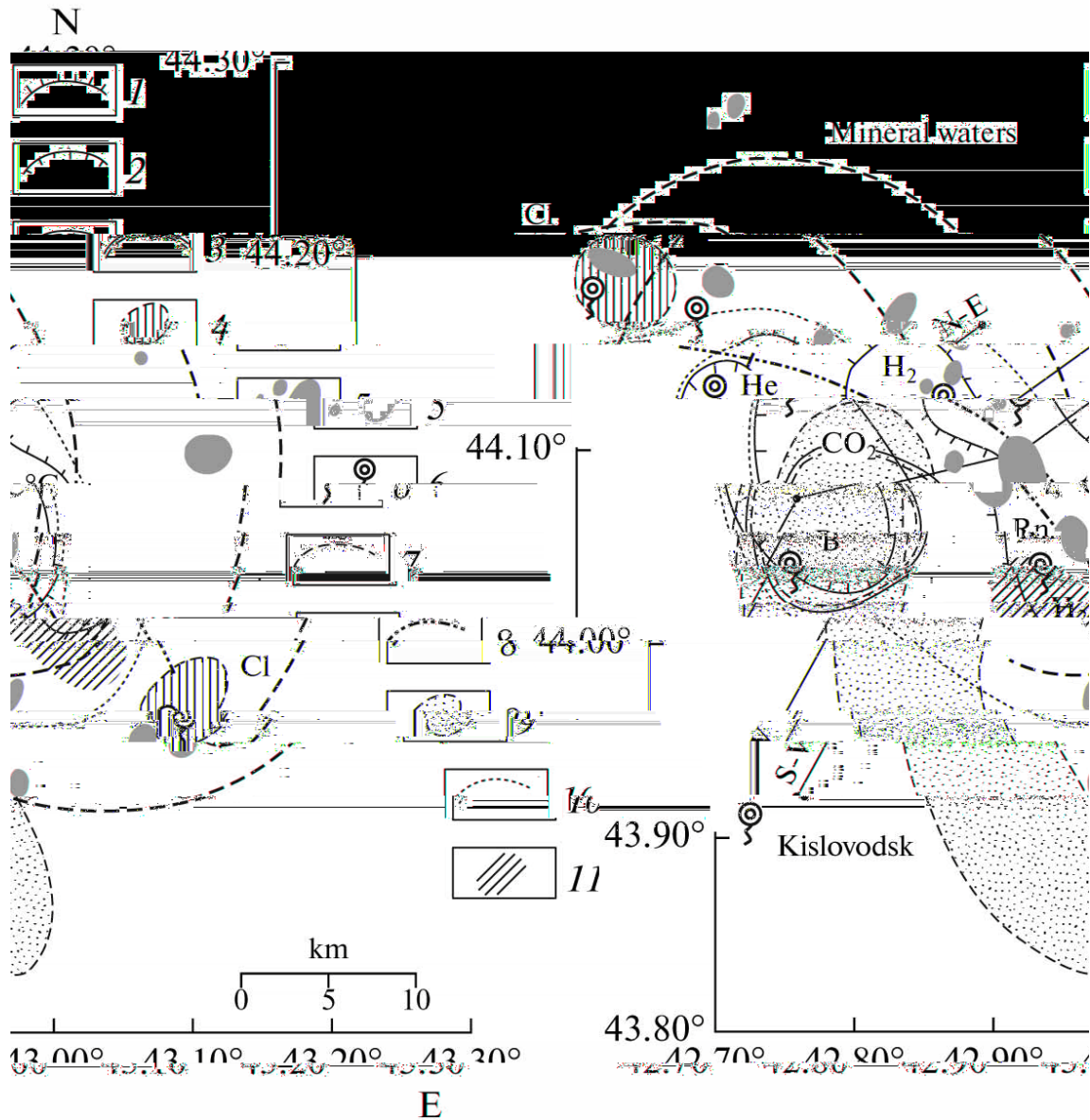


Figure 3.3.3. Combined scheme for location of parts with maximal geothermal gradients and maximal concentrations of chemical components in mineral waters and accompanying gases, and for zones of structural and geophysical peculiarities of the Pyatigorsk volcanic center: (1) contours of portions with a high (greater than 150°C per km) geothermal gradient, (2) portion with a high (greater than 6 g per liter) concentrations of hydrocarbonates, (3) portion with high (more than 55 mg per liter) concentrations of boric acid, (4) portion of high (greater than 9 g per liter) concentrations of chlorine in mineral waters, (5) laccoliths, (6) mineral water springs with higher hydrogen, helium, and radon content, (7) the most clearly revealed fragments of annular faults, (8) axis of mantle surface bend, (9) aseismic zone, (10) contour of

the probable zone of granitic layer rocks melting (peripheral magmatic source), (11) thinning zone in granitic layer.

Masurenkov Yu. P., A. L. Sobisevich, and N. I. Laverova, *Doklady Akad. Nauk* 428, 810 (2009) [*Doklady Earth Sci. (Engl. Transl.)* 429, 1359 (2009)].

Masurenkov Yu. P., Sobisevich A. L. *The Modern Fluid-Magmatic System of the Pyatogorsk Volcanic Center // Doklady Earth Sciences*, 2010, Vol. 435, Part 2, pp. 1699–1704. DOI: 10.1134/S1028334X10120305

The Modern Hydrothermal System of the Crust–Mantle Origin

Our previous data (see above) provide evidence for spatial closeness between mineral waters and magmatic manifestations but still do not prove their genetic relationships, because they may be interpreted as simple means of one (laccolith) for withdrawal of another (spring) to the surface. A common character or similar origin should be found in the composition and properties of both waters and magmatic rocks. However, some chemical components of mineral waters may be the components of magmatic volatiles and probably mantle fluid.

We mapped the CO₂, B, Cl and Na₂O in mineral waters and superimpose it with geological-tectonic map of Beshtau laccolith. Comparison of the components removed by carbonic acid mineral waters with the geochemical environment, which accompanied the magmatic regime 8–10 Ma in the period of existence and intrusion of magma during the formation of laccoliths demonstrates their striking consistence. A series of curves in Fig. 3.3.4b reflects the distribution of some components along the A–B profile in intruded magma (upper curve, wt % in arbitrary scale convenient for comparison) and in modern mineral waters (lower curves, g/l). Lines reflecting the distribution of components in magma are plotted by the data of their concentration in magmatic rocks.

On the magmatic level (upper curves) of the existence of the fluid–magmatic system, carbon dioxide was mainly concentrated in the center of the magmatic chamber with its concentration decreasing to the chamber periphery and endocontact zones. The data in reliably determined concentrations were obtained only for fluorine among all halogens.

Because of the similarity of its characteristics with those for chlorine, its behavior most likely may be analogous to that of chlorine. The concentration of fluorine in the magmatic melt demonstrates the opposite pattern in comparison with the behavior of carbon dioxide: the minimum in the central part of the chamber and relative saturation of endocontact zones. As this takes place, the zone of relative magma enrichment in fluorine forms a ring around the center of the chamber depleted in it. Water concentrations, petrochemical coefficients Q and n, and the degree of melt crystallization (not shown in Fig. 3.3.4) regularly changing the concentration from the center to the periphery of the chamber and reaching a maximum or minimum also undergo inversion along the ring zone located between the chamber center and its endocontact. This ring inversion zone in the chamber is indicated by horizontal hatching (3) in Fig. 3.3.4a.

Almost complete similarity of curves of the distribution of maximal chlorine and hydrocarbonate concentrations in mineral waters along the A–B profile to curves of fluorine and carbonic acid distribution in magma previously occurring there at some depth along the same profile and around it gives important grounds for such an assumption, if not being direct proof for the existence of the modern magmatic chamber. However, in our opinion, the presence of a concentrically zoned (in cross section) geochemical structure of the drainage fluid–magmatic system may be considered to be proved. In this connection, we suggest that the distribution of high chlorine concentrations around this system in near-surface crustal horizons follows the same regularity as that in the magmatic chamber.

This suggests that the revealed chloride–sodium anomalies near the northwestern and southeastern ends of the mantle surface bend are not the local spot areas of their high concentrations, but are elements of the same ring zone, only partly revealed by the fault system.

The position of this assumed ring zone is demonstrated in Fig. 3.3.4a by vertical hatching (2). The zone of the probable location of the magmatic chamber is assumed inside this chloride-sodium ring. It is indicated by a bold line along the A–B profile.

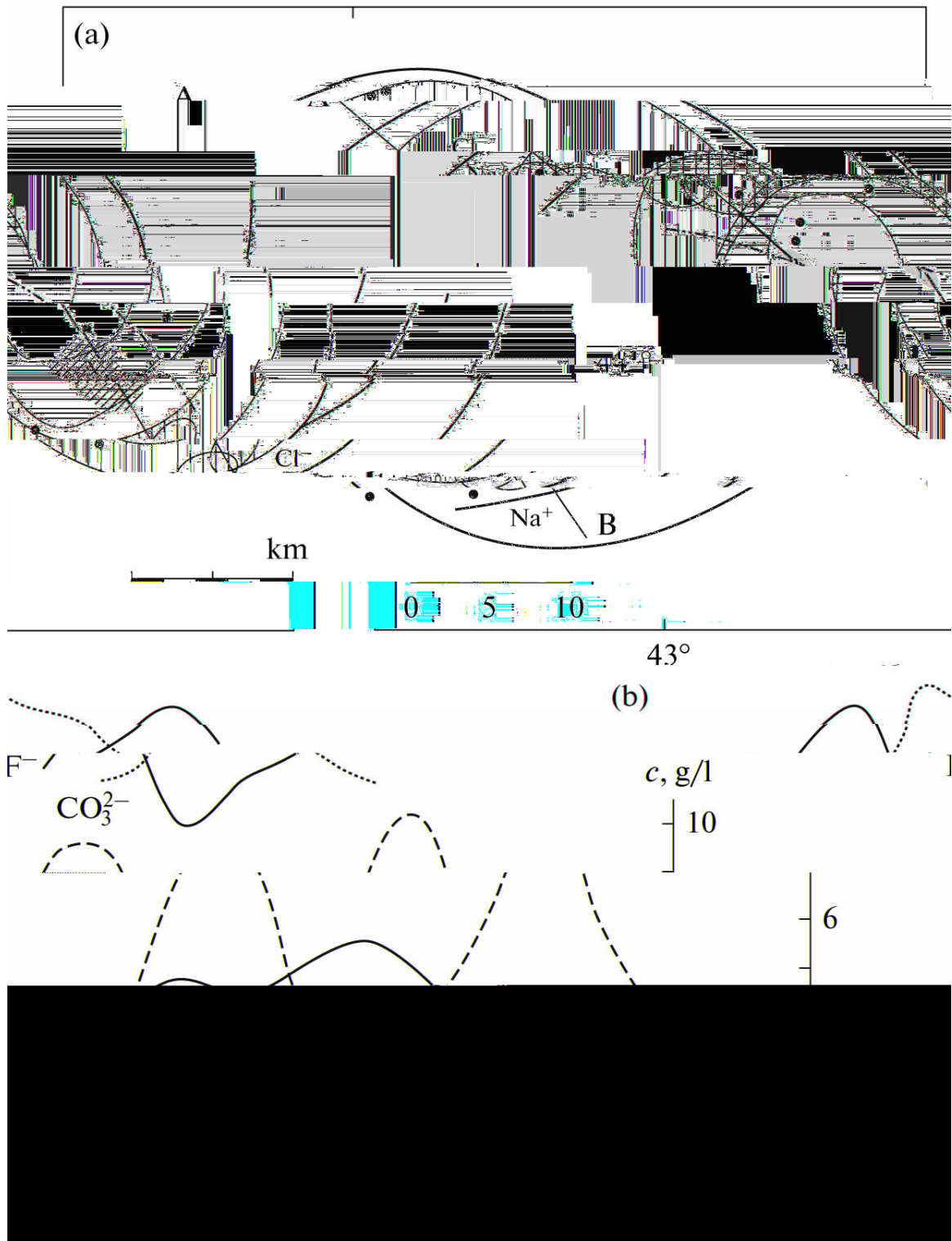


Fig. 3.3.4. Ring petrogeochemical and hydrochemical zonation in the structure of the Pyatigorsk volcanic center. (a): (1) zones of high concentrations of chlorine and alkalis in mineral waters, (2) assumed ring distribution of chlorine and alkalis in fluid flow from the mantle, (3) zone of inversions of the concentrations of petrogeochemical components in magmatic rocks of laccoliths, (4) laccoliths, (5) ring

and arch faults, (6) axis of the mantle surface bend, (7) zone of density decrease in the granite layer; (b): (8) distribution of carbon dioxide in rocks of laccoliths along the A–B profile, (9) distribution of chlorine and hydrocarbonates in mineral waters along the A–B profile; (10) A–B profile.

It should be mention that all the conclusions about the genesis of mineral waters are based on the data on the concentration of various chemical components in the most concentrated and heated waters, the closest to their endogenous predecessors.

Masurenkov Yu. P. and A. L. Sobisevich. Caucasian Mineral Waters: The Modern Hydrothermal System of the Crust–Mantle Origin. Doklady Earth Sciences, 2011, Vol. 436, Part 1, pp. 88–93.

4. Theoretical evidences in volcanology

4.1. The temporal organization of global volcanic activity

A.A. Gusev, *Institute of Volcanology and Seismology, Far East Division, Russian Academy of Sciences, Petropavlovsk-Kamchatsky, 683006, Russia; Kamchatka Branch, Geophysical Service, Russian Ac. Sci 9 Piip Blvd., 683006 Petropavlovsk-Kamchatsky, Russia*

To study the temporal organization of global volcanic activity over time scales from years to centuries, the following three event sequences were studied: two subsets of the regular catalog of eruptions after Siebert and Simkin [Siebert, L., Simkin, T., 2002. *Volcanoes of the World*... <http://www.volcano.si.edu/gvp/world/>], and the “ice core volcanic index” (IVI) sequence, based on the volcanic eruption record as acid layers in big glaciers (Robock, A., Free, M.P., 1996. *The volcanic record in ice cores for the past 2000 years*. In: Jones, P.D., Bradley, R.S., Jouzel, J. (Eds.), *Climatic Variations and Forcing Mechanisms of the Last 2000 Years*. Springer-Verlag, New York, pp. 533–546). To perform the statistical analysis in a meaningful way, data subsets were extracted from the original data, with size thresholds and time intervals carefully selected to make these subsets nearly homogeneous. The analysis has revealed, generally, the tendency to clustering, manifested in the following three forms: (1) The event rate is not uniform in time: event dates form active episodes (“common” clusters). (2) In the time-ordered, sequential list of sizes of eruptions, larger events do not appear purely randomly; instead, they form tight groups (“order clusters”). (3) The volcanic products discharge rate is significantly non-uniform, and shows episodic (intermittent or bursty) behavior. It was also found that for the volcanic sequences analyzed, the two types of clustering behavior mentioned in (1) and (2) are positively correlated: larger events are concentrated at the periods of higher event rate. Such a relationship is best demonstrated by the fact that there is clear negative correlation between the following two time series: (1) of the exponent b of the power law size–frequency distribution (the analog of b -value of the Gutenberg–Richter law for earthquakes) and (2) of the current event rate. Power spectra of the analyzed sequences mostly follow power laws, with negative exponent β . Thus, these sequences can be qualified as pulse flicker noises. In other words, they are fractal sequences with correlation dimension $D_c = \beta + 1 < 1$, and both their clustering and episodicity are of self-similar character. The revealed peculiarities of the global volcanic sequence suggest that some global-scale mechanism exists that is responsible for their origin. They are also of primary importance for understanding the impact of volcanism on climate.

Gusev A.A. Temporal structure of the global sequence of volcanic eruptions: order clustering and intermittent discharge rate // Physics of Earth and Planetary Interiors, Volume 166, Issues 3-4, February 2008, Pages 203-218.

4.2. Mechanism of lava fields generation

Slezin Yu. B., slezin@kscnet.ru, *Institute of Volcanology and Seismology, Far East Division, Russian Academy of Sciences, Petropavlovsk-Kamchatsky, 683006, Russia*

Two types of lava fields, *elongate* and *compact*, are generated by two types of discrete lava flows that are designated as *wide* and *narrow*. The width of a *wide* flow considerably

exceeds its thickness, the converse being true for a *narrow* one. *Wide* flows produce relatively narrow *elongate* lava fields, while *narrow* ones give rise to wider and *compact* lava fields of relatively smaller area and greater thickness, which is related to peculiarities in their dynamics causing branching and greater heat losses in such flows. Exact analytical formulas have been derived to relate the rate of lava in a flow to the flow geometry and lava rheology for idealized models of both flow types; a combination of these yields the approximate relationships for actual flows. We have found conditions for the generation of *narrow* flows showing strongly nonlinear behavior, which produces the peculiar features of the lava fields they create. Examples of lava fields generated by *narrow* flows from lateral vents on Klyuchevskoi Volcano are given. The conditions for their generation are more closely fulfilled in the upper part of the volcano's cone. It is hypothesized that such an arrangement of lava fields may facilitate slope instabilities and enhance the likelihood of major landslides.



Fig. 4.2.1. “Moving dam” (soliton) in one of the flows discharged by the Predskazannyi vent.

The generation of narrow flows is facilitated by high yield strengths and low lava discharges. Additional factors include unevennesses and ice on the slope. As a matter of fact, both lateral eruptions on Klyuchevskoi Volcano that have produced narrow flows with moving dams (IV VVS and Predskazannyi) were situated comparatively high, in the zone of present-day permanent glaciation, and had comparatively low discharges. The Predskazannyi discharge, measured by various methods on moving flows, was between 1 and 10 m³ s⁻¹, while the total yield strength was of the order of 10⁴ Pa [Panov et al., 1985], fitting the condition for the generation of narrow flows.

As also was shown by our earlier work [Panov and Slezin, 1985], moving lava dams in narrow flows enhance heat release, accelerate lava cooling, and thus decrease the length and area of the resulting lava field and increase its thickness. The flow branching due to dam action helps increase the relative width of the lava field. Since the eruptions that produce lava fields of this type mostly originate in the upper part of the volcanic cone, the erupted lava overloads this upper part and enhances the likelihood of landslides. Major sliding on volcanic slopes is an extremely

dangerous and rather widespread phenomenon of nature, the prediction of which would be of great practical value. All this imparts additional importance to a detailed study of the conditions for the generation of narrow lava flows.

Slezin Yu.B. Two Types of Lava Fields and the Mechanism of their Generation. Journal of Volcanology and Seismology, 2008, Vol. 2, No. 5, pp. 340–346.

Panov, V.K., Slezin, Yu.B., and Storcheus, A.V., The Mechanical Properties of Lava Discharged by the Predskazannyi Lateral Eruption (Klyuchevskoi Volcano, 1983), Vulkanol. Seismol., 1985, no. 1, pp. 21–28.

Panov, V.K. and Slezin, Yu.B., The Mechanism Generating the Lava Field of the Predskazannyi Lateral Eruption (Klyuchevskoi Volcano, 1983), Vulkanol. Seismol., 1985, no. 3, pp. 3–13.

4.3. Interaction of NaNO₃-NaOH fluids with sandstone rocks

Kiryukhin A.V., avk@kcsnet.ru, Institute of Volcanology and Seismology FED RAS, Petropavlovsk-Kamchatski, Russia

E. P. Kaymin, Zakharova E. V., Institute of Physical Chemistry and Electrochemistry RAS, Leninsky-31 Moscow 119991, Russia

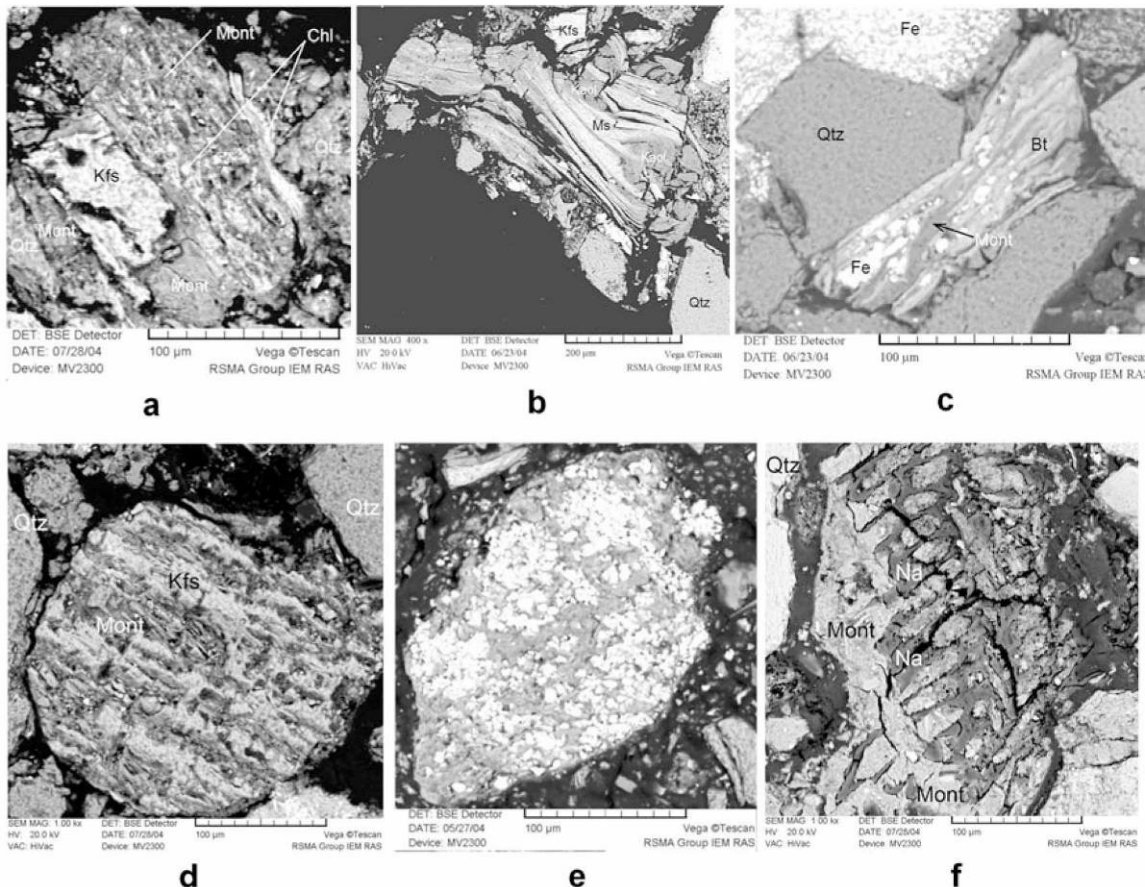


Fig. 4.3.1. Electron-scan images of samples (Kaymin data) after laboratory test: (a) chlorite (Chl) replacement by montmorillonite (Mont); (b) muscovite (Ms) replacement by kaolinite (Kaol); (c) biotite (Bt) replacement by montmorillonite (Mont); (d) K-feldspar (Kfs) replacement by montmorillonite (Mont); (e) grains of magnetite hosted in clay minerals; (f) sodium carbonates (Na) release in form of regions in montmorillonite (Mont). The black space is the polymeric matrix.

TOUGHREACT V1.0 modeling was used to reproduce laboratory tests involving sandstone samples collected from a deep radionuclide repository site at the Siberia Chemical Plant, Seversk, Russia. Laboratory tests included injection of alkaline fluids into sandstone samples at 708°C. Some minerals were constrained in the model to precipitate or dissolve, according to laboratory test results. A cation exchange option was used. Modeling results were compared with observed test data (mineral phase changes, transient concentration data at the outlet of a sample column). Reasonable agreement was obtained between calculated and measured mineral phases (Na-smectite and kaolinite precipitation, quartz, microcline, chlorite, and muscovite dissolution). After a cation exchange option was used in the model, the most abundant secondary mineral generated was dawsonite, which corresponds to sodium carbonates observed in the sample after an injection test. Time-dependent chemical concentrations (transient chemical concentration data) at the outlet of the sample column qualitatively matched the data observed.

A.V. Kiryukhin, E.P. Kaymin, E.V. Zakharova, A.A. Zubkov. MODELING OF THE LABORATORY TESTS OF INTERACTION OF THE NaNO₃-NaOH FLUIDS WITH SANDSTONE ROCKS FROM DEEP RADIONUCLIDE REPOSITORY SITE, USING TOUGHREACT. Proc. TOUGH Symposium, Berkeley, CA, LBNL, 15-17 May, 2006, 8 p.

A.V. Kiryukhin, E.P. Kaymin, and E.V. Zakharova THERMAL-HYDRODYNAMIC MODELING OF LABORATORY TESTS ON THE INTERACTION OF NaNO₃-NaOH FLUIDS WITH SANDSTONE ROCK AT A DEEP RADIONUCLIDE REPOSITORY SITE \\ Volcanology and Seismology Journal, #6, 2007, 20 p.

4.4.Simulation of earthquake ground motion

Gusev A.A., *Institute of Volcanology and Seismology, Far East Division, Russian Academy of Sciences, Petropavlovsk-Kamchatsky, 683006, Russia*

Pavlov V.M., *Kamchatka Branch, Geophysical Service RAS, 9 Piip Blvd, 683006 Petropavlovsk-Kamchatsky, Russia*

A kinematic, stochastic fault model and simulation procedure is proposed for realistic, application-oriented simulation of earthquake ground motion. An extended fault plane is discretized as a grid of point subsources. Subsource signal, in its low-frequency part, is produced by a dislocation strip sweeping the fault area. In its high-frequency part, it is defined by random local slip history, represented by a segment of pulsed noise. Subsource signals are convolved with broad-band Green functions for a layered half-space, and stacked, resulting in the ground motion at a site. Through a special choice of subsource signals, the Fourier spectrum of ground motion obeys an observation-based scaling law. Effects of the rupture velocity behavior, rise time, wavenumber spectrum for the final slip, the degree of spikiness of time functions etc can be easily analyzed. For illustration, several near-source 1994 Northridge earthquake records are simulated, and related uncertainties are estimated.

In the development of the proposed broad-band simulation procedure it was planned to incorporate most well-established properties of earthquake sources. The resulting procedure, though judging by a single test only, is quite attractive: in the mode of almost blind testing, the match to observations in the epicentral zone is quite satisfactory. Another attractive result is the demonstrated possibility to generate uncertainty estimates; this capability is important for any engineering-oriented application. More work is needed to verify wider applicability of the proposed technique. Also, recommendations must be elaborated for the choice of a few

parameters of the source model whose values are no more than guessed at present. There are no any analogous methods in Europe and in Russia.

Gusev A.A., Pavlov V.M. *Broadband Simulation of Earthquake Ground Motion by a Spectrum-Matching, Multiple-Pulse Technique* // *Earthquake Spectra*. 2009. V. 25, N 2, P. 257-276.

Gusev A.A., Guseva E.M., Pavlov V.M. *Modeling of the ground motion at earthquake in Petropavlovsk 24.11.1971 ($M_w=7.6$)* // *Physics of the Earth*. 2009. № 5. pp. 29-38 (in Russian).

4.5. Processes in the feeders of basaltic volcanoes

Ozerov A.Yu., ozero@ozero.ru, *Institute of Volcanology and Seismology, Far East Division, Russian Academy of Sciences, Petropavlovsk-Kamchatsky, 683006, Russia*

Processes in the feeders of basaltic volcanoes during Strombolian-type eruptions were examined with the use of a complex apparatus for modeling basaltic eruptions (CAMBE), which was designed and manufactured by the authors for this purpose (Fig. 4.5.1). The experimental setup consists of modeling and registering units and has a height of 18 m. It was designed with regard for the geometric dimensions of a natural feeding volcanic system: the ratio of the inner diameter of the feeder to its height is approximately 1 : 1000. CAMBE was the first modeling equipment making possible passing a flow of gas-saturated liquid through the conduit, which allowed us to study the nucleation of gas bubbles, their growth, coalescence, transformations of the gas structures, and the kinetics of the gas phase.

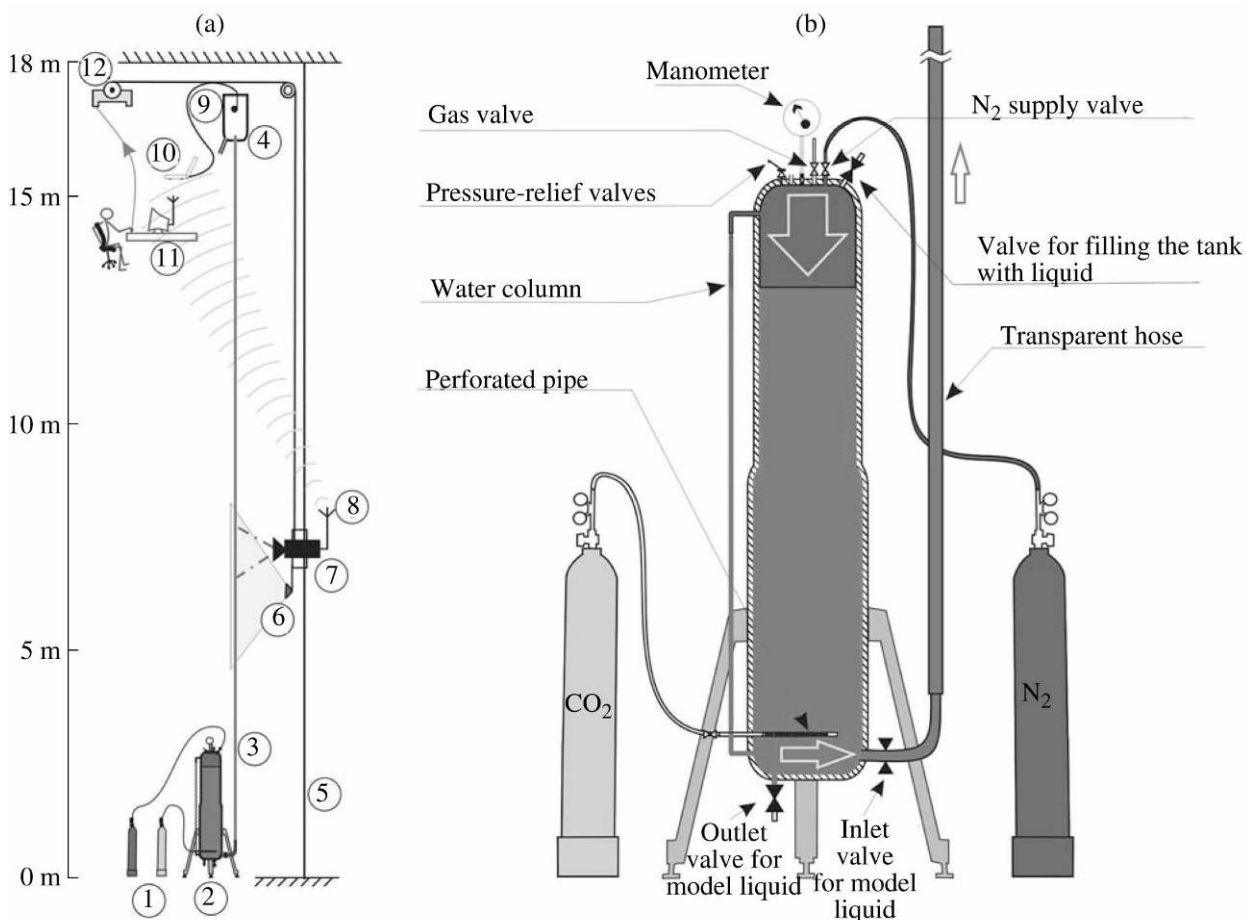


Fig. 4.5.1. CAMBE experimental equipment for modeling basaltic eruptions.

(a) Design of (1–4) the modeling and (5–14) units of CAMBE: (1) high-pressure gas tanks with CO₂ and N₂, (2) hermetically sealed tank for preparing modeling liquid, (3) transparent hose, (4) aquarium for receiving liquid, (5) cable for directing the movement of the dynamic video monitoring car, (6) source of light, (7) camcorder, (8) transmitting set and telemetry antenna, (9) microphone, (10) computer, (11) radio signal receiver and monitor, (12) electric motor. The operator is shown in the upper part of the figure. (b) Unit for preparing gas-rich model liquid and its pumping to the transparent hose.

Gas-hydrodynamic regime				Types of eruptive activity in volcanic vent (at a viscosity of the basaltic melt of 10 ³ –10 ⁵ Pa s)								
Regime		Phase of regime		Continuous and even delivery of material				Discrete delivery of material				
Increase in the gas content	Slug	mature	4b	Illustrations of gas-hydrodynamic regimes according to experimental data (1–4)	Lava eruptions	Weak ash emissions	Powerful ash emissions	Weak ash explosions with a low amount of bombs	Powerful bomb explosions	Powerful bomb explosions without ash	Powerful bomb explosions with ash emissions	
		initial	4a									
	Cluster	mature	3b									
		initial	3a									
	Bubbly	mature	2b									
		initial	2a									
	Liquid	1										1








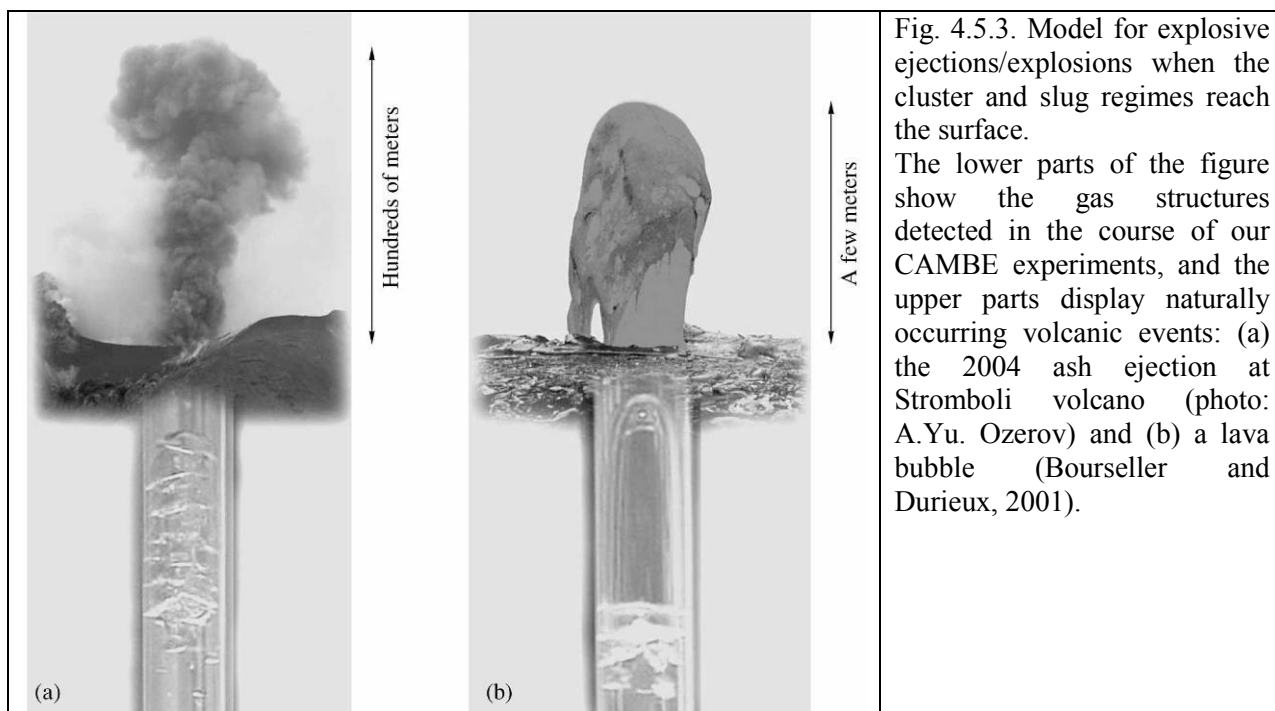








Fig. 4.5.2. Classification of the types of eruptive activity at basaltic volcanoes depending on the gas-hydrodynamic regimes in their vents.

The experiments were carried out in a manner that made it possible to eliminate effects of structural barriers and fluctuations in the liquid flow velocity. As a result of the experiments, a new (previously unknown) regime in the flow of two-phase systems through a vertical conduit was discovered: the cluster regime, which is characterized by systematically alternating dense accumulations of gas bubbles (bubble clusters) and liquid devoid of a free gas phase. It is demonstrated that the liquid, bubbly, cluster, and slug regimes systematically grade into one another and are polymorphic modifications of gas-saturated liquids moving through vertical conduits (Fig. 4.5.2). Our data led us to propose a new model for the gas-hydrodynamic movement of magmatic melt through the conduit of a basaltic volcano: depending on the gas-hydrodynamic regime in the volcanic vent, various types of eruptive activity (up to explosions) may take place (Fig. 4.5.3). The analyses of basaltic magma explosions allowed us to describe

them from a new standpoint and recognize the following four major modes of their manifestations at the surface: (1) weak ash explosions early during the cluster regime, (2) strong ash explosions during the mature cluster regime, (3) bomb explosions during the slug regime, (4) bomb grading to ash explosions during the slug regime associated with trains of small bubbles.



Ozerov A.Yu. *Experimental Modeling of the Explosion Mechanism of Basaltic Magmas* // *Petrology*, 2009. Vol. 17. № 7. P. 653–668.

Gavrilenko M.G., Ozerov A.Yu. *Geochemical similarities between the pre-caldera and modern evolutionary series of eruptive products from Gorely volcano, Kamchatka* // 2010 AGU Fall Meeting, Abstract V21B-2333

Ozerov A. Yu. *The Mechanism of Basaltic Explosions: Experimental Modeling*. *Journal of Volcanology and Seismology*, 2010, Vol. 4, No. 5, pp. 295–309.

4.6. Volcanology and climate

Murav'ev Ya. D., murjd@kscnet.ru, *Institute of Volcanology and Seismology, Far East Division, Russian Academy of Sciences, Petropavlovsk-Kamchatsky, 683006, Russia*

The problem of influence of volcanic activity on climatic changes has been already studied for more than 200 years. And only during the last quarter of the previous century, when methods of remote sounding of atmosphere were introduced into research practice, as well as ice core drilling of polar glaciers was mastered, some approaches to its solution were found. This review considers the results of works in this area. It is shown, that, despite an obvious progress, many issues of volcano-climate interaction remain unsolved, and especially thin processes of transformation of volcanic aerosols when carried in the atmosphere.

Murav'ev Ya. D., *Volcano eruptions and climate*. *Vestnik DVO RAS*. 2007. № 2. pp.71-82 (in Russian)

Vyatkina M.P., Kazakov N.I., Murav'ev Ya. D. Dynamic of the vegetation and soils in the valley of Bilchonok glacier after the deglaciation. The materials of the glaciological researchers. 2007. Issue 102. pp.178-186 (in Russian).

4.7. Rotational processes in geology

Vikulin A.V., *Institute of Volcanology and Seismology, Far East Division, Russian Academy of Sciences, Petropavlovsk-Kamchatsky, 683006, Russia*

In this book there present original works of geologists, physicists, geographers, geodesists and astronomers of various centers of sciences of Russia that are located in Moscow, Petropavlovsk-Kamchatsky, Vladivostok, Tomsk and other cities, and also in Poland and Bulgaria. The works are related to rotational, vortical and wave movements of wide range. Such movements are offered to be put in pawn in a basis of a new geological-physical paradigm known as rotational geodynamics. The book is recommended for the wide range of readers: from students-naturalists up to scientific employees of different ranks, which are interested in regularities and features of structure and evolution of the Earth, the planets and the universe.

Vikulin A.V., Melekestsev I.V. Rotational processes in geology and physics / Ed. by E.E. Milanovsky. M.: URSS, Moscow State university, 2007. 528 p.

4.8. Volcanic plumes and wind

Bursik M.I., S.E. Kobs, A. Burns, *Department of Geology, State University of New York at Buffalo, Buffalo, NY 14260, United States*

O.A. Braitseva, L.I. Bazanova, I.V. Melekestsev, *Institute of Volcanology and Seismology, Russian Academy of Sciences, Petropavlovsk-Kamchatskiy, 683006, Russia*

Kurbatov A., *Climate Change Institute, University of Maine, Orono, ME 04469, United States*

Pieri D.C., *Earth and Space Sciences Division, Jet Propulsion Laboratory, California Institute of Technology, Pasadena, CA 91109, United States*

Volcanic plumes interact with the wind at all scales. On smaller scales, wind affects local eddy structure; on larger scales, wind shapes the entire plume trajectory. The polar jets or jetstreams are regions of high [generally eastbound] winds that span the globe from 30 to 60° in latitude, centered at an altitude of about 10 km. They can be hundreds of kilometers wide, but as little as 1 km in thickness. Core windspeeds are up to 130 m/s. Modern transcontinental and transoceanic air routes are configured to take advantage of the jetstream. Eastbound commercial jets can save both time and fuel by "ying within it; westbound aircraft generally seek to avoid it.

Using both an integral model of plume motion that is formulated within a plume-centered coordinate system (BENT) as well as the Active Tracer High-resolution Atmospheric Model (ATHAM), we have calculated plume trajectories and rise heights under different wind conditions. Model plume trajectories compare well with the observed plume trajectory of the Sept 30/Oct 1, 1994, eruption of Kliuchevskoi Volcano, Kamchatka, Russia, for which measured maximum windspeed was 30–40 m/s at about 12 km. Tephra fall patterns for some prehistoric eruptions of Avachinsky Volcano, Kamchatka, and Inyo Craters, CA, USA, are anomalously elongated and inconsistent with simple models of tephra dispersal in a constant wind!eld. The Avachinsky deposit is modeled well by BENT using a windspeed that varies with height.

Two potentially useful conclusions can be made about air routes and volcanic eruption plumes under jetstream conditions. The first is that by taking advantage of the jetstream, aircraft are flying within an airspace that is also preferentially occupied by volcanic eruption clouds and particles. The second is that, because eruptions with highly variable mass eruption rate pump volcanic particles into the jetstream under these conditions, it is difficult to constrain the tephra grain size distribution and mass loading present within a downwind volcanic plume or cloud that has interacted with the jetstream. Furthermore, anomalously large particles and high mass loadings could be present within the cloud, if it was in fact formed by an eruption with a high mass eruption rate. In terms of interpretation of tephra dispersal patterns, the results suggest that extremely elongated isopach or isopleth patterns may often be the result of eruption into the jetstream, and that estimation of the mass eruption rate from these elongated patterns should be considered cautiously.

Bursik M.I., Kobs S.E., Burns A., Braitseva O.A., Bazanova L.I., Melekestsev I.V., Kurbatov A., Pieri D.C. Volcanic plums and wind: jetstream interaction examples and implications for air traffic // Journal of Volcanology and Geothermal Research. Elsevier. 2009. № 186. P. 60-67.